THE UNIVERSITY OF OKLAHOMA

GRADUATE COLLEGE

ANALYSIS OF MULTIPLE-SEALING-FAULT SYSTEMS AND CLOSED RECTANGULAR RESERVOIRS BY TYPE CURVE MATCHING

A DISSERTATION

SUBMITTED TO THE GRADUATE FACULTY

in partial fulfillment of the requirements for the degree of

DOCTOR OF PHILOSOPHY

BY

DJEBBAR TIAB

Norman, Oklahoma

1976

ANALYSIS OF MULTIPLE-SEALING-FAULT SYSTEMS AND CLOSED RECTANGULAR RESERVOIRS BY TYPE CURVE MATCHING

APPROVED BY

H. Crichlow

D E Menzie

F M Townsend

Martin E Chenevert

DISSERTATION COMMITTEE

ACKNOWLEDGEMENTS

The author wishes to express his appreciation to Dr. Henry B. Crichlow, Director of the School of Petroleum and Geological Engineering, who supervised this study and made valuable suggestions. The author also wishes to thank Dr. Donald E. Menzie, Professor of Petroleum and Geological Engineering, Dr. Martin E. Chenevert, Associate Professor of Petroleum and Geological Engineering, and Dr. Mark Townsend, Professor of Chemical Engineering and Material Science, for being members of the Dissertation Committee and their helpful comments.

The School of Petroleum and Geological Engineering of the University of Oklahoma furnished financial support.

ABSTRACT

Thus far, if a multiple-boundary situation is suspected in a hydrocarbon reservoir, about the best one can hope to do is obtain an estimate of the distance to the nearest boundary. Also, although a well in a closed rectangular drainage area presents a very important flow problem in conventional reservoir engineering, no comprehensive method exists in the literature to determine the location of the well with respect to each of the sealing boundaries of the drainage area.

This study presents a new technique for interpreting the pressure transient behavior of a well located in various multiple-fault systems and within closed rectangular reservoirs. The technique is principally based on the systematic use of the time rate of change of dimensionless well pressure. This function was systematically employed to explore the characteristics of drawdown and buildup well pressure behavior. A useful application of the time derivative of dimensionless well pressure function, as opposed to the conventional approach which employs the pressure itself as the significant function, is the generation of interpretive drawdown and buildup type-curve plots. Type-curve plots

generated in this manner can be used to match drawdown or buildup curves based on the time rate of change of field pressure data to determine several essential reservoir parameters such as permeability, porosity, drainage area, and distance to surrounding sealing faults.

The main reservoir systems considered in this study are: (a) two perpendicular sealing faults, (b) three perpendicular sealing faults, and (c) bounded rectangles whose sides are in integral ratios: 1:1 (square), 2:1, 4:1, 8:1 and 16:1. A large number of type-curve plots and corresponding numerical data in the form of tables are included.

TABLE OF CONTENTS

Chapter Page

LIST OF TABLES

Table | Page

Table Page

Table Page

LIST OF FIGURES

Figure | Page

Figure Page

Figure Page

ANALYSIS OF MULTIPLE-SEALING-FAULT SYSTEMS AND CLOSED RECTANGULAR RESERVOIRS BY TYPE CURVE MATCHING

CHAPTER I

INTRODUCTION

1.1 Literature Survey

The concept of analyzing pressure-time data from a producing or shut-in oil or gas well to obtain in-situ reservoir rock properties, such as permeability and porosity, was first applied in 1933. A classic study by Moore, Schilthius, and Hurst[1] in that year presented a solution to the diffusivity equation in terms of Bessel functions for a constant rate well and a constant pressure well in an infinite reservoir. In 1935, Theis[2] presented in groundwater hydrology literature the line source exponential integral solution to the diffusivity equation and its logarithmic approximation at large times. He also employed a semi-log graph which is commonly known as the Horner plot in the petroleum industry. Shortly afterwards, Muskat[3] developed a method to determine the eventual static pressure of a well in a

closed circular reservoir. Elkins[4] demonstrated in 1946 the use of the line source solution in interference testing between wells in an oil field to determine inter-well rock properties. Arps and Smith[5] presented a method to determine static pressure by plotting rate of change of well shut-in pressure versus shut-in pressure.

The preceding publications laid the foundation for two important papers in 1950. One paper by Horner[6] summarized methods for analyzing transient pressure data for a constant rate well in an infinite reservoir and in a closed reservoir. The second paper by Miller, Dyes and Hutchinson[7] presented the behavior of a constant rate well in a circular reservoir with no-flow and constant pressure conditions at the drainage boundary of the reservoir.

Although Muskat[3] had demonstrated the application of the method of images under steady-state flow conditions to simulate linear no-flow and flow boundaries near a well, Horner[6] presented in 1951 an application of the method to detect the presence of a sealing fault near a well from pressure data under transient flow conditions. Horner also presented a method to calculate the distance to the fault from buildup pressure data. Dolan, Einarson, and Hill[8] applied the technique to data from drill-stem tests. Davis and Hawkins[9] gave an equation to determine the distance from drawdown pressure data. Gray[10] reviewed these methods and discussed their limitations.

Bixel, Larkin, and van Poollen[11] considered a more general problem: a well located close to a linear discontinuity across which hydraulic diffusivity changes. They gave a method to calculate the distance to such a discontinuity.

Evrenos and Rejda[12] employed superposition techniques to simulate various combinations of linear boundaries of interest in gas storage systems, and showed how a match between the actual test data with various hypothetical model conditions can be used to arrive at a probable configuration of boundary conditions.

Overpeck and Holden[13] considered the effect of reservoir anisotropy on fault detection and showed that the distance calculated could differ by as much as 20 percent with those obtained by assuming an isotropic medium. They gave a procedure for imaging when the principal permeability axes are at some angle other than 0° or 90° to the fault boundary.

Rodgers and McArthur[14] employed a minimum standard deviation technique between observed pressures and a least squares straight line fit to determine boundary configuration. Prasad[15] presented a procedure to compute transient pressures for a well between two sealing faults intersecting at any angle.

Park Jones[16] in 1961 drew attention to the possible use of rate of change of well pressure with time in detecting reservoir boundaries. Van Poollen[17] presented graphs of time rate of change of well pressure during drawdown for

various well locations between faults intersecting at 90° and 36°. Although this approach yields interpretable drawdown behavior, it has not been widely used.

Witherspoon, et al.[18] considered the effect of a linear no-flow and flow boundary and presented the dimensionless pressure behavior caused by a constant rate producing well at an observation well some distance away. They discussed techniques to analyze drawdown test data.

For a well between two sealing parallel faults, Ramey, Kumar, and Gulati[19] presented dimensionless pressure data at the well and fourteen other points in the reservoir. These authors also presented a detailed study of constant pressure flow conditions at the reservoir boundary.

Matthews, Brons and Hazebroek[20] extended Horner's determination of static pressure for bounded circular reservoirs to the general case of a well in almost any position within a large variety of bounded drainage shapes. Later, Brons and Miller,[21] and Dietz[22] developed other pressure buildup interpretive methods for these closed shapes. These studies were followed by a large number of publications on well test interpretation in bounded reservoirs of various geometrical shapes such as a circle, square, rectangle, rhombus, ellipse, and right and equilateral triangle. Matthews and Russell[23] summarized the practical aspects of the findings of these studies in a monograph.

The Matthews-Brons-Hazebroek function may be used to obtain the dimensionless pressure only at the well, however.

For this reason, Earlougher, Ramey, Miller and Mueller[24] used superposition to produce a tabulation of the dimensionless pressure drop function at several locations within a bounded square (infinite-square array). These authors also demonstrated that the infinite-square array may be used to generate flow behavior for any rectangular shape whose sites are in integral ratios. In 1973, Earlougher and Ramey[25] presented tables of the dimensionless pressure at the well and at several other locations within a variety of closed rectangles with a well producing at a constant rate.

Tiab[26] and Tiab and Kumar[27,28] studied the behavior of the time rate of change of dimensionless pressure (p'_D) for a line source well and its application to interference analysis. These authors showed[27] that the p'_D function can be displayed as a family of curves on one graph for various r_D. They also showed[28] that for a well between two parallel sealing faults a log-log plot of time rate of change of well pressure versus time provides a unique behavior to detect and determine the distance to each of the two faults.

1.2 Statement of Problem

Pressure transient testing has been extensively applied to determine heterogeneities (sealing faults, fractures, sudden change in rock characteristics such as permeability and porosity, etc.) in petroleum reservoir systems, groundwater hydrology and other technological areas where the location of boundaries around a borehole is essential.

Methods to detect and locate one sealing fault (or no-flow boundary) in the vicinity of a producing oil or gas well by the conventional well pressure data were developed. Such methods, however, do not show interpretable characteristics in the presence of multiple-boundary situations. Thus far, if a multiple-boundary situation is suspected (with the exception of an infinite strip[28]), about the best one can hope to do is obtain an estimate of the distance to the nearest boundary. Furthermore, although a well in a closed rectangle presents a very important flow problem in conventional reservoir engineering, no systematic method exists in the literature to determine the location of the well with respect to each of the sealing boundaries of the rectangular reservoir.

1.3 Objectives of Study

The purpose of this study is to develop a systematic tool for interpreting the behavior of transient pressure functions, principally the derivatives, due to a constant rate well located (1) between two perpendicular sealing faults, (2) between three perpendicular sealing faults, and (3) anywhere inside a closed rectangle whose sides are in integral ratios of (a) 1:1 (square), (b) 2:1, (c) 4:1, (d) 8:1, and (e) 16:1. For this, type-curve plots based on the time rate of change of dimensionless well pressure will be presented for wells located in these oil reservoir systems.

Type-curve plots generated in this manner will be used to match the rate of change of well pressure drawdown (buildup) data for determination of permeability, porosity, drainage area, and number and location of boundaries.

1.4 Organization of Study

The next chapter presents the mathematical basis of drawdown and buildup well testing. For this, the continuous line source solution of the diffusivity equation, and its first two derivatives with respect to time are systematically discussed. The third chapter discusses the use of the theorem of superposition to generate no-flow boundaries existing in various oil reservoir systems of interest to this study.

Chapter four considers a well between two linear sealing faults intersecting at a right angle. The fifth chapter deals with the case of a well between three perpendicular sealing faults. Chapter six discusses the pressure behavior of a well at various locations inside a rectangular reservoir. The general conclusions reached by this study are presented in the seventh chapter.

CHAPTER II

THEORY

The pressure transient analysis technique presented in this study is based on the diffusivity equation describing the flow of fluids through porous media. This partial differential-type equation is generally written in cylindrical coordinates as:

$$\frac{\partial^2 p}{\partial r^2} + \frac{1}{r}\frac{\partial p}{\partial r} = \frac{\phi \mu c}{k}\frac{\partial p}{\partial t} \tag{2.1}$$

This equation is obtained by combination of the material balance equation and D'Arcy's flow equation. The assumptions implicit in the use of the diffusivity equation are as follows: (1) the porous medium is isotropic, horizontal, homogeneous, uniform in thickness, and has constant permeability and porosity; (2) a single-phase fluid is present and occupies the entire pore volume; (3) viscosity and compressibility of the fluid remain constant at all pressures; (4) the well completely penetrates the formation, and gravity forces are negligible; and (5) fluid density is governed by the equation:

$$\rho = \rho_o \exp[c(p - p_o)] \tag{2.2}$$

where ρ_o is the value of ρ at some reference pressure p_o, and c the compressibility. Applying the diffusivity equation in cases where these assumptions do not hold will obviously result in errors.

To obtain a dimensionless form of Equation 2.1 van Everdingen and Hurst[29] made the following transformations:

$$r_D = \frac{r}{r_w} \tag{2.3}$$

$$t_D = \frac{kt}{\phi \mu c r_w^2} \tag{2.4}$$

$$p_D(r_D,t_D) = \frac{2\pi kh}{q\mu} [p_i - p(r,t)] \tag{2.5}$$

After these transformations are made, the diffusivity equation can be written as:

$$\frac{\partial^2 p_D}{\partial r_D^2} + \frac{1}{r_D} \frac{\partial p_D}{\partial r_D} = \frac{\partial p_D}{\partial t_D} \tag{2.6}$$

This dimensionless form of the diffusivity equation is essential, as a single solution can be used for applications of different porosity, permeability and fluid properties. Several slightly different solutions of Eqs. 2.1 or 2.6 are presented in the petroleum literature.[30] The solution most convenient to the needs of this study is that for the case of flow into a well at a constant volumetric rate of production and located in a porous medium of infinite radial extent. This solution, which describes a classical flow problem, is referred to by many names: Lord Kelvin's

point source,[29] Theis solution,[2] and the continuous line source solution.[31]

2.1 The Continuous Line Source Solution

For a constant rate well with a vanishingly small radius ($r_w \to 0$) in an infinite system, the continuous line source solution to the diffusivity equation in dimensionless form is:

$$p_D(r_D,t_D) = -\frac{1}{2}\,Ei\left(-\frac{r_D^2}{4t_D}\right) , \qquad (2.7)$$

where Ei symbolizes the exponential integral and is defined as:

$$-Ei(-x) = \int_x^\infty \frac{1}{u}\,e^{-u}\,du . \qquad (2.8)$$

A mathematical formulation of the boundary conditions and derivation of this line source solution is presented in Appendix A.

Mueller and Witherspoon[32] investigated the validity of this solution in the case of a finite well bore radius. They concluded that the line source solution is an excellent approximation within one percent for all values of r_D when $(t_D/r_D^2) \geq 50$, and for $r_D \geq 20$ when $(t_D/r_D^2) \geq 0.5$. Therefore, for most r_D and t_D encountered in well-test analysis, Eq. 2.6 can be used to determine dimensionless pressures in an infinite radial system. This is evident from Fig. 2.1.

For small values of the argument, the exponential integral function may be approximated, within less than one

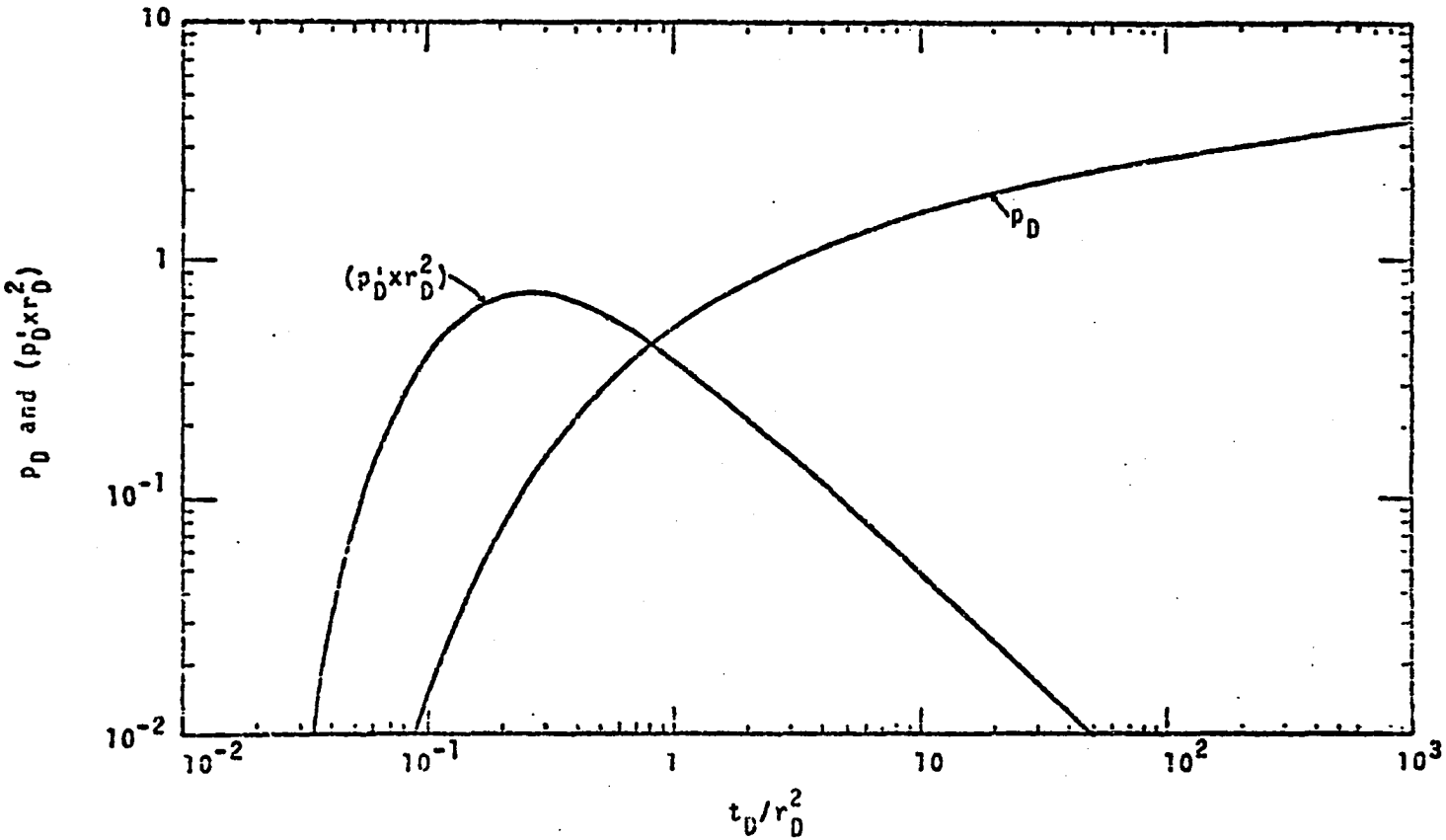

FIGURE 2.1: A log-log graph of p_D and $(p_D' \times r_D^2)$ vs (t_D/r_D^2) for a line source well in an infinite medium.

percent for $(t_D/r_D^2) \geq 70$, by a logarithmic function as follows:

$$-Ei\left(-\frac{r_D^2}{4t_D}\right) \simeq -\ln\left(\frac{r_D^2}{4t_D}\right) - 0.5772$$

$$\simeq \ln\left(\frac{t_D}{r_D^2}\right) + 0.80907 \qquad (2.9)$$

where the number 0.5772 is referred to as Euler's constant.[33] Equation 2.7 can then be written as:

$$p_D(r_D,t_D) = -\frac{1}{2}\left[\ln\left(\frac{r_D^2}{4t_D}\right) + 0.5772\right]$$

$$= \frac{1}{2}\left[\ln\left(\frac{t_D}{r_D^2}\right) + 0.80907\right] \qquad (2.10)$$

It is emphasized again that Eq. 2.10 is an approximation to Eq. 2.7 while the line source solution is itself an approximation for pressure behavior due to a finite radius wellbore in an infinite reservoir.

In this study, the continuous line source solution, Eq. 2.7, is used as a fundamental building block to simulate a number of useful solutions for flow into wells from finite and semi-finite reservoir systems by means of the theorem of superposition.

Tabulations of the dimensionless pressure drop at the well (i.e., $r_D = 1$) as well as for other r_D have been presented by several authors, including van Everdingen and Hurst,[30] Chatas,[34] Mortada,[35] Katz, et al.,[36] Witherspoon,

et al.,[18] Ramey, et al.,[19] and Edwardson, et al.[37] Tiab[26] presented the dimensionless pressure data in both graphical and tabular forms for $10^{-3} \leq t_D \leq 10^8$, and $1 \leq r_D \leq 30$.

2.2 First Derivative of the Line Source Solution

The continuous line source solution, Eq. 2.7, involves an exponential integral function which is defined in terms of an integral. The first derivative of the p_D-function would therefore require the use of the Leibnitz rule for differentiation under the integral sign, as shown in Appendix B, or

$$\frac{\partial p_D}{\partial t_D} = p_D' = \frac{1}{2t_D} \exp\left(-\frac{r_D^2}{4t_D}\right) \qquad (2.11)$$

A comparison of p_D'-data calculated using this equation with those for a finite radius wellbore (Figs. 2.2 and 2.3) indicates that the line source solution of Eq. 2.11 is an excellent approximation within less than one percent when $t_D \geq 250$ and within 2.5 percent when $t_D \geq 100$, at $r_D = 1$. However, at $r_D = 30$, p_D' is a good approximation within one percent for $t_D \geq 50$.

Equation 2.11 can be rearranged in the following form:

$$p_D' \times r_D^2 = \frac{1}{2(t_D/r_D^2)} \exp\left[-\frac{1}{4(t_D/r_D^2)}\right] \qquad (2.12)$$

It is evident that this equation is a function of the ratio t_D/r_D^2 only. This provides the basis for the type curve shown in Fig. 2.1. A log-log graph of $(p_D' \times r_D^2)$ vs (t_D/r_D^2)

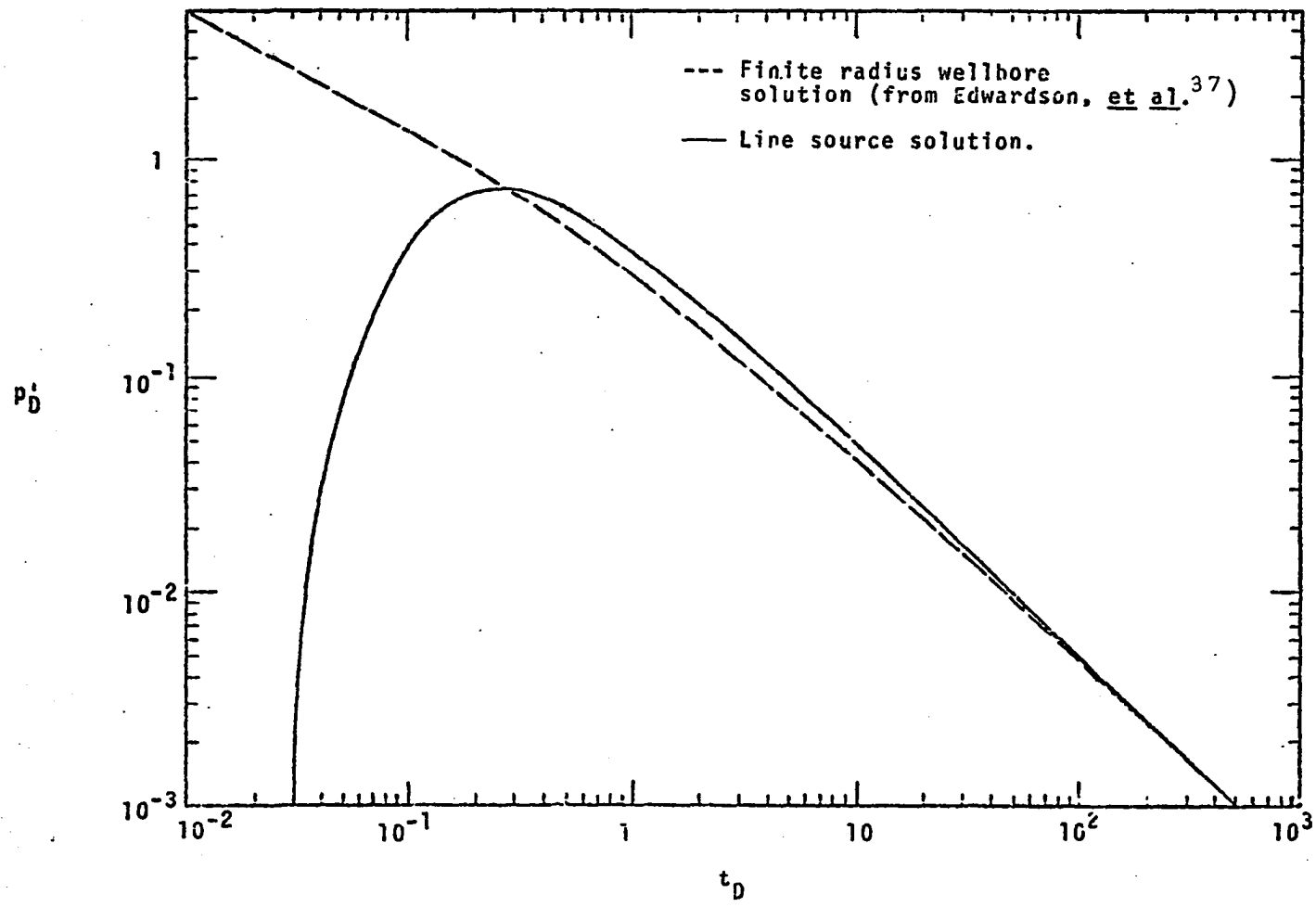

FIGURE 2.2: p'_D vs t_D at $r_D = 1$ for a constant rate well in an infinite reservoir.

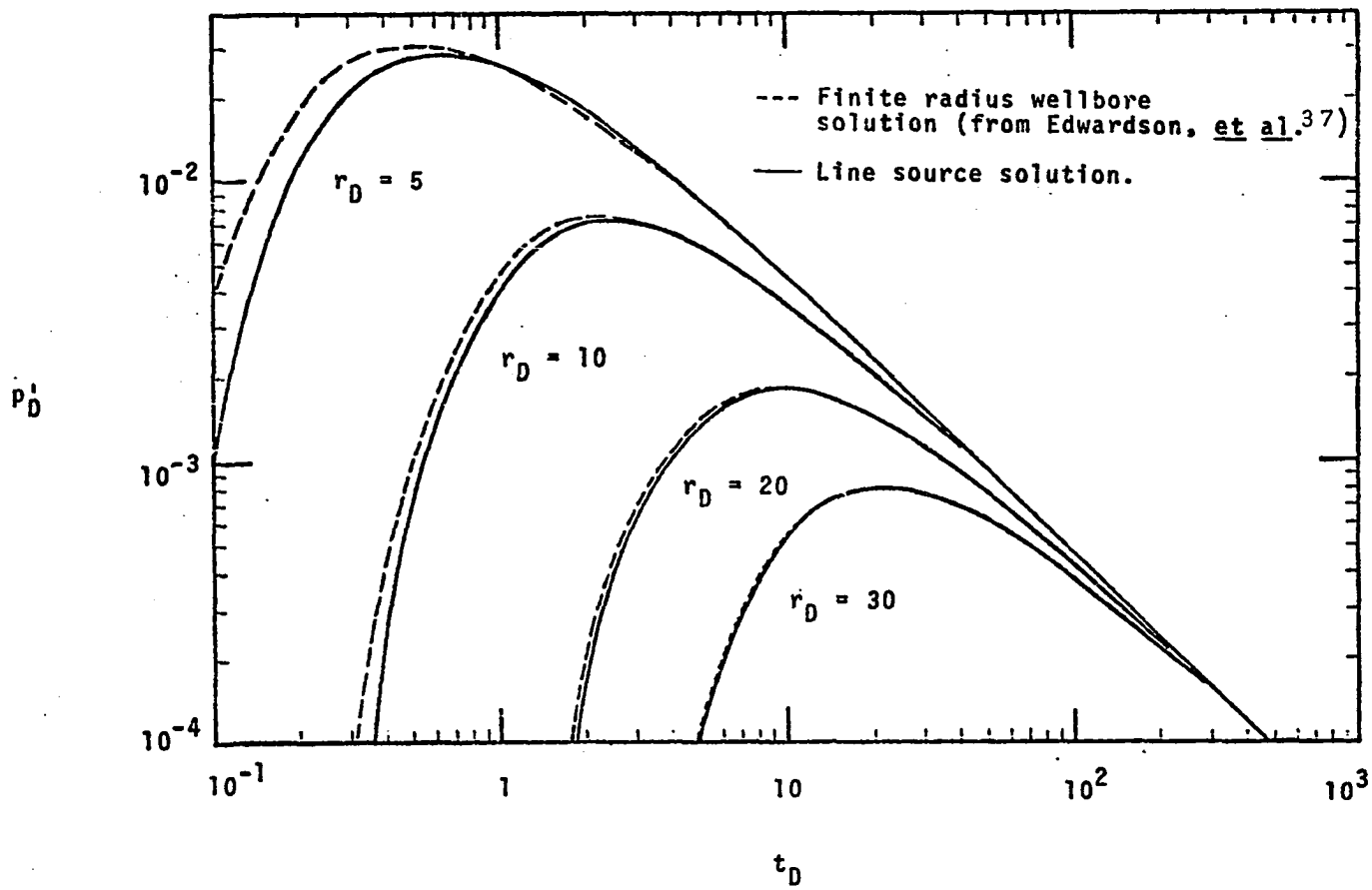

FIGURE 2.3: p'_D vs t_D for $r_D > 1$ for a constant rate well in an infinite reservoir.

is shown in Fig. 2.4 for various r_D. This figure indicates that the line source solution is a good approximation for $t_D/r_D^2 > 0.5$ when $r_D > 10$ and for $t_D/r_D^2 > 0.05$ when $r_D > 30$. Therefore, for practical purposes Eq. 2.11 can be used to compute p'_D for $t_D > 250$ at $r_D = 1$ and for $t_D > 50$ for all $r_D > 30$. These results are of considerable importance in interference testing between wells and between oil fields in a common aquifer and are traited in more details by Tiab and Kumar.[27]

In view of the above discussion, the rate of change with time of the dimensionless well pressure, i.e., $r_D = 1$, is given by

$$p'_{Dw} = \frac{1}{2t_D} \exp\left(-\frac{1}{4t_D}\right) \qquad (2.13)$$

for values of $t_D > 100$. The exponential term is close to unity for such values of t_D, and therefore Eq. 2.13 is approximated by

$$p'_{Dw} = \frac{1}{2t_D} \qquad (2.14)$$

A log-log graph of p'_{Dw} versus t_D would yield a straight line:

$$\log p'_{Dw} = -\log t_D - 0.30103 \qquad (2.15)$$

with a slope of -1. This is evident in Fig. 2.5 for $t_D > 100$. In terms of real parameters, the rate of change of pressure with time is given by Eq. B.8 of Appendix B:

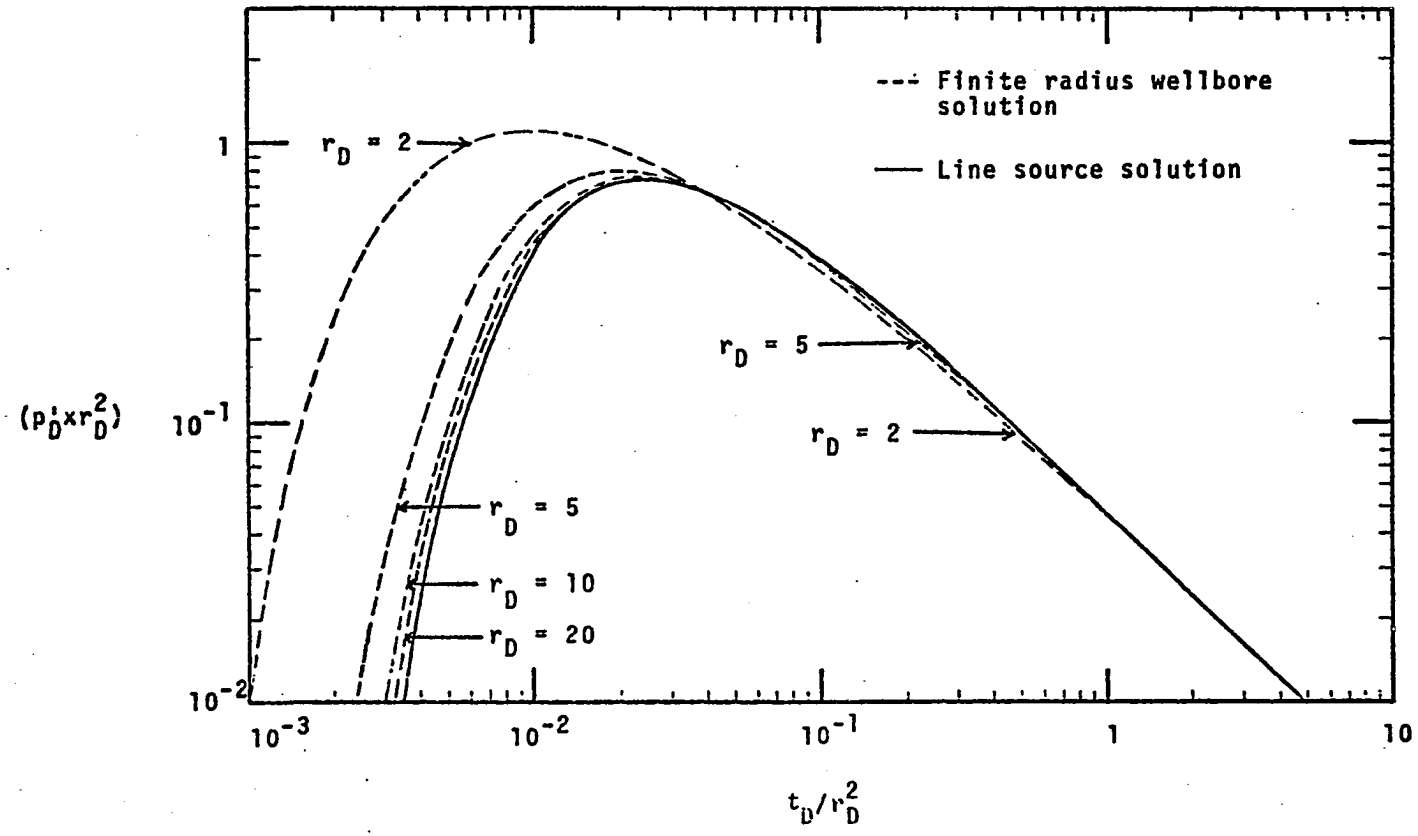

FIGURE 2.4: $(p'_D \times r_D^2)$ vs (t_D/r_D^2) for a constant rate well in an infinite reservoir.

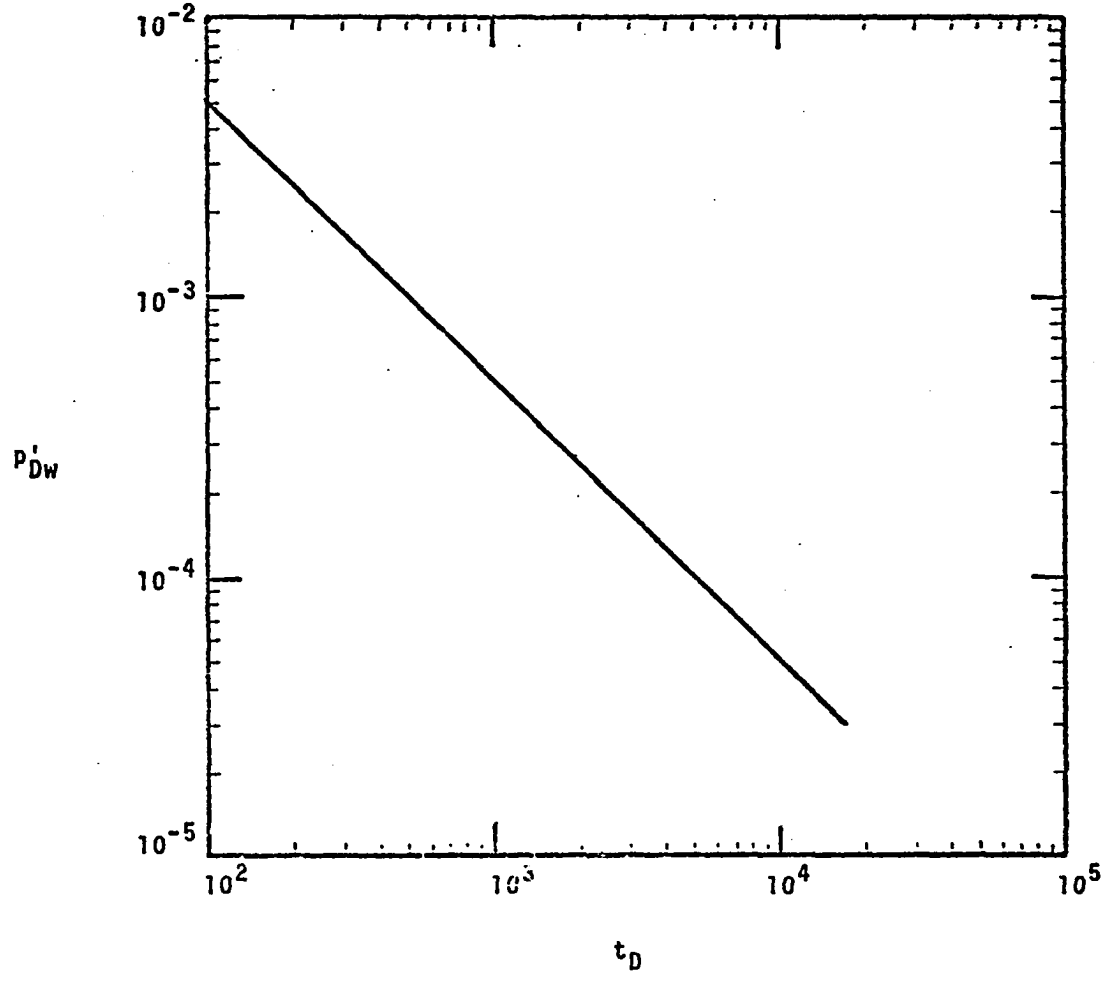

FIGURE 2.5: Time Rate of Change of Dimensionless Well Pressure vs Dimensionless Time for a Well in an Infinite Reservoir.

$$\frac{\partial p}{\partial t} = p' = -\frac{1}{t}\left(\frac{q\mu}{4\pi kh}\right)\exp\left(-\frac{\phi\mu c r^2}{4kt}\right) \tag{2.16}$$

which applied to well points for $\frac{kt}{\phi\mu c r_w^2} > 100$ yields

$$|p_w'| = \frac{1}{t}\left(\frac{q\mu}{4\pi kh}\right) \tag{2.17}$$

A log-log graph of $|p_w'|$ versus t would also yield a straight line:

$$\log |p_w'| = -\log t + \log\left(\frac{q\mu}{4\pi kh}\right) \tag{2.18}$$

It is evident that Eq. 2.15, in dimensionless quantities, is similar to Eq. 2.18, in real parameters. This similarity permits us to apply the type-curve matching technique to determine formation characteristics such as the kh and ϕc products.

This completes the discussion on the first derivative of the dimensionless pressure, the behavior of the second derivative is discussed next.

2.3 Second Derivative of the Line Source Solution

The second derivative with respect to time of the line source solution is obtained by direct differentiation of Eq. 2.11, as shown in Appendix C:

$$\frac{\partial^2 p_D}{\partial t_D^2} = \frac{1}{2t_D^2}\left(\frac{r_D^2}{4t_D} - 1\right)\exp\left(-\frac{r_D^2}{4t_D}\right) \tag{2.19}$$

or

$$p_D'' = \frac{p_D'}{t_D}\left(\frac{r_D^2}{4t_D} - 1\right) \tag{2.20}$$

In view of the discussion in previous sections regarding the approximation of the finite wellbore solution by the line source solution, it is estimated that equations 2.19 and 2.20 are valid at all $r_D \geq 50$ when $t_D \geq 250$, and at $r_D = 1$ when $t_D \geq 10^3$.

The second derivative of the dimensionless pressure at the well, i.e., $r_D = 1$, is

$$p''_{Dw} = \frac{1}{2t_D^2}\left(\frac{1}{4t_D} - 1\right)\exp\left(-\frac{1}{4t_D}\right) \qquad (2.21)$$

for $t_D \geq 10^3$. For such values of t_D the exponential term is very close to unity, while $\left(\frac{1}{4t_D} - 1\right) \simeq -1$, therefore, Eq. 2.21 can be approximated by

$$p''_{Dw} = -\frac{1}{2t_D^2} \qquad (2.22)$$

or

$$|p''_{Dw}| = \frac{1}{2t_D^2} \qquad (2.23)$$

A log-log graph of $|p''_{Dw}|$ versus t_D would yield a straight line:

$$\log |p''_{Dw}| = -2 \log t_D - 0.30103 \qquad (2.24)$$

with a slope of -2. This is evident in Fig. 2.6, where the straight line is obtained for $t_D > 10^2$ (rather than $t_D > 10^3$ as indicated earlier).

In terms of real parameters, the second derivative of pressure with time is given by Eq. 7 of Appendix C:

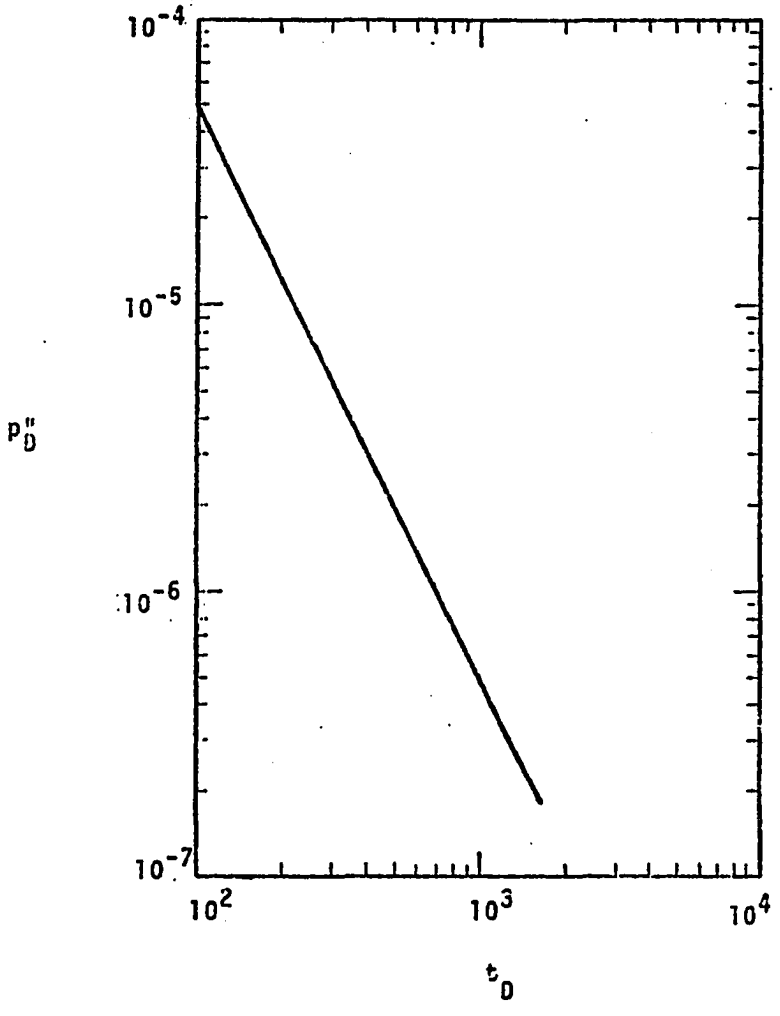

FIGURE 2.6: A log-log plot of $|p''_D|$ vs t_D for a line source well in an infinite medium, $t_D \geq 100$.

$$\frac{\partial^2 p}{\partial t^2} = p'' = -\frac{1}{t^2}\left(\frac{q\mu}{4\pi kh}\right)\left(\frac{\phi\mu c r^2}{4kt} - 1\right)\exp\left(-\frac{\phi\mu c r^2}{4kt}\right) \qquad (2.25)$$

which, applied to well points, i.e., $r = r_w$, for $\frac{kt}{\phi\mu c r_w^2} > 10^3$ yields

$$p''_w = \frac{1}{t^2}\left(\frac{q\mu}{4\pi kh}\right) \qquad (2.26)$$

or

$$\log p''_w = -2 \log t + \log \frac{q\mu}{4\pi kh} \qquad (2.27)$$

The similarity of Eq. 2.24 (in dimensionless parameters) with Eq. 2.27 (in real parameters) allows us to use type-curve matching techniques to determine the kh and ϕc products.

From comparison of equations 2.24 and 2.27 for p''_D with equations 2.15 and 2.18 for p'_D, it is evident that the second derivative yields no additional information over and above that obtainable from the first derivative. Furthermore, p''_D requires more computational time. In this study, however, p''_D has been systematically computed and tabulated solely for the sake of completeness.

2.4 Mathematical Basis for Well Testing (Infinite Reservoir)

Fundamentally, a change in well producing rate from a certain value constitutes a "well test." A change in well rate causes a perturbation in the reservoir system. The transient response of the reservoir to such a perturbation can be measured and used to determine various reservoir

parameters such as the kh and ϕc products, skin at the well, the number and types of boundaries, among others.

There are two kinds of well tests which are commonly used for this purpose: (1) a drawdown test consists in producing a well at constant rate and resulting pressures are measured at the well or at some other observation well, and (2) a buildup test is obtained by shutting in a producing well and measuring pressures at the well until it builds up to the average or static reservoir pressure. In the following, the concept of skin is briefly discussed.

2.4.1 Skin Factor

Van Everdingen and Hurst[30] pointed out that flow restrictions near a well cause an additional pressure drop. This can be thought of an an "infinitesimal skin" on the surface of the sand face at a well. The flowing well pressure p_{wf} in the presence of a skin s can be related to the dimensionless pressure as follows:

$$\frac{2\pi kh}{q\mu}(p_i - p_{wf}) = p_D(r_D, t_D) + s \qquad (2.28)$$

where the dimensionless skin factor s is given by

$$s = \frac{2\pi kh}{q\mu}\Delta p_{skin} \qquad (2.29)$$

where Δp is the additional pressure drop due to skin at the well.

2.4.2 Drawdown Well Test Analysis

The dimensionless well pressure after a flowing time t_D for a well in an infinite reservoir is given by Eq. 2.10

for $r_D = 1$:

$$p_D(1,t_D) = p_{Dw} = \frac{1}{2}[\ln t_D + 0.80907] \qquad (2.30)$$

for $t_D > 70$ which is always satisfied under normal well testing conditions. Eq. 2.30 implies that a plot of p_{Dw} versus logarithm of t_D would yield a straight line of slope 1.1513 ($= \frac{1}{2} \times 2.3026$) per log cycle as shown in Fig. 2.7.

The flowing well pressure p_{wf} in presence of skin s is obtained by substituting Eq. 2.30 into Eq. 2.28:

$$\frac{2\pi kh}{q\mu}(p_i - p_{wf}) = \frac{1}{2}[\ln t_D + 0.80907 + 2s] \qquad (2.31)$$

which in oil field units yields:

$$\frac{kh}{141.3\ q\mu B}(p_i - p_{wf}) = \frac{1}{2}\left[\ln \frac{0.000264\ kt}{\phi\mu c r_w^2} + 0.80907 + 2s\right] \qquad (2.32)$$

or

$$p_{wf} = p_i - \frac{162.6\ q\mu B}{kh}\left[\log t + \log \frac{k}{\phi\mu c r_w^2} - 3.23 + 0.878s\right] \qquad (2.33)$$

Thus a graph of p_{wf} versus actual flowing time produces a straight line on a semilog graph of slope m (absolute value):

$$m = \frac{162.6\ q\mu B}{kh} \qquad (2.34)$$

from which the kh product is determined as

$$kh = \frac{162.6\ q\mu B}{m} \qquad (2.35)$$

Eq. 2.33 can be further used to determine the skin s as shown by Ramey, et al.:[19]

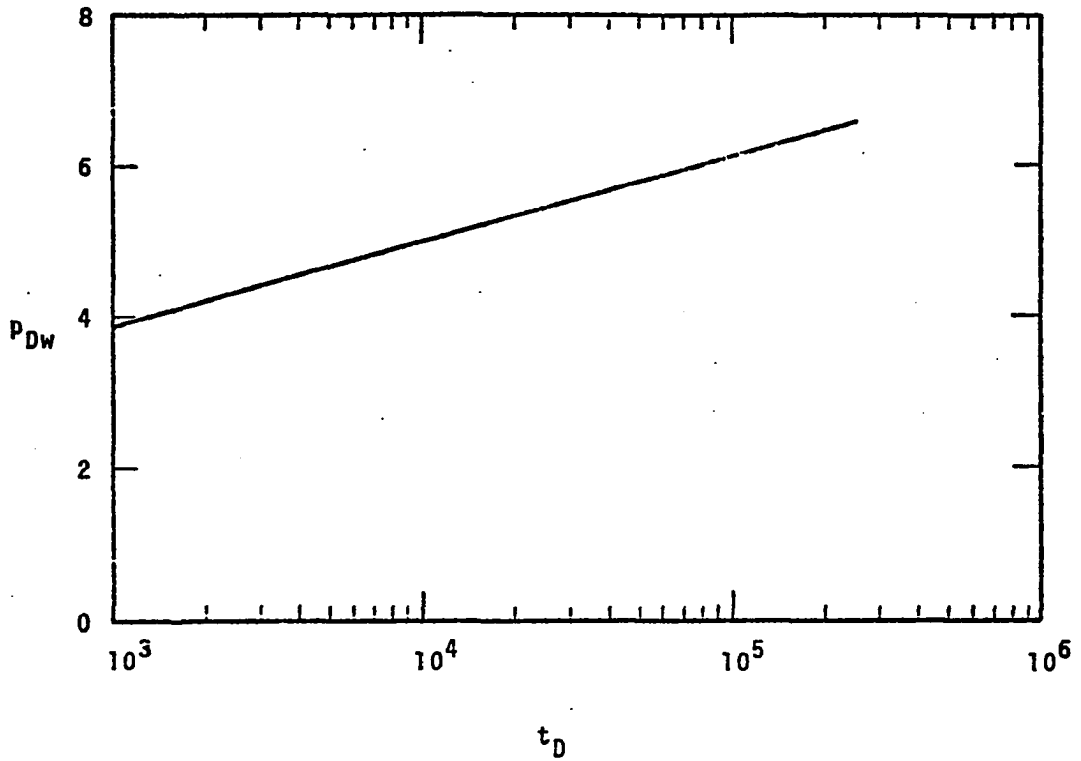

FIGURE 2.7: Dimensionless Well Pressure vs Dimensionless Time for a Well in an Infinite Reservoir.

$$s = 1.1513\left[\frac{p_i - p_{1hr}}{m} - \log \frac{k}{\phi\mu c r_w^2} + 3.23\right] \qquad (2.36)$$

where p_{1hr} is the value of p_{wf} at one hour flowing time and is estimated by extrapolation of the straight line obtained on the semilog graph. The pressure drop across the skin at the sand face is given by

$$\Delta p_{skin} = 0.87(m)s \qquad (2.37)$$

This completes the discussion on commonly used equations for interpretation of well pressure data. We next consider the equations employing the first derivative of flowing well pressure.

2.4.2.1 p'_{Dw}-Function

The time rate of change of dimensionless flowing well pressure for a well in an infinite reservoir is given by Eq. 2.15

$$\log p'_{Dw} = - \log t_D - 0.30103$$

for $t_D > 100$. In oilfield units, this equation yields the following from Eq. 2.18:

$$\log |p'_{wf}| = - \log t + \log\left(\frac{70.6\ q\mu B}{kh}\right) \qquad (2.38)$$

where p'_{wf} is in psi/hr and t in hours. Thus a plot of measured p'_{wf} versus time on a log-log graph can be overlaid on the type curve of Fig. 2.5 and a match point located. The value of dimensionless p'_{Dw} and t_D is read corresponding to measured p'_{wf} and t for the match point. The interpretive

equations to determine kh and ϕc products are respectively derived from Eq. B.16 and Eq. B.14 of Appendix B in oil field units:

$$kh = 141.3\ q\mu B\left(\frac{p'_{Dw}}{|p'_{wf}|}\right)\left(\frac{t_D}{t}\right) \qquad (2.39)$$

and

$$\phi c = \frac{qB}{26.856\ r_w^2 h}\left(\frac{p'_{Dw}}{|p'_{wf}|}\right) \qquad (2.40)$$

These two parameters are of significant importance since they provide an additional measure of the capacity of the flow system (kh), which is needed to predict deliverability and the reservoir volume parameters (ϕc), which is used to predict reserves in place.

Equation 2.38 provides an additional method to calculate the kh product. For flowing time of one hour, Eq. 2.38 becomes:

$$\log |p'_{wf}|_{1hr} = \log\left(\frac{70.6\ q\mu B}{kh}\right)$$

or

$$kh = \frac{70.6\ q\mu B}{|p'_{wf}|_{1hr}} \qquad (2.41)$$

where $|p'_{wf}|_{1hr}$ is the time rate change of well pressure at one hour flowing time.

2.4.2.2 p''_{Dw}-Function

In view of Eq. 2.24 and Eq. 2.27, one can plot the second derivative of the flowing well pressure p''_{wf} versus

time on a log-log graph which can be overlaid on the type-curve of Fig. 2.6 to determine both the kh and ϕc products from equations presented in Appendix C. The kh product is derived from Eq. C.16:

$$kh = 141.3\ q\mu B\left(\frac{|p''_{Dw}|}{p''_{wf}}\right)\left(\frac{t_D}{t}\right)^2 \tag{2.42}$$

while the ϕc product is obtained from Eq. C.11:

$$|p''_{Dw}| = \frac{t}{t_D}\left(\frac{26.856\ r_w^2 h\phi c}{qB}\right)p''_{wf} \tag{2.43}$$

or

$$\phi c = \frac{qB}{26.856\ r_w^2 h}\left(\frac{|p''_{Dw}|}{p''_{wf}}\right)\left(\frac{t_D}{t}\right) \tag{2.44}$$

where p''_{wf} = psi/hr^2, r_w = ft, h = ft, c = psi^{-1}, q = STB/D, t = hrs.

Note that the skin factor s does not occur in p'_{wf} and p''_{wf} versus time equations. This is normal since s is constant for a given well for the duration of the test and therefore time rate of change of s is zero.

2.4.3 Buildup Well Test Analysis

The dimensionless well pressure after a shut-in time Δt_D is obtained by employing superposition in time, which is discussed in detail in Chapter 4,

$$\frac{kh}{141.3\ q\mu B}(p_i - p_{ws}) = [p_D(r_{Dw}, t_D+\Delta t_D) + s] - [p_D(r_{Dw}, \Delta t_D) + s]$$

$$p_{Ds} = p_{Dw}(t_D + \Delta t_D) - p_{Dw}(\Delta t_D) \tag{2.45}$$

This equation is generally used to study the characteristics of buildup graphs and to derive interpretive equations. The three most widely used plotting techniques in pressure buildup analysis are: Horner graph,[6] Miller-Dyes-Hutchinson graph,[7] and Muskat graph.[3] Ramey and Cobb,[38] and Matthews and Russel[23] have presented in detail the basis for these graphs, and therefore, they will not be discussed here.

2.4.3.1 p'_{Ds}-Function

The time rate of change of the dimensionless buildup well pressure is obtained by differentiating Eq. 2.45 with respect to dimensionless shut-in time Δt_D:

$$p'_{Ds} = p'_{Dw}(t_D + \Delta t_D) - p'_{Dw}(\Delta t_D) \qquad (2.46)$$

where p'_{Dw} is calculated from Eq. 2.13 for a well in an infinite reservoir. Figure 2.8 presents p'_{Ds} as a function of dimensionless shut-in time Δt_D for various producing times. The behavior of p'_{Ds} on Fig. 2.7 is best understood by considering two time domains for interpretation purposes:

(1) $\Delta t_D << t_D$: When shut-in time is much less than the producing time, Eq. 2.46 yields:

$$\log |p'_{Ds}| = - \log \Delta t_D - 0.30103 \qquad (2.47)$$

This is shown in Appendix D. Thus a plot of $|p'_{Ds}|$ versus Δt_D on a log-log graph yields a straight line of slope -1. Such a characteristic is seen for $t_D = 10^4$ up to $\Delta t_D = 5 \times 10^2$, and for $t_D = 10^5$ up to $\Delta t_D = 5 \times 10^3$. Therefore, the condition of $\Delta t_D << t_D$ seems to be satisfied from Fig. 2.7

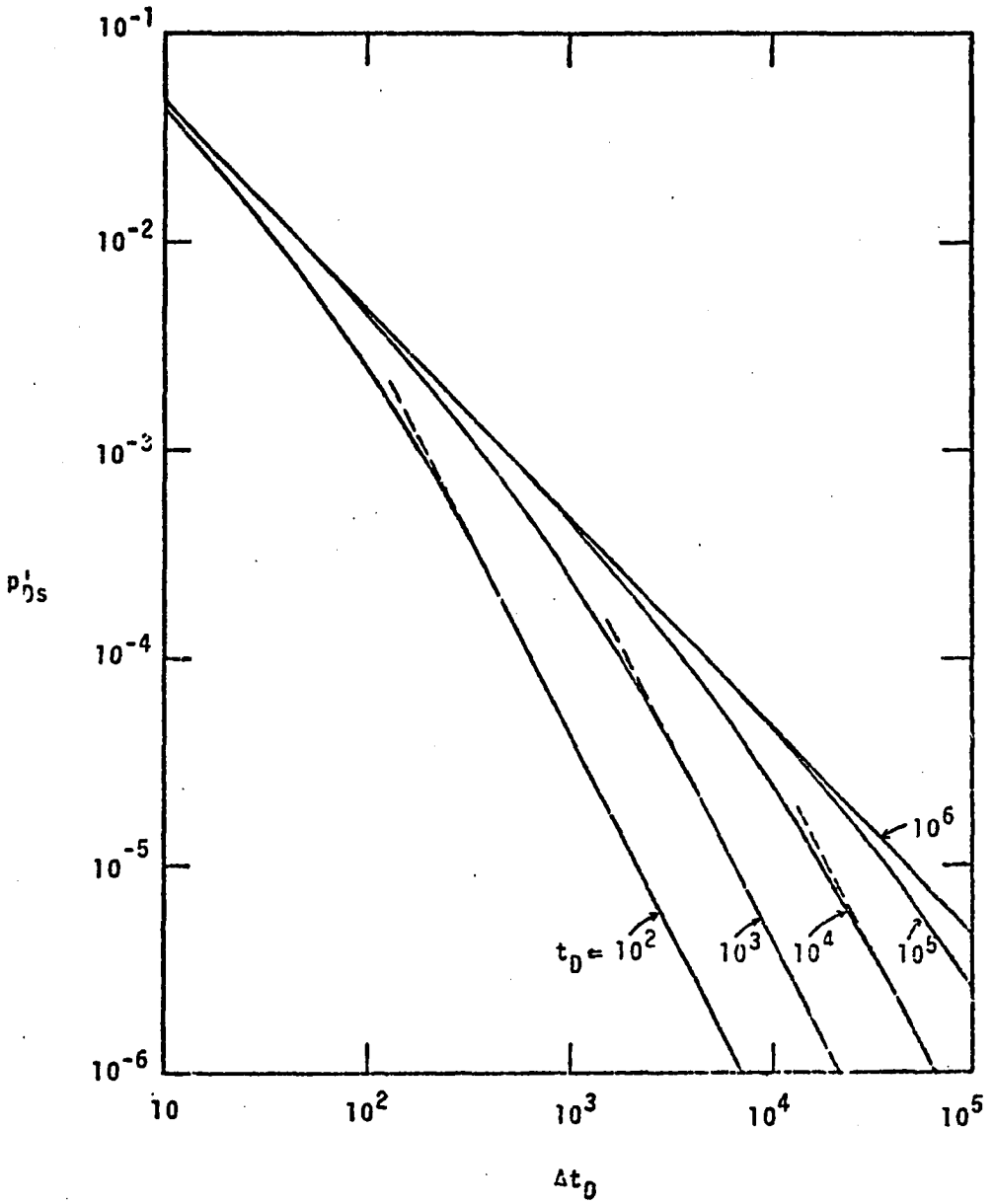

FIGURE 2.8: Time Rate of Change of Dimensionless Well Shut-in Pressure vs Dimensionless Shut-in Time for a Well in an Infinite Reservoir.

when $\Delta t_D \leq 0.05\ t_D$. In terms of real parameters (oilfield units) Eq. 2.47 becomes:

$$\log p'_{ws} = -\log \Delta t + \log \frac{70.6\ q\mu B}{kh} \tag{2.48}$$

Hence, a plot of the time rate of change of well shut-in pressure, p'_{ws}, versus shut-in time on a log-log graph yields a straight line of slope -1. If this plot of field data points is overlaid on the type-curve of Fig. 2.7, a match point would give the kh and ϕc products using the following equations derived in Appendix D:

$$kh = 141.3\ q\mu B\left(\frac{|p'_{Ds}|}{p'_{ws}}\right)\left(\frac{\Delta t_D}{\Delta t}\right) \tag{2.49}$$

$$\phi c = \frac{qB}{26.856\ r_w^2 h}\left(\frac{|p'_{Ds}|}{p'_{ws}}\right) \tag{2.50}$$

For a shut-in time of one hour, Eq. 2.48 becomes

$$\log(p'_{ws})_{1hr} = \log \frac{70.6\ q\mu B}{kh}$$

or

$$kh = \frac{70.6\ q\mu B}{(p'_{ws})_{1hr}} \tag{2.51}$$

where $(p'_{ws})_{1hr}$ is the time rate of change of shut-in well pressure at one hour.

(2) $\Delta t_D >> t_D$: When shut-in time is much longer than producing time, Eq. 2.46 assumes the following form, as shown in Appendix D.

$$\log |p'_{Ds}| = -2 \log \Delta t_D + \log(t_D/2) \tag{2.52}$$

Therefore, a straight line of slope -2 is obtained on a log-log graph of $|p'_{Ds}|$ vs. Δt_D. Such a straight line is shown in Fig. 2.8 for $t_D = 10^2$ when $\Delta t_D > 5 \times 10^2$, and $t_D = 10^3$ when $\Delta t_D > 5 \times 10^3$. Therefore, the condition of $\Delta t_D >> t_D$ is satisfied when $\Delta t_D \geq 5t_D$. In oilfield units, Eq. 2.52 becomes:

$$\log p'_{ws} = -2 \log \Delta t + \log t + \log \frac{70.6\ q\mu B}{kh} \qquad (2.53)$$

If the straight line of slope -2 is overlaid on the type-curve of Fig. 2.8, kh and ϕc products are then determined from Eqs. 2.49 and 2.50, respectively.

2.4.3.2 p''_{Ds}-Function

The second derivative of the dimensionless shut-in well pressure is given by differentiating Eq. 2.45 twice with respect to dimensionless shut-in time Δt_D:

$$p''_{Ds} = p''_{Dw}(t_D + \Delta t_D) - p''_{Dw}(\Delta t_D) \qquad (2.54)$$

where p''_{Dw} is computed from Eq. 2.21 for a well in an infinite reservoir. A plot of p''_{Ds} versus Δt_D on a log-log graph for various producing times is shown in Fig. 2.9. p''_{Ds} behaves differently in two separate time domaines as presented in Appendix E.

(1) $\Delta t_D << t_D$: When dimensionless shut-in time is much smaller than dimensionless producing time, Eq. 2.54 yields:

$$\log |p''_{Ds}| = -2 \log \Delta t_D - 0.30103 \qquad (2.55)$$

or in oilfield units

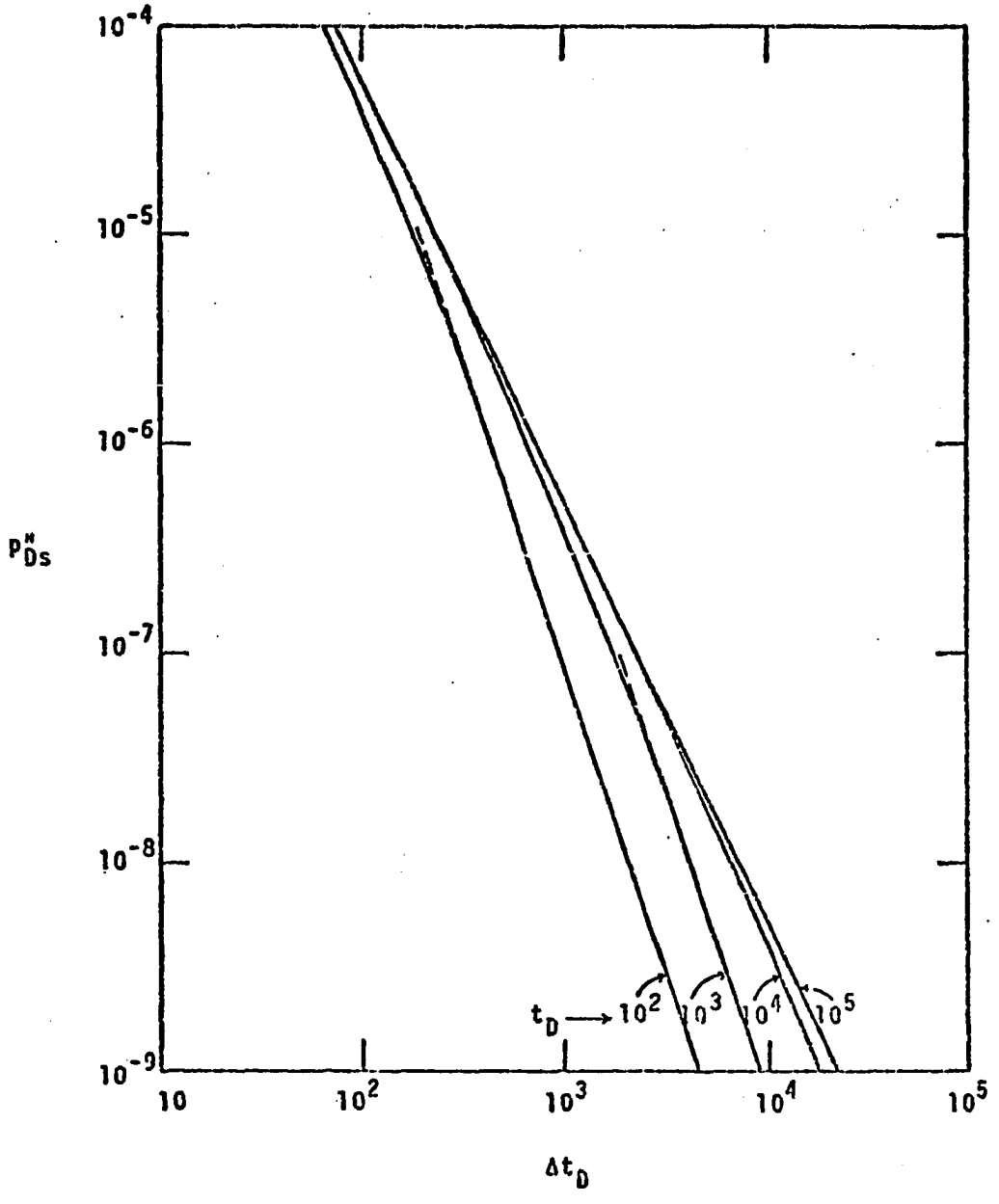

FIGURE 2.9: Second derivative of dimensionless well shut-in pressure vs shut-in time for a well in an infinite reservoir.

$$\log |p''_{ws}| = -2 \log \Delta t + \log \frac{70.6\ q\mu B}{kh} \qquad (2.56)$$

which results in similar interpretive equations as obtained for p'_{ws}. These are presented in Appendix E.

(2) $\Delta t_D >> t_D$: When dimensionless shut-in time is much longer than dimensionless producing time, Eq. 2.54 yields:

$$\log |p''_{Ds}| = -3 \log \Delta t_D + \log t_D \qquad (2.57)$$

or in oilfield units

$$\log |p''_{ws}| = -3 \log \Delta t_D + \log t + \log \frac{70.6\ q\mu B}{kh} \qquad (2.58)$$

which also results in similar interpretive equations (presented in Appendix E) as for p'_{ws}. Note, however, that a plot of p''_{ws} versus Δt on a log-log graph yields a straight line of slope -3.

In summary, this chapter has presented the behavior of the continuous line source solution and its first two derivatives with respect to time. A range of time and radii, under which the line source solution becomes a good approximation to a finite radius well bore, has been established. It is evident that the second derivative yields no additional information over that obtainable from the first derivative. Therefore, for the sake of practicallity, the analysis of the second derivative will not be pursued here, as it requires excessive computer plotting time. However, its values are systematically tabulated along with values of the first derivative.

Finally, this chapter has presented the mathematical basis for well testing. It is observed that analysis of p'_{wf} and p'_{ws} lead to new interpretive techniques which are simpler and more useful than currently used techniques based on the pressure function itself.

CHAPTER III

GENERATION OF BOUNDARY CONDITIONS

In a multiple well reservoir, the pressure at a point is simply the sum of pressure contributions due to all the wells at that point. More importantly: the pressure derivative at a point is also the sum of pressure derivatives due to all the wells. Consequently, we can put wells at certain locations to generate a desired boundary condition. This is known as the principle of superposition, which is probably the most powerful tool available in describing the single phase flow of a compressible fluid in any type of ideal reservoir. The so called "image" well method is simply another application of superposition. Muskat[3] used this principle to simulate the effect of no-flow and flow boundaries under steady state flow conditions. Horner[6] applied this method to study pressure buildup behavior for a well close to a sealing fault boundary under transient flow conditions.

3.1 Principle of Superposition

A common mathematical definition of superposition is that any sum of solutions to a linear partial differential

equation is also a solution. To understand the physical aspect of the principle of superposition and its application for simulating the effect of boundaries, such as sealing faults, consider an infinite porous medium which contains two wells (A and B) "$2b_x$" units of length apart. Let d_A and d_B be, respectively, the distances from well A and well B to a point F(x,y) within the reservoir, as shown in Fig. 3.1.

The classic approach to derive the pressure at point F would be to write the diffusivity equation, define two inner boundary conditions to include production of both wells, and define the initial and outer boundary conditions. But the principle of superposition offers a much simpler approach. The pressure at point F is simply the sum of the pressure drop caused by well A at a distance d_A and the pressure drop caused by Well B at a distance d_B. Thus we can use Eq. 2.5 to write the pressure p at point F(x,y) of Fig. 3.1(a):

$$\frac{2\pi kh}{q\mu}[p_i - p] = p_D(d_{AD},t_D) + p_D(d_{BD},t_D) \qquad (3.1)$$

or

$$p = p_i - \frac{q\mu}{2\pi kh}[p_D(d_{AD},t_D) + p_D(d_{BD},t_D)] \qquad (3.2)$$

where: $d_{AD} = d_A/r_w$

$d_{BD} = d_B/r_w$

Let now the point F(x,y) lie on the perpendicular bisector of the line segment connecting the two wells (Fig. 3.1(b)). Thus d_A and d_B will be equal, and the dimensionless

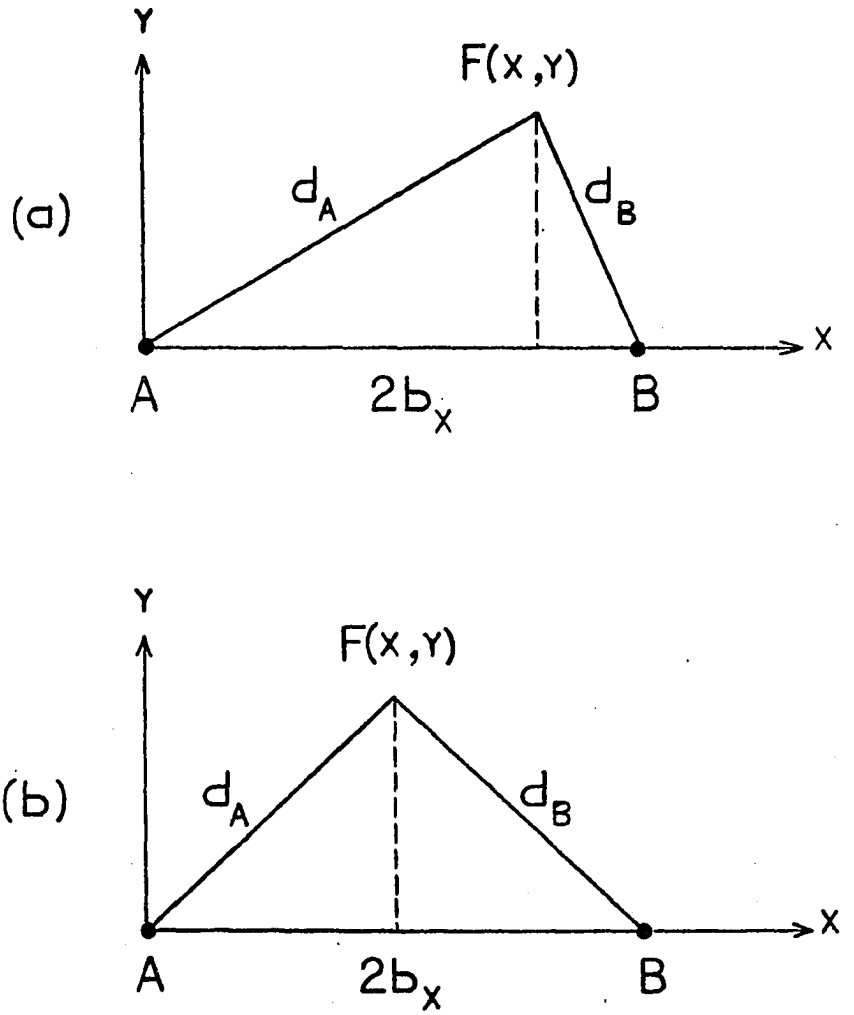

FIGURE 3.1: Pressure at any point in the reservoir caused by two wells producing at a constant rate well.

pressures at each well will be equal. Consequently, the pressure gradient in any direction through the point F caused by each well acting alone will be exactly the same, but opposite in sign. Thus the net pressure gradient along the perpendicular bisector will be zero and fluid connot cross the line. This line is generally referred to as a "no-flow boundary" which could be a sealing fault. Thus, the pressure distribution for one well producing at constant rate q located at a distance b_x from a linear sealing fault is similar to the pressure distribution for two wells producing at constant rate q each, both wells starting to produce at time zero, and spaced $2b_x$ units of length apart. This is shown in Fig. 3.2.

3.2 Well Between Two Perpendicular Sealing Faults

Consider a well between two linear sealing faults, or no-flow boundaries, intersecting at a right angle in an otherwise infinite system. Let the well be at a distance b_x from one fault and b_y from the other perpendicular fault as shown in Fig. 3.3(a). Then, locate two image wells at the same distances b_x and b_y on the other side of the boundaries as shown in Fig. 3.3(b). Finally the two image wells are also imaged giving a common third image well. Therefore, three image wells are required to simulate the pressure behavior of a real well between two perpendicular sealing faults.

a) REAL SYSTEM

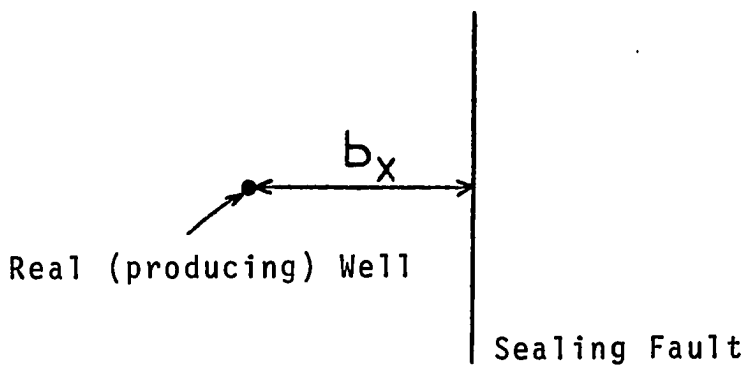

b) IMAGE SYSTEM

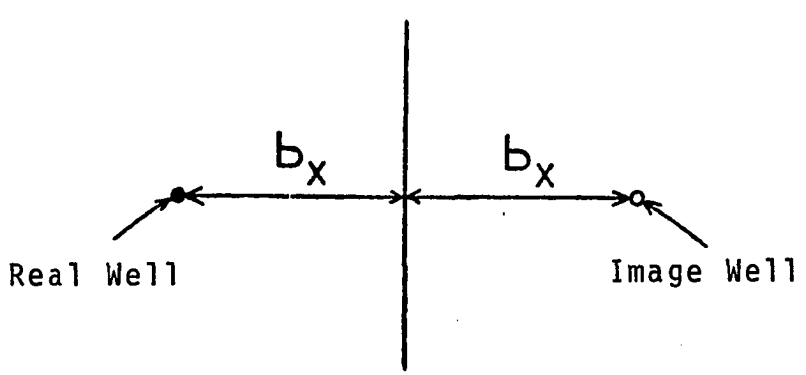

FIGURE 3.2: Generation of a linear sealing fault, or no-flow boundary.

a) REAL SYSTEM

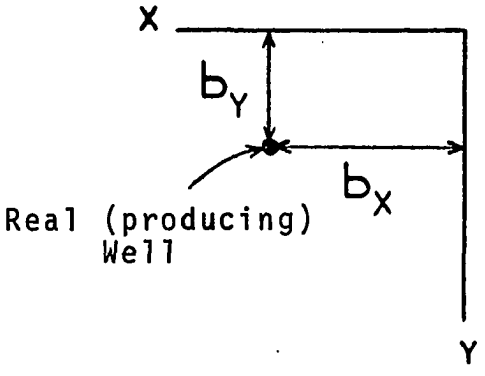

b) IMAGE SYSTEM

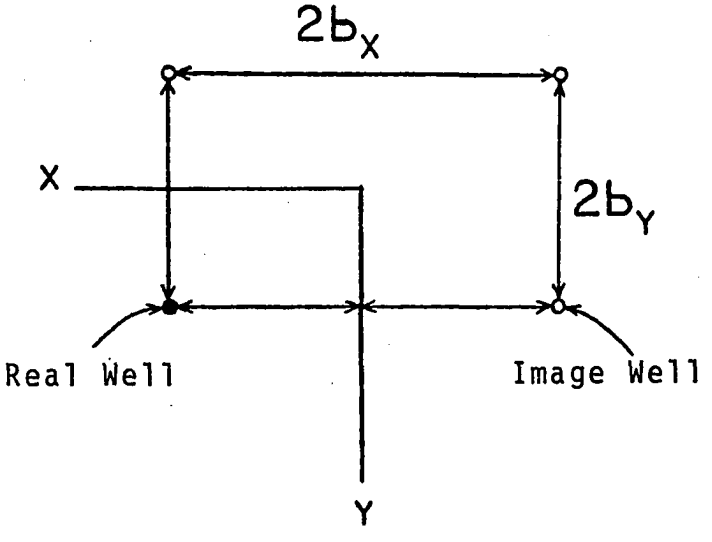

FIGURE 3.3: Generation of two perpendicular sealing faults.

3.2.1 Distance to Image Wells

The distances from the real well to the three image wells are given by:

$$r_x = 2b_x \tag{3.3}$$

$$r_y = 2b_y \tag{3.4}$$

$$r_{xy} = 2\sqrt{b_x^2 + b_y^2} \tag{3.5}$$

where r_x = distance to the image well across fault x

r_y = distance to the image well across fault y

r_{xy} = distance to the third image fault.

If the dimensionless distance is defined as a multiple of b_x, then Eqs. 3.3, 3.4 and 3.5 respectively become:

$$r_{Dx} = r_x/b_x = 1 \tag{3.6}$$

$$r_{Dy} = r_y/b_x = 2y_D \tag{3.7}$$

$$r_{Dxy} = r_{xy}/b_x = 2b_x\sqrt{1 + y_D^2} \tag{3.8}$$

where

$$y_D = b_y/b_x \tag{3.9}$$

Computer programs, which require the distance b_x and seven values of dimensionless integral ratio y_D: 1, 1/2, 1/4, 1/8, 1/16, 1/32 and 1/64, were developed to tabulate p_D, p_D' and p_D'', and plot only type-curves of p_D'. This approach is systematically applied in generating the three-fault system and rectangular reservoirs, which are discussed in later sections.

3.2.2 Dimensionless Time

For reasons to be discussed in the following chapter, the dimensionless time defined by Eq. 2.4 can be modified such that the wellbore radius (r_w) is replaced by a distance of interest.

Let t_{DA}, t_{Dby}, and t_{Dbb} be dimensionless times based respectively upon b_x, b_y and the product $b_x b_y$.

$$t_{DA} = \frac{kt}{\phi\mu c b_x^2} = t_D \left(\frac{r_w}{b_x}\right)^2 \tag{3.10}$$

$$t_{Dby} = \frac{kt}{\phi\mu c b_y^2} = t_{DA} \left(\frac{b_x}{b_y}\right)^2 \tag{3.11}$$

$$t_{Dbb} = \frac{kt}{\phi\mu c (b_x b_y)} = t_{DA} \frac{b_x^2}{(b_x b_y)} \tag{3.12}$$

3.2.3 Pressure Behavior at a Point

The dimensionless pressure behavior at a point between the two sealing faults intersecting at a right angle is given by the sum of pressure contributions due to the real well and the three image wells:

$$p_D(r_D, t_D) = p_{DR}(r_{DR}, t_{DA}) + \sum_{n=1}^{3} p_{DI}[r_{DI}(n), t_{DA}] \tag{3.13}$$

or

$$p_D(r_D, t_{DA}) = -\frac{1}{2}\left\{E_i\left[-\frac{(r/b_x)^2}{4t_{DA}}\right] + Ei\left[-\frac{1}{t_{DA}}\right] + Ei\left[-\frac{(b_y/b_x)^2}{t_{DA}}\right] + Ei\left[-\frac{(b_x^2 + b_y^2)/b_x^2}{t_{DA}}\right]\right\} \tag{3.13a}$$

The time rate of change of dimensionless pressure is obtained by direct differentiation of Eq. 3.13:

$$p'_D(r_D,t_{DA}) = p'_{DR}(r_{DR},t_{DA}) + \sum_{n=1}^{3} p'_{DI}[r_{DI}(n),t_{DA}] \quad (3.14)$$

or

$$p'_D(r_D,t_{DA}) = \frac{1}{2t_{DA}}\left\{\exp\left[-\frac{(r/b_x)^2}{4t_{DA}}\right] + \exp\left[-\frac{1}{t_{DA}}\right] + \exp\left[-\frac{(b_y/b_x)^2}{t_{DA}}\right] + \exp\left[-\frac{(b_x^2 + b_y^2)/b_x^2}{t_{DA}}\right]\right\} \quad (3.14a)$$

where

r_{DR} = dimensionless distance from the real well, r/b_x.

r_{DI} = dimensionless distance from the image well, r_I/b_x.

In the above equations p_{DR} and p_{DI} are calculated by using Eq. 2.7, and p'_{DR} and p'_{DI} by Eq. 2.11.

3.3 Well Between Three Perpendicular Sealing Faults

In theory, one needs an infinite number of image wells to simulate correctly the pressure behavior of a well located in a multiple sealing faults system. But, for most practical purposes, only a finite number of wells need be considered. This finite number should, however, be large enough such that the pressure contribution due to the last series of image wells is negligible.

Consider a well producing at a constant rate located between three sealing faults intersecting at right angles.

This system can be simulated by two (infinite) lines of image wells. The first line is generated as if there were only two parallel faults (Fig. 3.4). This author[26] studied this case and generated the line of image wells as follows: (1) the first pair of image wells is obtained by directly imaging the real well on each boundary, (2) successive pairs of image wells are generated by imaging the wells of the previous pair, and (3) the grid of images is expanded until the pressure contribution due to the last series of image wells is negligible at a point of interest. The second line of image wells is obtained by simply imaging the first line on the third sealing fault, which intersects the two parallel faults at right angles. This is shown in Fig. 3.5.

3.3.1 Distance to Image Wells

Assuming the real well to be at the origin in Fig. 3.4(b), the distance to image wells of the first line can be calculated as follows:

$$\begin{aligned} r_{xe} &= 2nW_x \\ r_{xo} &= 2(n-1)W_x + 2a_x \\ r_{xop} &= 2(n-1)W_x + 2b_x \end{aligned} \tag{3.15}$$

where

n = a positive integer, 1, 2, 3, $\cdots$

b_x = distance to the nearest of the 2 parallel boundaries

a_x = distance to the other parallel boundary, $W_x - b_x$

a) REAL SYSTEM

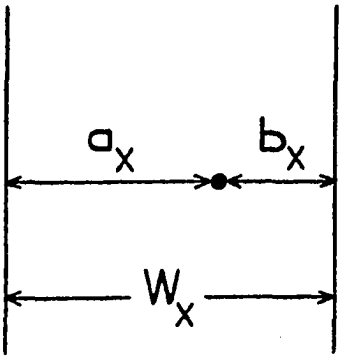

b) IMAGE SYSTEM

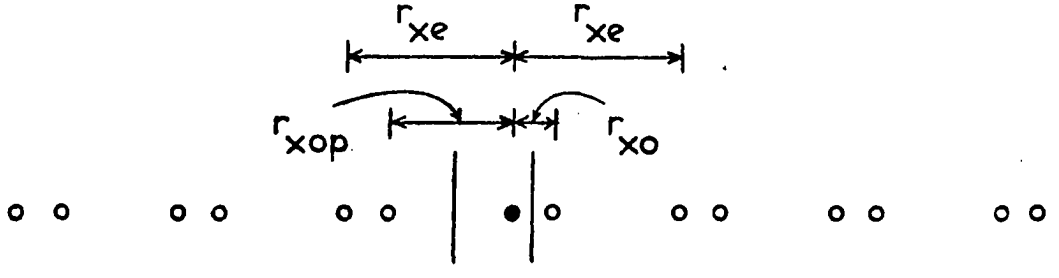

FIGURE 3.4: Generation of two parallel sealing faults.

a) REAL SYSTEM

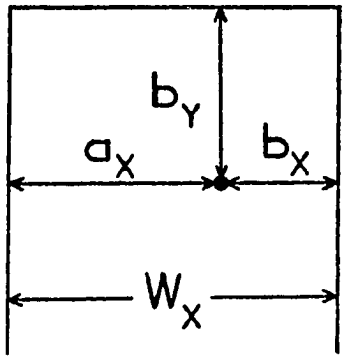

b) IMAGE SYSTEM

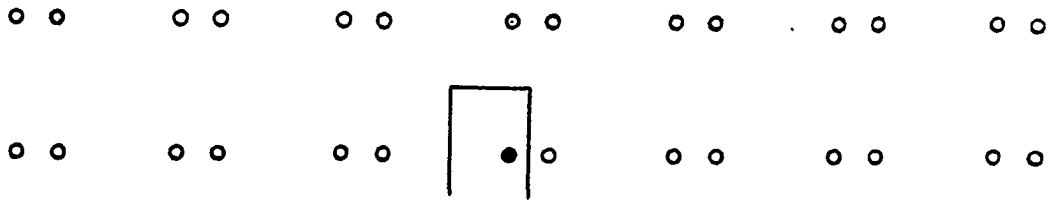

FIGURE 3.5: Generation of three perpendicular sealing faults.

W_x = distance between the two parallel boundaries, on the x-axis

r_{xe} = distance to image wells when n is even

r_{xo} = distance to image wells when n is odd

r_{xop} = distance to image wells when n is odd on the other side of the strip

The second line shown in Fig. 3.5(b) has (N + 1) image wells and the distance can be calculated using the following set of equations:

$$\begin{aligned} r_{Iy} &= 2b_y \\ r_{Ixe} &= (r_{Iy}^2 + r_{xe}^2)^{0.5} \\ r_{Ixo} &= (r_{Iy}^2 + r_{xo}^2)^{0.5} \\ r_{Ixop} &= (r_{Iy}^2 + r_{xop}^2)^{0.5} \end{aligned} \tag{3.16}$$

where

r_{Iy} = distance to image well of real well on the y-axis

r_{Ixe}, r_{Ixo}, r_{Ixop} = distance to image wells of the second line, where the subscripts are as defined above.

b_y = distance to the third fault which intersects the two parallel boundaries at right angles.

If dimensionless distance is defined as a multiple of distance W_x, the two sets of Equations 3.15 and 3.16 would become, respectively:

$$r_{Dxe} = r_{xe}/W_x = 2n$$

$$r_{Dxo} = r_{xo}/W_x = 2(n - 1) + a_{Dx} \tag{3.17}$$

$$r_{Dxop} = r_{xop}/W_x = 2(n - 1) + b_{Dx}$$

and

$$\begin{aligned} r_{DIy} &= r_{Iy}/W_x = 2b_{Dy} \\ r_{DIxe} &= r_{Ixe}/W_x = 2W_x[b_{Dy}^2 + n^2]^{0.5} \\ r_{DIxo} &= r_{Ixo}/W_x = 2W_x[b_{Dy}^2 + ((n-1) + a_{Dx})^2]^{0.5} \\ r_{DIxop} &= r_{Ixop}/W_x = 2W_x[b_{Dy}^2 + ((n-1) + b_{Dx})^2]^{0.5} \end{aligned} \tag{3.18}$$

where

$$a_{Dx} = a_x/W_x \tag{3.19}$$

$$b_{Dx} = b_x/W_x \tag{3.20}$$

$$b_{Dy} = b_y/W_x \tag{3.21}$$

3.3.2 Dimensionless Time

The dimensionless time defined by Eq. 2.4 can be modified such that the wellbore radius (r_w) is replaced by a distance of interest such as W_x, b_x, b_y and the product $b_x b_y$.

$$t_{DA} = \frac{kt}{\phi\mu c W_x^2} = t_D\left(\frac{r_w}{W_x}\right)^2 \tag{3.22}$$

$$t_{Db_x} = \frac{kt}{\phi\mu c b_x^2} = t_{DA}\left(\frac{W_x}{b_x}\right)^2 \tag{3.23}$$

$$t_{Db_y} = \frac{kt}{\phi\mu c b_y^2} = t_{DA}\left(\frac{W_x}{b_y}\right)^2 \tag{3.24}$$

$$t_{Dbb} = \frac{kt}{\phi\mu c b_x b_y} = t_{DA}\left(\frac{W_x^2}{b_x b_y}\right) \tag{3.25}$$

3.3.3 Pressure Behavior at a Point

The pressure contributions due to the real well and the two infinite lines of image wells at any point inside a three-perpendicular-sealing-fault system can be expressed by the following equation:

$$\begin{aligned} p_D(r_D,t_{DA}) = &- \frac{1}{2}\{Ei[-r_{DR}^2/4t_{DA}] + Ei[-b_{Dy}^2/t_{DA}]\} \\ &- \sum_{n=2k}^{\infty}\{Ei[-n^2/t_{DA}] + Ei[-W_x^2(b_{Dy}^2 + n^2)/t_{DA}]\} \\ &- \frac{1}{2}\sum_{n=2k-1}^{\infty}\{Ei[-[2(n-1) + a_{Dx}]^2/4t_{DA}] \\ &\quad + Ei[-W_x^2[b_{Dy}^2 + ((n-1) + a_{Dx})^2]/t_{DA}] \\ &\quad + Ei[-[2(n-1) + b_{Dx}]^2/4t_{DA}] \\ &\quad + Ei[-W_x^2[b_{Dy}^2 + ((n-1) + b_{Dx})^2]/t_{DA}]\} \end{aligned} \tag{3.26}$$

where $k = 1,2,3,\cdots$.

A similar expression for the time rate of change of dimensionless pressure can be written by simply differentiating Eq. 3.26 with respect to t_{DA}, or:

$$\begin{aligned} p_D'(r_D,t_{DA}) = &\frac{1}{2t_{DA}}\{exp[-r_{DR}^2/4t_{DA}] + exp[-b_{Dy}^2/t_{DA}]\} \\ &+ \frac{1}{t_{DA}}\sum_{n=2k}^{\infty}\{exp[-n^2/t_{DA}] + exp[-W_x^2(b_{Dy}^2 + n^2)/t_{DA}]\} \\ &+ \frac{1}{2t_{DA}}\sum_{n=2k-1}^{\infty}\{exp[-[2(n-1) + a_{Dx}]^2/4t_{DA}] \end{aligned}$$

$$+ \exp[-W_x^2[b_{Dy}^2 + ((n-1) + a_{Dx})^2]/t_{DA}]$$

$$+ \exp[-[2(n-1) + b_{DX}]^2/4t_{DA}]$$

$$+ \exp[-W_x^2[b_{Dy}^2 + ((n-1) + b_{Dx}]^2/t_{DA}]\} \qquad (3.27)$$

p_{DR} and p_{DI} are, of course, calculated by using Eq. 2.7.

3.4 Well Inside a Closed Rectangle

The pressure behavior in this system can be generated by an infinite number of infinite lines of image wells. However, as mentioned earlier, only a finite number of image wells need be considered. Let N be the number of image wells needed along the x-axis, and M the number needed along the y-axis, then the total number of images necessary to describe the behavior of a bounded single-well system is M x N. Note that in the case of a square, M = N. In the case of a rectangle, however, M must be increased as the ratio W_x:W_y increases from 2:1 to 16:1, where W_x and W_y are, respectively, the long and short sides of the rectangle. The number of image wells along the x-axis, N, in invariable as long as $W_x \geq W_y$.

Figure 3.6 presents part of the (infinite) image net required to generate the condition of zero flow across the outer boundary in a 2:1 rectangle.

3.4.1 Distance to Image Wells

The distance to image wells of the line coinciding with the x-axis is calculated by simply using the set of

a) REAL SYSTEM

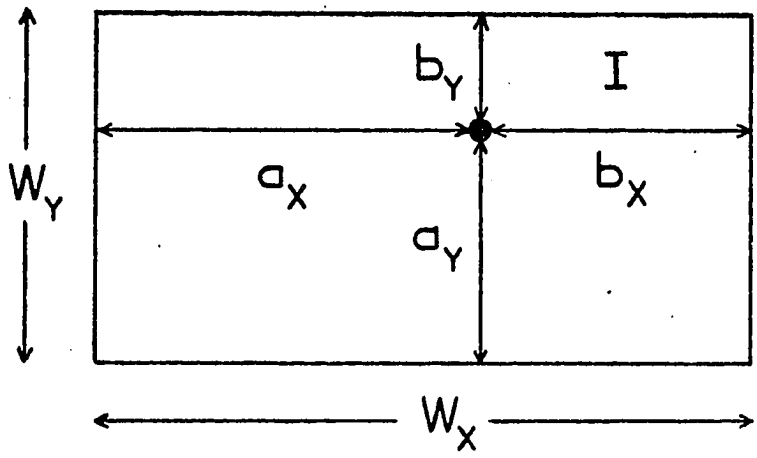

b) IMAGE SYSTEM

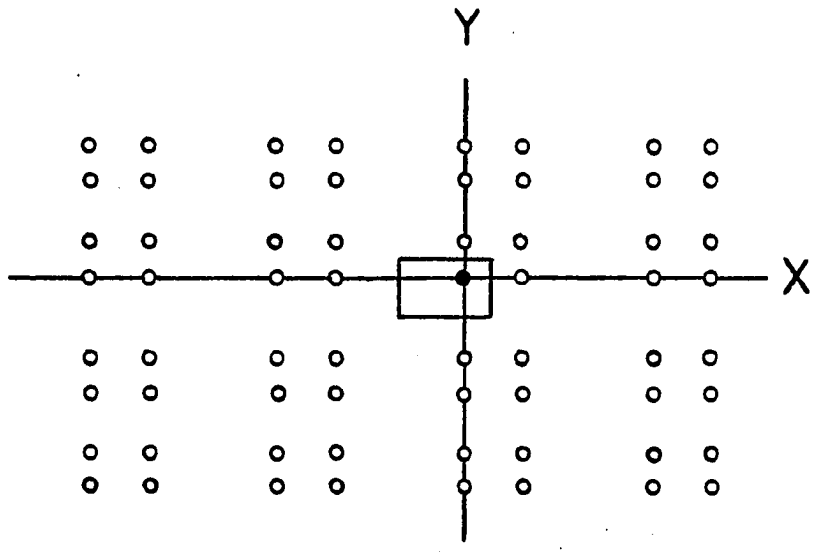

FIGURE 3.6: Rectangular drainage system showing well and part of the infinite image net.

equation 3.15. As to the distance to images of the line on the y-axis, the following equations are used:

$$\begin{aligned} r_{ye} &= 2mW_y \\ r_{yo} &= 2(m-1)W_y + 2a_y \\ r_{yop} &= 2(m-1)W_y + 2b_y \end{aligned} \tag{3.28}$$

The distance to image wells on lines parallel to the x-axis (not including images on the y-axis) are given by three sets of equations.

(1) m is even, i.e., m = 2j, where j = 1,2,3,$\cdots$

$$\begin{aligned} r_{Ee} &= (r_{ye}^2 + r_{xe}^2)^{0.5} \\ r_{Eo} &= (r_{ye}^2 + r_{xo}^2)^{0.5} \\ r_{Eop} &= (r_{ye}^2 + r_{xop}^2)^{0.5} \end{aligned} \tag{3.29}$$

(2) m is odd on the positive side of the y-axis, i.e., m = 2j - 1.

$$\begin{aligned} r_{Oe} &= (r_{yo}^2 + r_{xe}^2)^{0.5} \\ r_{Oo} &= (r_{yo}^2 + r_{xo}^2)^{0.5} \\ r_{Oop} &= (r_{yo}^2 + r_{xop}^2)^{0.5} \end{aligned} \tag{3.30}$$

(3) m is odd on the negative side of the y-axis, m = 2j -1.

$$\begin{aligned} r_{OPe} &= (r_{yop}^2 + r_{xe}^2)^{0.5} \\ r_{OPo} &= (r_{yop}^2 + r_{xo}^2)^{0.5} \\ r_{OPop} &= (r_{yop}^2 + r_{xop}^2)^{0.5} \end{aligned} \tag{3.31}$$

To obtain dimensionless distances, Eqs. 3.29, 3.30 and 3.31 can be divided by the drainage area $A = W_x \times W_y$, or:

$$\begin{aligned} r_{DEe} &= 2[m^2W_y^2 + n^2W_x^2]^{0.5}/A \\ r_{DEo} &= 2[m^2W_y^2 + ((n-1)W_x + a_x)^2]^{0.5}/A \\ r_{DEop} &= 2[m^2W_y^2 + ((n-1)W_x + b_x)^2]^{0.5}/A \end{aligned} \tag{3.32}$$

$$\begin{aligned} r_{DOe} &= 2[((m-1)W_y + a_y)^2 + n^2W_x^2]^{0.5}/A \\ r_{DOo} &= 2[((m-1)W_y + a_y)^2 + ((n-1)W_x + a_x)^2]^{0.5}/A \\ r_{DOop} &= 2[((m-1)W_y + a_y)^2 + ((n-1)W_x + b_x)^2]^{0.5}/A \end{aligned} \tag{3.33}$$

$$\begin{aligned} r_{DOPe} &= 2[((m-1)W_y + b_y)^2 + n^2W_x^2]^{0.5}/A \\ r_{DOPo} &= 2[((m-1)W_y + b_y)^2 + ((n-1)W_x + a_x)^2]^{0.5}/A \\ r_{DOPop} &= 2[((m-1)W_y + b_y)^2 + ((n-1)W_x + b_x)^2]^{0.5}/A \end{aligned} \tag{3.33a}$$

The two sets of equations 3.15 and 3.28 are also made dimensionless by making them multiples of the drainage area as follows:

$$\begin{aligned} r_{Dxe} &= 2nW_x/A \\ r_{Dxo} &= 2[(n-1)W_x + a_x]/A \\ r_{Dxop} &= 2[(n-1)W_x + b_x]/A \end{aligned} \tag{3.34}$$

$$\begin{aligned} r_{Dye} &= 2mW_y/A \\ r_{Dyo} &= 2[(m-1)W_y + a_y]/A \\ r_{Dyop} &= 2[(m-1)W_y + b_y]/A \end{aligned} \tag{3.35}$$

Finally, dimensionless locations are defined, as shown in Fig. 6.1 (rectangle) and Fig. 6.2 (square) by the following equations:

$$x_D = 2b_x/W_x \tag{3.36}$$

$$y_D = 2b_y/W_y \tag{3.37}$$

3.4.2 Dimensionless Time

The wellbore radius (r_w) in Eq. 2.4 can be replaced by several parameters of interest, such as b_x, b_y, $b_x b_y$ and the square root of the drainage area (A), to define new dimensionless times.

$$t_{DA} = \frac{kt}{\phi\mu cA} = t_D\left(\frac{r_w^2}{A}\right) \tag{3.38}$$

$$t_{Db_x} = \frac{kt}{\phi\mu cb_x^2} = t_{DA}\left(\frac{A}{b_x^2}\right) \tag{3.39}$$

$$t_{Db_y} = \frac{kt}{\phi\mu cb_y^2} = t_{DA}\left(\frac{A}{b_y^2}\right) \tag{3.40}$$

$$t_{Dbb} = \frac{kt}{\phi\mu cb_x b_y} = t_{DA}\left(\frac{A}{b_x b_y}\right) \tag{3.41}$$

where $A = W_x \times W_y$.

3.4.3 Pressure Behavior at a Point

The dimensionless pressure drop function at any point location inside a bounded rectangular system is:

$$p_D(r_D, t_{DA}) = p_{DR}(r_{DR}, t_{DA}) + \sum_{n=1}^{\infty} p_{DI}[r_{DI}(n), t_{DA}] \tag{3.42}$$

where: p_{DR} = dimensionless pressure at the real well

p_{DI} = dimensionless pressure at the image wells

r_{DR} = dimensionless radius of the real well, $r/\sqrt{A}$

r_{DI} = dimensionless distance of the image wells, $r_I/\sqrt{A}$

Substituting the five sets of equations 3.32, 3.33, 3.34, 3.35 and 3.36 into Eq. 3.42, yields:

$$
\begin{aligned}
p_D(r_D,t_{DA}) = & -\frac{1}{2}\,Ei[-r_{DR}^2/4t_{DA}] - \sum_{n=2k}^{\infty} Ei[-r_{Dxe}^2/4t_{DA}] \\
& - \frac{1}{2}\sum_{n=2k-1}^{\infty}\{Ei[-r_{Dxo}^2/4t_{DA}] + Ei[-r_{Dxop}^2/4t_{DA}]\} \\
& - \sum_{m=2j}^{\infty} Ei[-r_{Dye}^2/4t_{DA}] \\
& - \frac{1}{2}\sum_{m=2j-1}^{\infty}\{Ei[-r_{Dyo}^2/4t_{DA}] + Ei[-r_{Dyop}^2/4t_{DA}]\} \\
& + \sum_{m=2j}^{\infty}\{\sum_{n=2k}^{\infty} Ei[-r_{DEe}^2/4t_{DA}] \\
& + \sum_{n=2k-1}^{\infty}\{Ei[-r_{DEo}^2/rt_{DA}] + Ei[-r_{DEop}^2/4t_{DA}]\}\} \\
& - \frac{1}{2}\sum_{m=2j-1}^{\infty}\{\sum_{n=2k}^{\infty} Ei[-r_{DOe}^2/4t_{DA}] \\
& + \sum_{n=2k-1}^{\infty}\{Ei[-r_{DOo}^2/4t_{DA}] + Ei[-r_{DOop}^2/4t_{DA}]\}\} \\
& - \frac{1}{2}\sum_{m=2j-1}^{\infty}\{\sum_{n=2k}^{\infty} Ei[-r_{DOPe}^2/4t_{DA}] \\
& + \sum_{n=2k-1}^{\infty}\{Ei[-r_{DOPo}^2/4t_{DA}] + Ei[-r_{DOPop}^2/4t_{DA}]\}\}
\end{aligned}
\tag{3.43}
$$

A similar expression for p_D' can be obtained by replacing the exponential integral "Ei" symbol by the exponential function "exp" symbol, and multiplying the whole right-hand-side part of Eq. 3.43 by the ratio $(-1/t_{DA})$.

In summary, this discussion has outlined the use of the principle of superposition to generate the pressure behavior due to a single well producing at a constant rate in presence of multiple-sealing-fault systems and rectangular reservoirs. However, unlike the general approach to these systems which consisted of using highly idealized models in the laboratory, this study is based on an actual field case which is discussed next.

3.5 Field Case: The Hassi Touareg Anticlinorium, Algeria

The Hassi Touareg Anticlinorium is located in the central part of the Mesozoic Basin of the Eastern Algerian Sahara (Fig. 3.7). It is characterized by its rather complex structure which was caused by the occurence of an orogenic phase (called Austrian phase). The productive levels are located under the salt cover of the Upper Trias. The Southern section of this Anticlinorium extends into the so-called Gassi Touil oil Province, while the Rhourde el Baguel oilfield in the North seems to enter another oil province, the Hassi Messaoud one. The history and geological aspect of the Hassi Touareg Anticlinorium are discussed in detail by Claret and Tempère.[39]

Figure 3.8 shows the six main structural units of the oriental basin of the Algerian Sahara: (1) Haut-Fond d'El Biod (A), (2) Dorsale d'El Agreb and Messaoud (A1), (3) Hassi Touareg Anticlinorium (A2), (4) Oued Mya (B1), (5) Oriental Erg (B2), and (6) Sillon de Dorbane (S). Figure 3.9 presents the structural map of the Hassi Touareg

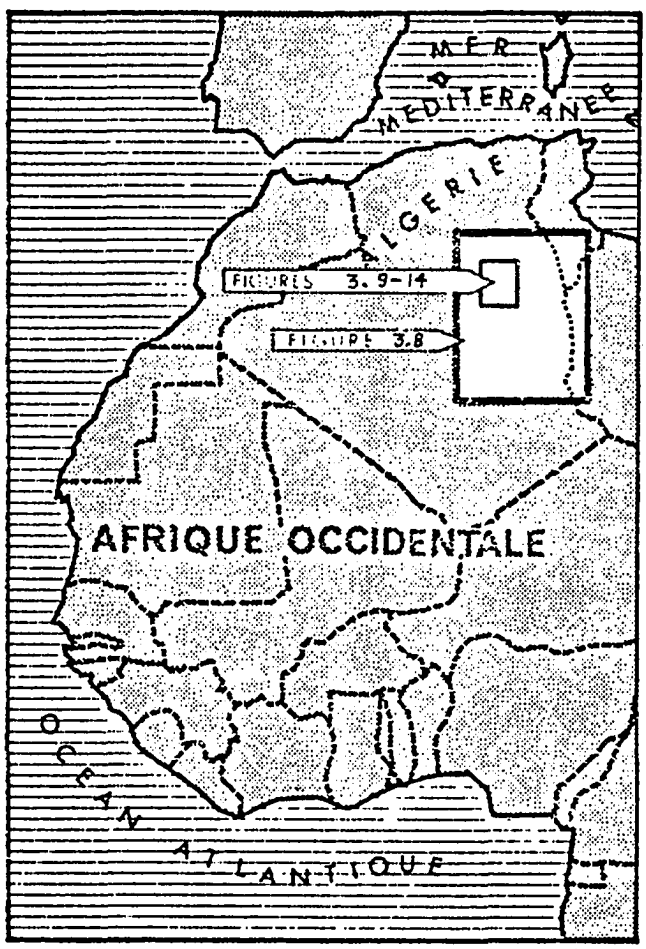

FIGURE 3.7: Location of the Hassi Touareg Anticlinorium, Algeria.

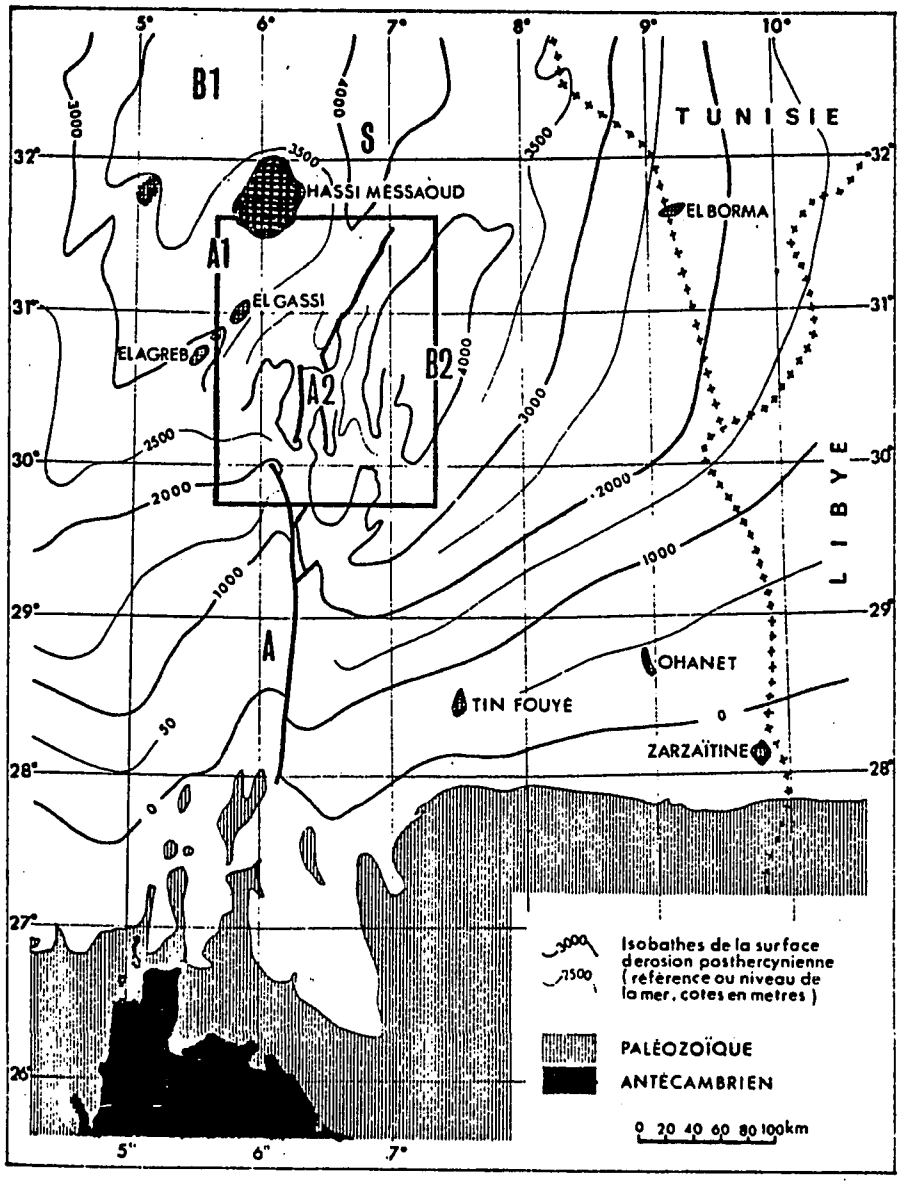

FIGURE 3.8: Structural Units of the Oriental Basin of the Algerian Sahara.

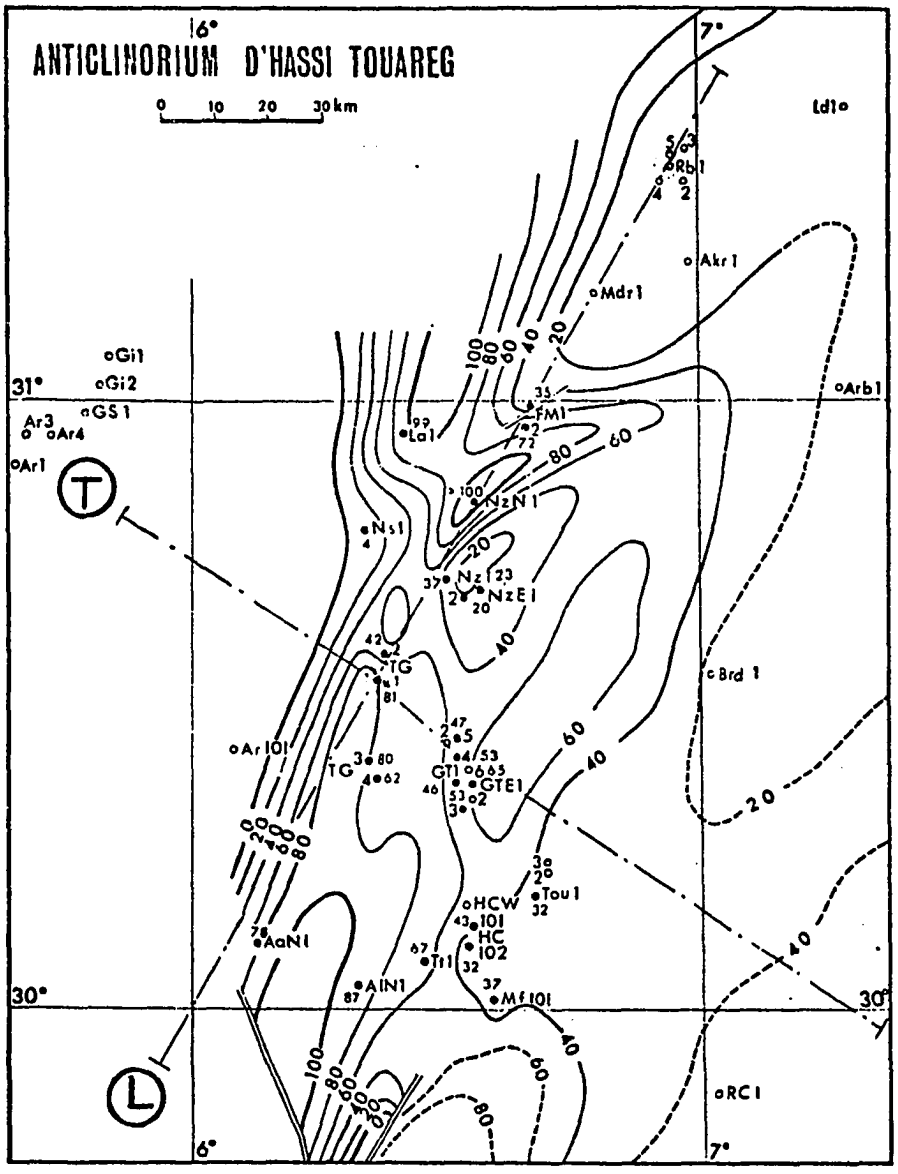

FIGURE 3.9: Structural map showing the eroded surface of the Hassi Touareg Anticlinorium.

Anticlinorium, and the two lines L and T along which the cross-sections of Figures 3.10, 3.11, 3.12 and 3.13 were drawn from a combination of geophysical, geological and drilling data. Figures 3.10 and 3.11 are transversal cross-sections along line T showing, respectively, the lithology and the location of petroleum reservoirs. Figures 3.12 and 3.13 are longitudinal cross-sections along line L. These cross-sections show the existence of four sealing faults parallel to line L and two sealing faults parallel to line T, as shown in Fig. 3.14.

Thus the Hassi Touareg oil province is actually composed of three closed rectangular reservoirs, eight systems of three perpendicular faults and four systems of two perpendicular faults. A comprehensive and economical planning of well location in such systems is practically impossible with the presently used pressure buildup and drawdown techniques for fault distance calculations. The type-curve matching technique presented in this study is strongly recommended for such multiple-boundary situations. This technique is discussed in detail in the following chapters.

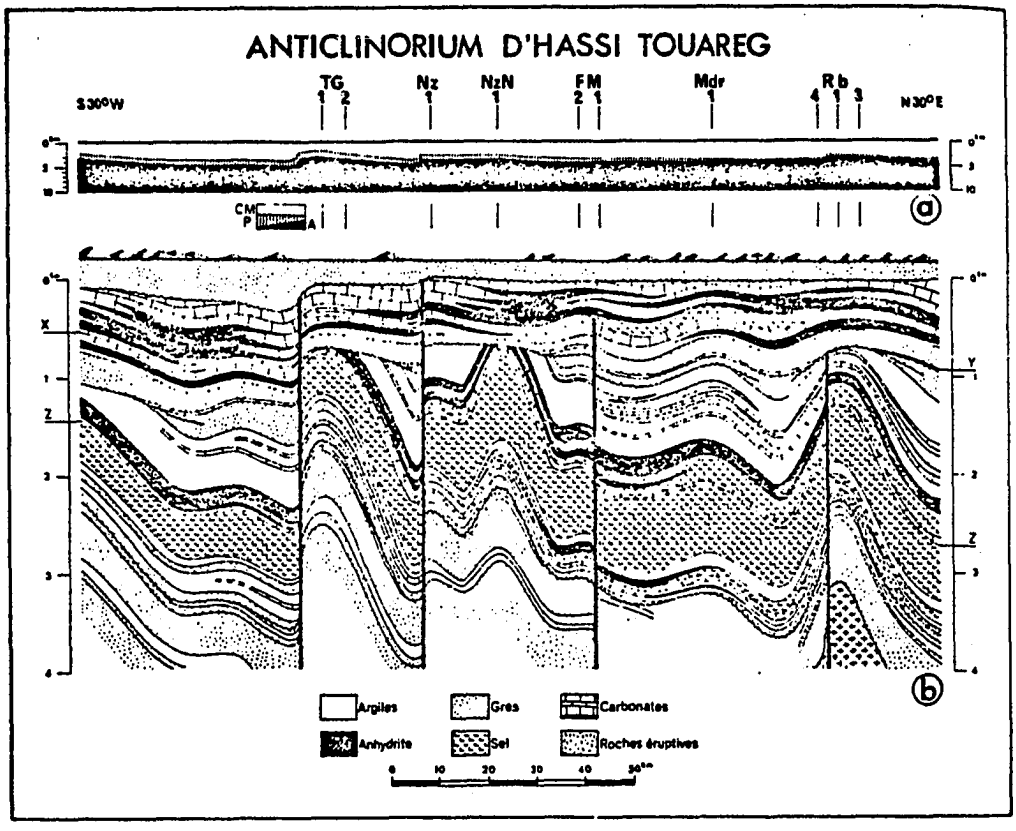

FIGURE 3.10: Transversal cross-section showing the lithology of the Hassi Touareg Anticlinorium.

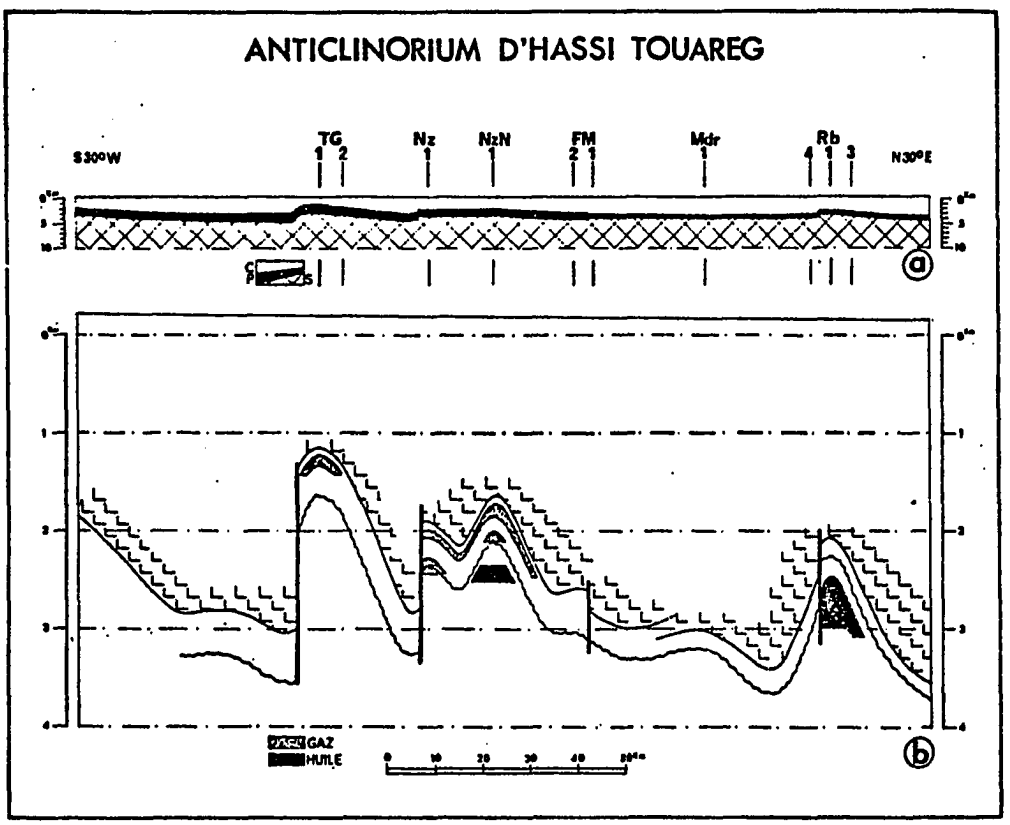

FIGURE 3.11: Transversal cross-section showing the location of petroleum reservoirs in the Hassi Touareg Anticlinorium.

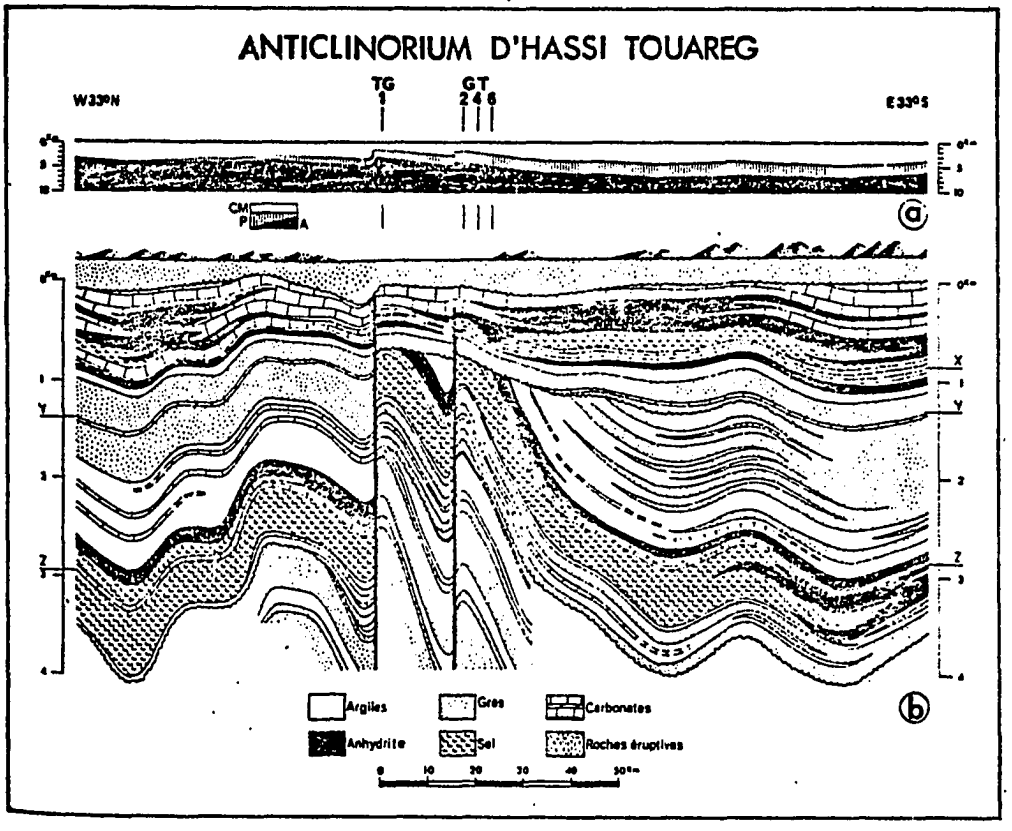

FIGURE 3.12: Longitudinal cross-section showing the lithology of the Hassi Touareg Anticlinorium.

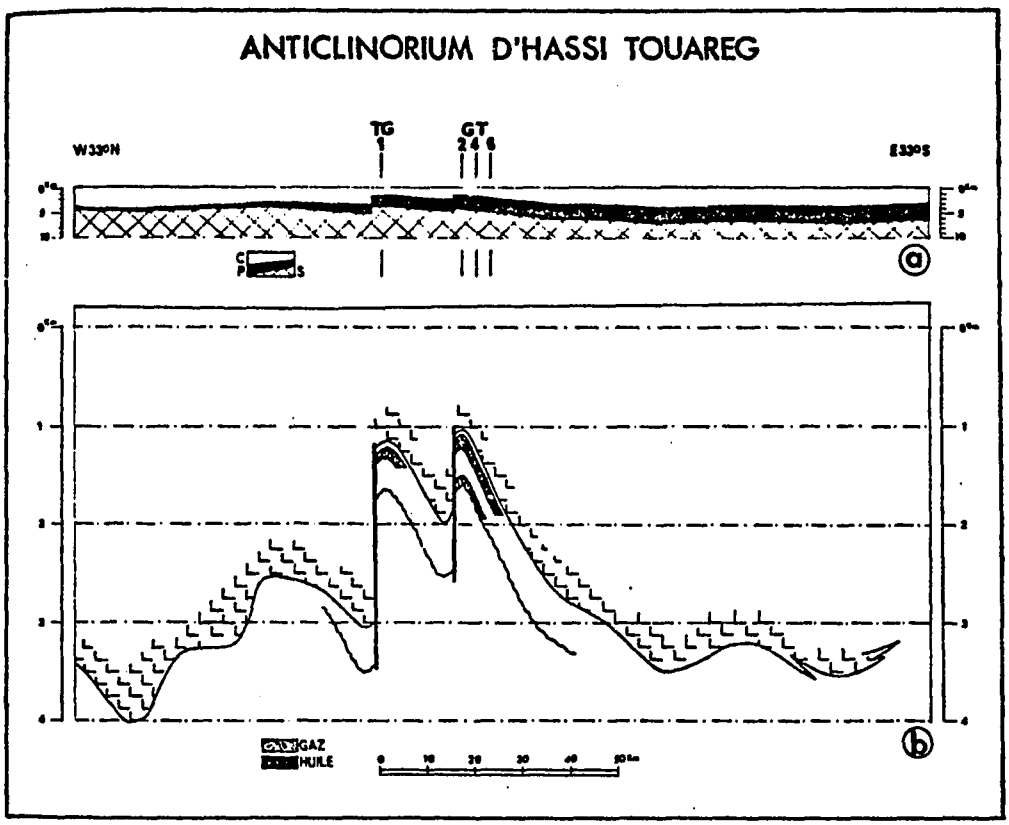

FIGURE 3.13: Longitudinal cross-section showing the location of the petroleum reservoirs in the Hassi Touareg Anticlinorium

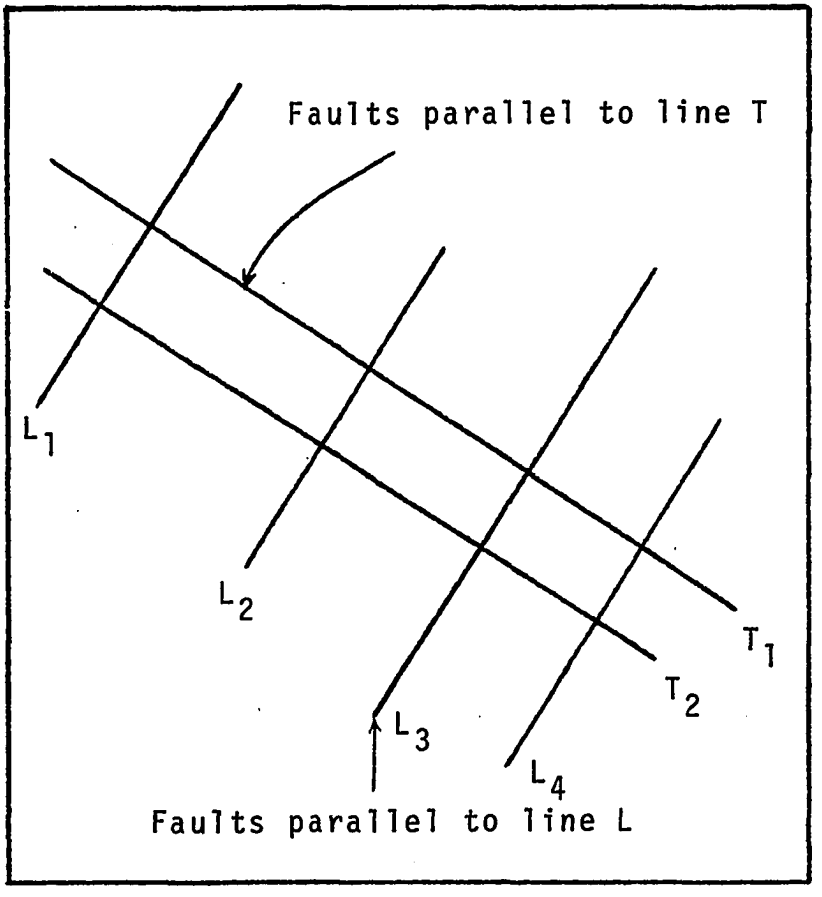

FIGURE 3.14: Plane view of the internal structure of the Hassi Touareg Anticlinorium, Algeria.

CHAPTER IV

WELL BETWEEN TWO PERPENDICULAR SEALING FAULTS

Transient behavior equations for wells located near linear discontinuities have been described in the literature. Horner[6] presented a technique based on the method of images to analyze the transient data of a well in the vicinity of a single fault. Van Poollen[17] utilized the method of images to generate pressure drawdown curves for a well located near two intersecting faults in an otherwise infinite system.

The present discussion will be concerned with the generation of type curve plots for a single well producing at constant rate and located between two no-flow boundaries intersecting at a right angle. The continuous line source solution to the diffusivity equation and the first derivative of the dimensionless well pressure with respect to time are systematically employed to develop pressure drawdown and buildup type-curve plots.

4.1 Pressure Drawdown Analysis

It is appropriate, first, to discuss the simple case of a well near a single sealing fault. Tiab[26] demonstrated that when a well is at a distance "b_x" from a no-flow boundary,

as shown in Fig. 3.2, the dimensionless well pressure is given by:

$$p_{Dw} = p_{DR}(r_{DR},t_{DA}) + p_{DI}(r_{DI},t_{DA}) \qquad (4.1)$$

where

$$t_{DA} = \frac{kt}{\phi\mu c b_x^2} \qquad (4.2)$$

r_{DR} = dimensionless distance of the real well, r_w/b_x

r_{DI} = dimensionless distance of the image well, $2b_x/b_x = 2$.

With these transformations, Eq. 4.1 can be written as:

$$p_{Dw} = -\frac{1}{2}\left\{Ei\left[-\frac{(r_w/b_x)^2}{4t_{DA}}\right] + Ei\left[-\frac{1}{t_{DA}}\right]\right\} \qquad (4.3)$$

A plot of p_{Dw} versus t_{DA} is shown in the semilog graph of Fig. 4.1 for three values of r_{DR}. Independently of r_{DR}, we observe two intersecting straight lines. The first line of slope 1.1513 corresponds to the infinite reservoir behavior shown in Fig. 2.7. The second straight line of slope 2.303 (double the slope of the first line) indicates the presence of a no-flow boundary. The two straight lines intersect at t_{DA} of 1.781 which is the exponential of Euler's constant. This observation provides a way to determine the distance b_x to the boundary from Eq. 4.2.

The time rate of change of dimensionless well pressure in presence of a no-flow boundary is, of course, obtained by direct differentiation of Eq. 4.3 with respect to

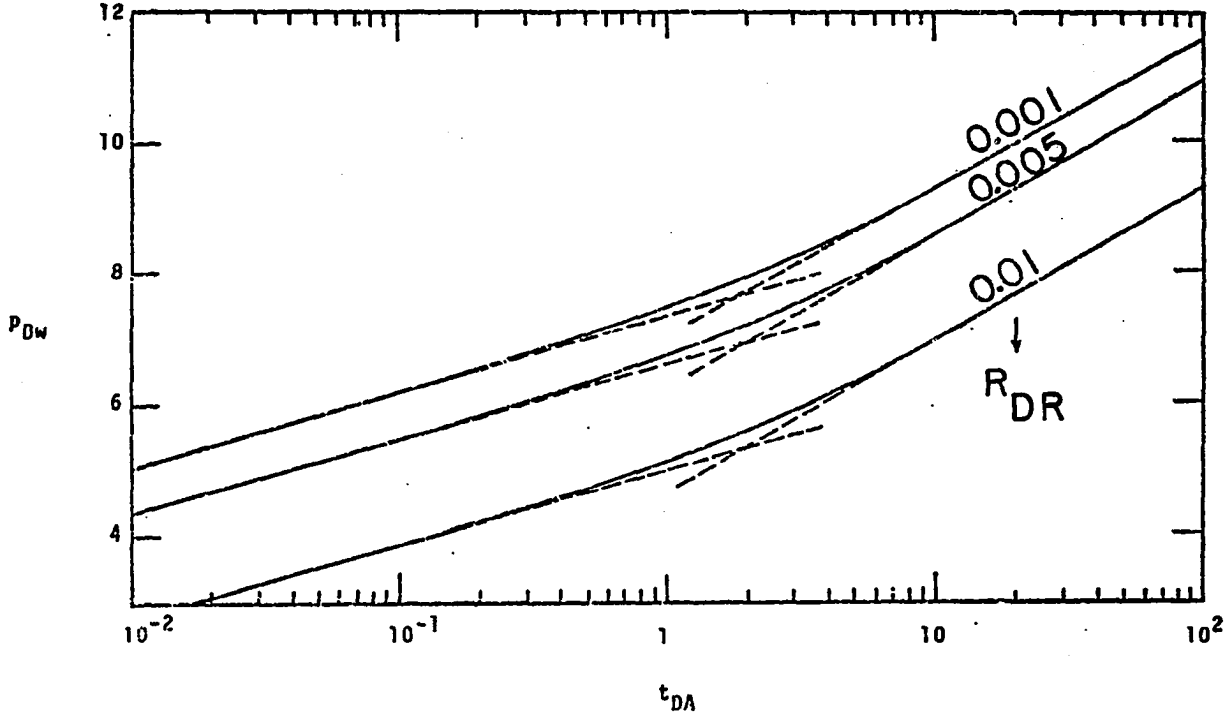

FIGURE 4.1: Dimensionless pressure vs dimensionless time for a well near a linear sealing fault.

t_{DA}:

$$p'_{Dw} = \frac{1}{2t_{DA}}\left\{\exp\left[-\frac{(r_w/b_x)^2}{4t_{DA}}\right] + \exp\left[-\frac{1}{t_{DA}}\right]\right\} \qquad (4.4)$$

A type-curve of p'_{Dw} versus t_{DA} on a log-log graph is shown in Fig. 4.2. We observe that the initial and final portions of the curve are straight lines of same slope -1. If a type curve data plot, i.e., $\partial p/\partial t$ vs. t, is placed over the master type curve of Fig. 4.2 such that the best match is obtained, then any convenient match point can be used to determine the distance to the fault as follows:

$$b_x = \left[\left(\frac{0.000264\ k}{\phi\mu c}\right)(t/t_{DA})_M\right]^{0.5} \qquad (4.5)$$

where $(t)_M$ and $(t_{DA})_M$ are the abscissa of the match point on the data plot and the master curve, respectively. This match point can also be used to calculate the kh product from Eq. 2.39 and the ϕc product from Eq. 2.40 with r_w replaced by b_x.

This brief discussion on the pressure behavior of a well near a single fault has pointed to the usefulness of p'_{Dw} in detecting sealing faults in an otherwise infinite reservoir. This technique will be applied in the following sections to analyze the behavior of dimensionless pressure and its first time derivative of a well near two perpendicular sealing faults, or no-flow boundaries.

4.1.1 Behavior of Dimensionless Flowing Well Pressure

The dimensionless pressure behavior of a well between two sealing faults intersecting at a right angle is given

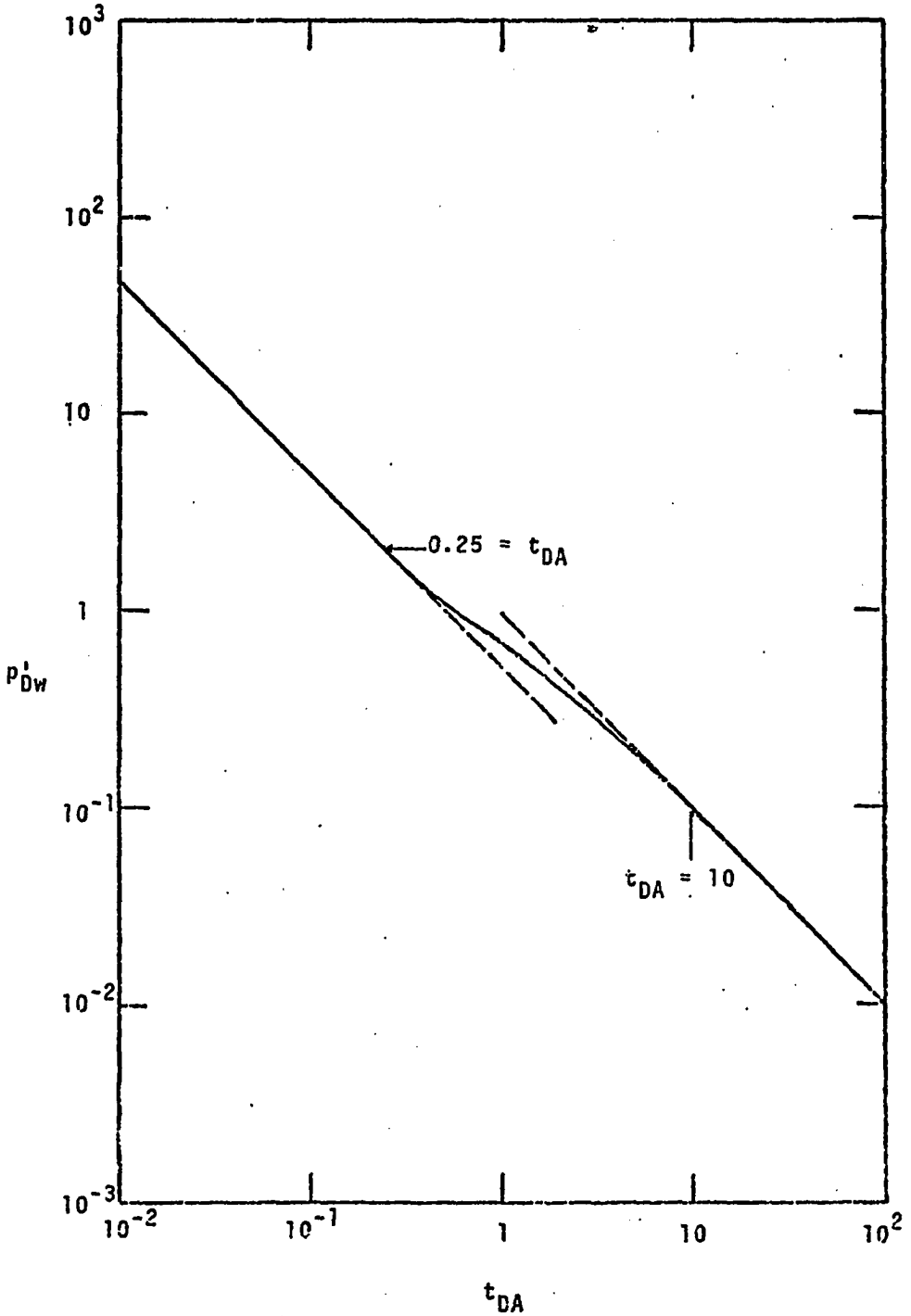

FIGURE 4.2: Time rate of change of dimensionless pressure vs dimensionless time for a well near a sealing fault.

by Eq. 3.13a, where the distance r is replaced by the well-bore radius r_w in the dimensionless radius r_{DR}. Figure 4.3 presents a semilog plot of p_{Dw} versus t_{DA} for the five well locations shown in Fig. 4.4. Computed values of p_{Dw} and its derivatives for y_D = 1, 1/2, 1/4 and 1/8 are respectively presented in Tables 1-4. For each y_D we observe a common straight line of slope 1.151 at early time representing infinite media without the effects of boundaries. The slope of this line can be used to determine the kh product and skin s from Eq. 2.35 and Eq. 2.36 respectively.

Figure 4.3 indicates that a second straight line of slope twice that of the first one is observed for $y_D \leq 1/16$, corresponding to the effect of the closest no-flow boundary. For values of $y_D \geq 1/16$, i.e., $b_y \geq b_x/16$, this second straight line vanishes. However, a third straight line of slope 4.6 (= 4 x 1.1513) is observed for all y_D. It is evident, therefore, that graphs of the type shown in Fig. 4.3 are useful only in cases where the well is very close to the boundaries. In the following section, we show that p'_{Dw} offers a much better method to detect and locate both boundaries.

4.1.2 Behavior of p'_{Dw}

The time rate of change of dimensionless pressure for a well located between two no-flow boundaries, or sealing faults, intersecting at a right angle is given by the sum of pressure contributions due to the real well and the three image wells as indicated by Eq. 3.14a, where the

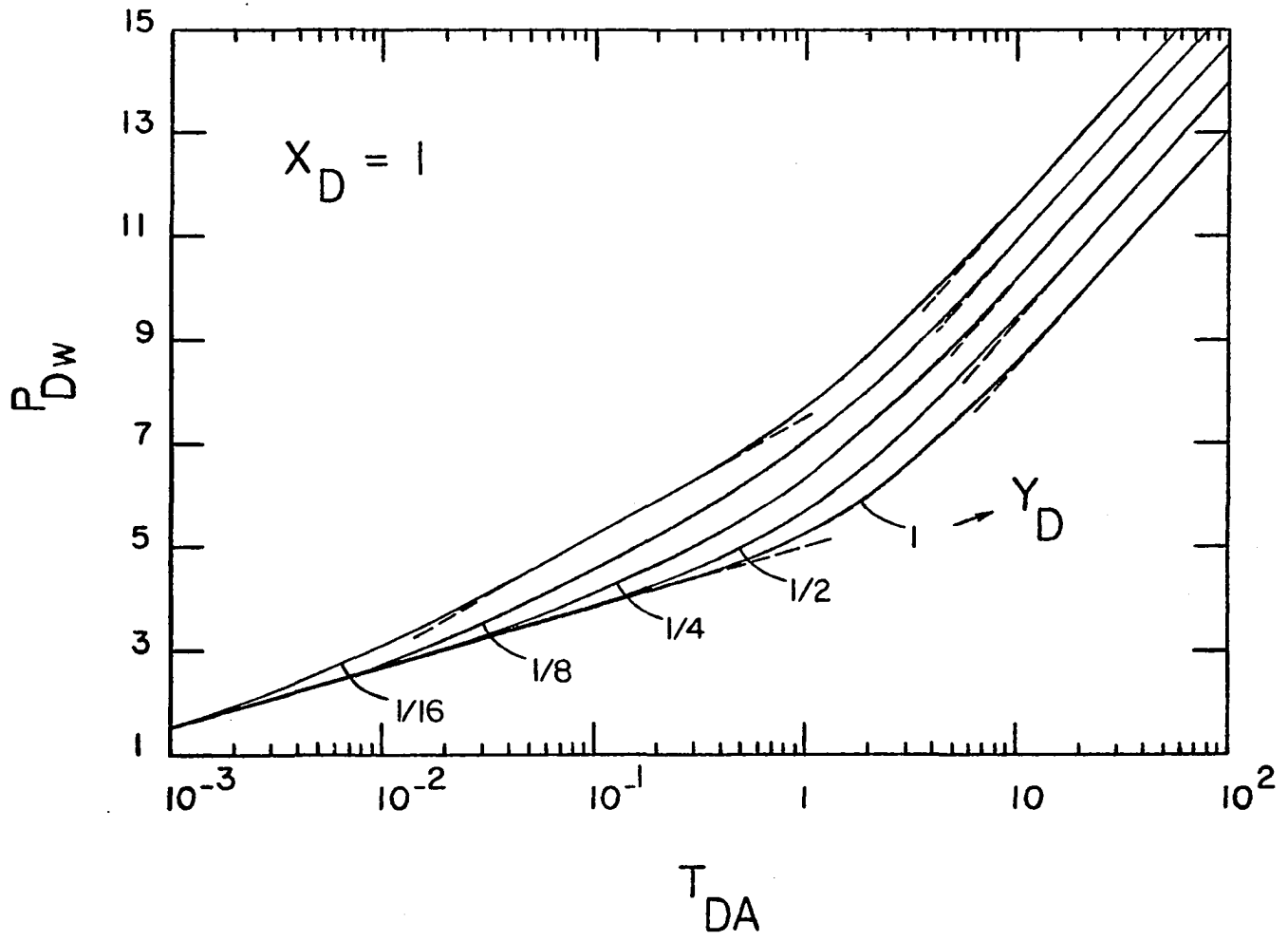

FIGURE 4.3: Semilog plot of p_{Dw} vs t_{DA} for a well between two perpendicular sealing faults.

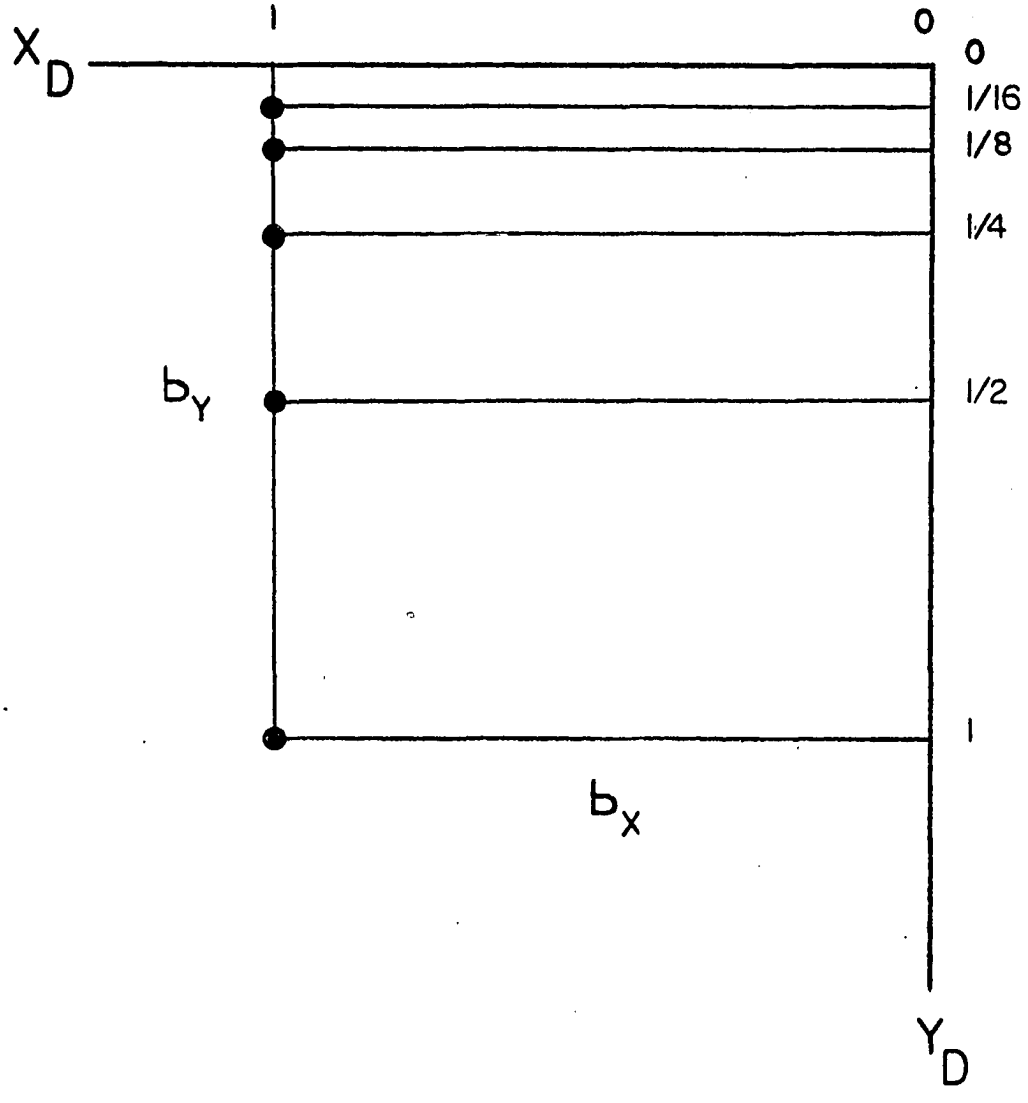

FIGURE 4.4: Two-perpendicular-fault system showing well locations.

distance r is replaced by the wellbore radius r_w in r_{DR}. A type curve of p'_{Dw} versus t_{DA} on a log-log graph is presented in Fig. 4.5 for various well locations between the two boundaries. This graph shows the existence of three parallel straight line portions of slope -1: (1) The first straight line at early time represents infinite reservoir behavior without the effect of faults. (2) The second straight line, corresponding to the effect of the closest fault, vanishes for values of $y_D \geq 1/8$. However, it is not necessary to have a second straight line since the type curve data plot must appear like the corresponding master type curve for all times. (3) The third straight line (which starts at $t_{DA} = 20$) is common to the family of curves. It indicates the existence of the second fault.

When a well is located on the bisector between the intersecting faults, i.e., $b_x = b_y$ or $y_D = 1$, the effect of both faults is felt at the same time. This causes the first straight line to extend up to a t_{DA} of 0.2, and, as expected, the second line is not observed. As a result, from comparison of Fig. 4.5 for $y_D = 1$ or 1/2 with Fig. 4.2, it appears that there is no way of telling whether we are in the presence of a single fault or two faults, since for these values of y_D, Fig. 4.5 shows no second straight line. However, it is evident from this figure that the total shift to the right of the final straight line in the case of two perpendicular faults is double the shift in the case of a single fault. The shift of the second straight line of

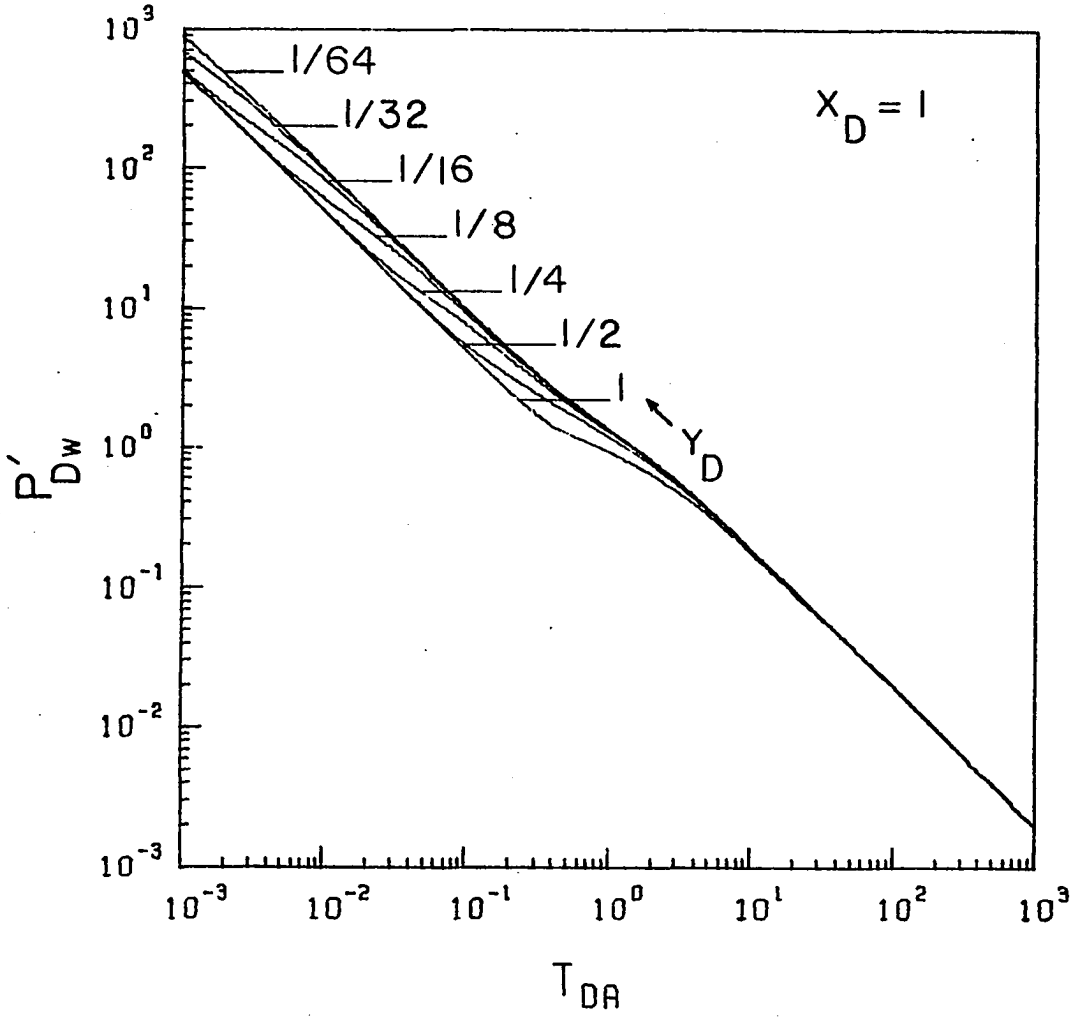

FIGURE 4.5: Type-curve plot of p'_{Dw} vs t_{DA} for various well locations between two perpendicular sealing faults.

Fig. 4.5 for $y_D \leq 1/8$ is, of course, equal to the shift obtained in the presence of a single fault. This is the distinguishing feature of the behavior of the time rate of change of pressure of a well near two sealing faults intersecting at a right angle.

The distance to both faults, b_x and b_y, and several other reservoir parameters such as the kh and ϕc products can be determined by type curve matching from Fig. 4.5. The following approach can be used.

Drawdown Type-Curve Matching Procedure

1. Plot rate of change of well pressure data with time $\Delta p_{wf}/\Delta t = p'_{wf}$ (psi/hr) on the ordinate vs t (hr) on the abscissa of log-log paper of the same size as the original master type curve, of which a reduced copy is shown in Fig. 4.5. (A full scale copy of the master type curve is available from the author on request.) Note that $\Delta p_{wf}/\Delta t$ can be simply obtained by using the conventional two-point derivative approach. The simplicity of this method as opposed to more complex ones, such as the five-point derivative method, will allow a practicing engineer without a formal training in differential analysis and computer application to use this type-curve technique.

2. Place the type curve data plot of p'_{wf} vs. t over the master type curve plot of p'_{Dw} vs. t_{DA}, such that corresponding axes are parallel.

3. Slide the field curve, keeping axes parallel, until the best match is obtained with one of the curves of the

master graph, and read $(y_D)_M$. To get a good match, it may be necessary to approximate for values of y_D not included in the master type curve. In any case, the first point of the final straight line of the field curve must be placed over the corresponding point of the master curve.

4. Pick any convenient match point and read the corresponding values of $(p'_{Dw})_M$ and $(t_{DA})_M$ from the master type curve of Fig. 4.5, and $|p'_{wf}|_M$ and $(t)_M$ from the type curve data plot. These values are used to calculate various reservoir parameters as follows:

(a) Distance to boundaries

$$b_x = \left[\left(\frac{0.00264\ k}{\phi\mu c}\right)(t/t_{DA})_M\right]^{0.5} \tag{4.6}$$

and

$$b_y = b_x(y_D)_M \tag{4.7}$$

(b) Flow capacity (or kh-product)

$$kh = 141.3\ q\mu B(p'_{Dw}/p'_{wf})_M(t_{DA}/t)_M \tag{4.8}$$

(c) Storage capacity: the ϕc product is obtained by overlaying the first straight line portion of plot of step 1 on Fig. 2.5:

$$\phi c = (qB/26.856\ hr_w^2)(p'_{Dw}/p'_{wf})_{M,\text{Fig. 2.5}} \tag{4.9}$$

This curve matching approach will give a much more accurate value of the distance to boundaries and other reservoir parameters than presently used well test analysis techniques, as field data curves must appear like the proper analytic solution for all times.

To spread out the curves for various values of y_D, we use a dimensionless time based upon the distance to the nearest fault, b_y, as defined in Eq. 3.11, or in oilfield units:

$$t_{Db_y} = \frac{0.000264\ kt}{\phi\mu c b_y^2} \tag{4.10}$$

A plot of p'_{Dw} versus t_{Db_y} on a log-log graph is shown in Fig. 4.6 for various well locations between two perpendicular sealing faults. The general behavior in Fig. 4.6 is, of course, the same as in Fig. 4.5 except that we have a distinct curve for each well location. Figure 4.6 can be used to determine the distance to the nearest boundary and other reservoir parameters using the type curve technique described above.

The distance to the nearest fault is given by

$$b_y = \left[\left(\frac{0.000264\ k}{\phi\mu c}\right)(t/t_{Db_y})_M\right]^{0.5} \tag{4.11}$$

and the distance to the other fault is given by

$$b_x = b_y/(y_D)_M \tag{4.12}$$

The products kh and ϕc are respectively given by Eq. 4.8 and 4.9 where t_{DA} is replaced by t_{Db_y} (in Eq. 4.8) and b_x is replaced by b_y (in Eq. 4.9).

A dimensionless time based upon the product of distances b_x and b_y, as defined in Eq. 3.12, can also be used to spread out the curves for various well locations. In oil

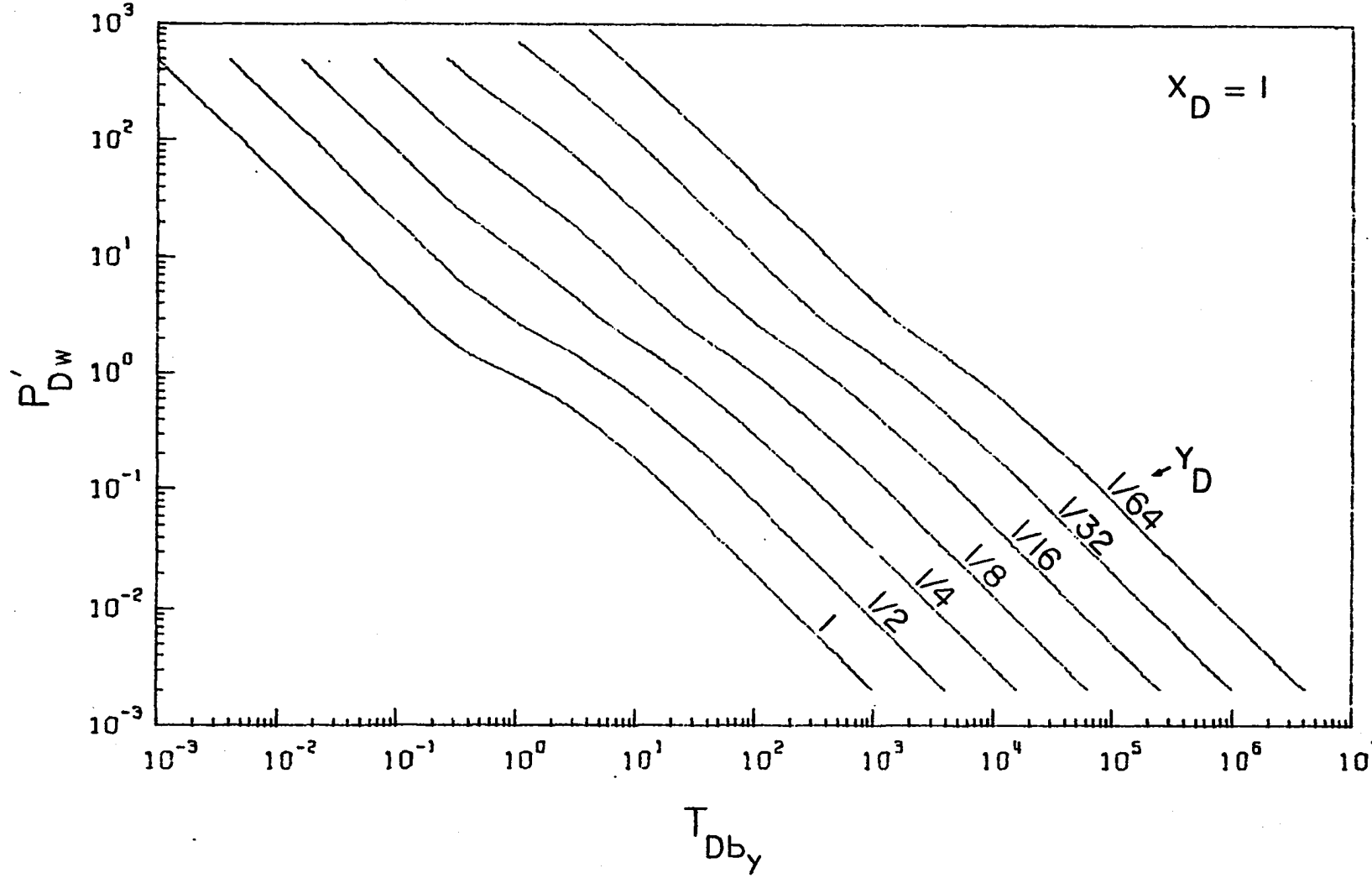

FIGURE 4.6: Type-curve plot of p'_{Dw} vs t_{Db_y} for various well locations between two perpendicular sealing faults.

field units

$$t_{Dbb} = \frac{0.000264\ kt}{\phi\mu c b_x b_y} \tag{4.13}$$

A graph of p'_{Dw} versus t_{Dbb} is shown in Fig. 4.7 which exhibits the same general character as Figs. 4.5 and 4.6. As before, the type curve matching technique can be used to determine the product $b_x b_y$ from the match point, or

$$b_x b_y = \frac{0.000264\ k}{\phi\mu c} (t/t_{Dbb})_M \tag{4.14}$$

Then, the distance to the nearest boundary is given by

$$b_y = \sqrt{(b_x b_y)(y_D)_M} \tag{4.15}$$

Finally, it is evident that a match point in Fig. 4.7 can be used to determine the ϕc and kh products from Eqs. 4.8 and 4.9 where t_{DA} and b_x are respectively replaced by t_{Dbb} and the square root of $b_x b_y$.

4.1.3 Drawdown Type-Curve Match Example

Consider a new producing oil well located between the two perpendicular faults L_4 and T_2 of the Hassi Toureg Anticlinorium as shown in Fig. 3.14. Assuming the reservoir and well data below, determine the permeability, the porosity and the well location with respect to the two faults.

$q = 425$ STB/D

$\mu = 0.65$ cp

$B = 1.14$ res.bbl/STB

$c = 7.5 \times 10^{-6}$ psi^{-1}

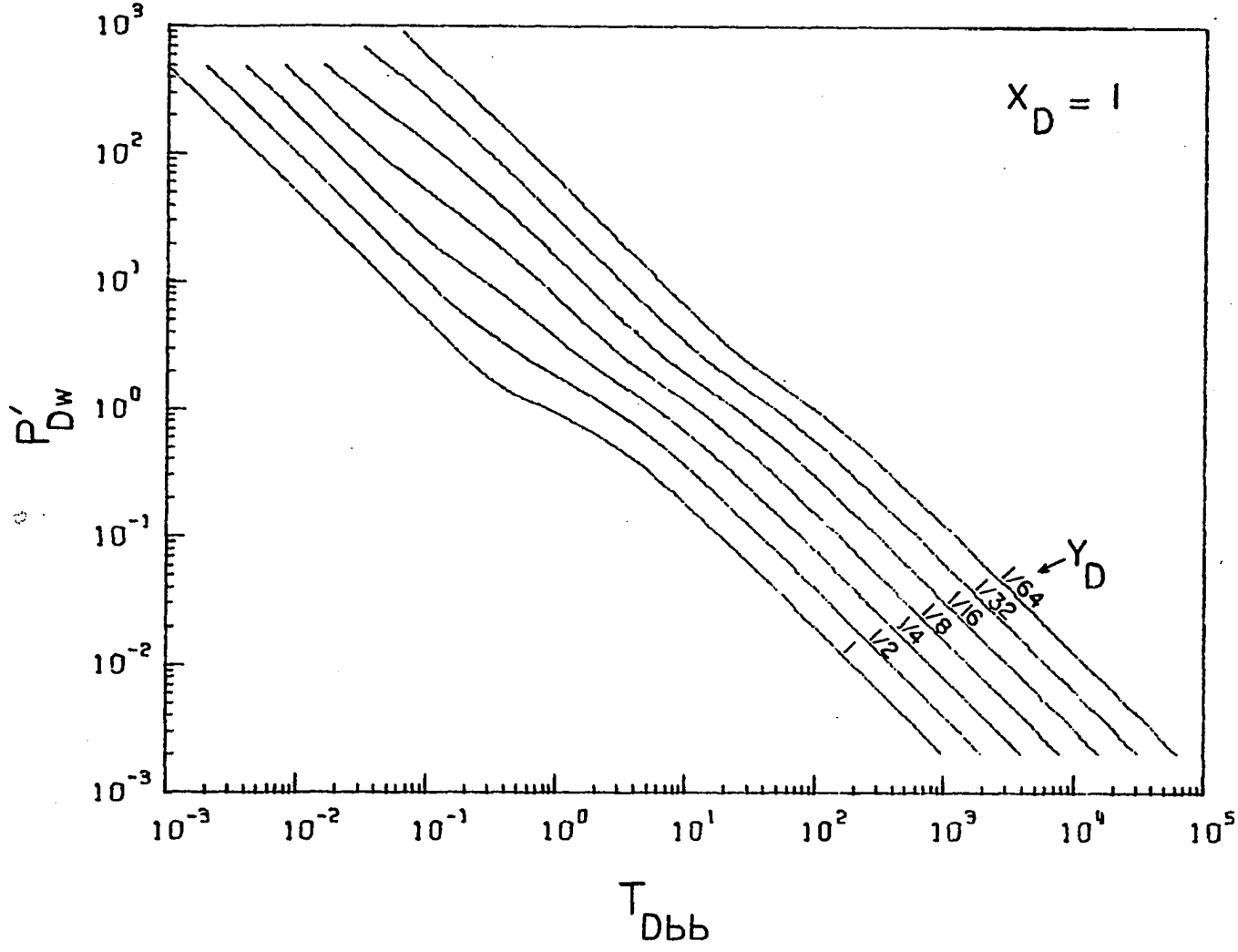

FIGURE 4.7: Type-curve plot of p'_{Dw} vs t_{Dbb} for various well locations between two perpendicular sealing faults.

$h = 36$ ft

$r_w = 0.316$ ft

The time rate of change of flowing well pressure (p'_{wf}) field data is plotted against producing time on a log-log graph paper (Fig. 4.8) with the same grid size as the master type-curve of Fig. 4.5. This field data curve is then placed on Fig. 4.5 as shown in Fig. 4.8. The resulting match point has the following coordinates:

$(t_{DA})_M = 1$ $\qquad$ $(p'_{Dw})_M = 1.357$ psi/hr

$(t)_M = 2.796$ $\qquad$ $(p'_{wf})_M = 5.356$

The kh-product can be determined from Eq. 4.8:

$$kh = (141.3)(425)(0.65)(1.14)(1.357/5.356)(1/2.796)$$
$$= 4032 \text{ md-ft}$$

then

$$k = \frac{4032}{36} = \underline{112 \text{ md}}$$

The field data curve is then overlayed on Fig. 2.5 according to step (c) of the Drawdown Type-Curve Matching Procedure, such that

$$[(p'_{Dw} \times t_{DA})/(p'_{wf} \times t)]_{M,\text{Fig. } 4.5}$$
$$= [(p'_{Dw} \times t_D)/(p'_{wf} \times t)]_{M,\text{Fig. } 2.5} = \frac{kh}{141.3\ q\mu B}$$

Using the reservoir data we find that

$$\frac{kh}{141.3\ q\mu B} = \frac{(112)(36)}{(141.3)(425)(0.65)(1.14)} = \frac{1}{11.04}$$

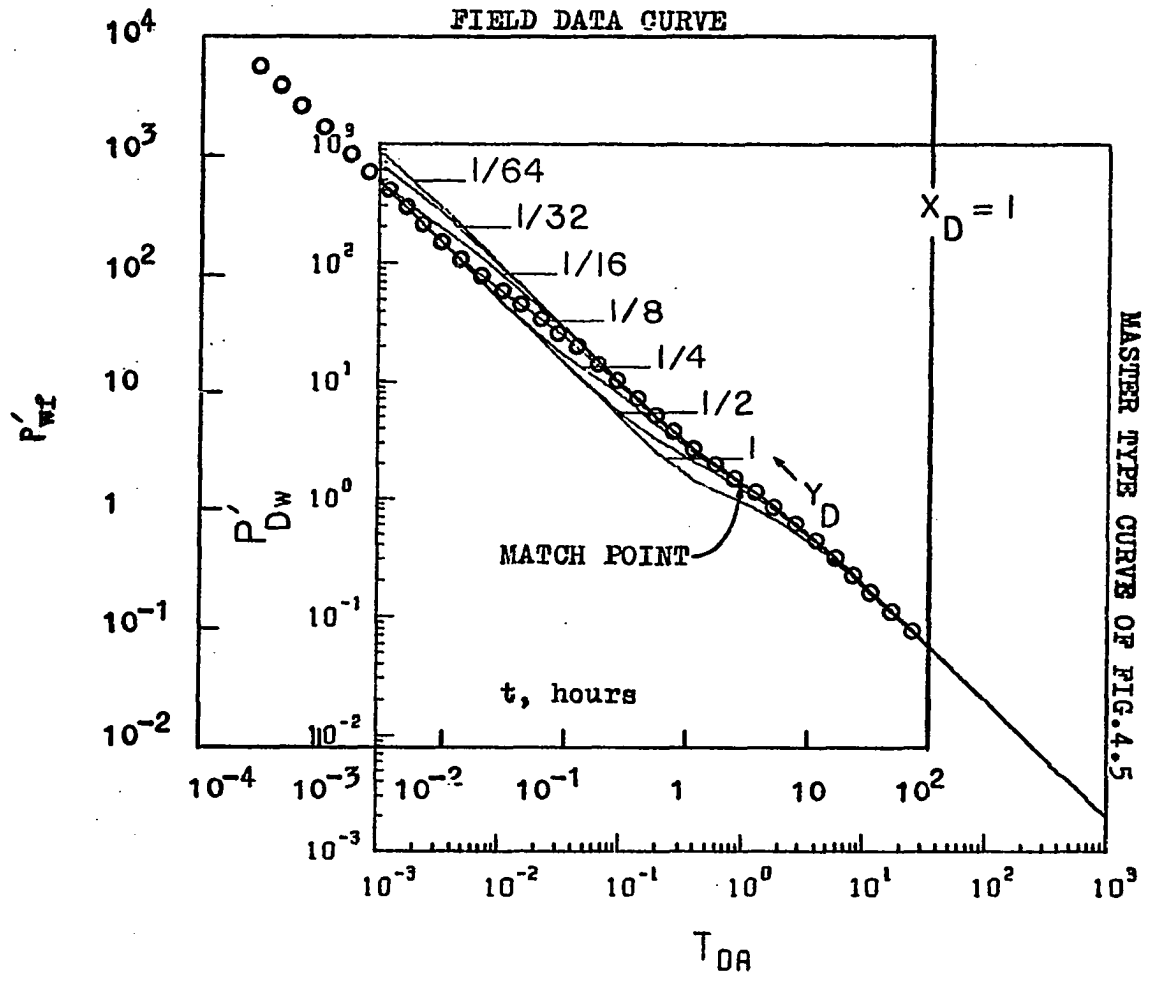

FIGURE 4.8: Drawdown type-curve match example.

Note that the product $(p'_{Dw} \times t_D)_{Fig.\ 2.5}$ is always equal to 0.5 (see Eq. 2.14). Thus

$$(p'_{wf} \times t)_{M,Fig.\ 2.5} = 11.04(p'_{Dw} \times t_D)_{M,Fig.\ 2.5}$$
$$= (11.04)(0.5)$$
$$= 5.52$$

Hence, any point on the first straight line (which corresponds to the infinite reservoir behavior without the effects of the boundaries) with $p'_{wf} \times t = 5.52$ is a match point. Thus a choice of $(t_D)_M = 10^4$ from Fig. 2.5 yields $(p'_{Dw})_M = 0.5 \times 10^{-4}$ and $(t)_M = 0.02$ from the field data curve yields $(p'_{wf})_M = 2.78 \times 10^2$.

The ϕc-product can be calculated from Eq. 4.9:

$$\phi c = \frac{(425)(1.14)}{(26.856)(36)(0.316)^2}\left[\frac{0.5 \times 10^{-4}}{2.78 \times 10^2}\right] = 0.9026 \times 10^{-6} \text{ psi}^{-1}$$

$$\phi = \frac{0.9026 \times 10^{-6}}{7.5 \times 10^{-6}} = \underline{0.12}$$

Finally, Fig. 4.8 shows that the match is obtained for $(y_D)_M = 1/8$. The distance to the furthest of the two faults is determined from Eq. 4.6.

$$b_x = \left[\frac{(0.000264)(112)}{(0.12)(0.65)(7.5 \times 10^{-6}}\frac{2.796}{1}\right]^{0.5} = \underline{376 \text{ ft}}$$

The distance to the closest fault is calculated from Eq. 4.7.

$$b_y = (376)(1/8) = \underline{47 \text{ ft}}$$

We could just as well have matched the type-curve of Fig. 4.6. In that case, we would have calculated b_y from Eq. 4.11, then we would have used Eq. 4.12 to calculate b_x. We could also have matched Fig. 4.7, in which case we would have determined the product $b_x b_y$ from Eq. 4.14, the distance b_y from Eq. 4.15, and, of course, b_x from the ratio $b_x b_y / b_y$.

In summary, this section has discussed the behavior of p_{Dw} and p'_{Dw} for a well located between two sealing faults intersecting at a right angle in an otherwise infinite reservoir. It is demonstrated that the type curve technique based on the rate of change of dimensionless well pressure provides unique solutions for locating multiple sealing faults and calculating several important reservoir parameters such as the kh and ϕc products.

4.2 Pressure Buildup Analysis

The powerful principle of superposition, which was used in the previous chapter to generate boundary conditions, can also be used to develop interpretative methods for analyzing the behavior of shut-in well pressure, p_{ws}, during buildup well testing. Consider a well in an infinitely large reservoir which is produced at the rate (+q) for a time period t. At a time t, a second well, located in exactly the same position as the first well, is produced for a time period Δt at the rate (-q), thus making the net production rate due to both wells become zero. Therefore, the

total pressure drop at some point in the reservoir is the sum of the pressure drop due to the first well producing for $(t + \Delta t)$ and the pressure drop caused by the second well producing only for Δt, or:

$$\frac{2\pi kh}{\mu}(p_i - p_s) = \{(+q)[p_D(r_D,(t+\Delta t)_D) + s]\} + \{(-q)[p_D(r_D,\Delta t_D) + s]\}$$

or

$$\frac{2\pi kh}{q\mu}(p_i - p_s) = p_{Ds} = p_D[r_D,(t+\Delta t)_D] + p_D[r_D,\Delta t_D] \quad (4.16)$$

The shut-in well pressure at the well, i.e., $r = r_w$ and $r_D = 1$, is then given by the following equation, in oilfield units:

$$\frac{kh}{141.3\ q\mu B}(p_i - p_{ws}) = -\frac{1}{2}Ei\left[-\frac{1}{4(t+\Delta t)_D}\right] + \frac{1}{2}Ei\left[-\frac{1}{4\Delta t_D}\right] \quad (4.17)$$

A simpler and shorter form of this equation is given by Eq. 2.45, which we write again:

$$p_{Ds} = p_{Dw}(t_D + \Delta t_D) - p_{Dw}(\Delta t_D)$$

This approach to buildup analysis, which is similar to that of Ramey and Cobb [38] is preferred here over the conventional one which generally consists of replacing dimensionless pressures with analytical solutions, such as Eq. 2.33, which are subject to too many assumptions and approximations.

4.2.1 Behavior of Dimensionless Shut-In Well Pressure (p_{Ds})

The behavior of the dimensionless shut-in well pressure for a well between two perpendicular no-flow boundaries, or sealing faults, is obtained from the following equation:

$$p_{Ds} = -\frac{1}{2}\left\{Ei\left[-\frac{(r_w/b_x)^2}{4(t+\Delta t)_{DA}}\right] + Ei\left[-\frac{1}{(t+\Delta t)_{DA}}\right] + Ei\left[-\frac{(b_y/b_x)^2}{(t+\Delta t)_{DA}}\right] + Ei\left[-\frac{(b_x^2+b_y^2)/b_x^2}{(t+\Delta t)_{DA}}\right]\right\} + \frac{1}{2}\left\{Ei\left[-\frac{(r_w/b_x)^2}{4\Delta t_{DA}}\right] + Ei\left[-\frac{1}{\Delta t_{DA}}\right] + Ei\left[-\frac{(b_y/b_x)^2}{\Delta t_{DA}}\right] + Ei\left[-\frac{(b_x^2+b_y^2)/b_x^2}{\Delta t_{DA}}\right]\right\} \quad (4.18)$$

This equation was used to generate computed buildup graphs of Horner and MDH type for various values of dimensionless producing time t_{DA} (before shut-in). Computed values of p_{Ds} and its derivatives for $(x_D,y_D) = (1, 1/8)$ are presented in Tables 5, 6, 7 and 8 for $t_{DA} = 0.01$, 0.1, 1 and 10, respectively.

4.2.1.1 Horner Method

This method conventionally consists of plotting shut-in well pressure, p_{ws}, versus the logarithm of the time ratio $(t + \Delta t)/\Delta t$. The Horner graph for a well located at $(x_D,y_D) = (1, 1/8)$ between two sealing faults intersecting at a right angle is presented in Fig. 4.9 for $t_{DA} = 0.1$, 1, 10, and 100. As expected, a straight line of slope 1.1513 per log cycle is observed for each producing time at early shut-in times, which corresponds to the infinite reservoir

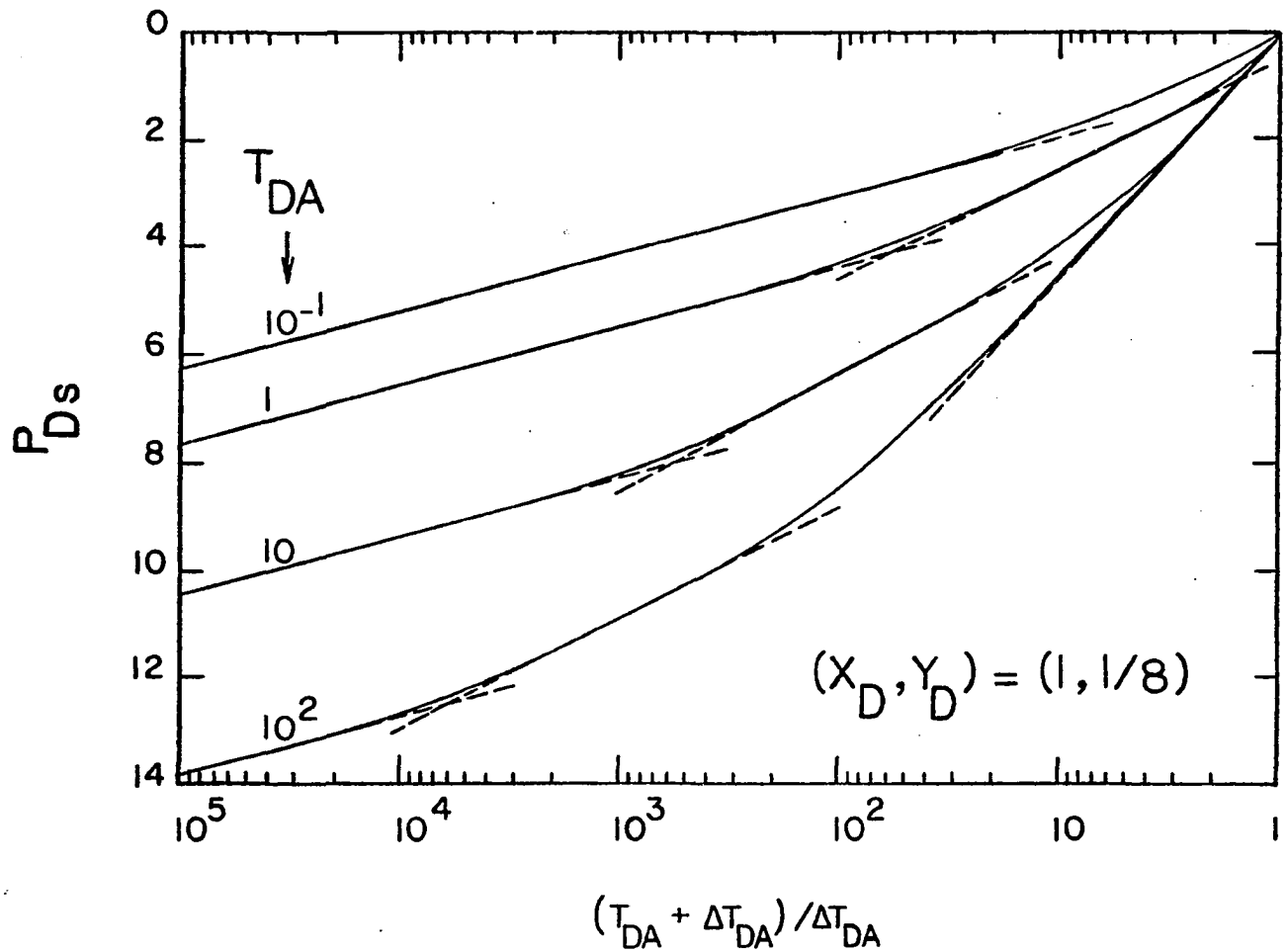

FIGURE 4.9: Horner buildup graph for a well located at $(x_D, y_D) = (1, 1/8)$ between two perpendicular sealing faults.

behavior. The slope of this line can be used to calculate the kh product from Eq. 2.35. At long shut-in times and for producing times $t_{DA} \geq 1$, we observe a second straight line of slope twice that of the first line, which is an indication of the effect of the closest fault. The two lines intersect at time ratios $(t + \Delta t)/\Delta t$ of 6×10^3, 6×10^2 and 6×10 for dimensionless producing times t_{DA} of 10^2, 10 and 1, respectively. These intersection points can be used to calculate the distance to the nearest boundary as demonstrated by Horner.[6]

When producing times (before shut-in) are long, i.e., $t_{DA} \geq 10^2$, a third straight line of slope four times that of the first line can be obtained, indicating the presence of the second perpendicular boundary. This third line is, however, too short (less than a log cycle) to be correctly used to locate the second boundary. It is evident from Fig. 4.9 that this line requires excessively high long shut-in times, and therefore, in most cases, it will not be observed.

When producing times are short, i.e., $1 \leq t_{DA} < 10^2$, the third straight line is not observed at all. For $t_{DA} \leq 0.1$ only the first line of slope 1.1513 is obtained.

The Horner graph for $(x_D, y_D) = (1, 1/2)$ is shown in Fig. 4.10. Note that in this case, only the first and third straight lines are shown for $t_{DA} = 10^2$, while for $t_{DA} \leq 10$ only the first one is observed.

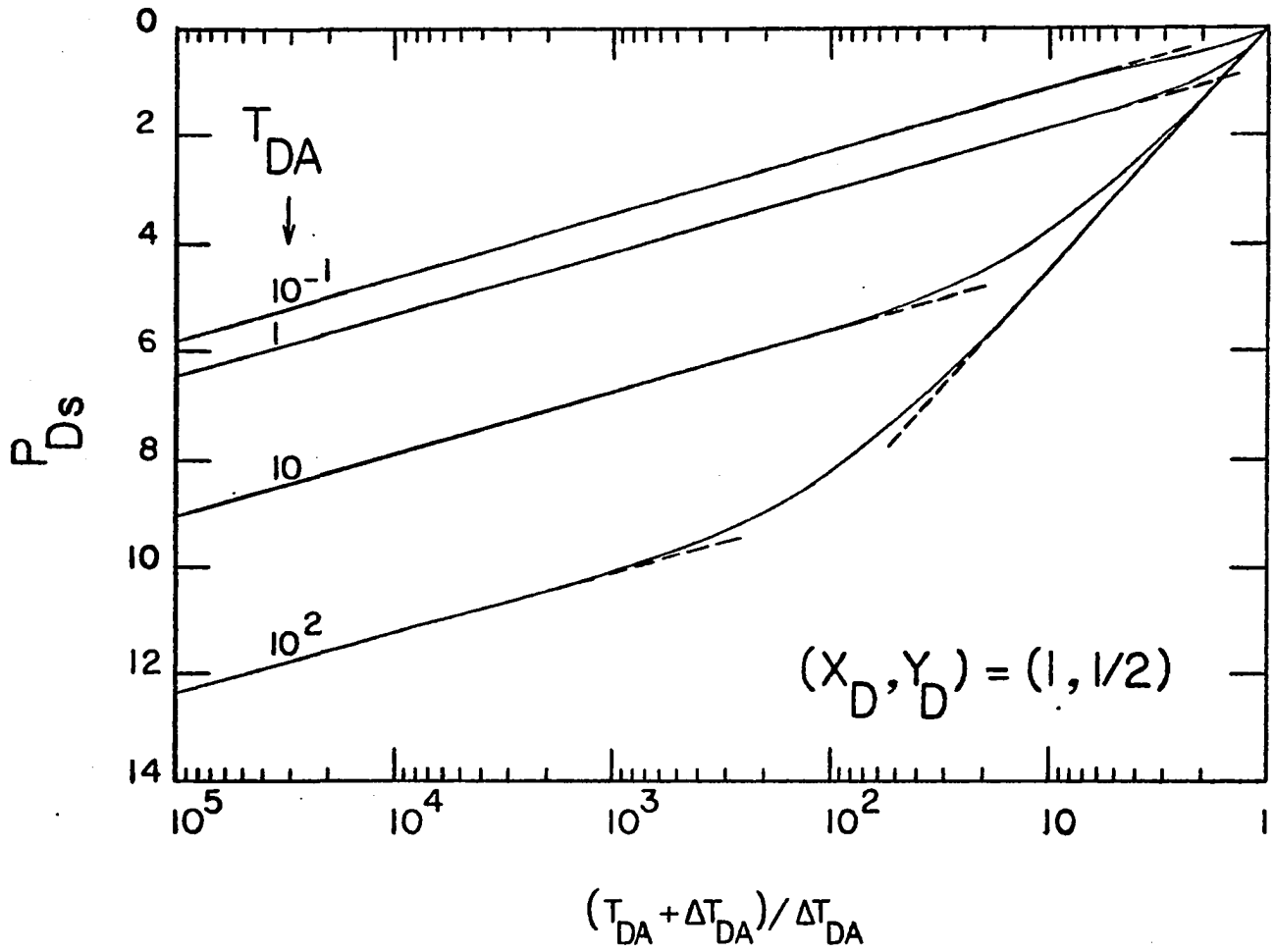

FIGURE 4.10: Horner buildup graph for a well located at $(x_D, y_D) = (1, 1/2)$ between two perpendicular sealing faults.

It is evident, therefore, that for a well between two perpendicular faults, the Horner method is useful in detecting only one fault since the third straight line of slope 4.6 is obtained only at infinite shut-in time (which, of course, implies that this line can never be observed).

4.2.1.2 Miller, Dyes and Hutchinson Method

The MDH graph for a well at $(x_D, y_D) = (1, 1/8)$ between two perpendicular sealing faults is illustrated in Fig. 4.11 for producing times from 0.1 to 100. A straight line of slope 1.1513 is obtained at early times corresponding to infinite reservoir behavior. The slope of this line can be used to determine the flow capacity of the well, kh. For long producing times, i.e., $t_{DA} \geq 100$ and long shut-in times we observe three distinct straight lines which can be used to estimate the distance to each fault. For $t_{DA} = 10$, only the first and second straight lines are shown, while for $t_{DA} < 10$, not even the second line is obtained.

Figure 4.12 presents the MDH graph for a well located at $(x_D, y_D) = (1, 1/2)$ between two perpendicular faults. This figure indicates that it is possible to observe only the first and third lines when $t_{DA} = 100$. However, when $t_{DA} \leq 10$ only the first line is obtained.

In conclusion, the MDH method also is not practical in the presence of multiple sealing fault systems.

Muskat is another well-known method used to analyze pressure buildup data. However, this author[26] showed that the Muskat graph offers no distinguishing features in the

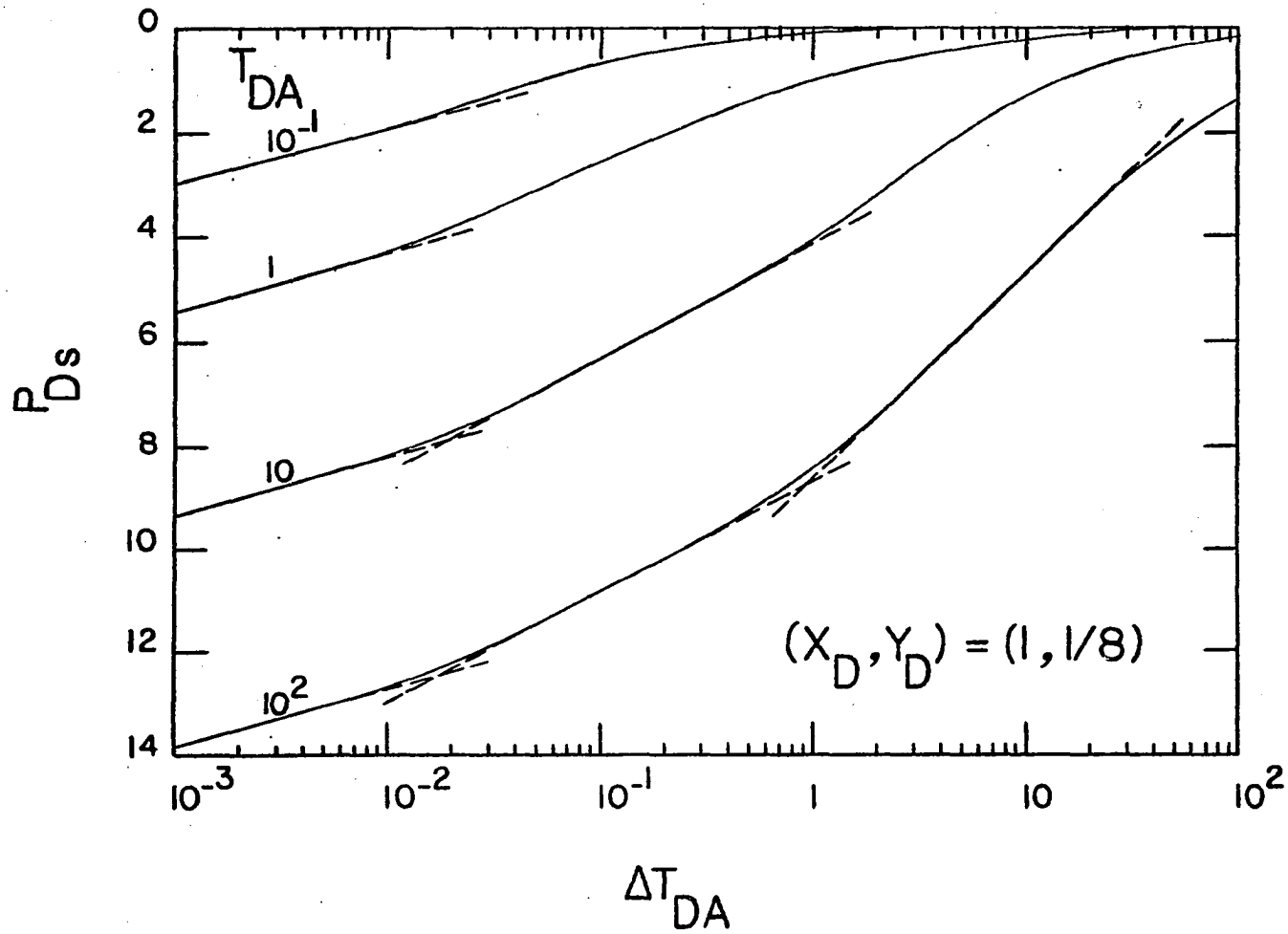

FIGURE 4.11: Miller-Dyes-Hutchinson buildup graph for a well located at $(x_D.y_D) = (1,1/8)$ between two perpendicular sealing faults.

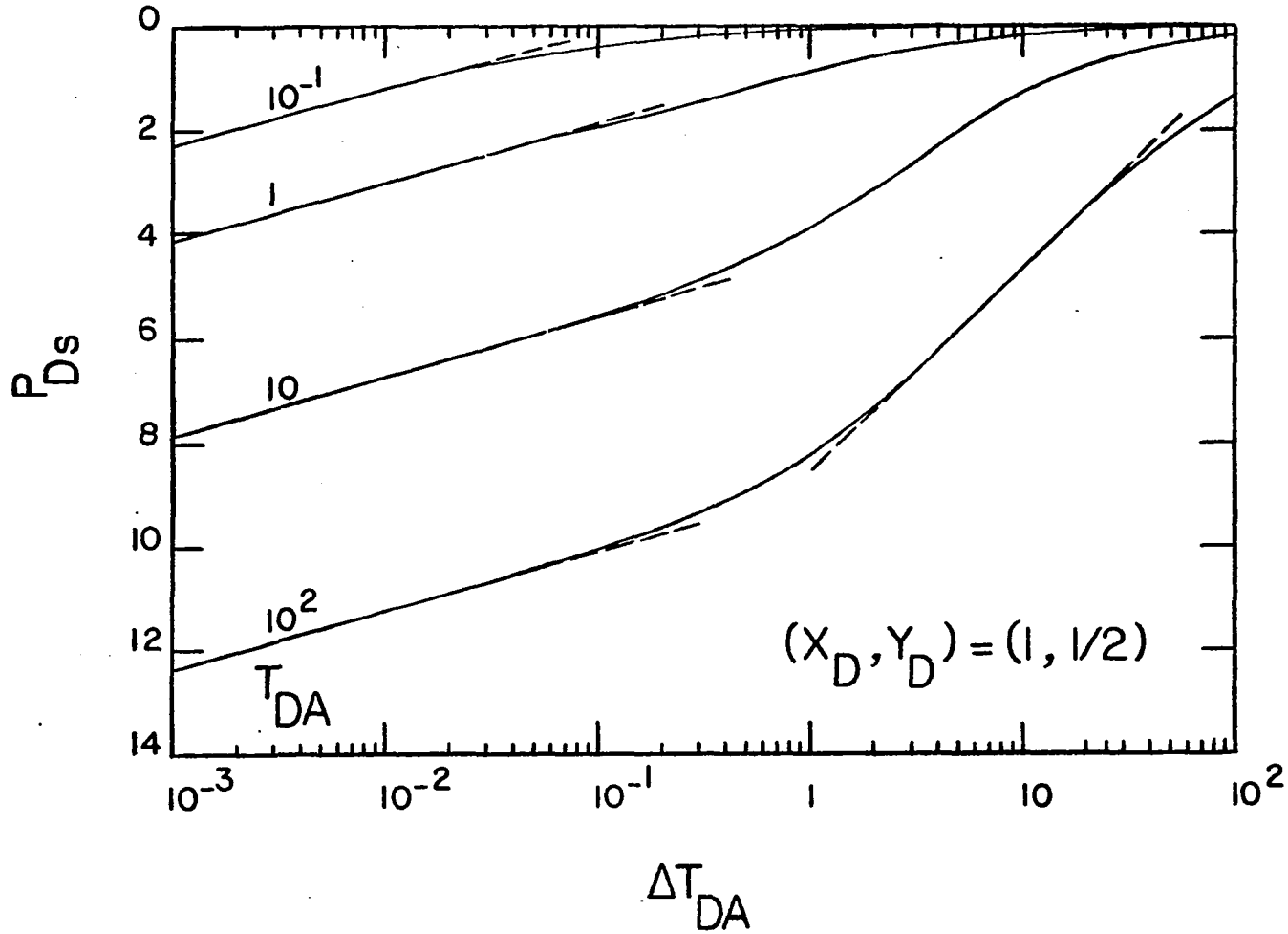

FIGURE 4.12: Miller-Dyes-Hutchinson buildup graph for a well located at $(x_D, y_D) = (1, 1/2)$ between two perpendicular sealing faults.

presence of semi-infinite systems, and therefore will not be discussed here.

4.2.2 Behavior of p'_{Ds}

The behavior of the time rate of change of dimensionless shut-in well pressure for a well located between two perpendicular sealing faults, or no-flow boundaries, is given by:

$$p'_{Ds} = \frac{1}{2(t + \Delta t)_{DA}}\left\{\exp\left[-\frac{(r_w/b_x)^2}{4(t + \Delta t)_{DA}}\right] + \exp\left[-\frac{1}{(t + \Delta t)_{DA}}\right]\right.$$

$$\left. + \exp\left[-\frac{(b_y/b_x)^2}{(t + \Delta t)_{DA}}\right] + \exp\left[-\frac{(b_x^2 + b_y^2)/b_x^2}{(t + \Delta t)_{DA}}\right]\right\}$$

$$- \frac{1}{2\Delta t_{DA}}\left\{\exp\left[-\frac{(r_w/b_x)^2}{4\Delta t_{DA}}\right] + \exp\left[-\frac{1}{\Delta t_{DA}}\right]\right.$$

$$\left. + \exp\left[-\frac{(b_y/b_x)^2}{\Delta t_{DA}}\right] + \exp\left[-\frac{(b_x^2 + b_y^2)/b_x^2}{\Delta t_{DA}}\right]\right\} \qquad (4.19)$$

A log-log graph of $|p'_{Ds}|$ versus Δt_{DA} for seven different values of producing time is shown in Fig. 4.13 for $(x_D, y_D) = (1, 1/8)$. Computed values of p'_{Ds} are also presented in tabular form in Appendix F2. The behavior of p'_{Ds} in Fig. 4.13 can be interpreted by considering three time domains:

(1) $t_{DA} \geq 10^3$: It is evident from Fig. 4.13 that, for such producing times, p'_{Ds} yields three common parallel straight lines of slope -1. This behavior, in view of Fig. 4.5, is the distinguishing feature of a two perpendicular

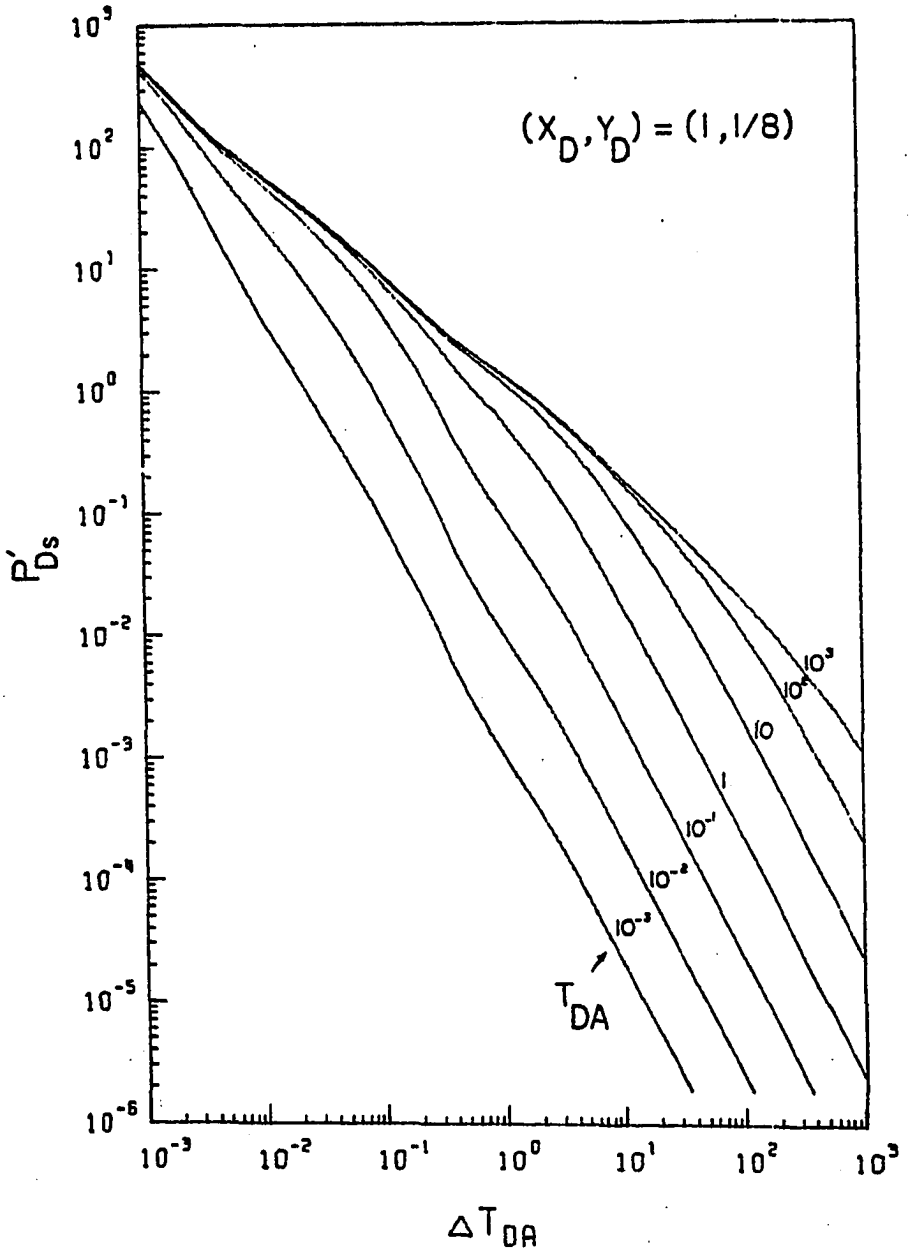

FIGURE 4.13: Type-curve plot of p'_{Ds} vs Δt_{DA} for a well located at (x_D, y_D) = (1,1/8) between two perpendicular sealing faults.

sealing faults system. Note that the dimensionless shut-in time must be at least equal to 10^2.

(2) $10 \leq t_{DA} < 10^3$: Figure 4.13 indicates that for this range of producing times and $\Delta t_{DA} = 1$, we only obtain the first two parallel straight lines. This implies that, under these time conditions, only the closest fault will be detected. However, when the well is closed-in for $\Delta t_{DA} > 1$, p'_{Ds} bends over the second straight line before it becomes a straight line of slope twice that of the first one. This upward bend suggests the existence of another boundary, and the doubling of slope simply means that the well was shut in longer than it produced (see Sec. 2.4.3.1).

(3) $t_{DA} \leq 1$: In this case, the effect of boundaries is not observed at all for $\Delta t_{DA} \leq 0.01$. However, for $\Delta t_{DA} > 0.01$, the curve bends upward then becomes a straight line of slope -2.

Figure 4.14 is another plot of p'_{Ds} versus Δt_{DA} on a log-log graph for $(x_D, y_D) = (1, 1/2)$. Note that only the first and third parallel straight lines are obtained for $t_{DA} \geq 10^3$. Three more plots for $(x_D, y_D) = (1,1)$, $(1, 1/4)$, and $(1, 1/16)$ are included in Appendix I.

Therefore, a log-log plot of p'_{Ds} vs. Δt_{DA} for a well located between two perpendicular faults can be correctly used only when the well was produced for a long time; so old wells are excellent candidates. Under this condition, reservoir parameters such as the kh and ϕc products, and the distance to both boundaries can be estimated by the type curve matching technique, according to the following procedure.

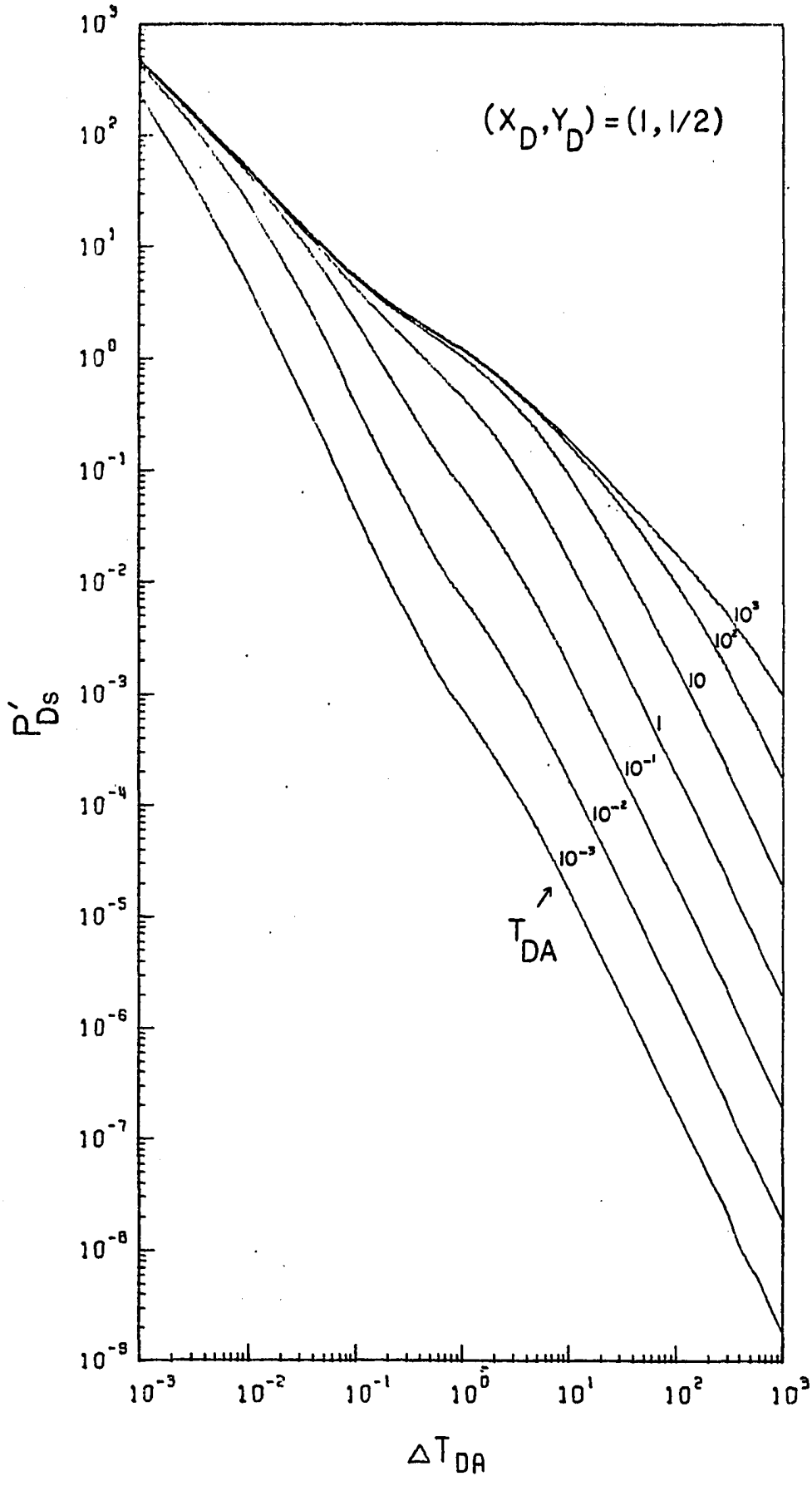

FIGURE 4.14: Type-curve plot of p'_{Ds} vs Δt_{DA} for a well located at $(x_D, y_D) = (1, 1/2)$ between two perpendicular sealing faults.

Buildup Type Curve Matching Procedure

1. Plot the actual time rate of change of shut-in well pressure data $p'_{ws} = \Delta p_{ws}/\Delta(\Delta t)$ against real shut-in time (hr) on log-log tracing paper of the same size cycle as the master type curve (Fig. 4.13).

2. The type curve data plot is placed over the corresponding master type curve, the coordinate axes of the two curves being kept parallel and shifted to a position which represents the best fit of the data to the master curve. More than one of the type curves presented in this chapter and Appendix F may have to be tried to obtain a best fit of all data. This number of trials, however, can be reduced by observing the following distinguishing features.

(a) When all three parallel straight lines are obtained (Fig. 4.13), it implies that the well must be located much closer to one of the boundaries than the other, thus $y_D \leq 1/8$. Further, if the second straight line is one log cycle long (or more), then $y_D \leq 1/16$ (Fig. F3).

(b) When only the first and third straight lines are obtained, it is an indication that the well is far from both faults. If the transition line shows a short flattening as in Fig. F2, the $1/4 \leq y_D < 1/2$. When the effect of both boundaries is felt at the same time, i.e., the well is at equal distances to the boundaries, the first straight line corresponding to the infinite reservoir behavior is unusually long, as shown in Fig. F1 for $y_D = 1$.

If none of the type curves presented here will reasonably fit all the data, it is recommended to use Eq. 4.18 to generate type curves within the range of the suspected value of y_D. A complete set of type curves (full scale), including those for values of y_D not presented here, is available from the author on request.

3. Once the best match is obtained with one of the type curves, pick any convenient match point, and read the corresponding values of $(p'_{Ds})_M$ and $(\Delta t_{DA})_M$ from the master type curve and $(p'_{ws})_M$ and $(t)_M$ from the type curve data plot. These values can then be used to determine the following reservoir parameters.

(a) Flow Capacity:

$$kh = 141.3\ q\mu B(p'_{Ds}/p'_{ws})_M(\Delta t_{DA}/\Delta t)_M \qquad (4.20)$$

(b) Storage Capacity: the ϕc product is obtained by overlaying the first straight line portion of the plot obtained in step 1 over Fig. 2.7.

$$\phi c = (qB/26.856\ r_w^2 h)(p'_{Ds}/p'_{ws})_{M,Fig.\ 2.7} \qquad (4.21)$$

Generally, values of porosity and rock compressibility estimated from laboratory tests (core analyses or logging techniques) are directly used in pressure equations for the entire life of the reservoir. Even though we know that, on one hand, the effective values of these two factors in the reservoir are different from the measured values, and, on the other hand, both factors are nonlinear. The change in

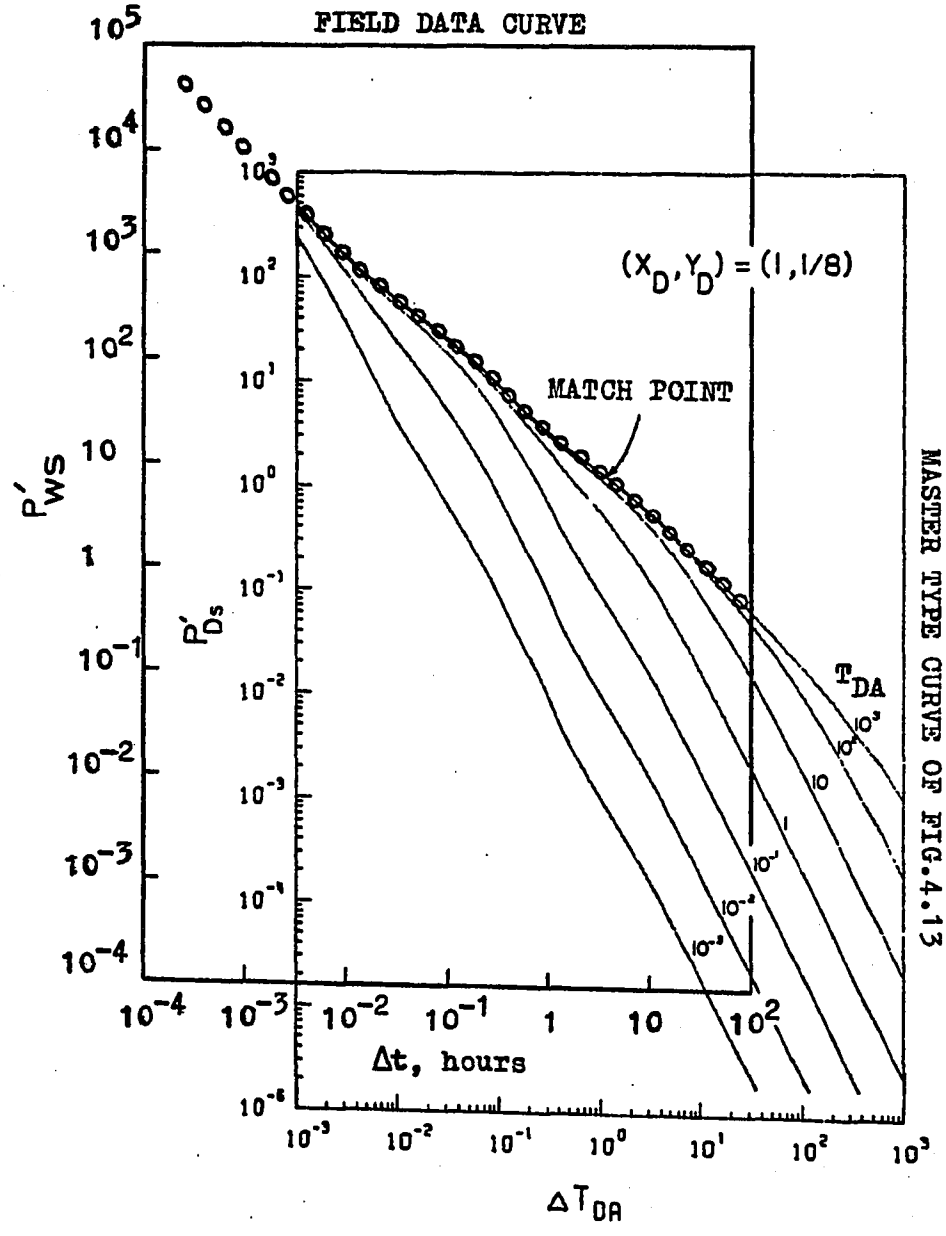

FIGURE 4.15: Buildup type-curve match example.

pore volume and rock compressibility is important in reservoirs or aquifers which contain fluid compressibilities in the range of 3 to 25 x 10^{-6} psi^{-1}, as in oil reservoirs above the bubble point. Even though the rock compressibilities are small figures, their effect, combined with that of porosity, may be considerable on calculations to predict reserves in place. Hence, the in-situ measurements of the product of these two parameters using the technique presented here, whether based on drawdown (last section) or buildup well testing, will be very useful in predicting correctly the reserves in place.

(c) Distance to boundaries

$$b_x = \left[\left(\frac{0.000264\ k}{\phi\mu c}\right)(\Delta t/\Delta t_{DA})_M\right]^{0.5} \qquad (4.22)$$

$$b_y = b_x(y_D)_M$$

4.2.3 Buildup Type-Curve Match Example

The following data was assumed to be taken on a shut-in oil well located between the two perpendicular sealing faults T_1 and L_1 (outside angle) of the Hassi Touareg field (Fig. 3.14) after it had produced 145,550 bbls at an average rate of 355 STB/D. Determine the permeability, the porosity and the distances to faults T_1 and L_1.

$q = 355$ STB/D

$N_p = 145{,}550$ bbls

$h = 18$ ft

$B = 1.084$ res.bbl/STB

$$\mu = 0.42 \text{ cp}$$

$$c = 3.4 \times 10^{-6} \text{ psi}^{-1}$$

$$r_w = 0.30 \text{ ft}$$

The time rate of change of shut-in well pressure (p'_{ws}) field data is shown in Fig. 4.15. The field data curve was placed on the master type-curve of Fig. 4.13 according to the Buildup Type Curve Matching Procedure. The resulting match point has the following data:

$$(\Delta t_{DA})_M = 1 \qquad (p'_{Ds})_M = 1.355$$

$$(\Delta t)_M = 3.538 \text{ hrs} \qquad (p'_{ws})_M = 7.836 \text{ psi/hr}$$

The kh-product can be calculated from Eq. 4.20:

$$kh = (141.3)(355)(0.42)(1.084)\left(\frac{1.355}{7.836}\right)\left(\frac{1}{3.538}\right) = \underline{1116 \text{ md-ft}}$$

then

$$k = \frac{1116}{18} = \underline{62 \text{ md}}$$

Now, place the first straight line portion of the field data curve on the straight line portion of slope -1 ($\Delta t_D << t_D$) of Fig. 2.8 according to step 3.b of the Buildup Type Curve Matching Procedure such that the following relationship holds:

$$(p'_{Ds} \times \Delta t_{DA}/p'_{ws} \times \Delta t)_{M,\text{Fig. } 4.13}$$

$$= (p'_{Ds} \times \Delta t_D/p'_{ws} \times \Delta t)_{M,\text{Fig. } 2.8} = \frac{kh}{141.3\ q\mu B}$$

Using the reservoir data we obtain

$$\frac{kh}{141.3\ q\mu B} = \frac{(62)(18)}{(141.3)(355)(0.42)(1.084)} = \frac{1}{20.46}$$

The effective production life of the well is given by:

$$t = \frac{N_p}{q} = \frac{(24)(145{,}550)}{355} = 9{,}840 \text{ hrs}$$

Thus $t >> \Delta t$ (in this case $\Delta t = 96$ hrs), which indicates that we are in the time domain $t_D >> \Delta t_D$ of Fig. 2.8. Under this condition, we know that the product $p'_{Ds} \times \Delta t_D$ is equal to 0.5 (see Eq. 4 of Appendix D). Hence

$$\begin{aligned}(p'_{ws} \times \Delta t)_{M,\text{Fig. 2.8}} &= 20.46(p'_{Ds} \times \Delta t_D)_{M,\text{Fig. 2.8}} \\ &= (20.46)(0.5) \\ &= 10.23\end{aligned}$$

Any point on the first straight line of the field data curve with $p'_{ws} \times \Delta t = 10.23$ is therefore a match point. Thus a choice of $(\Delta t_D)_M = 10^3$ from Fig. 2.8 yields $(p'_{Ds})_M = 0.5 \times 10^{-3}$ and $(\Delta t)_M = 1.18 \times 10^{-3}$ from the field data curve yields $(p'_{ws})_M = 8.67 \times 10^3$. The ϕc-product is then determined from Eq. 4.21:

$$\phi c = \frac{(355)(1.084)}{(26{,}856)(0.3)^2(18)}\left[\frac{0.5 \times 10^{-3}}{8.67 \times 10^3}\right] = 0.51 \times 10^{-6} \text{ psi}^{-1}$$

then

$$\phi = \frac{0.51 \times 10^{-6}}{3.4 \times 10^{-6}} = \underline{0.15}$$

The distance to the furthest of the two faults can be calculated from Eq. 4.22.

$$b_x = \left[\frac{(0.000264)(62)}{(0.15)(0.42)(3.4 \times 10^{-6})}\left[\frac{3.538}{1}\right]\right]^{0.5} = \underline{512 \text{ ft}}$$

Finally, Fig. 4.15 indicates that the match was obtained for $(x_D,y_D)_M = (1, 1/8)_M$. The distance to the closest fault is determined from Eq. 4.7.

$$b_y = (512)(1/8) = \underline{65 \text{ ft}}$$

In summary, this chapter discussed the drawdown and buildup well pressure behavior for a well located between two sealing faults, or no-flow boundaries, intersecting at a right angle in an otherwise infinite reservoir. As demonstrated, type curves based on the time rate of change of dimensionless well pressure, p'_{Dw}, offer a simple but powerful tool for measuring the distance to both boundaries. Interpretive equations were also developed to calculate flow capacity (kh) and storage capacity (ϕc).

The behavior of dimensionless shut-in well pressure using Horner and Miller-Dyes-Hutchinson methods was presented. Both methods were found to be useful only for long producing and shut-in times. Type curves based on the time rate of change of dimensionless shut-in well pressure, p'_{Ds}, can be used to measure the distance to the two perpendicular sealing faults and both kh and ϕc products.

In the next chapter, the transient pressure behavior for a well located between three perpendicular sealing faults, or no-flow boundaries, is presented.

CHAPTER V

WELL BETWEEN THREE PERPENDICULAR SEALING FAULTS

The type curve technique outlined in the last chapter is systematically applied here to analyze the transient pressure behavior of a single well located inside a system of three linear no-flow boundaries, or sealing faults, intersecting at right angles, in an otherwise infinitely large reservoir. It is, of course, assumed that the well is producing at a constant rate and the reservoir fluid is slightly compressible. The formation is isotropic and of constant thickness.

Note that this system of three sealing faults has not been analyzed to the author's knowledge in the petroleum literature and is therefore original to this study.

5.1 Pressure Drawdown Analysis

Figure 5.1 shows the main locations considered for pressure analysis of a well between three perpendicular no-flow boundaries, or sealing faults. The well location is defined, through this chapter, as follows:

$$(x_D, y_D) = (2b_x/W_x,\ 2b_y/W_x) \qquad (5.1)$$

where:

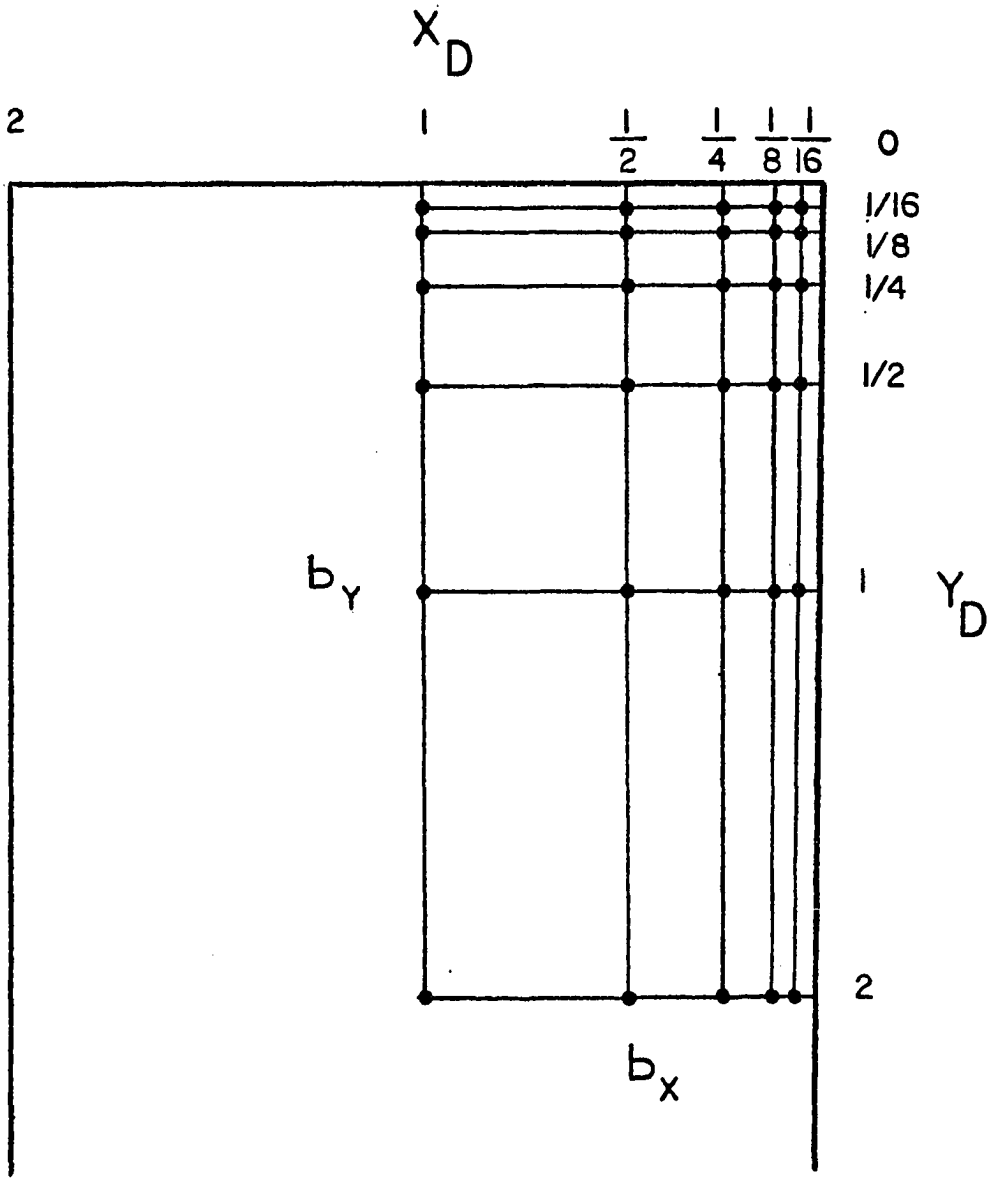

FIGURE 5.1: Three-perpendicular-fault system showing well locations.

W_x = distance between the two parallel boundaries

b_x = distance to the nearest of the two parallel boundaries

b_y = distance to the boundary which is perpendicular to the two parallel ones

5.1.1 Behavior of p_{Dw}

The dimensionless well pressure at any location (x_D, y_D) is the sum of pressure contributions of the two infinite lines of image wells and the real well itself, or

$$p_{Dw} = p_{DR}[r_{DR}, t_{DA}] + p_{DI}[r_{DIy}, t_{DA}] + 2 \sum_{n=2k}^{\infty} \{p_{DI}[r_{Dxe}, t_{DA}] + p_{DI}[r_{DIxe}, t_{DA}]\} + \sum_{n=2k-1}^{\infty} \{p_{DI}[r_{Dxo}, t_{DA}] + p_{DI}[r_{DIxo}, t_{DA}] + p_{DI}[r_{Dxop}, t_{DA}] + p_{DI}[r_{DIxop}, t_{DA}]\} \quad (5.2)$$

This equation is simply another form of Eq. 3.26 where r is replaced by r_w in the dimensionless radius r_{DR}, which was defined as r/W_x.

Figure 5.2 shows dimensionless well pressure, p_{Dw}, versus dimensionless time, t_{DA}, on a semi-log graph, for various locations of the well within a semi-finite system of three boundaries. At location (1/32, 1/8), i.e., the well is very close to two perpendicular boundaries, we observe three straight lines. The first line, of slope 1.15, corresponds to the infinite reservoir behavior. The second line, of slope 2.30, represents the effect of the closest fault, which in this case is the closest of the two parallel

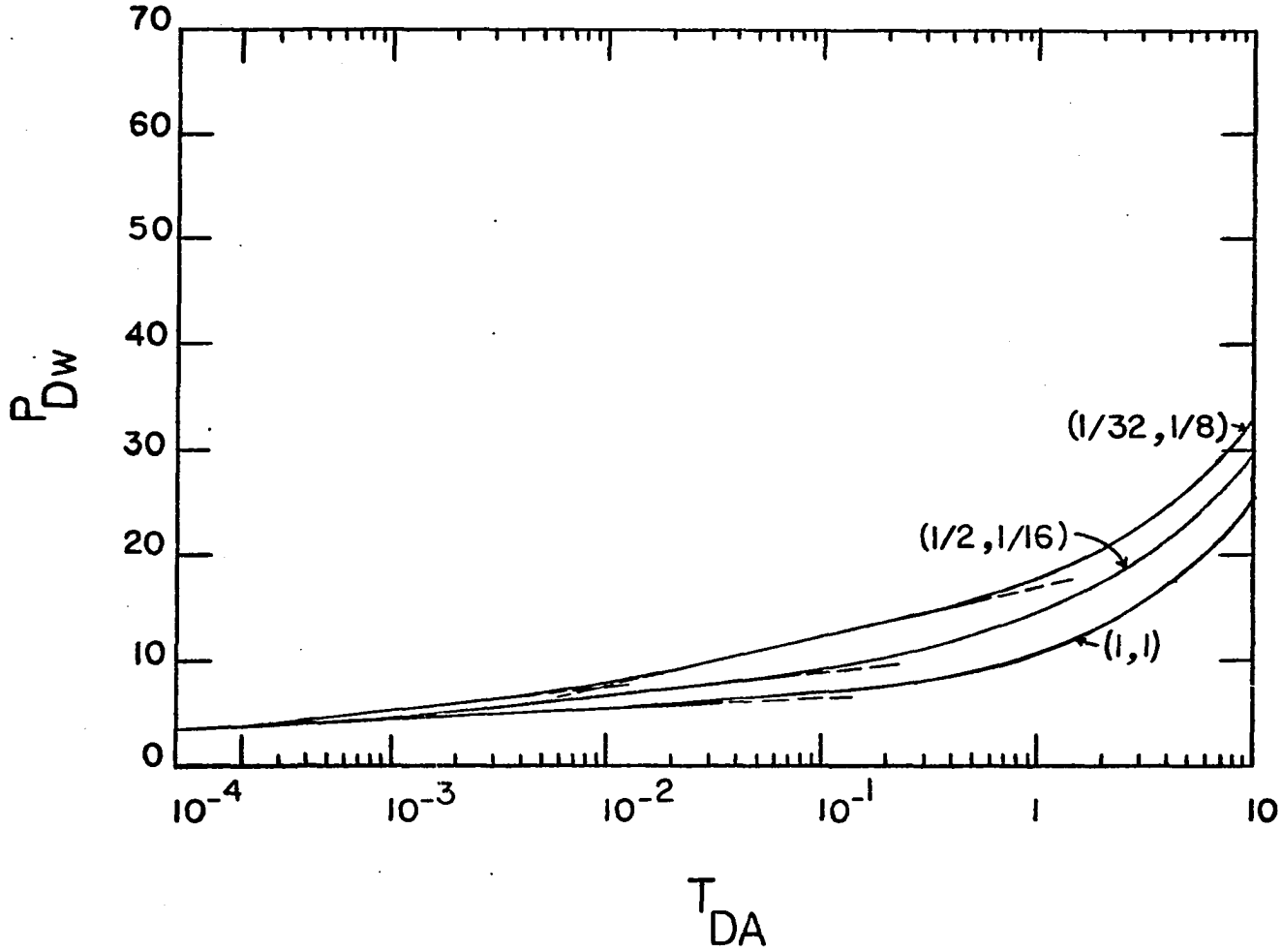

FIGURE 5.2: Semilog plot of p_{Dw} vs t_{DA} for a well between three perpendicular sealing faults.

faults. Finally, the third line of slope 4.6 is caused by the effect of the perpendicular fault. The effect of the third boundary is not observed at all. At location (1/2, 1/16) the well is much closer to the perpendicular fault than to either parallel one. In this case, only the closest fault is indicated by a straight line of slope 2.3. This implies that the two parallel faults will not be detected for such a well location. When the well is at equal distance from all three faults of the system, i.e., $(x_D,y_D) = (1,1)$, Fig. 5.2 indicates that a plot of p_{Dw} vs. t_{DA} cannot be used to determine the distance to each fault, since there are no straight lines observed. This behavior is due to the interference effects of the two infinite lines of image wells.

Figure 5.2 points to the limitations of the drawdown well pressure function in detecting multiple sealing faults. It is clear that, at the most, only the two closest perpendicular boundaries can be located. It is shown in the following section that the time rate of change of well pressure offers a much better description of a multiple sealing fault system.

5.1.2 Behavior of p'_{Dw}

The behavior of the rate of change of dimensionless well pressure of a single well located in a semi-finite system composed of three perpendicular no-flow boundaries, or sealing faults, is obtained by differentiating Eq. 5.2 or 3.26 with respect to the dimensionless time t_{DA}, or:

$$p'_{Dw} = p'_{DR}[r_{DR}, t_{DA}] + p'_{DI}[r_{DIy}, t_{DA}] + 2 \sum_{n=2k}^{\infty} \{p'_{DI}[r_{Dxe}, t_{DA}] + p'_{DI}[r_{DIxe}, t_{DA}]\} + \sum_{n=2k-1}^{\infty} \{p'_{DI}[r_{Dxo}, t_{DA}] + p'_{DI}[r_{DIxo}, t_{DA}] + p'_{DI}[r_{Dxop}, t_{DA}] + p'_{DI}[r_{DIxop}, t_{DA}]\} \quad (5.3)$$

Type curve plots of p'_{Dw} versus t_{DA} for eleven values of y_D are presented in figures 5.3 and 5.4, respectively, for $x_D = 1/32$ and $1/8$. This plot shows the existence of four distinct straight line portions: (1) The first straight line, observed at early production, has a slope $m_1 = -1$. This line represents infinite media without the effects of faults as shown in Fig. 2.5. (2) The second and third straight lines correspond to the effects of two perpendicular sealing faults as shown in Fig. 4.5, and have the same slopes as the first line, i.e., $m_3 = m_2 = m_1$. (3) The fourth straight line of slope $m_4 = -0.5$ is influenced by the third boundary, which is parallel to the first boundary observed. Note that a slope of -0.5 is a distinguishing feature of parallel sealing faults as demonstrated by this author[26] in the case of an infinite strip.

Figure 5.5 shows an additional illustration of the behavior of the time rate of change of dimensionless drawdown pressure, p'_{Dw}, versus dimensionless time, t_{DA}, for eleven well locations along the symmetrical axis of the semi-infinite strip. For these well locations, the effects of the two parallel boundaries are felt at the same time and

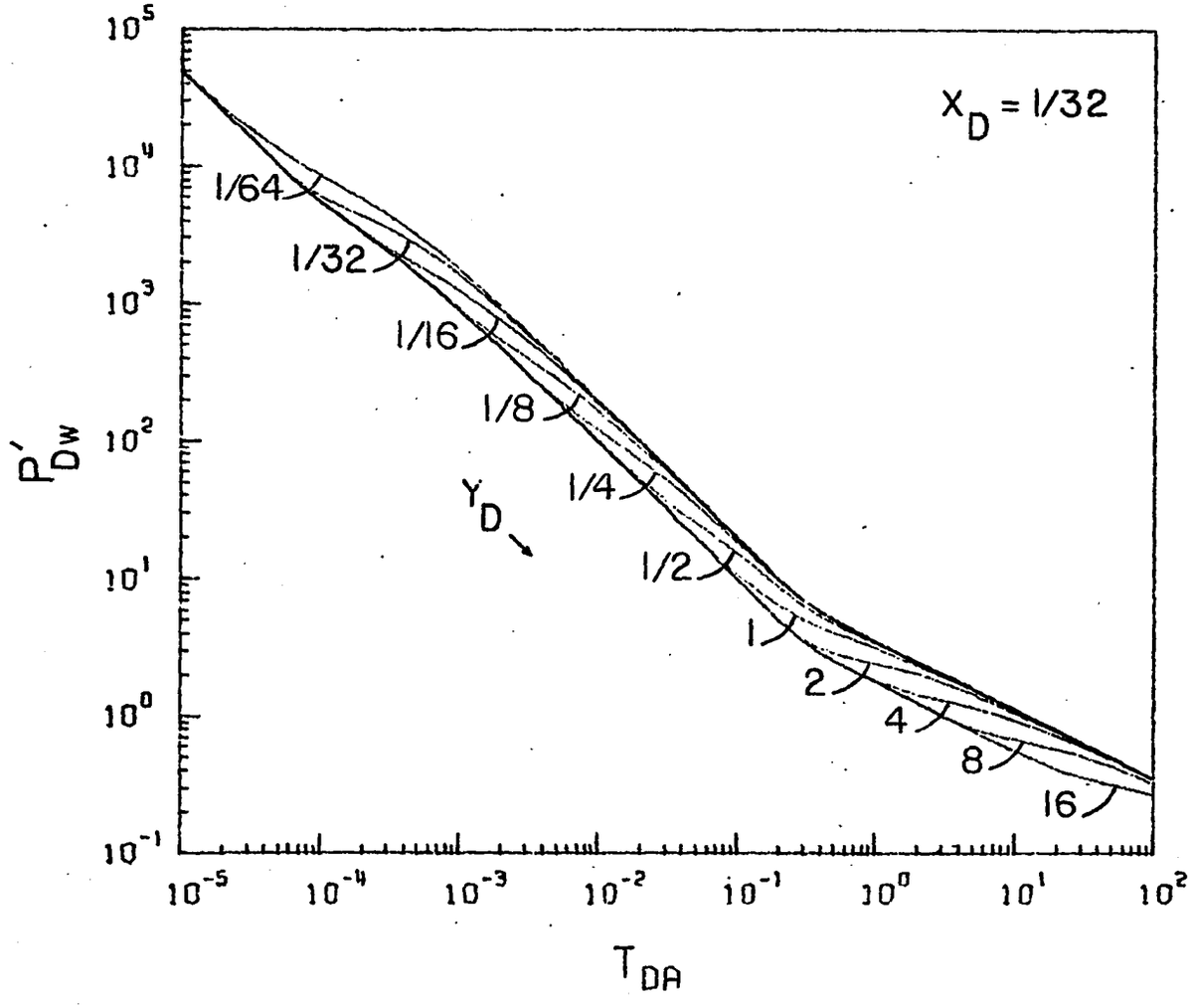

FIGURE 5.3: Type-curve plot of p'_{Dw} vs t_{DA} for a well between three perpendicular sealing faults, when $x_D = 1/32$ and $1/64 \leq y_D \leq 16$.

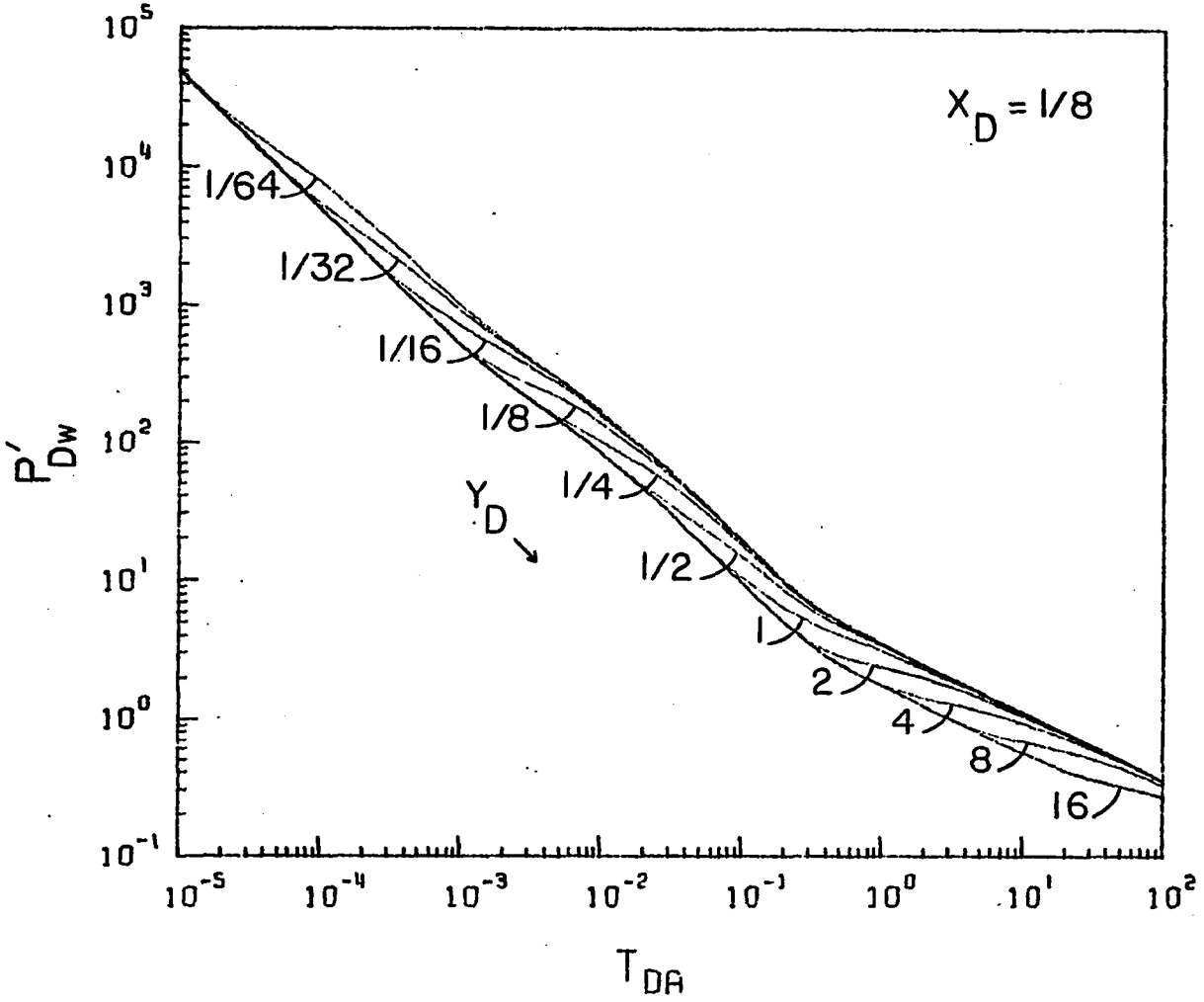

FIGURE 5.4: Type-curve plot of p'_{Dw} vs t_{DA} for a well between three perpendicular sealing faults, when $x_D = 1/8$ and $1/64 \leq y_D \leq 16$.

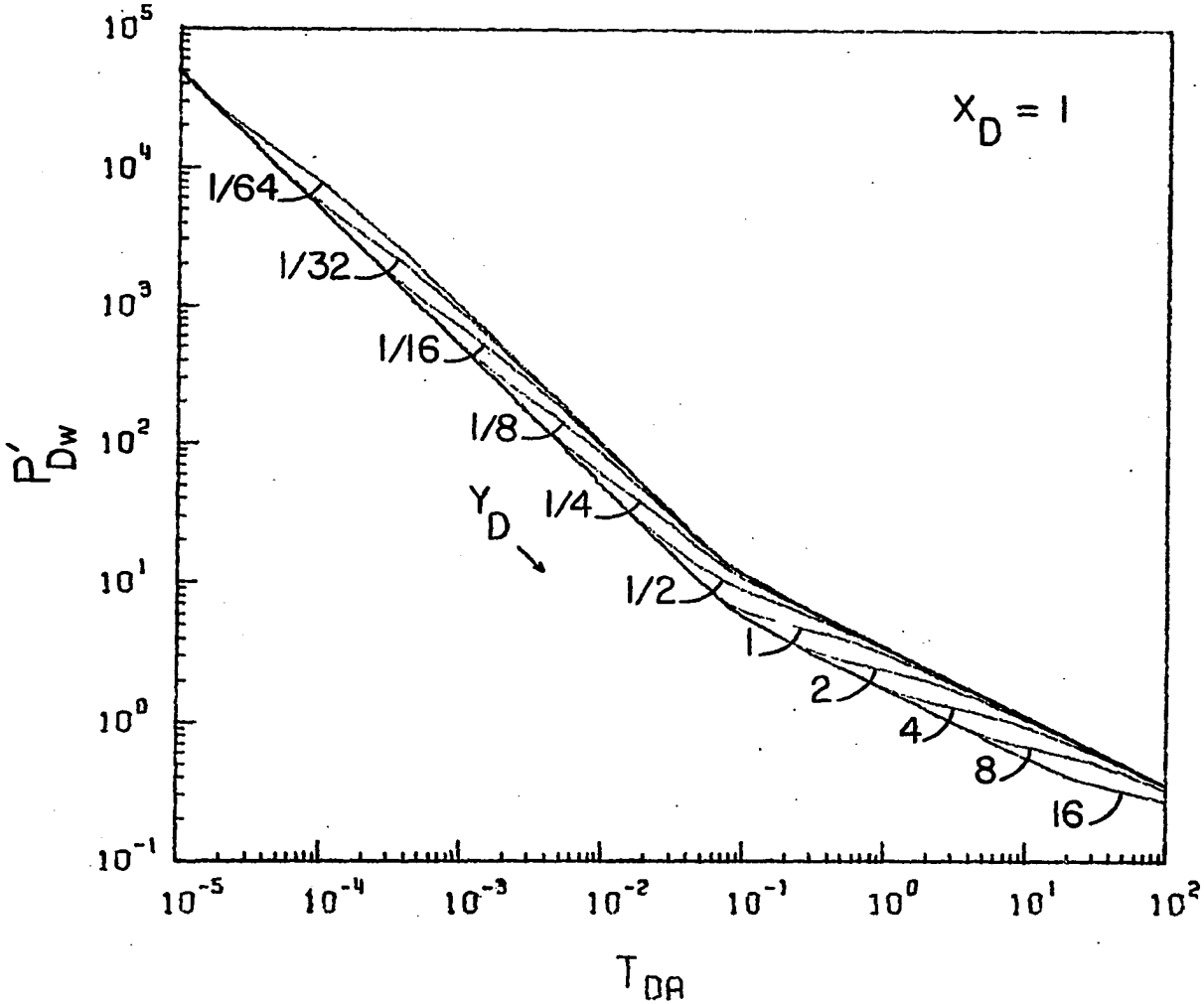

FIGURE 5.5: Type-curve plot of p'_{Dw} vs t_{DA} for a well between three perpendicular sealing faults, when $x_D = 1$ and $1/64 \leq y_D \leq 16$.

therefore we obtain only three straight line portions. The first line of slope -1 and corresponding to the infinite reservoir behavior is observed over a long period of time as opposed to its counterpart of Fig. 5.3 or Fig. 5.4. For values of $y_D \leq 1$, the second straight line has a slope of -1 and represents the effects of the perpendicular fault while the third straight line of slope -0.5 corresponds to the effects of the two parallel faults. However, when $y_D > 1$, both second and third straight lines have a slope of -0.5. This is normal since when $y_D > x_D$, the effects of the two parallel boundaries are felt first, giving a slope of -0.5, then followed by the effects of the perpendicular boundary yielding a third straight line which has a slope of -1 and shifted to the right.

The distance to all three boundaries, a_x, b_x, and b_y, and other reservoir parameters such as the flow capacity kh can be determined by type curve matching technique described in the last chapter. The width W_x is calculated from the match point as follows:

$$W_x = \left[\left(\frac{0.000264\ k}{\phi\mu c}\right)(t/t_{DA})_M\right]^{0.5} \qquad (5.4)$$

The distance to the nearest of the two parallel faults is determined from the value of x_D at the match point, $(x_D)_M$, or

$$b_x = \frac{1}{2} W_x (x_D)_M \qquad (5.5)$$

The distance to the second parallel fault is simply given by:

$$a_x = W_x - b_x \tag{5.6}$$

Finally, the distance to the perpendicular fault is determined from the value of y_D at the match point, $(y_D)_M$, or:

$$b_y = \frac{1}{2} W_x (y_D)_M \tag{5.7}$$

The flow capacity (kh) and storage capacity (ϕc) of this semi-infinite strip can be calculated from the match point, using Eqs. 4.8 and 4.9, respectively.

All three figures, 5.3, 5.4 and 5.5, point out that for values of y_D greater than unity, the effects of the two parallel faults dominate the behavior of the time rate of change of dimensionless drawdown pressure, p'_{Dw}, versus dimensionless time, t_{DA}, which becomes similar to that of an infinite strip. This system is presented in reference 26 and 28. For this reason and also to emphasize the effects of the three perpendicular faults Fig. 5.6 presents the relationship between p'_{Dw} and t_{DA} for $y_D \leq 1$ and $x_D = 1/8$. To spread out the curves of this figure, we plot p'_{Dw} against the dimensionless time t_{Db_x} defined by Eq. 3.23, or in oilfield units:

$$t_{Db_x} = (0.000264\ kt)/(\phi \mu c b_x^2) \tag{5.8}$$

A plot of p'_{Dw} versus t_{Db_x} on a log-log graph is shown in Fig. 5.7 for values of $y_D \leq 1$ and $x_D = 1/8$. The general behavior of the time rate of change of dimensionless well pressure, p'_{Dw}, in Fig. 5.7 is obviously similar to that in Fig. 5.6, except now we have a distinct curve for each well

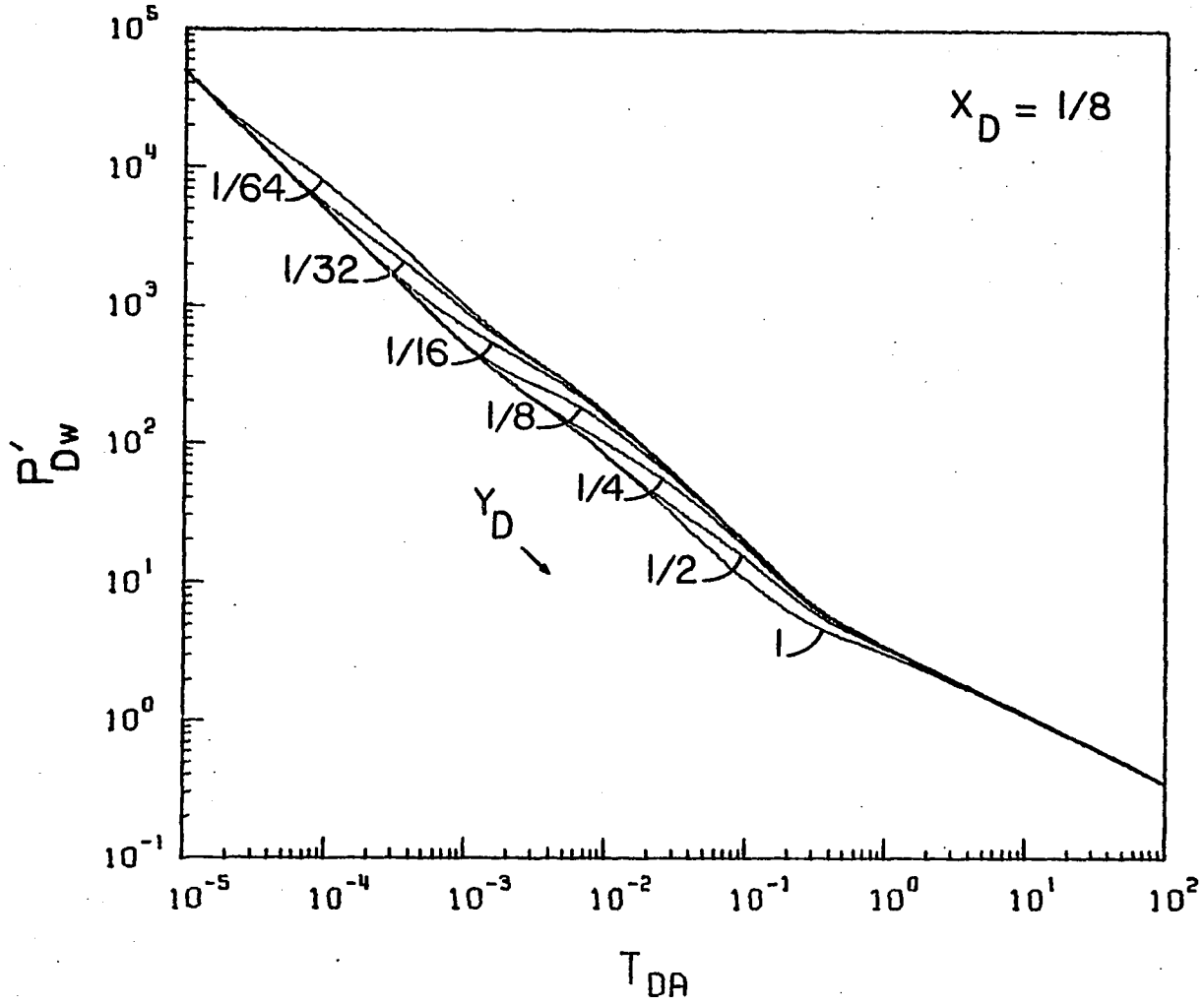

FIGURE 5.6: Type-curve plot of p'_{Dw} vs t_{DA} for a well between three perpendicular sealing faults, when $x_D = 1/8$ and $1/64 \leq y_D \leq 1$.

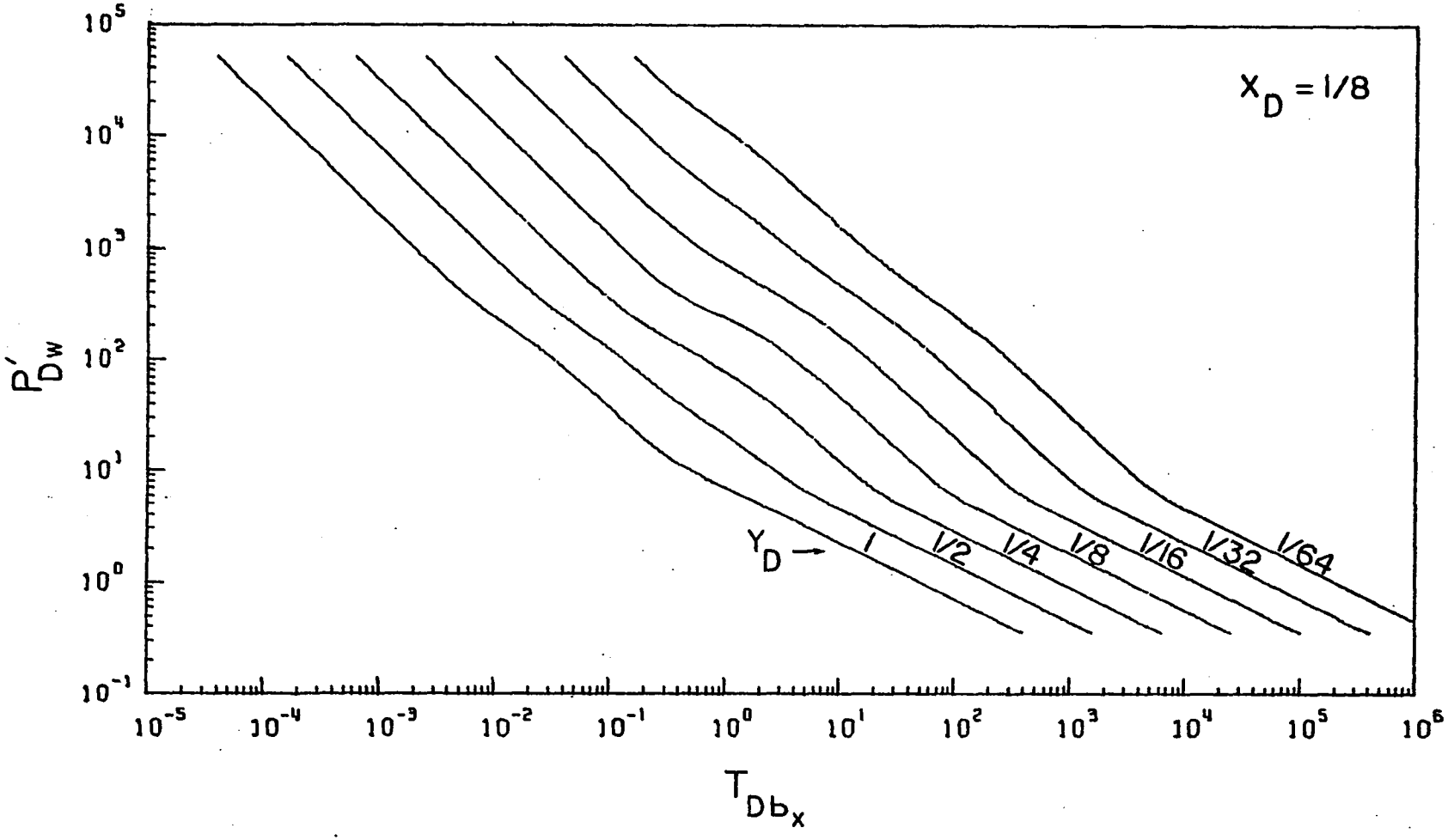

FIGURE 5.7: Type-curve plot of p'_{Dw} vs t_{Db_x} for a well between three perpendicular sealing faults, when $x_D = \frac{1}{8}$ and $1/64 \leq y_D \leq 1$.

location. Figure 5.7 can also be used to determine the distance to each fault in the system, by applying the type curve matching technique described earlier. The distance b_x is calculated first from Eq. 5.8:

$$b_x = \left[\left(\frac{0.000264\ k}{\phi\mu c}\right)(t/t_{Db_x})\right]^{0.5} \tag{5.9}$$

The distance between the two parallel boundaries is given by

$$W_x = 2b_x/(x_D)_M \tag{5.10}$$

The distances a_x and b_y can be calculated from the match point using, respectively, Eqs. 5.6 and 5.7. This match point can also be used to determine the kh and ϕc products from Eqs. 4.8 and 4.9, where t_{DA} is replaced by t_{Db_x}. Finally, just as we plotted p'_{Dw} against t_{DA} and t_{Db_x}, we can plot it against t_{Dbb} which is defined by Eq. 3.41. In oilfield units t_{Dbb} is defined as follows:

$$t_{Dbb} = (0.000264\ kt)/(\phi\mu c b_x b_y) \tag{5.11}$$

Figure 5.8 shows a plot of p'_{Dw} versus t_{Dbb} on a log-log graph for values of y_D less than or equal to unity and $x_D = 1/8$. The general behavior of the family of curves in this figure is, of course, similar to that in Figures 5.4, 5.6 and 5.7. By applying the type curve matching technique to Fig. 5.8, we can estimate the distance to the perpendicular fault from Eq. 11 as follows:

$$b_x b_y = \left[\left(\frac{0.000264\ k}{\phi\mu c}\right)(t/t_{Dbb})_M\right]^{0.5} \tag{5.12}$$

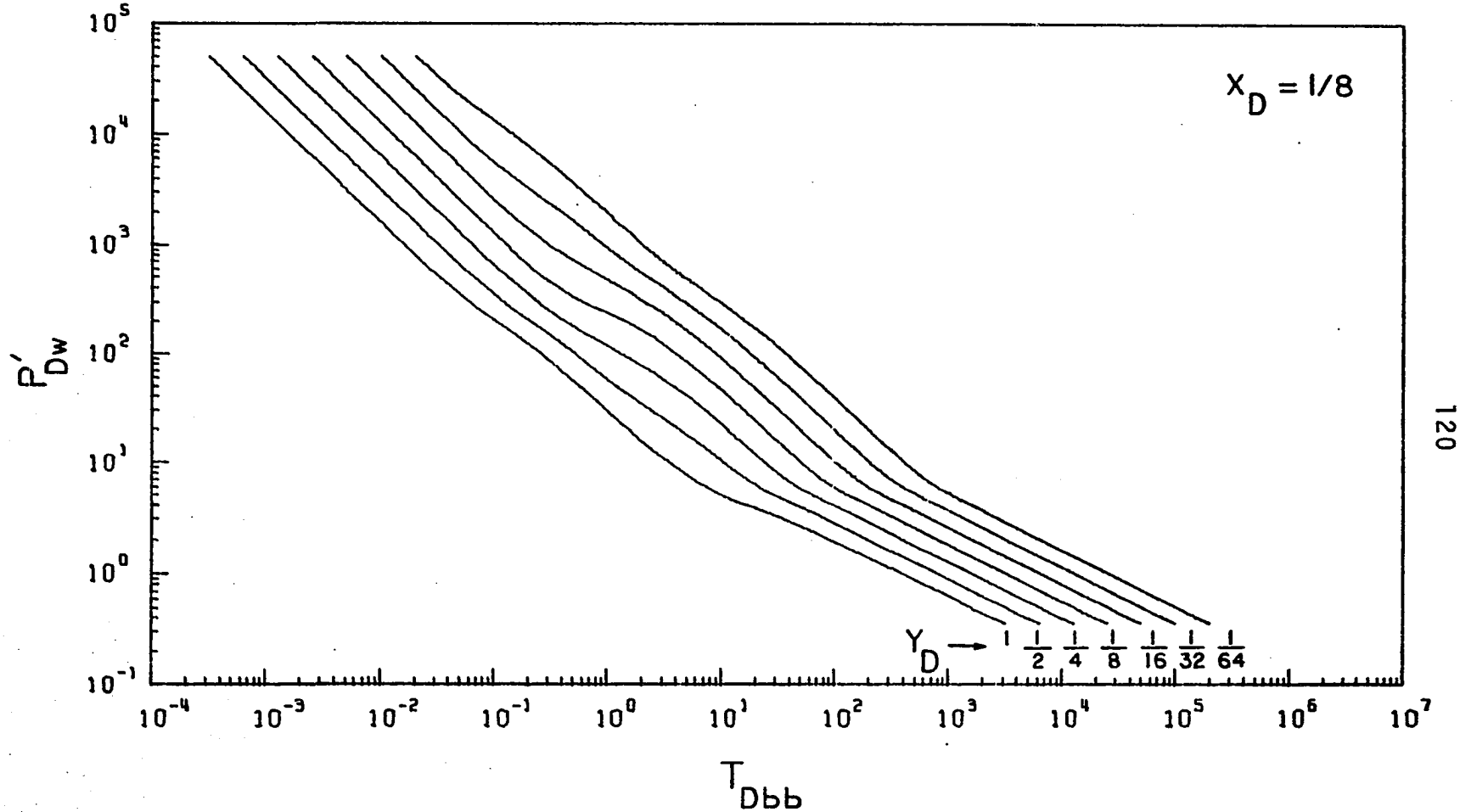

FIGURE 5.8: Type-curve plot of p'_{Dw} vs t_{Dbb} for a well between three perpendicular sealing faults, when $x_D = 1/8$ and $1/64 \leq y_D \leq 1$.

Then, the width W_x can be calculated from the following relationship

$$W_x = 2[(b_x b_y)(x_D)_M(y_D)_M]^{0.5} \qquad (5.13)$$

The distances b_x and a_x, and the products kh and ϕc are respectively determined from equations 5.5, 5.6, 4.8 and 4.9, where t_{DA} is replaced by t_{Db_y}.

Computed values of p_{Dw} and its derivatives for various well locations are presented in Tables 9-12. Figures F.4-9 are additional type-curve plots based on p'_{Dw} for several well locations between three perpendicular sealing faults.

In summary, a type-curve plot of the time rate of change of dimensionless drawdown pressure, p'_{Dw}, against dimensionless times based on any distance of interest, offers several unique characteristics for a single well located between three perpendicular sealing faults. These characteristics can be used to determine the distance to each fault, by using the type curve matching technique presented in the last chapter. The products kh and ϕc can also be estimated from the type curve of p'_{Dw} vs. t_{DA}.

This section has also pointed to the usefulness of p'_{Dw} in detecting multiple sealing boundaries as opposed to p_{Dw} which can at most help locate the nearest boundary.

5.2 Pressure Buildup Analysis

The pressure buildup behavior of a single well located between three sealing boundaries in an otherwise infinitely

large reservoir may be generated by using superposition in time to Eq. 3.26 or Eq. 5.2.

$$p_{Ds} = \frac{1}{2}\left\{Ei\left(-\frac{r_{DR}^2}{4\Delta t_{DA}}\right) + Ei\left(-\frac{r_{DIy}^2}{4\Delta t_{DA}}\right) + 2\sum_{n=2k}^{\infty}\left[Ei\left(-\frac{r_{Dxe}^2}{4\Delta t_{DA}}\right)\right.\right.$$

$$\left. + Ei\left(-\frac{r_{DIxe}^2}{4\Delta t_{DA}}\right)\right] + \sum_{n=2k-1}^{\infty}\left[Ei\left(-\frac{r_{Dxo}^2}{4\Delta t_{DA}}\right) + Ei\left(-\frac{r_{DIxo}^2}{4\Delta t_{DA}}\right)\right.$$

$$\left.\left. + Ei\left(-\frac{r_{Dxop}^2}{4\Delta t_{DA}}\right) + Ei\left(-\frac{r_{DIxop}^2}{4\Delta t_{DA}}\right)\right]\right\} - \frac{1}{2}\left\{Ei\left(-\frac{r_{DR}^2}{4(t+\Delta t)_{DA}}\right)\right.$$

$$+ Ei\left(-\frac{r_{DIy}^2}{4(t+\Delta t)_{DA}}\right) + 2\sum_{n=2k}^{\infty}\left[Ei\left(-\frac{r_{Dxe}^2}{4(t+\Delta t)_{DA}}\right)\right.$$

$$\left. + Ei\left(-\frac{r_{DIxe}^2}{4(t+\Delta t)_{DA}}\right)\right] + \sum_{n=2k-1}^{\infty}\left[Ei\left(-\frac{r_{Dxo}^2}{4(t+\Delta t)_{DA}}\right)\right.$$

$$+ Ei\left(-\frac{r_{DIxo}^2}{4(t+\Delta t)_{DA}}\right) + Ei\left(-\frac{r_{Dxop}^2}{4(t+\Delta t)_{DA}}\right)$$

$$\left.\left. + Ei\left(-\frac{r_{DIxop}^2}{4(t+\Delta t)_{DA}}\right)\right]\right\} \qquad (5.14)$$

where the variables r_D's are defined by the two sets of equations 3.17 and 3.18, and

Δt = shut-in time

t = production time equal to the ratio of total produced fluid to last stabilized flow rate before shut-in, N_p/q.

For analyzing pressure buildup data of a well with constant flow rate before shut-in, there are two plotting procedures that are used most frequently: the Horner method[6] and the Miller-Dyes-Hutchinson method.[7]

5.2.1 Horner Method

This pressure buildup graph is a plot of shut-in pressure data on the ordinate versus the time ratio $(t + \Delta t)/\Delta t$ on the abscissa of a semi-log paper. Equation 5.14 provides the basis for computation of synthetic Horner graphs for different producing times and different well locations. Such a graph is presented in Fig. 5.9 for $(x_D, y_D) = (1/2, 1/2)$. As can be seen from this figure, all producing times yield a straight line of slope 1.151 which corresponds to the infinite media without the effects of faults. The slope of this line is conventionally used to determine the kh product and skin s from Eq. 2.35 and Eq. 2.36, respectively. At time ratio of unity, this line appears to extrapolate to initial pressure (see Eq. 2.45).

Figure 5.9 points to two important results: (1) when t_{DA} is equal to 0.01 (or less), we observe only one straight line of slope 1.151 which extends to infinite shut-in time, i.e., $(t + \Delta t)/\Delta t = 1$, implying that the well is located in an infinitely large reservoir with no faults. This is, of course, a misleading implication. (2) No other straight line is observed that might indicate the existence of sealing faults in the reservoir. Thus, for such a well location, the presence of even one fault would not be suspected.

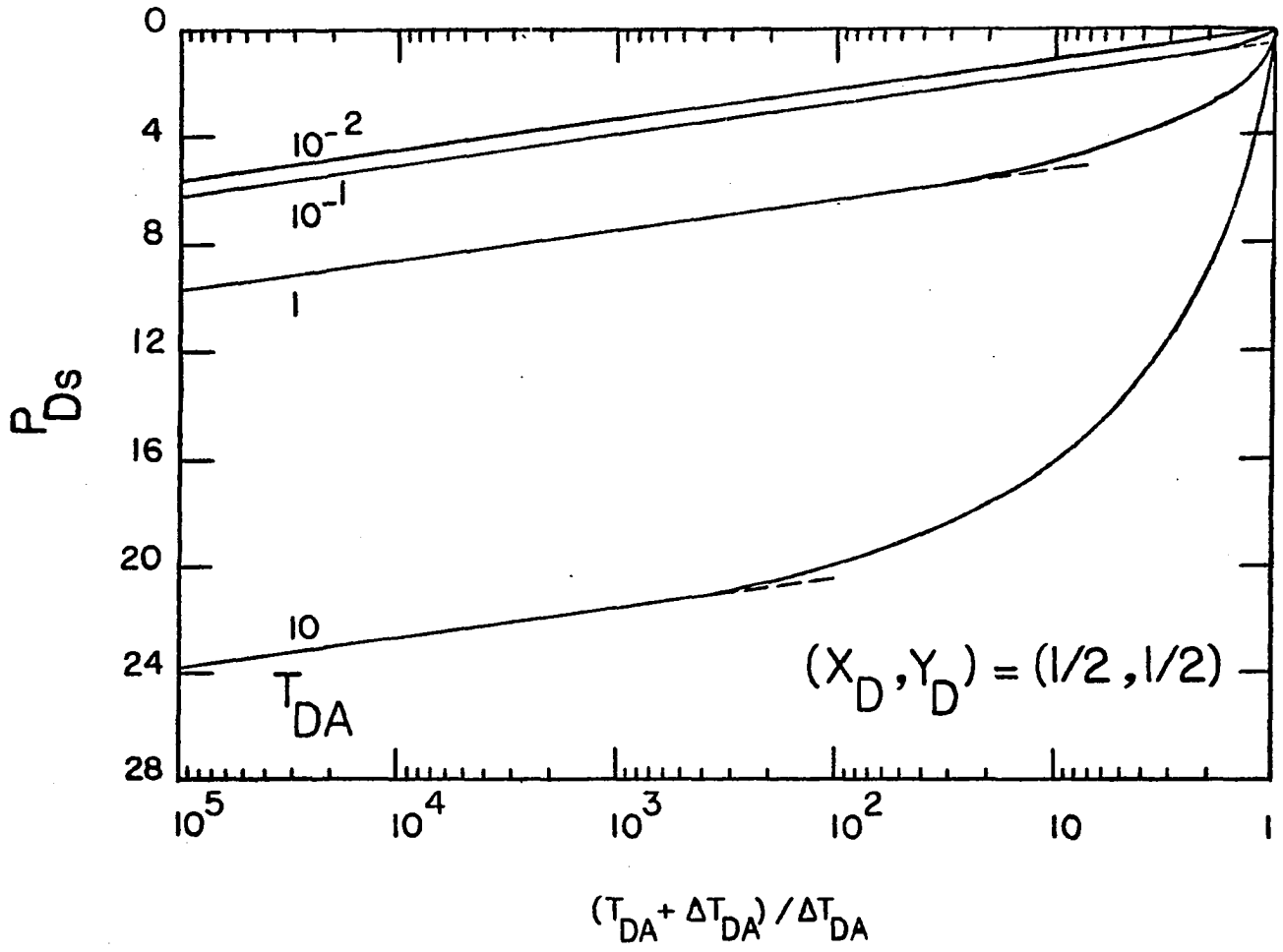

FIGURE 5.9: Horner buildup graph for a well located at (x_D, y_D) = (1/2, 1/2) between three perpendicular sealing faults.

The Horner graph for $(x_D,y_D) = (1/64, 1/2)$, i.e., the well is close to one of the parallel no-flow boundaries, is presented in Fig. 5.10. Note that in this case, we can observe a second straight line of slope 2.3 which can be used to locate the nearest fault. The first line (not fully plotted in this graph) has, of course, a slope of 1.1513.

The preceding has shown that for a well located between three sealing faults intersecting at right angles, the Horner graph will detect only the closest fault.

5.2.2 Miller-Dyes-Hutchinson Method

This method suggests that a graph of shut-in well pressure versus the logarithm of shut-in time should provide a straight line whose slope is proportional to the flow capacity product (kh). The same data computed for the Horner method, using Eq. 5.14, may also be plotted in this fashion to explore the properties of this method for a well located between three perpendicular no-flow boundaries, or sealing faults. Figure 5.11 presents such a buildup graph for various producing times for a well located at $(x_D,y_D) = (1/2, 1)$. A straight line of slope 1.151 is obtained for all $t_{DA} \geq 0.10$. The slope of this line, which corresponds to the infinite reservoir behavior without the effects of faults, may be used to calculate the kh product and the skin factor s from Eq. 2.35 and Eq. 2.36, respectively. Note that the length of this straight line becomes very short as the producing time shortens, then vanishes completely for t_{DA} less than or equal to 0.01. Figure 5.12 is another MDH graph

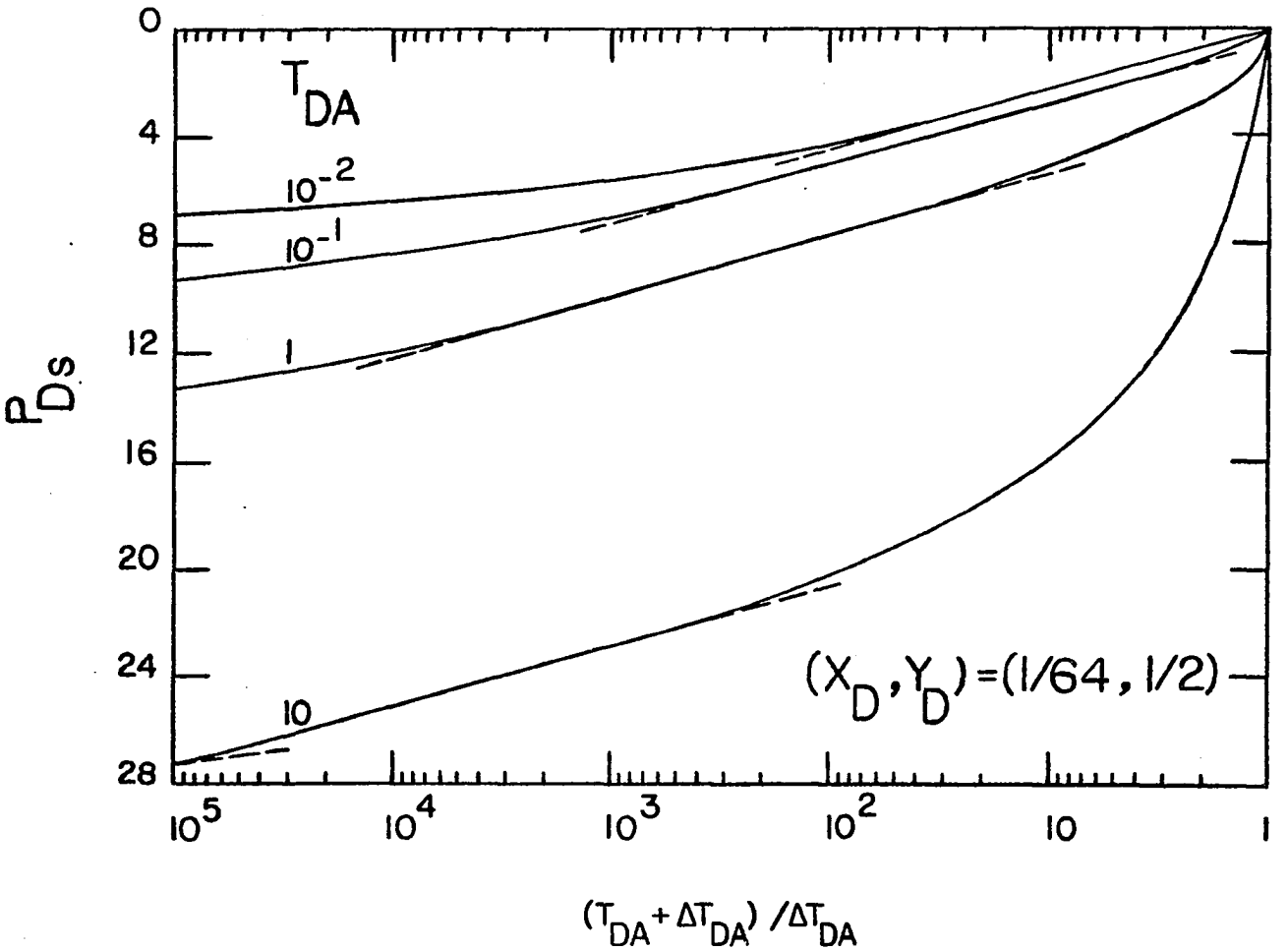

FIGURE 5.10: Horner buildup graph for a well located at (x_D, y_D) = (1/64, 1/2) between three perpendicular sealing faults.

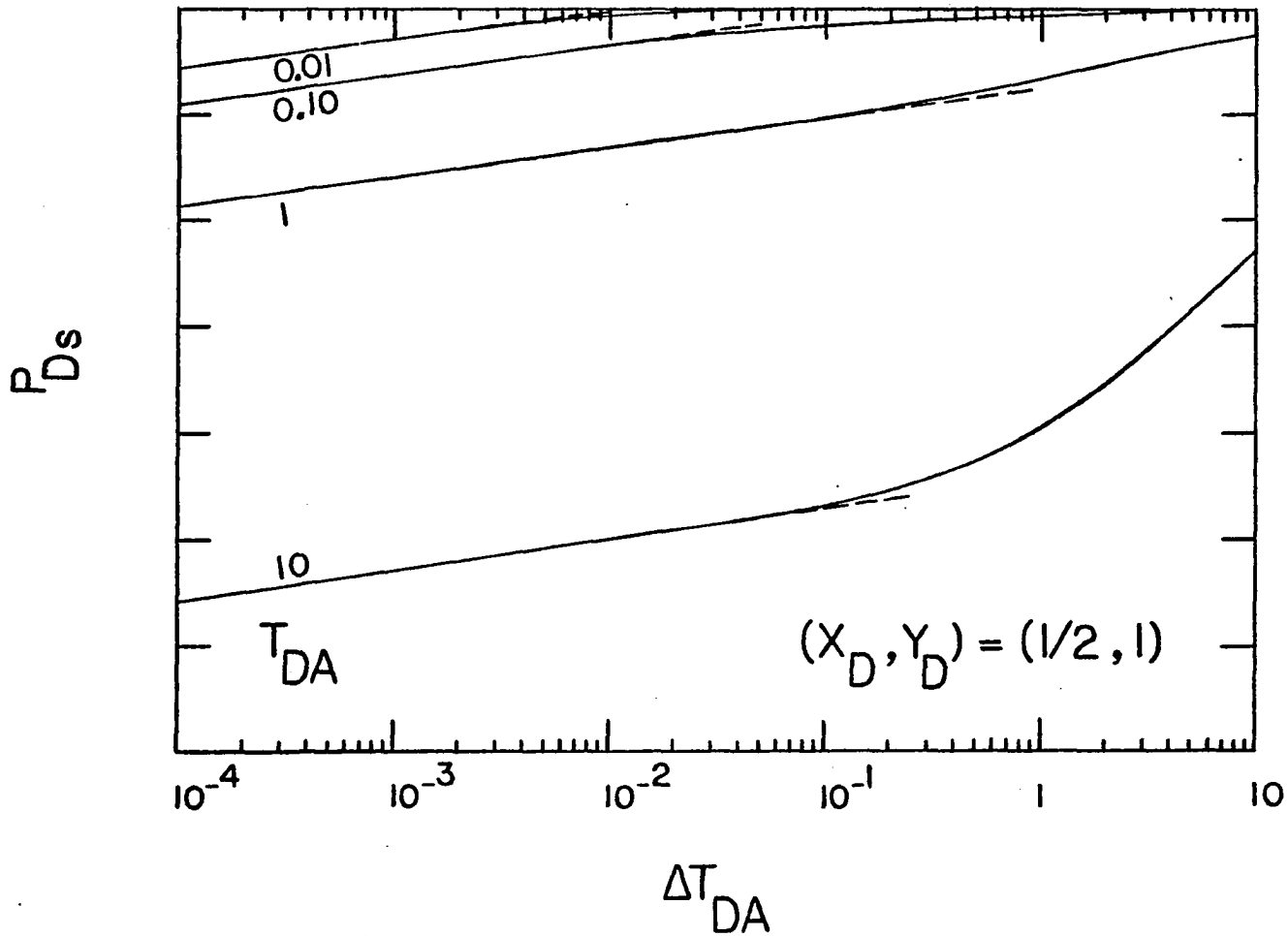

FIGURE 5.11: Miller-Dyes-Hutchinson buildup graph for a well located at (x_D, y_D) = (1/64, 1) between three perpendicular sealing faults.

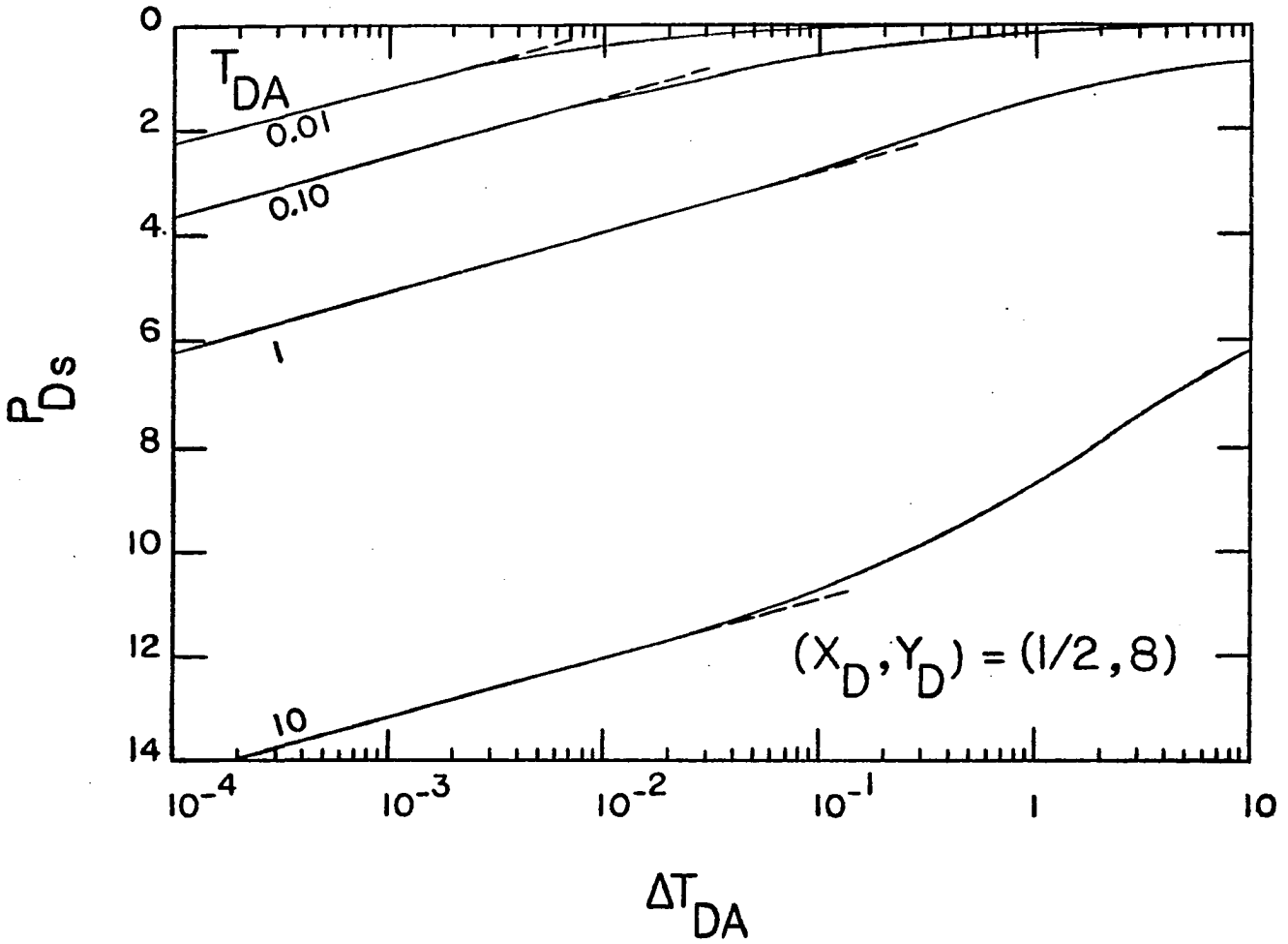

FIGURE 5.12: Miller-Dyes-Hutchinson buildup graph for a well located at $(x_D, y_D) = (1/2, 8)$ between three perpendicular sealing faults.

for $(x_D, y_D) = (1/2, 8)$. The general behavior is similar to that of Fig. 5.11. Both figures fail to indicate the presence of even one fault. However, a second straight line of slope 2.3 would have been observed if we had used the same well locations of Figs. 5.9 and 5.10 for the Horner graph.

Therefore, both Horner and Miller-Dyes-Hutchinson methods cannot be used to locate each boundary of a system composed of three perpendicular sealing faults.

5.2.3 Behavior of p'_{Ds}

The derivative of shut-in well pressure may be obtained by differentiating Eq. 5.14 with respect to time, or

$$
\begin{aligned}
p'_{Ds} = \frac{1}{2(t+\Delta t)_{DA}} \Bigg\{ & \exp\left(-\frac{r_{DR}^2}{4(t+\Delta t)_{DA}}\right) + \exp\left(-\frac{r_{DIy}^2}{4(t+\Delta t)_{DA}}\right) \\
& + 2 \sum_{n=2k}^{\infty} \left[\exp\left(-\frac{r_{Dxe}^2}{4(t+\Delta t)_{DA}}\right) + \exp\left(-\frac{r_{DIxe}^2}{4(t+\Delta t)_{DA}}\right) \right] \\
& + \sum_{n=2k-1}^{\infty} \left[\exp\left(-\frac{r_{Dxo}^2}{4(t+\Delta t)_{DA}}\right) + \exp\left(-\frac{r_{DIxo}^2}{4(t+\Delta t)_{DA}}\right) \right. \\
& \left. + \exp\left(-\frac{r_{Dxop}^2}{4(t+\Delta t)_{DA}}\right) + \exp\left(-\frac{r_{DIxop}^2}{4(t+\Delta t)_{DA}}\right) \right] \Bigg\} \\
& - \frac{1}{2\Delta t_{DA}} \Bigg\{ \exp\left(-\frac{r_{DR}^2}{4\Delta t_{DA}}\right) + \exp\left(-\frac{r_{DIy}^2}{4\Delta t_{DA}}\right) \\
& + 2 \sum_{n=2k}^{\infty} \left[\exp\left(-\frac{r_{Dxe}^2}{4\Delta t_{DA}}\right) + \exp\left(-\frac{r_{DIxe}^2}{4\Delta t_{DA}}\right) \right]
\end{aligned}
$$

$$+ \sum_{n=2k-1}^{\infty} \left[\exp\left(- \frac{r_{Dxo}^2}{4\Delta t_{DA}} \right) + \exp\left(- \frac{r_{DIxo}^2}{4\Delta t_{DA}} \right) + \exp\left(- \frac{r_{Dxop}^2}{4\Delta t_{DA}} \right) \right.$$

$$\left. + \exp\left(- \frac{r_{DIxop}^2}{4\Delta t_{DA}} \right) \right] \Bigg\} \qquad (5.15)$$

Figure 5.13 presents p'_{Ds} as a function of shut-in time, Δt_{DA}, for six producing times of various lengths. The well is located at $(x_D, y_D) = (1/2, 1/64)$. Computed data of p'_{Ds} are presented in Tables 13-16. As discussed in the last chapter, the p'_{Ds} function behaves according to three distinct time domains:

(1) $t_{DA} \geq 10$: When producing times are equal to or greater than 10, Fig. 5.13 yields four parallel straight lines of slope -1, up to $t_{DA} = \Delta t_{DA}$. Then, for $\Delta t_D > t_{DA}$ a fifth straight line of slope -1.5 is observed. This is the distinguishing feature of three perpendicular sealing fault systems. Note, however, that the third straight line is very short (less than half log cycle) for $t_{DA} = 10$.

(2) $10^{-2} \leq t_{DA} \leq 1$: For intermediate values of producing time t_{DA}, we can only observe the first two parallel straight lines of slope -1, which are followed by a long transition period. The last portion of these curves is a straight line of slope -1.5. This characteristic is unique to a system of three perpendicular faults.

(3) $t_{DA} \leq 10^{-3}$: For short producing times, Fig. 5.13 yields three straight line portions of different slopes. The first line of slope -1 represents the infinite reservoir

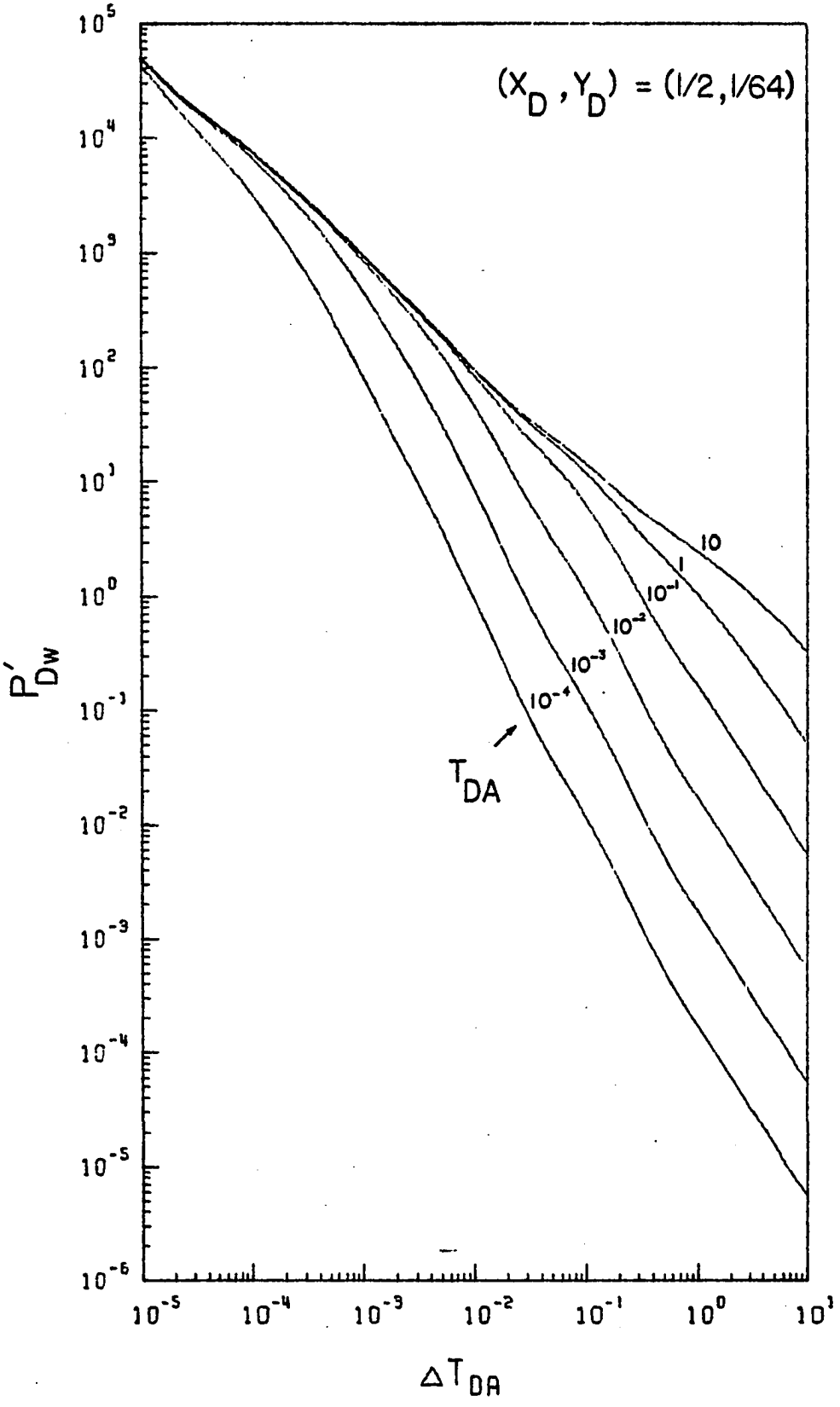

FIGURE 5.13: Type-curve plot of p'_{Ds} vs Δt_{DA} for a well located at $(x_D, y_D) = (1/2, 1/64)$ between three perpendicular sealing faults.

behavior without the effects of faults. The second straight line portion of slope -2 indicates the existence of a perpendicular sealing boundary. When the effects of the second parallel fault are felt, we obtain the third straight line portion of slope -1.5.

Hence, a plot of time rate of field shut-in pressure, p'_{ws}, versus shut-in time on a log-log graph should yield unique characteristics that may be used to locate each fault of the system, and estimate other reservoir parameters such as kh and ϕc products. The type curve matching technique presented in the previous chapter should be followed step by step.

Figure 5.14 shows a plot of p'_{Ds} vs. Δt_{DA} for a single well located between three perpendicular sealing faults at $(x_D, y_D) = (1, 1/64)$. It is evident from this figure that, for such a well location, the third parallel straight line is not observed at all, even when $t_{DA} \geq 10$. However, the double shift to the right of the fourth parallel straight line implies the existence of two parallel faults at equal distances from the well.

A set of type curve plots of p'_{Ds} vs. Δt_{DA}, for various well locations inside a system of three perpendicular faults is included in Appendix F (Fig. F.10-12).

In summary, this chapter presented the behavior of the pressure function and its first derivative for a well located between three perpendicular no-flow boundaries, or sealing faults. It is concluded that the semi-log graph of

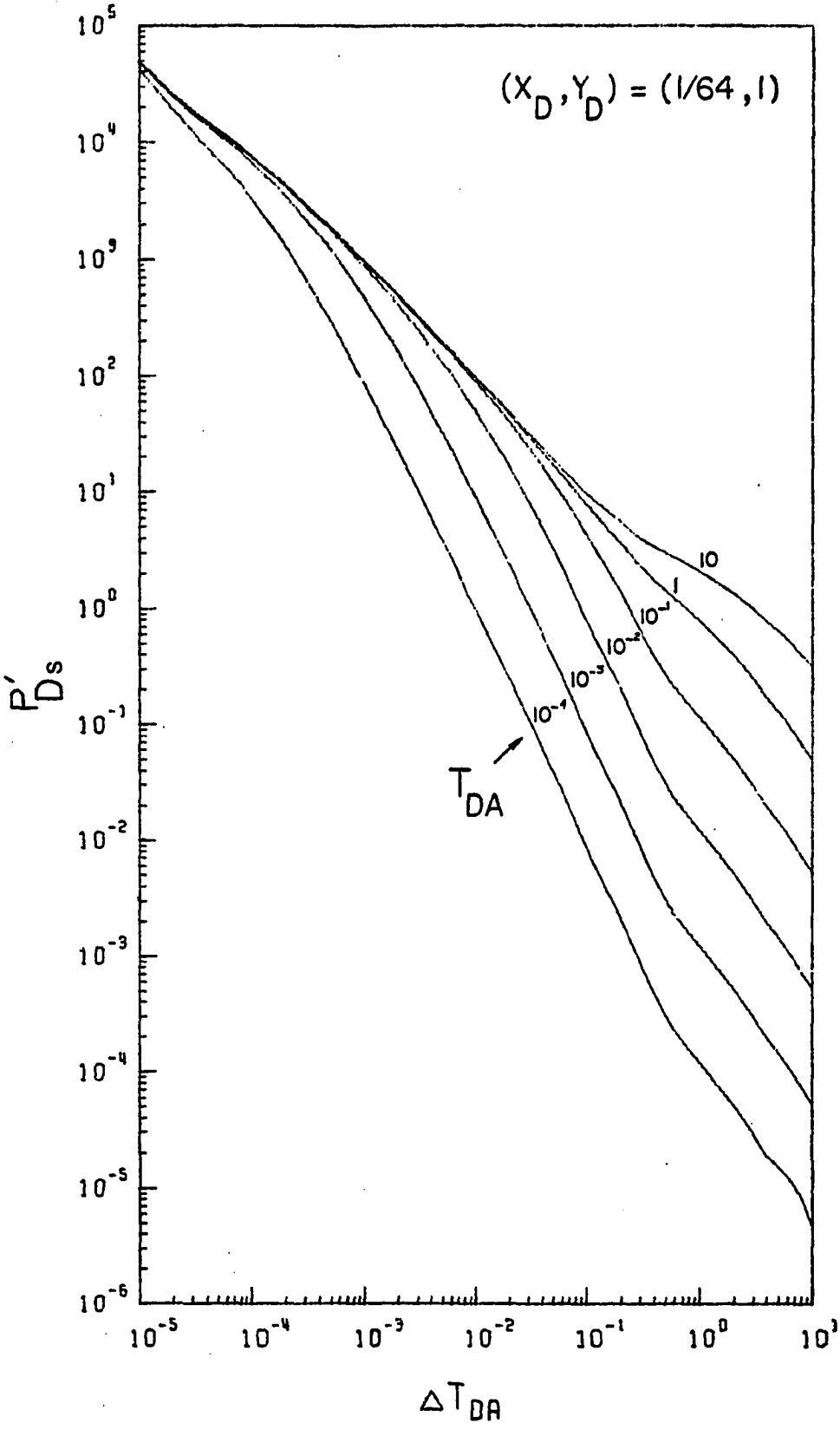

FIGURE 5.14: Type-curve plot of p'_{Ds} vs Δt_{DA} for a well located at $(x_D, y_D) = (1/64, 1)$ between three perpendicular sealing faults.

p_{Dw} vs. t_{DA} can, at the most, help locate the closest fault. However, a plot of p'_{Dw} vs. t_{DA} on a log-log graph offers several unique characteristics which may be used to determine the distance to each fault. The shut-in well pressure behavior as exhibited on both Horner and Miller-Dyes-Hutchinson plots is presented. These common graphs can at most only identify the nearest boundary. Finally, a plot of the time rate of change of dimensionless buildup pressure against dimensionless shut-in time on a log-log graph also shows unique characteristics which may be used to calculate the distance to all three faults.

CHAPTER VI

PRESSURE BEHAVIOR IN CLOSED RECTANGULAR RESERVOIRS

The purpose of this chapter is to present the behavior of the time rate of change of well pressure at several well locations within a variety of rectangular drainage areas with no-flow outer boundaries. The type curve matching technique employed in the last two chapters is systematically applied to locate the well with respect to each boundary of the closed system, and to determine several essential reservoir parameters such as the flow capacity (kh), the storage capacity (ϕc), the initial pressure and extent (A) of the drainage area.

6.1 Pressure Drawdown Analysis

In 1954, Matthews, Brons and Hazebroek[20] demonstrated that the continuous line source solution can be superposed to simulate the behavior of bounded drainage areas. These authors generated the pressure behavior of a bounded single well producing at a constant rate by adding together the pressure disturbances caused by the appropriate array of an infinite number of image wells. Later, Earlougher et al.[24] and Earlougher and Ramey[25] used superposition to produce a

tabulation of the dimensionless pressure drop function at the well and other locations within several closed rectangular drainage shape.

However, none of these authors presented in the literature an analytical equation giving the dimensionless pressure drop of the rectangular drainage system. Also, no interpretive method was developed to locate the well with respect to each boundary of the system. Such information is essential in planning future well locations.

6.1.1 Behavior of p_{Dw}

Consider a well producing at a constant rate anywhere within a closed rectangular reservoir as shown in Fig. 3.6(a). The dimensionless pressure drop function at the well, p_{Dw}, is given by Eq. 3.43, where r is replaced by r_w in r_{DR}. Figure 6.1 shows some of the well locations considered in this study. Dimensionless well locations are defined by:

$$(x_D, y_D) = (2b_x/W_x,\ 2b_y/W_y) \tag{6.1}$$

where

W_x = width of rectangle in the x-direction

W_y = width of rectangle in the y-direction

b_x = distance to the nearest boundary in the x-direction

b_y = distance to the nearest boundary in the y-direction

Because of the symmetry of the rectangular system, it is

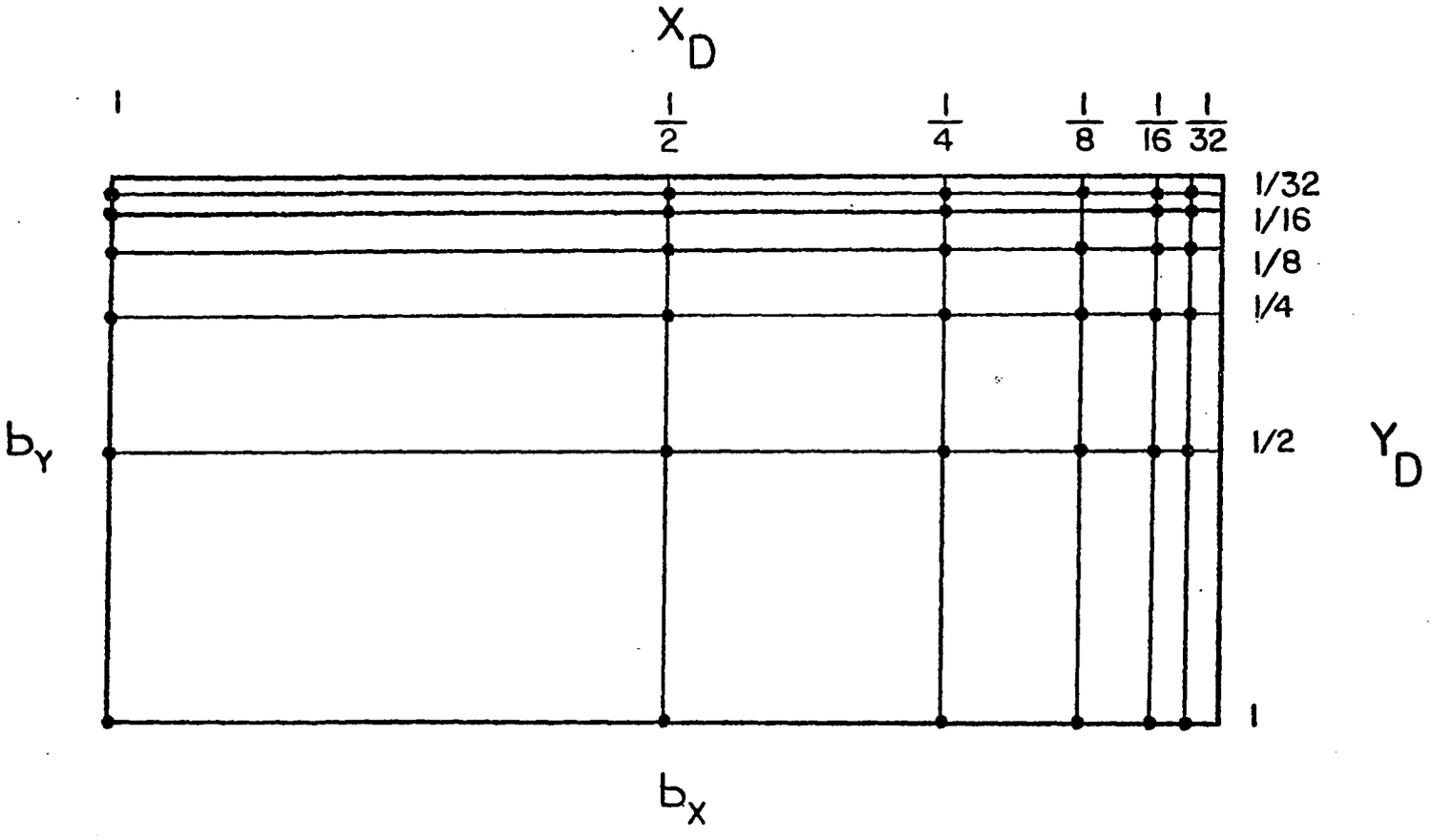

FIGURE 6.1: Quarter I of a rectangular drainage system showing well locations.

necessary to compute pressures only within the quarter shown in Fig. 6.1. This explains the coefficient 2 in Eq. 6.1. In the case of a square the symmetry is not only along the x and y axes, but also along the diagonals; therefore, we need to compute p_{Dw} only within the octant shown in Fig. 6.2. Tables 17 through 21 present the dimensionless functions p_{Dw}, p'_{Dw} and p''_{Dw} as functions of dimensionless drawdown times for various well locations in several closed rectangular drainage systems. The main drainage systems considered in this study are rectangles whose sides are in the following integral ratios: 1:1 (square), 2:1, 4:1, 8:1, and 16:1.

The pressure p at any point of the rectangular reservoir can be computed from Eq. 3.42 or 3.43 by using

$$p = p_i + \frac{70.6\ q\mu B}{kh}\{Ei[-r_{DR}^2/4t_{DA}] + \sum_{n=1}^{\infty} Ei[-r_{DI}^2/4t_{DA}]\} \quad (6.2)$$

where r_{DR} and r_{DI} are the dimensionless distances to the real well and image wells, respectively, and t_{DA} is defined (in oilfield units) as follows:

$$t_{DA} = \frac{0.000264\ kt}{\phi\mu cA} \quad (6.3)$$

where A is the drainage area of the reservoir.

At the well point, Eq. 6.2 becomes

$$p_{wf} = p_i + \frac{70.6\ q\mu B}{kh}[Ei(-r_{Dw}^2/4t_{DA}) + \sum_{n=1}^{\infty} Ei(-r_{DI}^2/4t_{DA})] \quad (6.4)$$

where

$$r_{Dw} = r_w/\sqrt{A} \quad (6.5)$$

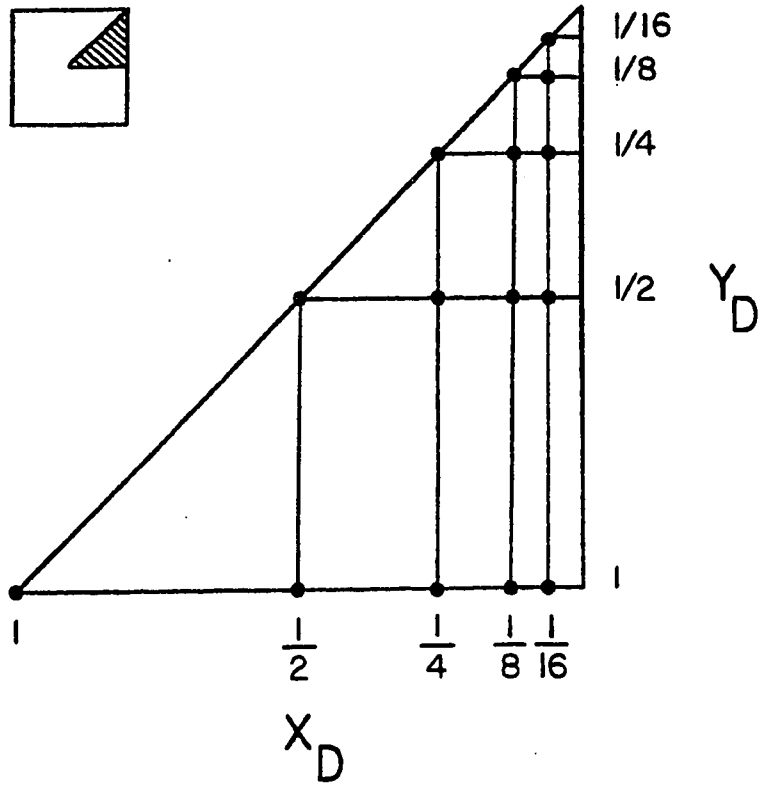

FIGURE 6.2: Octant of a square drainage system showing well locations.

This equation indicates that only the dimensionless pressure at the real well depends on the dimensionless ratio r_{Dw}. The most common value of r_{Dw} used in the literature[24,25] is 0.5×10^{-3}. This value of r_{Dw} is also used in this study solely for the purpose of comparison. For different values of r_{Dw}, Tables 17 through 21 may be modified by subtracting $Ei[-(0.5 \times 10^{-3})^2/4t_{DA}]$ and then adding the appropriate value of $Ei[-r_{Dw}^2/4t_{DA}]$. Using the logarithmic approximation of the exponential integral we find that this operation is equivalent to adding (to tables 17 through 21) directly the "correction factor," ψ_w, which is given by

$$\psi_w = \ln(0.5 \times 10^{-3}/r_{Dw}) \qquad (6.6)$$

where r_{Dw} is any given value different from the one used here. It should be emphasized that the pressure contributions of image wells are independent of the value of r_{Dw}.

Figure 6.3 is a classical plot of p_{Dw} vs. t_{DA} presented by Earlougher et al.,[24] Ramey and Cobb,[38] and Kumar and Ramey.[40] It is clear from this figure that the dimensionless pressure becomes a linear function of dimensionless time, when $t_{DA} \geq 0.010$. This behavior is commonly referred to as pseudo-steady state. Every point within a closed reservoir will eventually reach this state of constant rate pressure decline. However, the time at which p_{Dw} vs. t_{DA} becomes linear depends on the location of the point. This linear portion can be represented (for $t_{DA} \geq 0.010$) by

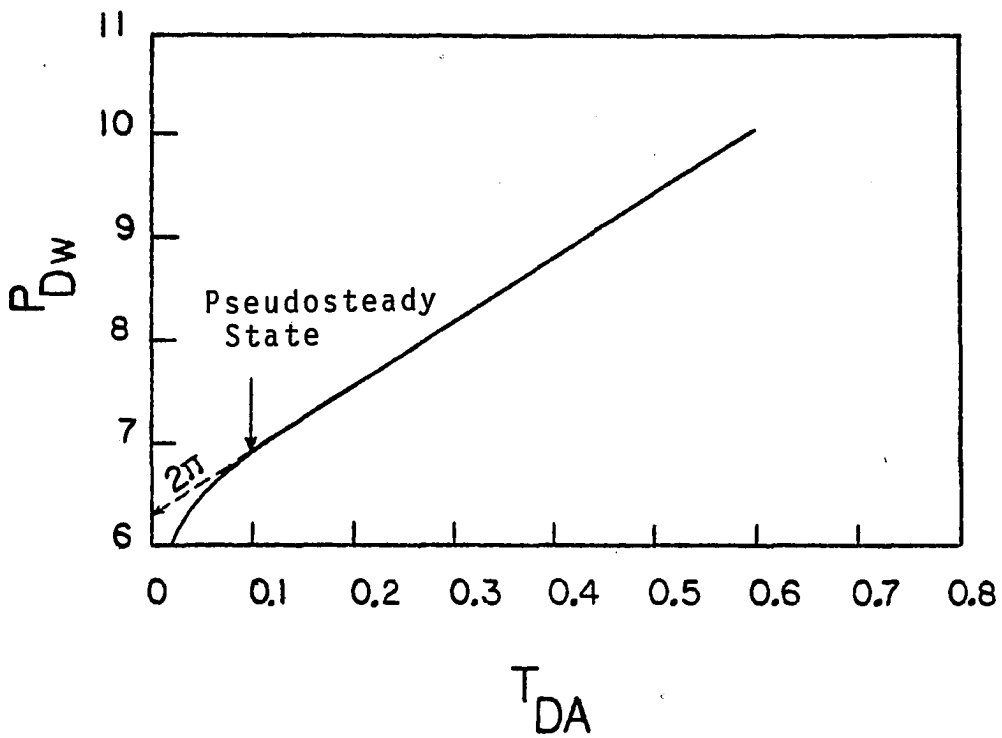

FIGURE 6.3: Linear graph of p_{Dw} vs t_{DA} for a well in the center of a square.

$$p_D(r_{Dw}, t_{DA}) = \ln\left(\frac{1.5}{r_{Dw}\sqrt{C_A}}\right) + 2\pi t_{DA} \qquad (6.7)$$

where C_A is the shape factor of the drainage area for a given well location and closed reservoir. This factor was introduced in the literature by Brons and Miller.[21] Later, Dietz[22] tabulated shape factors for an extensive list of drainage shapes and well locations. For values of C_A not included in the Dietz' tabulations, the techniques of Earlougher et al.[24] and Ramey[31] can be used to determine the needed shape factor. However, the graphical method presented by Earlougher[41] is preferred here because of its simplicity. For example, the shape factor for a well in the center of a closed square is 30.8828. For the same well location, the shape factor of a 2:1 rectangle is 21.8448. Note that a slightly different form of Eq. 6.7 was first published by Ramey and Cobb.[38]

The early portion of the plot of p_{Dw} versus t_{DA} of Fig. 6.3 ($t_{DA} < 0.010$) corresponds to the so-called initial transient period.[40] The equation of this line is, of course, given by the familiar expression

$$p_{Dw} = \frac{1}{2}\left[\ln t_D + 0.80907\right]$$

or

$$p_{Dw} = \frac{1}{2}\left[\ln \frac{t_{DA}}{r_{Dw}^2} + 0.80907\right] \qquad (6.8)$$

Figure 6.4 presents a graph of p_{Dw} versus logarithm of t_{DA} for various well locations in a closed 2:1 rectangle. A straight line of slope 1.151 results for small values of t_{DA} for all locations. This line is represented by Eq. 6.8. For the case of a well in the center of the rectangular reservoir, i.e., $(x_D,y_D) = (1,1)$, we can only observe one straight line which extends to $t_{DA} = 0.08$. The slope of this line can be used, as usual, to estimate the kh product and skin factors from Eqs. 2.35 and 2.36, respectively. When $(x_D,y_D) = (1/32, 1/4)$, i.e., the well is located much closer to the short side of the rectangle than to the longer side, Fig. 6.4 shows the existence of a total of three straight lines. The first line corresponds to the infinite reservoir behavior without the effects of boundaries. The second line of slope 2.3 is caused by the short side, while the third line of slope 4.6 is caused by the long side of the rectangle. Thus, for such well location the two distances b_x and b_y can be estimated by any of the existing techniques. There is a speculation in the literature[16] that one would observe two more straight lines of slopes 8 x 1.151 and 16 x 1.151 which can be used to determine the distances a_x and a_y to the other two boundaries of the closed system. Figure 6.4 shows that such speculation is incorrect and unfounded. It is shown in the following section that p'_{Dw} offers a much better description of all boundaries of a closed rectangular reservoir.

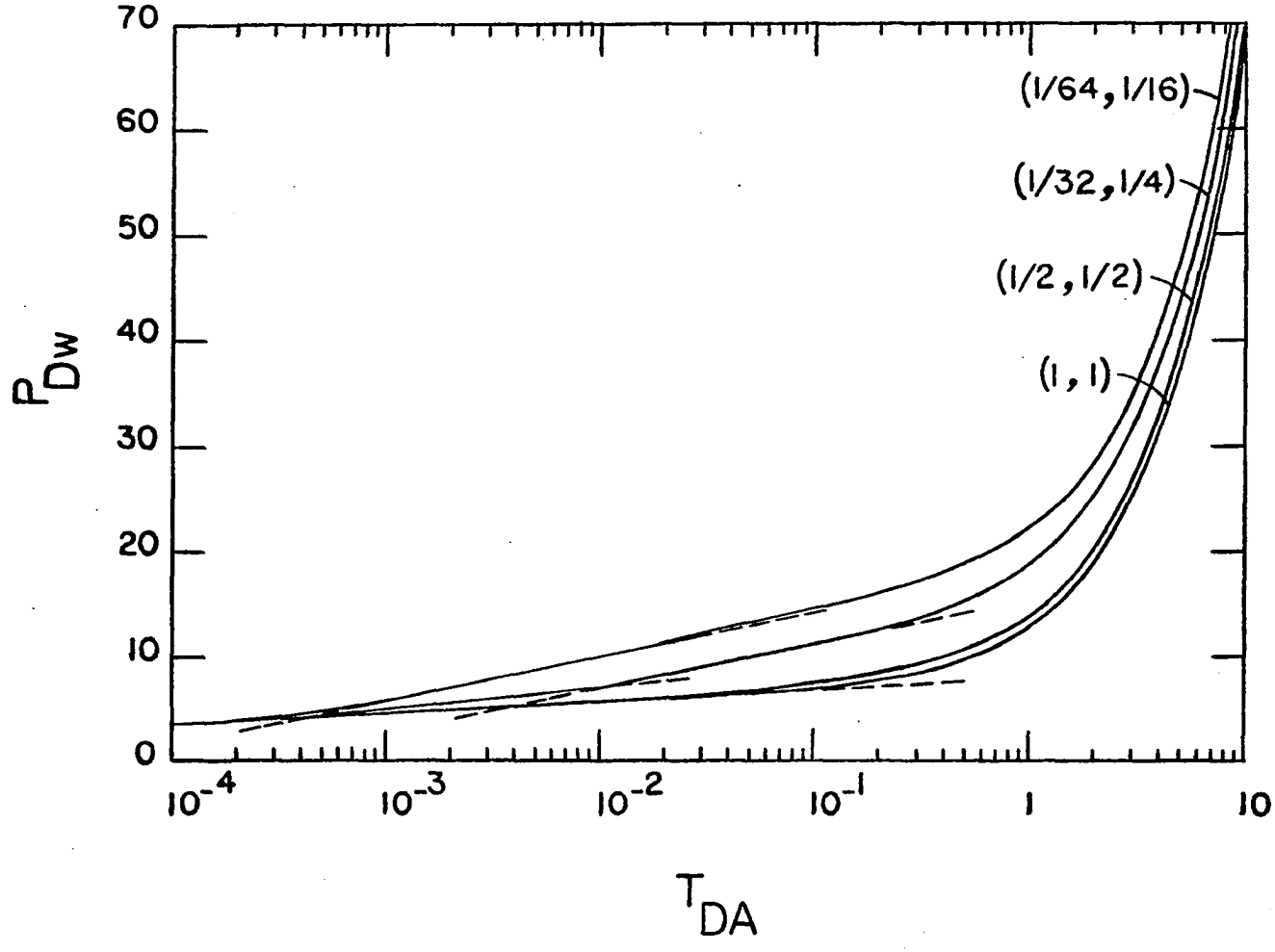

FIGURE 6.4: Semilog plot of p_{Dw} vs t_{DA} for various well locations inside a closed 2:1 rectangle.

6.1.2 Behavior of p'_{Dw}

The time rate of change of dimensionless pressure drop can be obtained by differentiating Eq. 3.43 with respect to t_{DA}, or simply by replacing the exponential integral symbol, "Ei," by the exponential function symbol, "exp," and multiplying the right hand side of Eq. 3.43 by $(-1/t_{DA})$. At the well, r is replaced by r_w in the dimensionless ratio r_{DR}.

Figure 6.5 is a linear plot of p'_{Dw} versus t_{DA} for a well in the center of a square. This figure shows that the pseudo-steady state is reached for $t_{DA} \geq 0.175$, not 0.010 as suggested in Fig. 6.3. This conforms with the behavior of p'_{Dw} described in chapter 2, where it was found that the line source solution to the diffusivity equation becomes an excellent approximation for dimensionless times much longer for p'_{Dw} than for p_{Dw}. It is evident from Fig. 6.5 that, for $t_{DA} \geq 0.175$, p'_{Dw} is constant and is equal to 6.283 or 2π. This constant can also be obtained by differentiating Eq. 6.7 with respect to t_{DA}:

$$p'_{Dw} = 2\pi \tag{6.9}$$

It is clear that every point within a closed drainage area will eventually yield a constant rate of change of dimensionless of 2π. However, not all points yield this value at the same time.

A typical type curve plot of p'_{Dw} vs. t_{DA} on a log-log graph is presented in Fig. 6.6 for seven different well

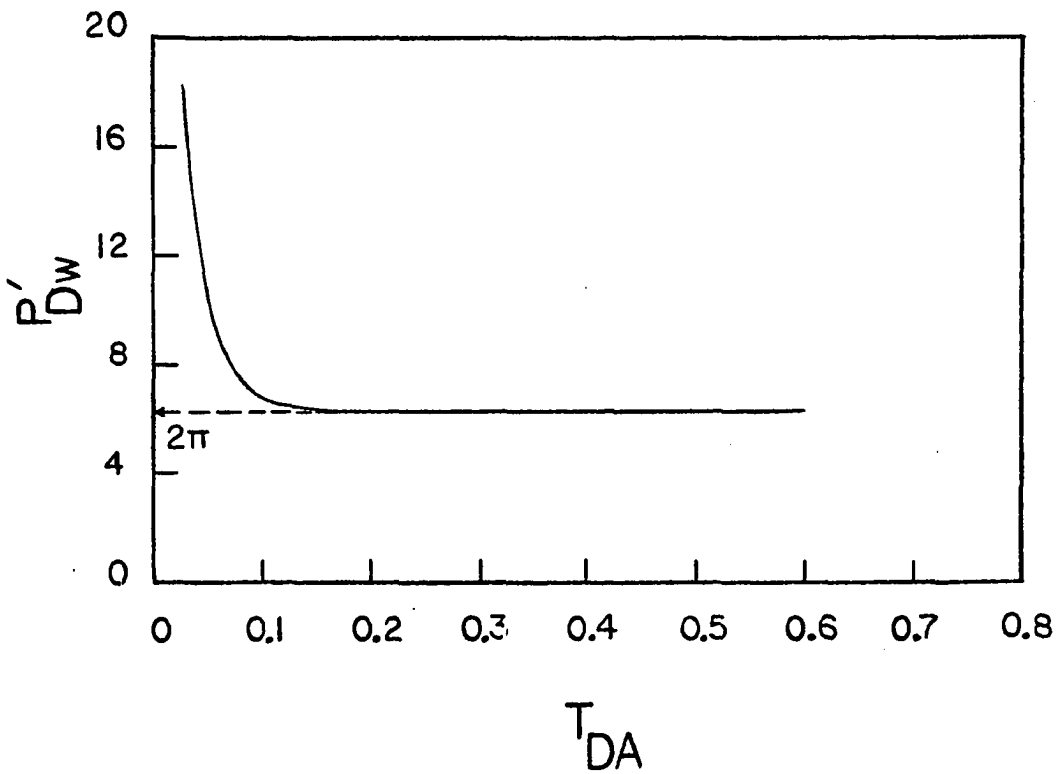

FIGURE 6.5: Linear graph of p'_{Dw} vs t_{DA} for a well in the center of a closed square.

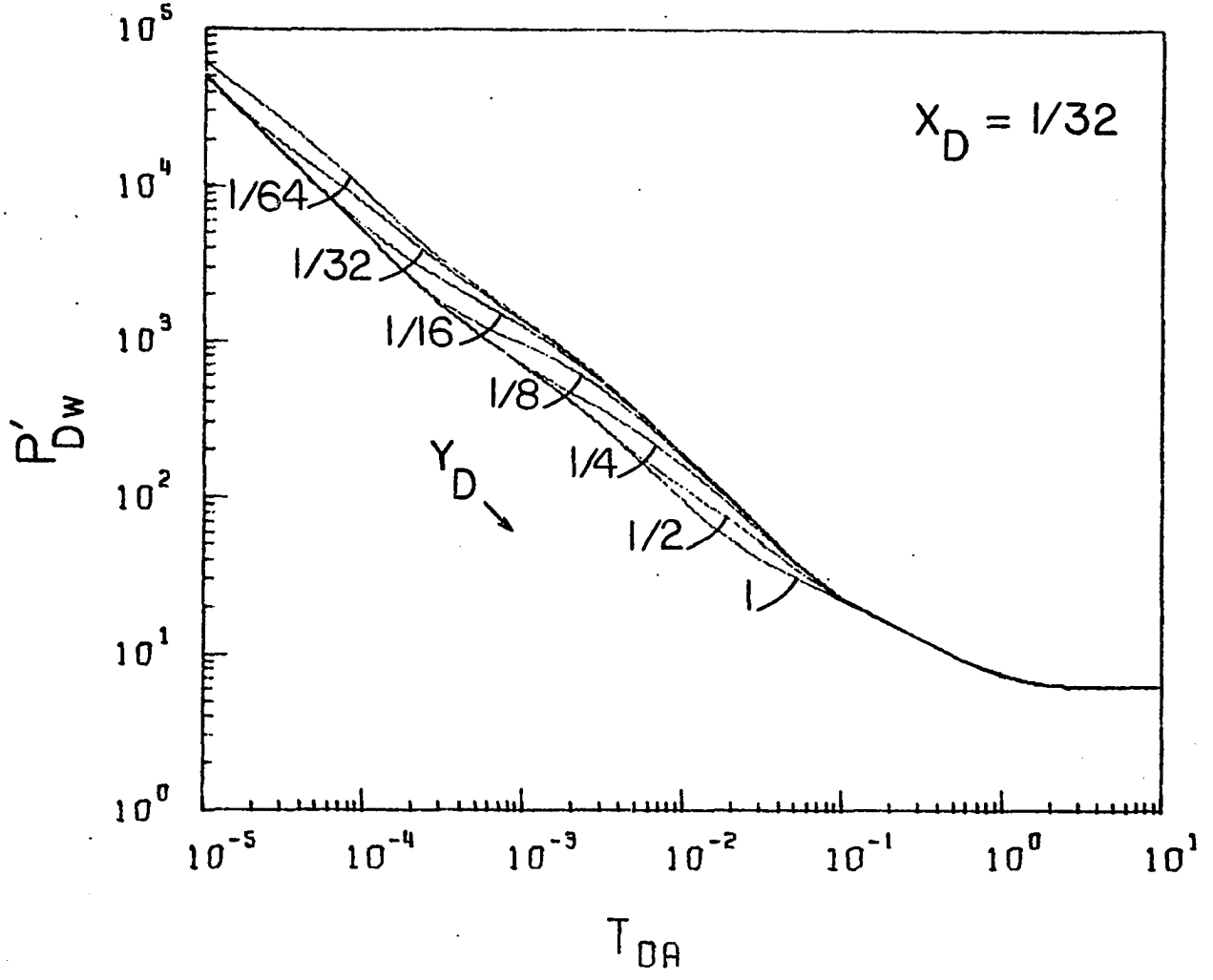

FIGURE 6.6: Type-curve plot of p'_{Dw} vs t_{DA} for a well located inside a closed 4:1 rectangle, when $x_D = 1/32$ and $1/64 \leq y_D \leq 1$.

locations within a closed 4:1 rectangle. This graph shows the existence of five distinct straight line portions for each curve corresponding to a well location. This behavior is best observed for $y_D = 1/64$. (1) The first straight line, of slope -1, corresponds to the infinite reservoir behavior without the effects of the surrounding no-flow boundaries. Note that this line extends up to $t_{DA} = 2.5 \times 10^{-4}$ for $y_D = 1$. (2) The second straight line portion is parallel to the first one. It is caused by the nearby long side of the rectangle. (3) The third line represents the effects of the short side of the rectangle, and has the same slope as the two previous ones. (4) When the effects of the second long side of the rectangle are felt, a fourth straight line is obtained. This line, however, has a slope of -0.5 which is a common characteristic of two parallel no-flow boundaries, already observed in the case of a closed infinite strip[26] and the case of three perpendicular sealing faults (Chapter 5). (5) The last straight line is obtained when pseudo-steady state is reached. Note that this state begins at $t_{DA} = 2.5$. It is clear that this linear portion is represented by Eq. 6.9, i.e., $p'_{Dw} = 2\pi$.

When the well is located at $(x_D, y_D) = (1/32, 1)$, Fig. 6.6 shows that only four straight lines can be observed. This is normal, since $y_D = 1$ implies that the well is at equal distance between the two long sides of the rectangle. Therefore, their effects are felt at the same time, yielding a straight line which has a characteristic slope of -0.5.

The distances to all four sides of the rectangular reservoir b_x, b_y, a_x and a_y and other essential parameters such as the extent of the drainage area, A, and the kh and ϕc products can be estimated from Fig. 6.6, according to the type-curve matching technique developed in the last two chapters. Once the best match is obtained with one of the curves of the master type-curve, the flow capacity can be determined from Eq. 4.8, which we write again.

$$kh = 141.3\ q\mu B(p'_{Dw}/p'_{wf})_M(t_{DA}/t)_M$$

Note that a convenient match point would be the point at which the pseudo-steady state is reached. Thus, for example, if Fig. 6.6 is the master curve from which the best match is obtained, the above equation becomes

$$kh = 141.3\ q\mu B(2\pi/p'_{wf})_M(2.5/t)_M$$

or

$$kh = 2.22 \times 10^3\ q\mu B/(p'_{wf}t)_M \qquad (6.10)$$

It is stressed that Eq. 6.10 is valid <u>only</u> for Fig. 6.6, as different values of x_D will yield different values of t_{DA} at which the pseudo-steady state is reached. Thus for $x_D = 1$, Fig. 6.7 shows that this state is reached at $t_{DA} = 7$.

The ϕc product can be calculated from Eq. 4.9 by overlaying the first straight line of the type curve field data on Fig. 2.5. The extent of the drainage area can be calculated from the following equation:

$$A = \frac{0.000264\ k}{\phi\mu c}\ (t/t_{DA})_M \qquad (6.11)$$

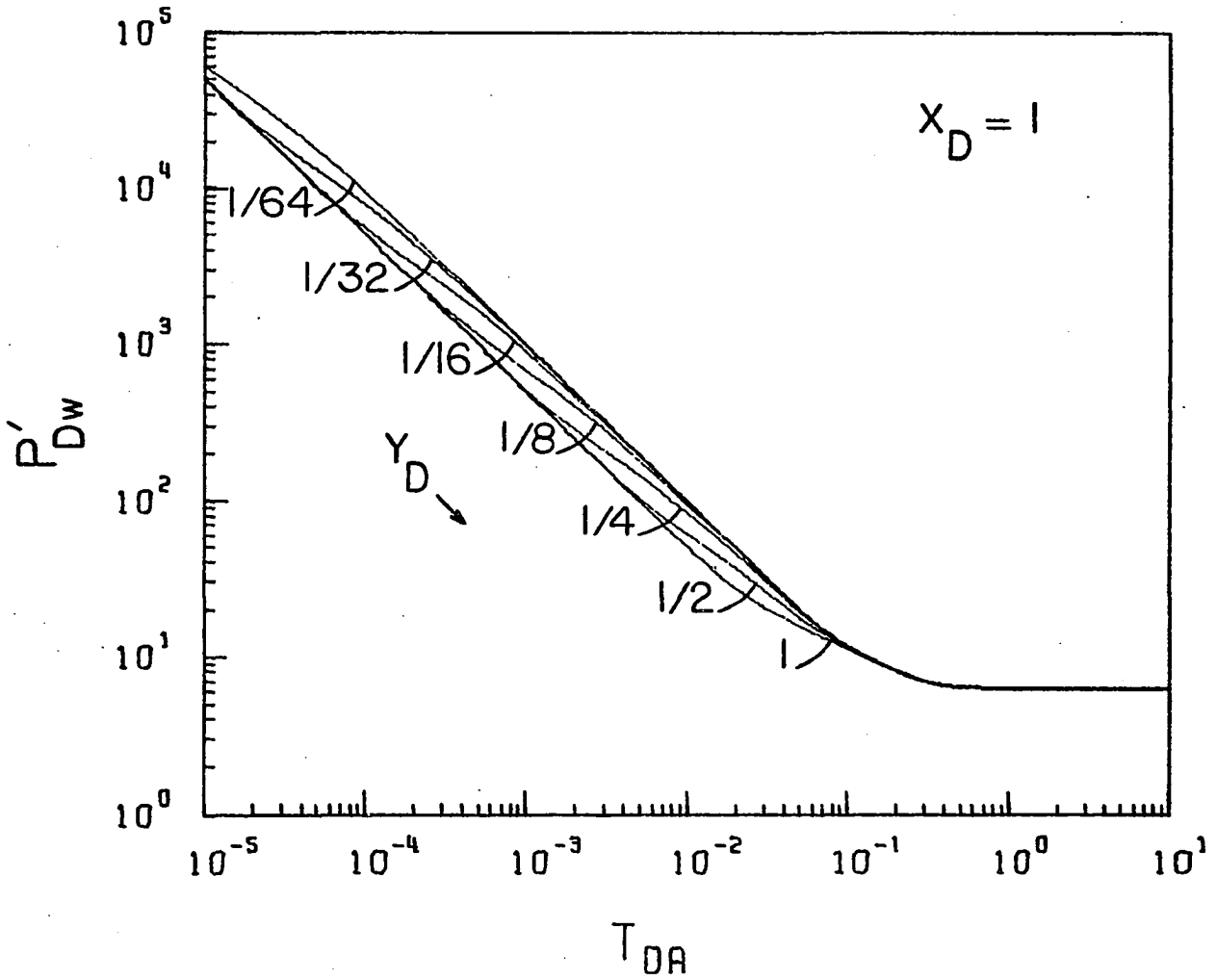

FIGURE 6.7: Type-curve plot of p'_{Dw} vs t_{DA} for a well located inside a closed 4:1 rectangle, when $x_D = 1$ and $1/64 \leq y_D \leq 1$.

The length to width ratio of the drainage area (2:1, 2:1,$\cdots$) corresponding to the master curve from which the best match is obtained, can be used to calculate W_x and W_y from the value of A. For example, if the match is obtained from Fig. 6.6, where $(W_x/W_y)_M = 4/1$, then $W_y = 2\sqrt{A}$ and $W_x = 4W_y$. Finally, the distances to the four sides of the rectangle can be determined as follows:

$$b_x = \frac{1}{2} W_x (x_D)_M \tag{6.12}$$

$$b_y = \frac{1}{2} W_y (y_D)_M \tag{6.13}$$

$$a_x = W_x - b_x \tag{6.14}$$

$$a_y = W_y - b_y \tag{6.15}$$

Figure 6.8 is a typical type-curve plot of p'_{Dw} versus t_{DA} for a well located inside a square. Note that in this case the straight line portion of slope -0.5, which was observed in Fig. 6.6 for a 4:1 rectangle, has vanished. This is a unique characteristic of a square shaped reservoir. It is evident from Fig. 6.7 that the pseudo-steady state is reached earlier for a square than for a 4:1 rectangle. Figures 6.9, 6.10 and 6.11 are similar type-curve plots for rectangles whose sides are in integral ratios of 2:1, 8:1 and 16:1, respectively. Several more typical graphs of this nature are included in Appendix F.

A second method for for locating the well with respect to the closed boundaries of a rectangular reservoir is obtained from a combination of Figs. 6.12 and 6.13 which

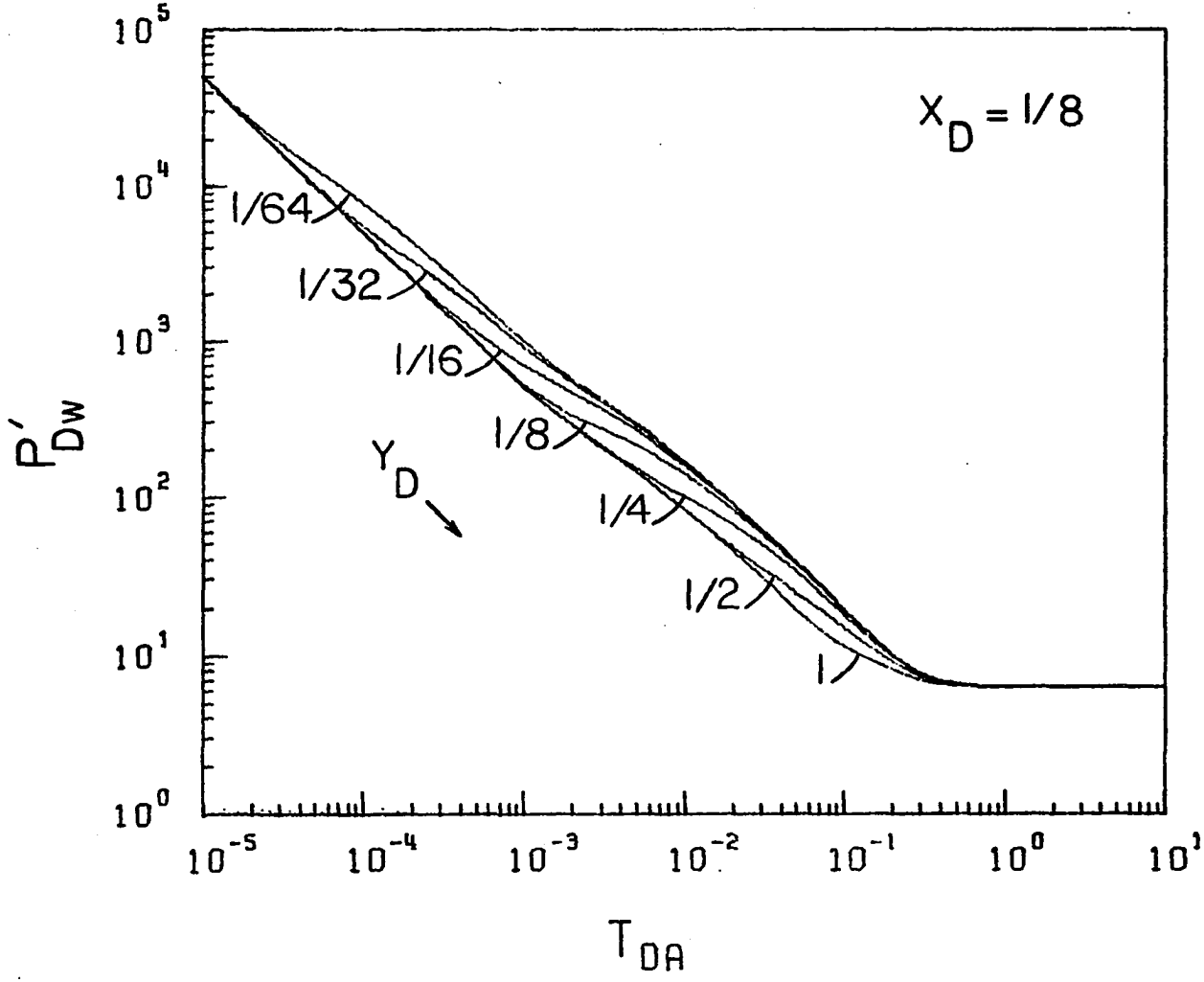

FIGURE 6.8: Type-curve plot of p'_{Dw} vs t_{DA} for a well located inside a closed square, when $x_D = 1/8$ and $1/64 \leq y_D \leq 1$.

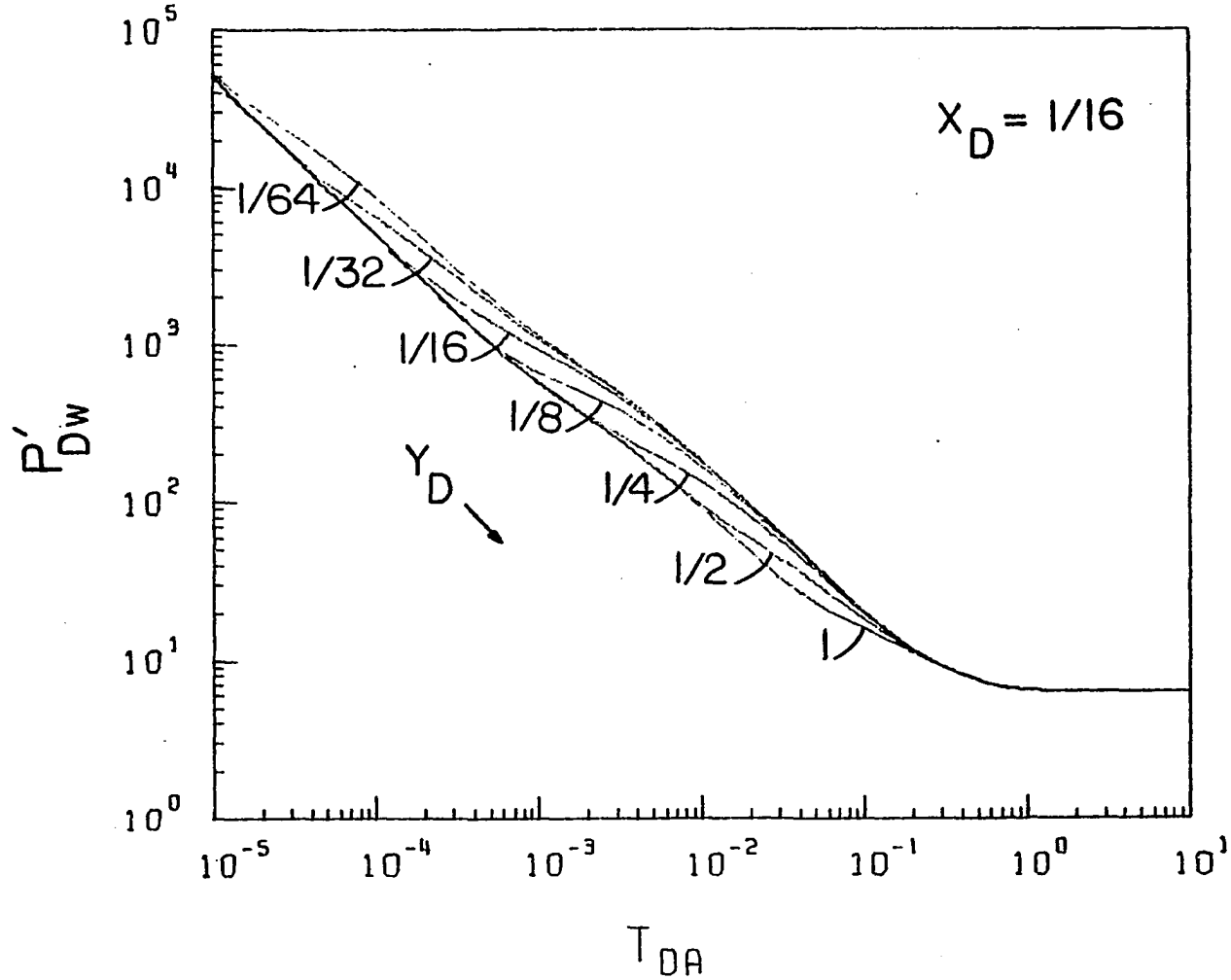

FIGURE 6.9: Type-curve plot of p'_{Dw} vs t_{DA} for a well located inside a closed 2:1 rectangle, when x_D = 1/64 and $1/64 \leq y_D \leq 1$.

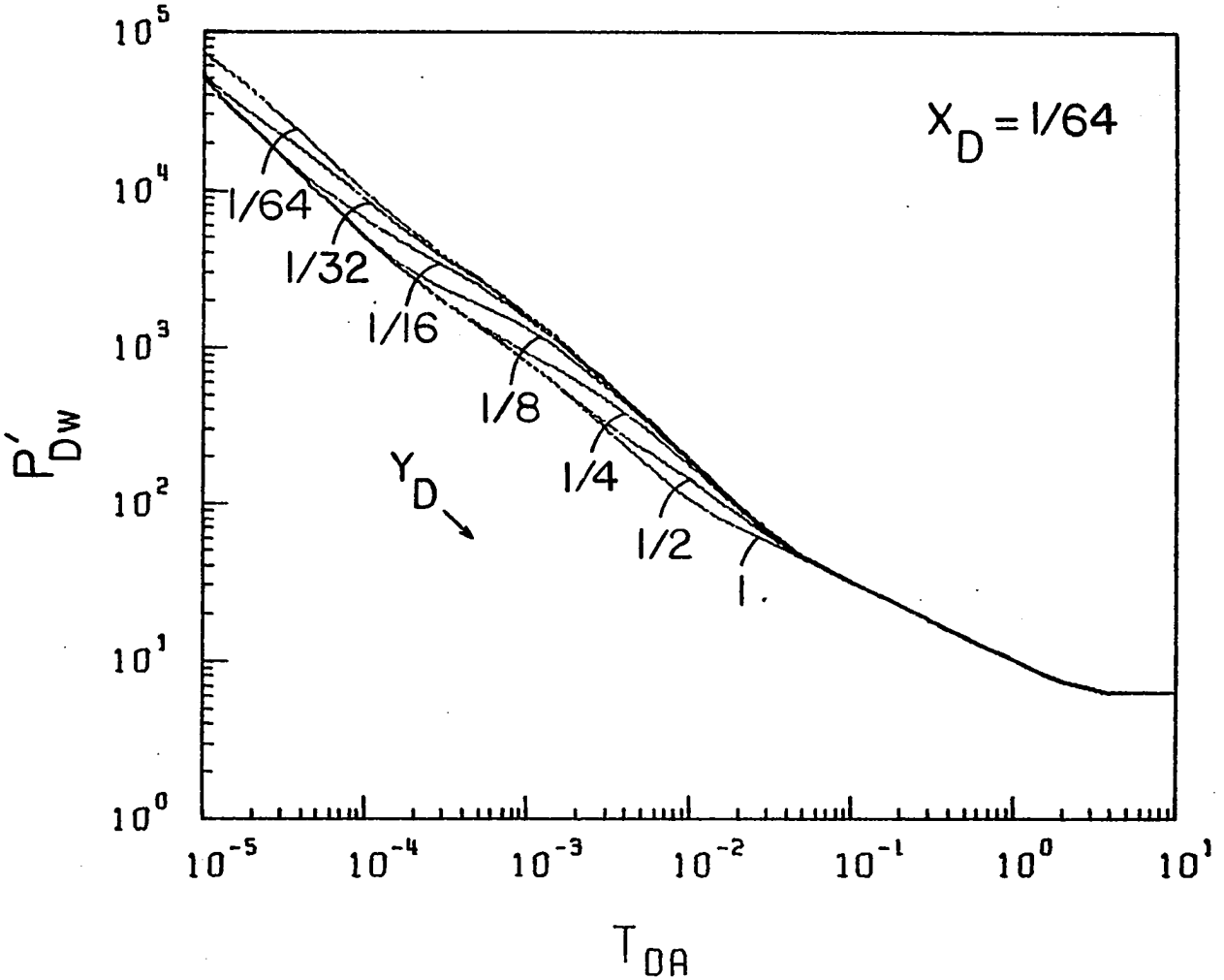

FIGURE 6.10: Type-curve plot of p'_{Dw} vs t_{DA} for a well located inside a closed 8:1 rectangle, when x_D = 1/64 and $1/64 \leq y_D \leq 1$.

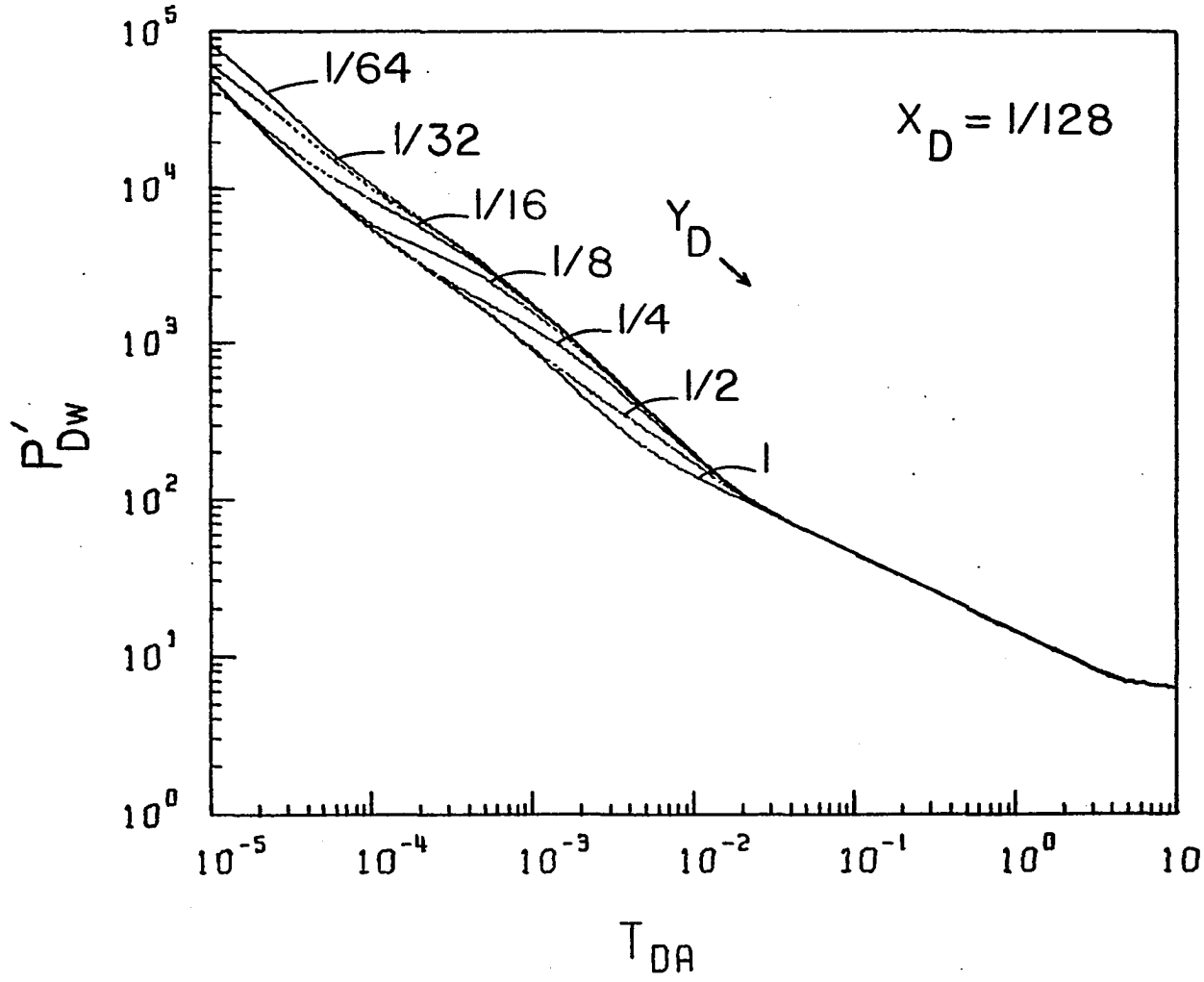

FIGURE 6.11: Type-curve plot of p'_{Dw} vs t_{DA} for a well located inside a closed 16:1 rectangle, when $x_D = 1/128$ and $1/64 \leq y_D \leq 1$.

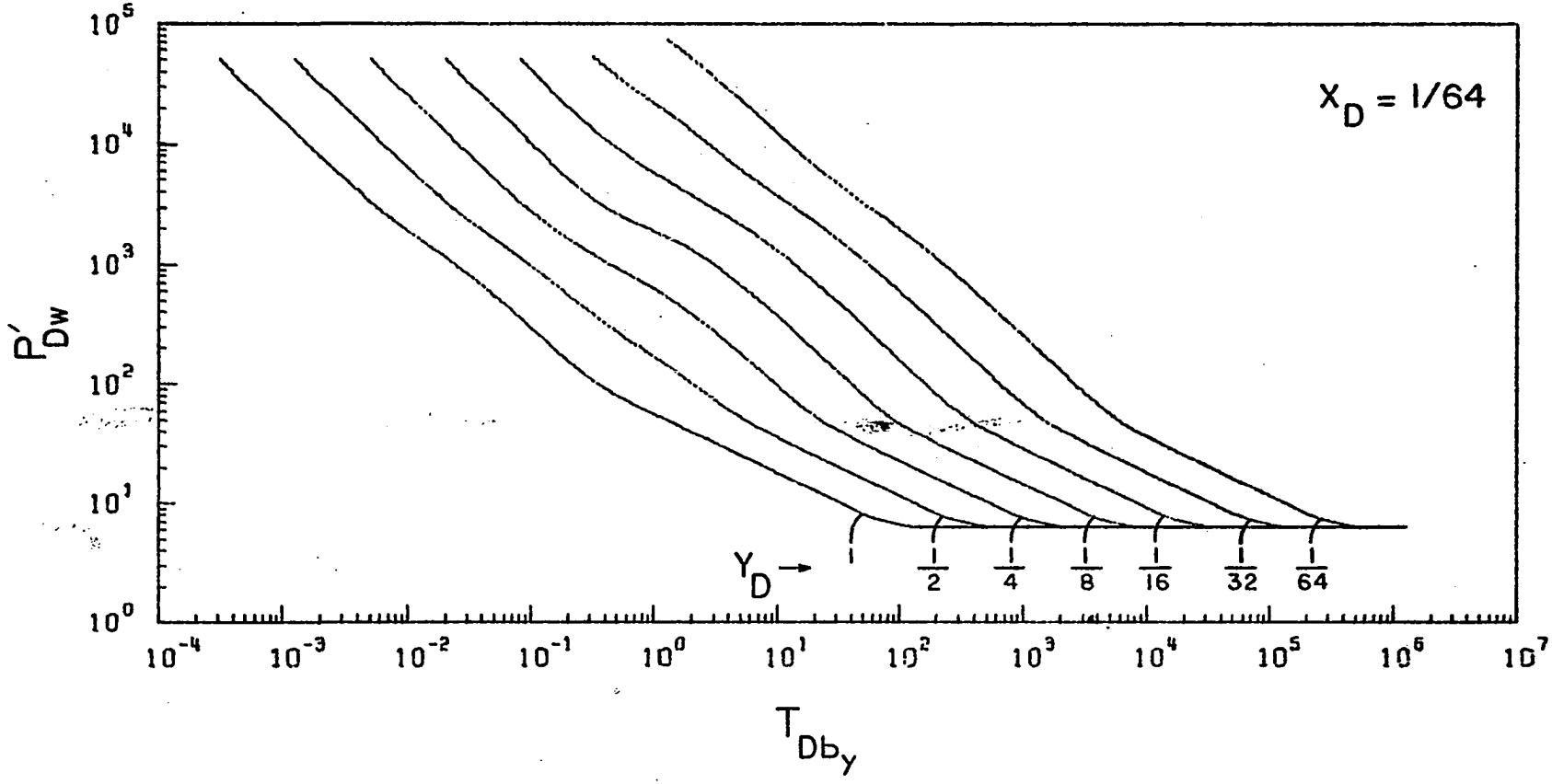

FIGURE 6.12: Type-curve plot of p'_{Dw} vs t_{Db_y} for a well located inside a closed 8:1 rectangle, when x_D = 1/64 and 1/64 $\leq y_D \leq$ 1.

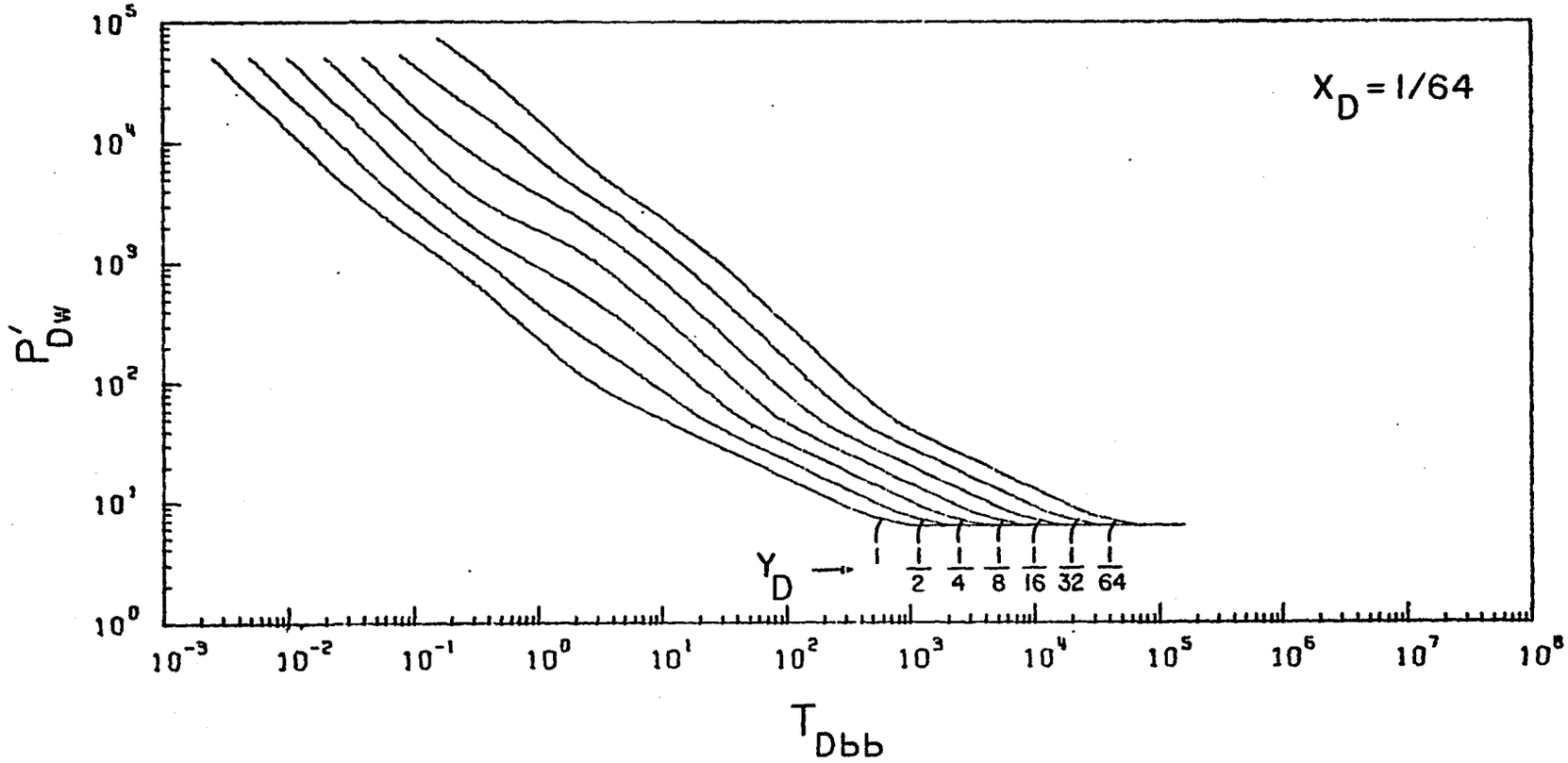

FIGURE 6.13: Type-curve plot of p'_{Dw} vs t_{Dbb} for a well located inside a closed 8:1 rectangle, when $x_D = 1/64$ and $1/64 \leq y_D \leq 1$.

are, respectively, type-curve plots of p'_{Dw} against t_{Db_y} and t_{Dbb} for $x_D = 1/64$ and $1 \leq y_D \leq 1/64$. The dimensionless times t_{Db_y} and t_{Dbb} are defined in Eqs. 3.39 and 3.41. This method involves the following steps.

(1) Plot the type-curve field data p'_{ws} vs. t.

(2) Obtain a match from Fig. 6.12 and Fig. 6.13. Note that since the value of x_D is the same in both figures, the y_D value will also be the same.

(3) Read: x_D, y_D, W_x/W_y, t_{Db_y}, t_{Dbb} and t corresponding to the match point. Then

$$b_x b_y = \frac{0.000264\ k}{\phi \mu c} (t/t_{Dbb})_M \tag{6.16}$$

$$b_y = \left[\frac{0.000264\ k}{\phi \mu c} (t/t_{Db_y})_M\right]^{0.5} \tag{6.17}$$

The distance b_x is determined from these two equations. The extent of the drainage area, A, can be calculated as follows,

$$A = (4b_x b_y)/(x_D)_M (y_D)_M \tag{6.18}$$

The length to width ratio of the master type curve from which the match is obtained can be used to calculate W_x and W_y from the value of A. Finally, equations 6.14 and 6.15 can be used to determine the distances a_x and a_y.

Thus, a plot of p'_{Dw} vs. dimensionless time on a log-log graph offers several unique characteristics for a well inside bounded systems which can be used to determine the distance to each boundary. The ϕc and kh products can also be determined by type curve matching techniques. Additional

type-curve plots of p'_{Dw} are presented in Appendix F (Figures F.13-18).

6.2 Pressure Buildup Analysis

The behavior of dimensionless buildup pressure can be expressed by applying the powerful superposition principle in time to Eq. 3.43. The dimensionless pressure at times Δt_{DA} is subtracted from the dimensionless pressure at times $(t + \Delta t)_{DA}$ causing a net production rate of zero. This is expressed by Eq. 2.45. This procedure can be employed to generate synthetic buildup graphs of Horner, Miller-Dyes, Hutchinson, and Muskat-type for various well locations and for varying lengths of producing times. However, this subject has been extensively investigated in the literature by a large number of authors,[19-23] and, therefore, will not be repeated here. The most important of these publications is that of Ramey and Cobb[38] who derived general interpretative equations describing the behavior of dimensionless buildup pressure for closed drainage areas. These authors made a thorough analysis of the characteristics of Muskat, Horner and Miller-Dyes-Hutchinson buildup graphs, and outlined their use in estimating the initial pressure and average pressure of the drainage area. They also presented conditions under which each of these graphs can be employed to determine the permeability and porosity of the reservoir. But, these graphs are of no use when it comes to locating the well with respect to the boundaries of the closed drainage

area. This problem is the subject of the following section, which discusses the behavior of the time rate of change of dimensionless buildup pressure for various rectangular reservoirs.

6.2.1 Behavior of p'_{Ds}

The time rate of change of dimensionless shut-in pressure for a well located inside a closed rectangular reservoir is obtained by applying the principle of superposition in time to the derivative of Eq. 3.43. Figure 6.14 presents a type-curve plot of p'_{Ds} versus Δt_{DA} for the case of a well located inside a closed 4:1 rectangle at $(x_D, y_D) = (1/64, 1/2)$. A family of curves is shown with producing time as a parameter. Computed data for p'_{Ds} used to plot Fig. 6.11 and other figures in this section are presented in Tables 22-26. As usual, the behavior of p'_{Ds} is best understood by considering three time domains:

(1) $t_{DA} \geq 1$: For such values of producing times, p'_{Ds} yields five distinct straight lines. The first three lines are parallel and have a slope of -1. The first one (not fully shown in Fig. 6.14) corresponds to the infinite reservoir behavior without the effects of the surrounding no-flow boundaries. The second and third parallel lines correspond, respectively, to the effects of the closest long and short sides of the rectangular drainage area.

The fourth straight line has a slope of -2. It represents the effects of the other long side of the rectangle. The last linear portion has a slope of -2π implying that

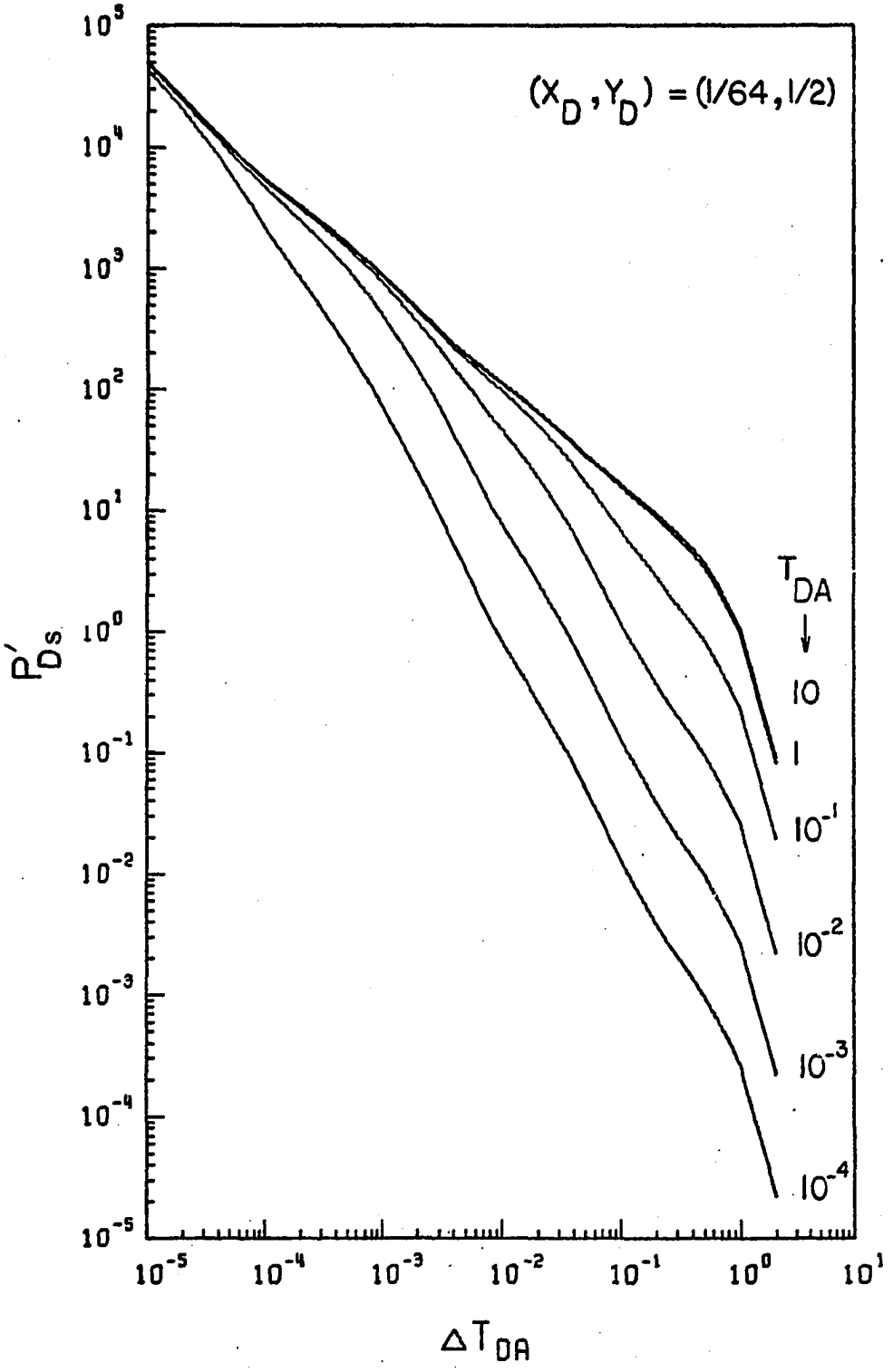

FIGURE 6.14: Type-curve plot of p'_{Ds} vs Δt_{DA} for a well located at $(x_D, y_D) = (1/64, 1/2)$ inside a closed 4:1 rectangle.

the well has been produced long enough to reach pseudo-steady state.

(2) $t_{DA} \leq 10^{-3}$: It is evident from Fig. 6.14 that the first and the last two linear portions remain unchanged, while the second and third straight lines become steeper with a slope of -2.

(3) $10^{-3} < t_{DA} < 1$: For intermediate values of producing time t_{DA}, only the third straight line becomes steeper with a slope of -2.

Thus, a plot of time rate of shut-in well pressure, p'_{ws}, versus Δt on a log-log graph should yield unique characteristics which may be used to locate the well with respect to the boundaries of a closed rectangular drainage area. Using the type-curve matching technique presented in Chapter 4, we can calculate the distance to each boundary as follows:

$$A = \frac{0.000264\ k}{c} (t/\ t_{DA})_M \tag{6.19}$$

$$W_y = [A/(W_x/W_y)_M]^{0.5} \tag{6.20}$$

$$W_x = A/W_y \tag{6.21}$$

The distances b_x, b_y, a_x and a_y can be calculated using, respectively, Eqs. 6.12, 6.13, 6.14 and 6.15. As to the kh and ϕc products, they can be determined from Eq. 4.20 and Eq. 4.21.

Figure 6.15 shows a type-curve plot of the time rate of change of dimensionless buildup pressure versus dimensionless

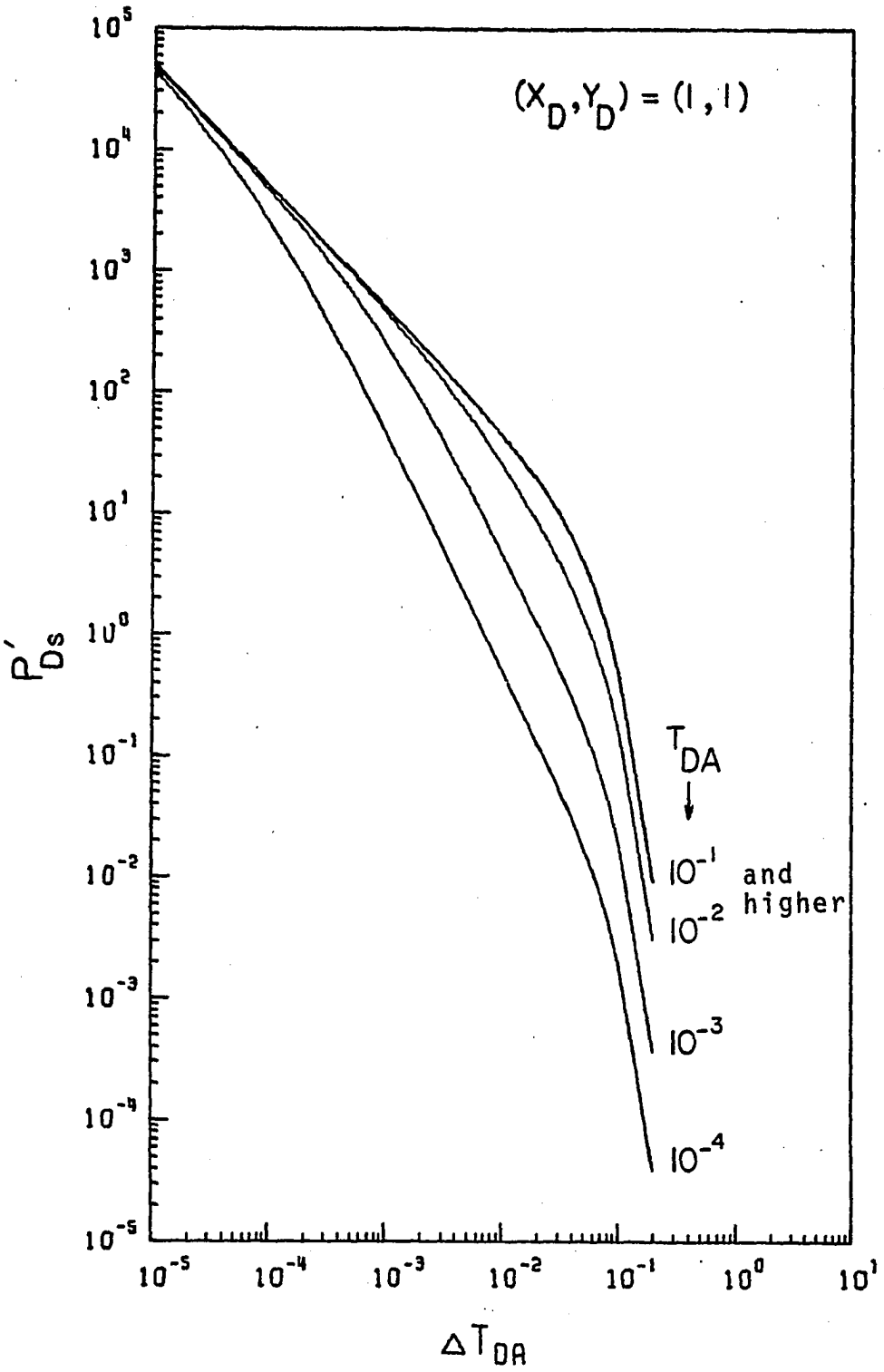

FIGURE 6.15: Type-curve plot of p'_{Ds} vs Δt_{DA} for a well located at $(x_D, y_D) = (1,1)$ inside a closed square.

time for a well located in the center of a square. It is evident from this figure that for such a well location, we can observe only two straight lines of slope -1 and -2π for $t_{DA} \geq 10^{-2}$. However, then $t_{DA} \leq 10^{-3}$ we observe three linear portions of slopes -1, -2 and -2π. Finally, a set of type-curve plots of p'_{Ds} vs. Δt_{DA} for various well locations and reservoir sizes is included in Appendix F (Figures F.19-23).

In summary, although many excellent publications have established pressure buildup theory for a well in a closed drainage area, no method was presented to locate the well with respect to all boundaries involved. The three main buildup analysis methods of Muskat, Miller-Dyes-Hutchinson, and Horner, as discussed by Ramey and Cobb,[38] can at best be used to locate the closest boundary. It has been shown in this chapter that the time rate of change of drawdown or buildup pressure offers unique characteristics which can be used to calculate the distance to each boundary for a well located inside a closed rectangular reservoir.

CHAPTER VII

CONCLUSIONS

The principle of superposition was systematically applied to the continuous line source solution and its time derivative to generate the pressure drawdown and buildup behavior of a constant-rate well in a multiple-sealing faults situation and bounded rectangular reservoir. The usual reservoir assumptions, as listed on page 8, were made, i.e., the porous media is assumed to be isotropic, horizontal, homogeneous, of uniform thickness, etc. A thorough analysis of the following three reservoir systems was conducted: (1) a well near two perpendicular sealing faults, or no-flow boundaries, (2) a well between a semi-infinite strip, or three sealing faults intersecting at right angles, and (3) a well inside closed rectangular reservoirs whose sides are in integral ratios of 1:1 (square), 2:1, 4:1, 8:1, and 16:1.

It was found that the type-curve matching technique based on the time rate of change of dimensionless well pressure is a powerful tool in detecting boundaries. Procedures based on this technique were outlined to determine the distance to all boundaries involved. This type-curve matching approach will also give much more accurate values of various essential reservoir parameters such as the kh and ϕc products and the extent of drainage area A.

The calculation technique used to produce pressure distributions in rectangular reservoirs is based on analytical equations as opposed to the conventional approach which consists of applying superposition to a square, that has a well at its center, to generate other rectangular shapes. These equations should enable a practicing petroleum engineer who had no training in formal solution of the diffusivity equation or application of the principle of superposition to generate dimensionless pressure data for bounded systems. Although this study concerned itself with rectangles whose sides are in integral ratios of 1:1, 2:1, 4:1, 8:1 and 16:1, the method can be employed for any rectangular reservoir size with any well location, and with any length-to-width ratio.

The type-curve matching technique based on the time rate of change of well pressure function not only has a solid fundamental basis, but provides a tool with more interpretive power than that based on the well pressure function itself. Log-log type-curves of p_D' versus dimensionless time have a tremendous interpretive power because field data curves must appear like the proper analytic solution for all times, thus allowing a more accurate estimate of reservoir characteristics such as permeability, porosity, drainage area and location of the well with respect to surrounding sealing faults, or no-flow boundaries. This information is essential for planning well locations in these systems.

The presently used pressure buildup and drawdown techniques for fault distance calculation based on semi-log graphs of the well pressure function should not be applied if a multiple-sealing-fault situation is suspected. The type-curve matching technique outlined in this study is strongly recommended for such situations, especially when a pressure drawdown test is run.

The results of this study are of considerable importance in interference testing between oil fields in common aquifers. This technique is not only valid in petroleum reservoirs, but also in other areas where the location of boundaries, sealing faults or other discontinuities, around the borehole is essential. Some examples of these areas are geothermal systems and groundwater hydrology.

The following specific conclusions are reached from this study.

I. Well Between Two Perpendicular Sealing Faults

1. A plot of flowing well pressure versus time on a semilog graph for $y_D \leq 1/16$ yields three distinct straight line portions which can be used to calculate the distance to both faults. However, for values of y_D greater than 1/16 (which is a more common situation), only the first and last straight lines of slope 1.151 and 4.6, respectively, are observed. Hence, in most cases, a semilog graph of p_{wf} vs. t should not be used for the purpose of locating the well with respect to two perpendicular boundaries. The

first straight line, which corresponds to the infinite reservoir behavior without the effects of nearby boundaries, can be used to estimate the kh product and skin factor s.

2. Both the Horner and Miller-Dyes-Hutchinson buildup graphs are equally reliable for detecting the closest fault. However, under very unusual conditions such as long shut-in times, long producing times, and $y_D < 1/8$, these graphs can be used to detect both boundaries.

3. A type-curve plot of the time rate of change of dimensionless drawdown well pressure, p'_{Dw}, versus dimensionless producing time, t_{DA}, yields three parallel straight line portions of slope -1. The distance to both faults, b_x and b_y, and several other reservoir parameters such as the kh and ϕc products can be accurately calculated by type-curve matching. The total shift to the right of the final straight line (with respect to the first one) is double that of the second line. This is the distinguishing feature of the behavior of p'_{Dw} for a well near two sealing boundaries intersecting at a right angle.

4. A log-log plot of the time rate of change of dimensionless buildup pressure, p'_{Ds}, versus dimensionless shut-in time can be used to calculate the distance to both faults, b_x and b_y, and the kh and ϕc products. It is recommended, however, to use these buildup type-curves only for very long producing times; so old wells are excellent candidates.

II. Well Between Three Perpendicular Sealing Faults

1. A semilog graph of flowing well pressure versus producing time can, generally, detect only the closest of the three faults. For values of (x_D, y_D) smaller than (1/32, 1/8) this graph yields three distinct straight lines of slope 1.151, 2.3 and 4.6, which may be used to calculate the distance to the two closest boundaries. The slope of the first line can give the kh product and skin factor.

2. The Horner and Miller-Dyes-Hutchinson buildup graphs should not be used for fault distance calculation if a multiple-sealing-fault situation is suspected. Thus in the case of three perpendicular sealing boundaries, about the best one can hope to do is obtain an estimate of the distance to the nearest boundary from the intersection point of the two straight line portions observed at long shut-in times. The first straight line of slope 1.151 can be used to determine the kh product, skin factor and initial pressure.

3. A type-curve plot of the time rate of change of dimensionless flowing well pressure, p'_{Dw}, versus dimensionless producing time, t_{DA}, yields four distinct straight line portions. The first three lines are parallel and have a slope of -1. The fourth straight line section has a slope of -0.5. This is the distinguishing feature of a three perpendicular sealing fault system. The type-curve matching technique presented in this study can be used to calculate

the distance to each boundary, b_x, b_y and a_x, the kh and ϕc products.

4. A type-curve plot of the time rate of change of dimensionless shut-in well pressure, p'_{Ds}, versus dimensionless shut-in time, Δt_{DA}, yields four parallel straight line portions of slope -1 when $t_{DA} >> \Delta t_{DA}$. A fifth straight line of slope -1.5 should be observed as Δt_{DA} becomes longer than t_{DA}, which is a very unusual case. For short and intermediate values of t_{DA} these graphs should show two early straight lines of slope -1, followed by another line of slope -2 and a final line of slope -1.5. Under these time conditions, the curve matching technique can be used to calculate various reservoir parameters such as the distance to each fault and both kh and ϕc products. It is emphasized that the use of these type-curve plots based on p'_{Ds} should be favored only when $t_{DA} >> \Delta t_{DA}$.

III. Well Inside a Closed Rectangular Reservoir

1. For drawdown, the initial semilog period of dimensionless well pressure, p_{Dw}, changes abruptly, for all practical purposes, into pseudo-steady state flow for a well at the center of a rectangular drainage area. The so-called "late transient" flow regime reported by Russel[42] for off-center wells corresponds, in fact, to the effects of the two closest boundaries. Thus, for a well located inside a 2:1 rectangle at $(x_D, y_D) = (1/32, 1/4)$ a total of three straight lines of slopes 1.151, 2.3 and 4.6 can be observed. This finding is original to this study as it has always been

believed that bounded systems yield only the first straight line of slope 1.151 corresponding to the infinite reservoir behavior without the effects of the surrounding boundaries.

2. A linear plot of p'_{Dw} versus t_{DA} for a well in the center of a square shows that the pseudo-steady state is reached at a drawdown time of 0.175, and for $t_{DA} > 0.175$, $p'_{Dw} = 2\pi$.

3. A type-curve plot of the time rate of change of dimensionless drawdown pressure versus dimensionless producing time, for a well inside a closed rectangular drainage area, yields five distinct straight line portions. The first three lines are parallel and have a slope of -1. The fourth line of slope -0.5 is observed just before the pseudo-steady flow is reached. The last linear portion is expressed by $p'_{Dw} = 2\pi$.

4. A log-log plot of the time rate of change of dimensionless buildup pressure versus dimensionless shut-in time also shows five distinct straight lines for off-center wells closer to any of the corners of the rectangle. However, all the five lines are observed only when $t_{DA} >> \Delta t_{DA}$. The first three straight lines are parallel and have a slope of -1. The fourth line has a slope of -2. The last straight line has a slope of -2π indicating pseudo-steady state.

5. The distances to all four sides of the rectangular reservoir, a_x, a_y, b_x and b_y and other essential parameters such as the extent of drainage area, A, and the kh and ϕc products can be estimated according to the type-curve

matching technique developed in this study. The most accurate results are obtained using this technique to drawdown type curves.

APPENDICES

APPENDIX A

SOLUTION FOR TRANSIENT PRESSURE BEHAVIOR DUE TO A CONSTANT RATE WELL IN AN INFINITE MEDIUM

The fundamental partial differential equation describing fluid flow in reservoir rocks is Eq. 2.1:

$$\frac{\partial^2 p}{\partial r^2} + \frac{1}{r}\frac{\partial p}{\partial r} = \frac{\phi \mu c}{k}\frac{\partial p}{\partial t}\ , \qquad (A.1)$$

subject to the following initial and boundary conditions:

1. Initial Condition: $p(r,0) = p_i\ ,\ \forall r$ (A.2)

2. Inner Boundary Condition: $\left(r\cdot\frac{\partial p}{\partial r}\right)_{r_w} = \frac{q\mu}{2\pi kh}\ ,\ \forall\ t > 0$ (A.3)

3. Outer Boundary Condition: $p(r,t) = p_i$ as $r \to \infty$ and $\forall\ t > 0$ (A.4)

The solution technique presented here follows that of Matthews and Russell. To develop the solution, we first replace the second boundary condition by the condition

$$\lim_{r\to 0} r\frac{\partial p}{\partial r} = \frac{q\mu}{2\pi kh}\ , \qquad \text{for } r > 0. \qquad (A.5)$$

This condition is the "line-source" approximation to the original boundary condition.

Substituting the Boltzmann Transformation:

$$z = \frac{\phi\mu c r^2}{4kt}$$

into Eq. A.1 and boundary conditions A.2 and A.5 gives

$$z \frac{d^2p}{dz^2} + \frac{dp}{dz}(1 + z) = 0 \qquad (A.6)$$

1. $p \to p_i$ as $z \to \infty$ (A.7)

2. $\lim_{z \to 0} 2z \frac{dp}{dz} = \frac{q\mu}{2\pi kh}$ (A.8)

Let $p' = \frac{dp}{dz}$, and Eq. A.6 becomes

$$z \frac{dp'}{dz} + (1 + z)p' = 0 \qquad (A.9)$$

Separation of variables and integration yield

$$\int \frac{dp'}{p'} = -\int \left(\frac{1}{z} + 1\right) dz$$

$$\ln p' = -\ln z - z + c_1$$

or

$$\ln p' + \ln z - \ln c = -z$$

$$\ln \frac{p'z}{c} = -z$$

$$\frac{p'z}{c} = e^{-z}$$

and

$$p' = \frac{dp}{dz} = c \frac{e^{-z}}{z} \qquad (A.10)$$

where c_1 and c are constants of integration.

Substitution of Eq. A.10 into boundary condition A.8 gives

$$\lim_{z\to 0} 2c\, e^{-z} = \frac{q\mu}{2\pi kh} = 2c$$

Thus,

$$c = \frac{q\mu}{4\pi kh} \tag{A.11}$$

Equation A.10 now becomes

$$\frac{dp}{dz} = \frac{q\mu}{4\pi kh} \frac{e^{-z}}{z}$$

Separation of variables and integration yield

$$\int dp = \frac{q\mu}{4\pi kh} \int \frac{e^{-z}}{z}\, dz$$

$$p = \frac{q\mu}{4\pi kh} \int^{z} \frac{e^{-z}}{z}\, dz + c_2$$

Assigning arbitrarily $z = \infty$ to the lower limit of the integral, we obtain

$$p = \frac{q\mu}{4\pi kh} \int_{\infty}^{z} \frac{e^{-z}}{z}\, dz + c_2 \tag{A.12}$$

or

$$p = -\frac{q\mu}{4\pi kh} \int_{z}^{\infty} \frac{e^{-z}}{z}\, dz + c_2$$

or

$$p = \frac{q\mu}{2\pi kh} [\tfrac{1}{2}Ei(-z)] + c_2$$

Applying the boundary condition A.7 to the above, we find $c_2 = p_i$ and therefore

$$p(r,t) = \frac{q\mu}{2\pi kh} [\tfrac{1}{2}Ei(-z)] + p_i \tag{A.13}$$

$$p_i - p(r,t) = \frac{q\mu}{2\pi kh}\left[-\tfrac{1}{2}Ei\left(-\frac{\phi\mu c r^2}{4kt}\right)\right]$$

or

$$\frac{2\pi kh[p_i - p(r,t)]}{q\mu} = -\frac{1}{2}\,Ei\left(-\frac{\phi\mu c r^2}{4kt}\right) \qquad (A.14)$$

which takes the following form in terms of dimensionless variables defined in the text by Eqs. 2.3, 2.4, and 2.5:

$$p_D(r_D,t_D) = -\frac{1}{2}\,Ei\left(-\frac{r_D^2}{4t_D}\right) \qquad (A.15)$$

This is the same as Eq. 2.6 of the text.

APPENDIX B

FIRST DERIVATIVE WITH TIME OF THE CONTINUOUS LINE SOURCE SOLUTION, EQ. 2.6

The continuous line source solution of Eq. 2.6 involves the Ei-function which is defined in terms of an integral. The first derivative of p_D would therefore involve differentiation under the integral sign which requires the use of Leibnitz' Rule.

B.1 Leibnitz' Rule

If

$$F(\alpha) = \int_{a(\alpha)}^{b(\alpha)} \phi(x,\alpha)\, dx \qquad (B.1)$$

where a and b are differentiable functions of α and where $\phi(x,\alpha)$ and $\partial\phi/\partial\alpha$ are continuous in x and α, then

$$\frac{\partial F}{\partial \alpha} = \int_{a(\alpha)}^{b(\alpha)} \frac{\partial \phi(x,\alpha)}{\partial \alpha}\, dx + \phi[b(\alpha),\alpha] \frac{db(\alpha)}{d\alpha} - \phi[a(\alpha),\alpha] \frac{da(\alpha)}{d\alpha} \qquad (B.2)$$

B.2 First Derivative of p_D with Time

Writing $x = r_D^2/(4t_D)$, from Eq. 2.6 we have

$$p_D(r_D,t_D) = -\frac{1}{2} Ei(-x) = \frac{1}{2} \int_x^\infty (e^{-u}/u)\, du \qquad (B.3)$$

and

$$\frac{\partial}{\partial t_D} p_D(r_D,t_D) = p_D' = \frac{1}{2} \frac{\partial}{\partial t_D} \left[\int_x^\infty (e^{-u}/u)\, du\right]$$

Applying Leibnitz' Rule as stated above:

$$p_D' = \frac{1}{2} \left(- \frac{e^{-x}}{x}\right) \frac{\partial x}{\partial t_D} \tag{B.4}$$

Substituting the value of x and its derivatives:

$$p_D' = - \frac{1}{2}\left(\frac{4t_D}{r_D^2}\right) \exp\left(- \frac{r_D^2}{4t_D}\right)\left[\frac{r_D^2}{4}\left(- \frac{1}{t_D^2}\right)\right]$$

$$p_D' = \frac{1}{2t_D} \exp\left(- \frac{r_D^2}{4t_D}\right) \tag{B.5}$$

Equation B.5 gives the rate of change of dimensionless pressure with time for a line source well in an infinite medium.

B.3 Conversion to Real Parameters

If we substitute equations 2.3, 2.4, and 2.5 for r_D, t_D, and p_D respectively in Eq. B.5 we obtain:

$$p_D' = \frac{\phi\mu c r_w^2}{2kt} \exp\left(- \frac{\phi\mu c r^2}{4kt}\right) \tag{B.6}$$

and

$$p_D' = \frac{\partial\left[\frac{2\pi kh}{q\mu} (p_i - p_{r,t})\right]}{\partial[kt/(\phi\mu c r_w^2)]}$$

or

$$p_D' = -2\pi r_w^2 h\phi c \frac{1}{q} \left(\frac{\partial p}{\partial t}\right) \tag{B.7}$$

Equating Eq. B.6 to B.7 we have:

$$\frac{\partial p}{\partial t} = p' = -\left(\frac{1}{t}\right)\left(\frac{q\mu}{4\pi kh}\right)\exp\left(-\frac{\phi\mu c r^2}{4kt}\right) \qquad (B.8)$$

or

$$p_D' \times t_D = \left(\frac{2\pi kh}{q\mu}\right)(|p'| \times t) \qquad (B.10)$$

and therefore:

$$kh = \left(\frac{q\mu}{2\pi}\right)(p_D'/|p'|)(t_D/t). \qquad (B.11)$$

B.4 Conversion to Oil Field Units

All the equations derived above are in Darcy units. In oil field units, Eq. B.9 is

$$\frac{\partial p}{\partial t} = |p'| = \left(\frac{1}{t}\right)\left(70.6\ \frac{q\mu B}{kh}\right)\exp\left(-\frac{\phi\mu c r^2}{0.001055\ kt}\right) \qquad (B.12)$$

where p' = psi/hr, q = STB/D, μ = cp, k = md, h = ft, B = formation volume factor, vol/vol, and t = hours.

Equation B.7 in oil field units becomes

$$p_D' = 2\pi r_w^2 h\phi c\left(\frac{1}{5.615}\ \frac{Bbl}{cu\ ft}\right)\left(\frac{1}{qB}\ \frac{D}{STB}\right)(24\ Hr/D)|p'|$$

$$= (1.119 \times 24) r_w^2 h\phi c\ \frac{1}{qB}\ |p'| \qquad (B.13)$$

or

$$p_D' = 26.856\ r_w^2 h\phi c\ \frac{1}{qB}\ |p'| \qquad (B.14)$$

where p' = psi/hr, r_w = ft, h = ft, ϕ = fraction, c = vol/vol/psi, q = STB/D and t = hrs.

If t is in days, then Eq. B.14 is

$$p_D' = 1.119\ r_w^2 h\phi c\ \frac{1}{qB}\ |p'| \qquad (B.15)$$

where p' = psi/day.

Further, Eq. B.11 in oil field units is:

$$kh = (141.3\ q\mu B)(p_D'/|p'|)(t_D/t) \ . \qquad (B.16)$$

APPENDIX C

SECOND DERIVATIVE WITH TIME OF THE CONTINUOUS LINE SOURCE SOLUTION, EQ. 2.6

C.1 Second Derivative of p_D with Time

The second derivative with time of the dimensionless pressure is obtained by differentiation of Eq. 2.10 and is given by:

$$\frac{\partial^2 p_D}{\partial t_D^2} = \frac{1}{2}\left[\left(-\frac{1}{t_D^2}\right) + \frac{1}{t_D}\left(-\frac{r_D^2}{4}\right)\left(-\frac{1}{t_D^2}\right)\right]\exp\left(-\frac{r_D^2}{4t_D}\right)$$

or

$$p_D'' = \frac{1}{2t_D^2}\left(\frac{r_D^2}{4t_D} - 1\right)\exp\left(-\frac{r_D^2}{4t_D}\right) \qquad (C.1)$$

or

$$p_D'' = p_D' \cdot \frac{1}{t_D}\left(\frac{r_D^2}{4t_D} - 1\right) \qquad (C.2)$$

C.2 Conversion to Real Parameters

$$p_D'' = \frac{\partial}{\partial t_D}\left(\frac{\partial p_D}{\partial t_D}\right)$$

$$= \frac{\partial}{\partial\left(\frac{kt}{\phi\mu c r_w^2}\right)}\left(-2\pi r_w^2 h\phi c\,\frac{1}{q}\,\frac{\partial p}{\partial t}\right)$$

or

$$p''_D = \frac{\phi\mu c r_w^2}{k} (-2\pi r_w^2 h\phi c) \frac{1}{q} \frac{\partial^2 p}{\partial t^2} \tag{C.3}$$

or

$$|p''_D| = \left(\frac{\phi\mu c r_w^2}{k}\right)^2 \left(\frac{2\pi kh}{q\mu}\right) \frac{\partial^2 p}{\partial t^2} \tag{C.4}$$

Further,

$$p''_D = \frac{\partial}{\partial t_D}\left[\frac{\phi\mu c r_w^2}{2kt} \exp -\left(\frac{\phi\mu c r^2}{4kt}\right)\right] \tag{C.5}$$

$$= \frac{\phi\mu c r_w^2}{k} \frac{\partial}{\partial t}\left[\frac{1}{2}\left(\frac{\phi\mu c r_w^2}{k}\right)\frac{1}{t} \exp\left(-\frac{\phi\mu c r^2}{4kt}\right)\right]$$

$$= \frac{1}{2}\left(\frac{\phi\mu c r_w^2}{k}\right)^2 \left[\left(-\frac{1}{t^2}\right)\left(\frac{1}{t}\right)\left(-\frac{\phi\mu c r^2}{4k}\right)\left(-\frac{1}{t^2}\right)\right] \exp\left(-\frac{\phi\mu c r^2}{4kt}\right)$$

or

$$p''_D = \frac{1}{2}\left(\frac{\phi\mu c r_w^2}{kt}\right)^2 \left(\frac{\phi\mu c r^2}{4kt} - 1\right) \exp\left(-\frac{\phi\mu c r^2}{4kt}\right) \tag{C.6}$$

Equating Eq. C.4 with Eq. C.6 we get

$$\frac{\partial^2 p}{\partial t^2} = -\frac{1}{t}\left(\frac{q\mu}{4\pi kh}\right) \exp\left(-\frac{\phi\mu c r^2}{4kt}\right)\left[\frac{1}{t}\left(\frac{\phi\mu c r^2}{4kt} - 1\right)\right] \tag{C.7}$$

or

$$\frac{\partial^2 p}{\partial t^2} = \left(\frac{\partial p}{\partial t}\right)\left(\frac{1}{t}\right)\left(\frac{\phi\mu c r^2}{4kt} - 1\right) \tag{C.8}$$

Consider the product:

$$|p''_D| \times t_D^2 = \frac{2\pi kh}{q\mu} (p'' \times t^2) \tag{C.9}$$

then

$$kh = \frac{q\mu}{2\pi} (|p_D''|/p'')(t_D/t)^2 \qquad (C.10)$$

C.3 Conversion to Oil Field Units

The equations in the previous section are in darcy units. In oil field units, Eq. C.3 is:

$$p_D'' = - \frac{\phi\mu c r_w^2}{0.000264\ k} (26.856\ r_w^2 h\phi c)\ \frac{p'}{qB} \qquad (C.11)$$

$$|p_D''| = (1.0184 \times 10^5)\left(\frac{\phi\mu c r_w^2}{k}\right)^2 \frac{kh}{q\mu B}\ p'' \qquad (C.12)$$

where $p'' = psi/hr^2$, $r_w = ft$, $h = ft$, $\phi = fraction$, $c = psi^{-1}$, $q = STB/D$ and $t = hrs$.

When t is in days, Eq. C.11 becomes:

$$p_D'' = - \frac{\phi\mu c r_w^2}{0.00634\ k} (1.119\ r_w^2 h\phi c)(p''/q\mu B) \qquad (C.13)$$

or

$$|p_D''| = (1.765 \times 10^2)\left(\frac{\phi\mu c r_w^2}{k}\right)^2 \frac{kh}{q\mu B}\ p'' \qquad (C.14)$$

where p" is in psi/day^2.

Equation C.7 in oil field units is

$$|p''| = \frac{1}{t^2}\left(70.6\ \frac{q\mu B}{kh}\right)\exp\left(-\ \frac{\phi\mu c r^2}{0.001055\ kt}\right)\left(\frac{\phi\mu c r^2}{0.001055kt} - 1\right) \qquad (C.15)$$

where p" is in psi/hr^2 and t is in hr.

Further, in oil field units Eq. C.10 yields:

$$kh = (141.3\ q\mu B)(|p_D''|/p'')(t_D/t)^2 \qquad (C.16)$$

APPENDIX D

TIME RATE OF CHANGE OF SHUT-IN WELL PRESSURE FOR A WELL IN AN INFINITE RESERVOIR

D.1 Equations for p'_{Ds}

The time rate of change of shut-in well pressure is given by Eq. 4.23 of the text:

$$p'_{Ds} = p'_{Dw}(t + \Delta t)_D - p'_{Dw}(\Delta t)_D \qquad (4.23)$$

where p'_{Dw} is the derivative of p_{Dw} with respect to t_D.

For a well in an infinite reservoir, p'_{Dw} is given by Eq. 2.11 of the text, and therefore the above equation yields:

$$p'_{Ds} = \frac{1}{2(t + \Delta t)_D} - \frac{1}{2(\Delta t)_D} \qquad (D.1)$$

or

$$p'_{Ds} = -\frac{1}{2}\frac{t_D}{(t + \Delta t)_D(\Delta t)_D} \qquad (D.2)$$

Two limiting forms for p'_{Ds} under various time domains of interest are obtained as follows:

Case 1: For $\Delta t_D << t_D$, Eq. D.2 can be rearranged into the following form:

$$p'_{Ds} = -\frac{1}{2}\frac{t_D}{t_D(1 + \Delta t_D/t_D)(\Delta t_D)} = -\frac{1}{2}\frac{1}{(1 + \Delta t_D/t_D)(\Delta t_D)} \tag{D.3}$$

which results in:

$$p'_{Ds} = -\frac{1}{2\Delta t_D} \qquad \text{as } \Delta t_D/t_D \to 0 \text{ when } \Delta t_D \ll t_D.$$

or

$$|p'_{Ds}| = 1/(2\Delta t_D) \ . \tag{D.4}$$

Thus,

$$\log |p'_{Ds}| = -\log \Delta t_D - 0.30103 \tag{D.5}$$

which is similar to Eq. 2.12 for well pressures during drawdown.

Case 2: When $\Delta t_D \gg t_D$: In view of Eq. D.1, p'_{Ds} approaches zero when $\Delta t_D \gg t_D$ because $(t + \Delta t)_D \simeq \Delta t_D$. But, if we take logarithms of both sides of Eq. D.2 we have:

$$\log |p'_{Ds}| = \log(t_D/2) - \log(t + \Delta t)_D - \log \Delta t_D \tag{D.6}$$

which yields

$$\log |p'_{Ds}| = -2 \log \Delta t_D + \log(t_D/2) \ . \tag{D.7}$$

Equation D.7 shows the influence of producing time t_D on the shut-in well pressure behavior.

D.2 Conversion to Real Parameters

In view of Eq. B.7, dimensionless p'_{Ds} is related to real p'_{ws} by:

$$p'_{Ds} = -2\pi r_w^2 h\phi c \frac{1}{q} [\partial p_{ws}/\partial(\Delta t)] \ . \qquad (D.8)$$

Multiplying the above equation by Δt_D, we have:

$$|p'_{Ds}| \cdot \Delta t_D = \frac{2\pi kh}{q\mu} (p'_{ws})(\Delta t) \ . \qquad (D.9)$$

From Eq. B.9 of Appendix B, we get for Eq. D.4:

$$p'_{ws} = \frac{1}{\Delta t} \frac{q\mu}{4\pi kh} \qquad (D.10)$$

or

$$\log p'_{ws} = - \log \Delta t + \log[q\mu/(4\pi kh)] \ . \qquad (D.11)$$

Further, we get from Eq. D.7:

$$|p'_{Ds}| = \frac{t_D}{2\Delta t_D^2} = \frac{\frac{kt}{\phi\mu c r_w^2}}{2\left(\frac{k\Delta t}{\phi\mu c r_w^2}\right)^2} \qquad (D.12)$$

or

$$p'_{ws} = \frac{t}{\Delta t^2} \frac{q\mu}{4\pi kh} \qquad (D.13)$$

or

$$\log p'_{ws} = -2 \log \Delta t + \log t + \log[q\mu/(4\pi kh)] \ . \qquad (D.14)$$

D.3 Conversion to Oil Field Units

In oil field units, Eq. D.8 is given by

$$|p'_{Ds}| = (26.856\ r_w^2 h\phi c)[p'_{ws}/(qB)] \qquad (D.15)$$

and Eq. D.9 by

$$|p'_{Ds}| \cdot \Delta t_D = \frac{kh}{141.3\ q\mu B} (p'_{ws})(\Delta t) \ . \qquad (D.16)$$

Further, from the above two equations we have:

$$\phi c = [qB/(26.856\ r_w^2 h)][|p'_{Ds}|/p'_{ws}] \qquad (D.17)$$

and

$$kh = 141.3\ q\mu B(|p'_{Ds}|/p'_{ws})(\Delta t_D/\Delta t)\ . \qquad (D.18)$$

APPENDIX E

SECOND DERIVATIVE OF SHUT-IN WELL PRESSURE FOR A WELL IN AN INFINITE RESERVOIR

E.1 Equations for p''_{Ds}

The second derivative of shut-in well pressure is obtained from Eq. 4.31 of the text:

$$p''_{Ds} = p''_{Dw}(t + \Delta t)_D - p''_{Dw}(\Delta t)_D$$

where p''_{Dw} is the second derivative of p_{Dw} with respect to Δt_D. For a well in an infinite reservoir, p''_{Dw} is given by Eq. 2.22 and therefore the above equation yields:

$$p''_{Ds} = -\frac{1}{2(t + \Delta t)_D^2} - \left[-\frac{1}{2\Delta t_D^2}\right] \tag{E.1}$$

$$= -\frac{1}{2}\left[\frac{1}{(t + \Delta t)_D^2} - \frac{1}{\Delta t_D^2}\right] \tag{E.2}$$

$$= -\frac{1}{2}\left[\frac{1}{(t + \Delta t)_D} - \frac{1}{\Delta t_D}\right]\left[\frac{1}{(t + \Delta t)_D} + \frac{1}{\Delta t_D}\right] \tag{E.3}$$

or

$$p''_{Ds} = +\frac{1}{2}\left[\frac{t_D}{(t + \Delta t)_D(\Delta t)_D}\right]\left[\frac{t_D + 2\Delta t_D}{(t + \Delta t)_D(\Delta t)_D}\right]. \tag{E.4}$$

Two limiting forms for p''_{Ds} are obtained as follows:

Case 1: For $\Delta t_D << t_D$: Eq. E.4 can be rearranged in the following form:

$$p''_{Ds} = \frac{1}{2}\left[\frac{t_D}{t_D(1 + \Delta t/t)\Delta t_D}\right]\left[\frac{t_D(1 + 2\Delta t/t)}{t_D(1 + \Delta t/t)\Delta t_D}\right] \qquad (E.5)$$

which yields when $(\Delta t/t)$ approaches zero:

$$p''_{Ds} = 1/(2\Delta t_D^2) \qquad (E.6)$$

or

$$\log p''_{Ds} = -2 \log \Delta t_D - 0.30103 \qquad (E.7)$$

which is similar to Eq. 2.24 for drawdown testing.

Case 2: For $\Delta t_D >> t_D$: Eq. E.4 can be rearranged as:

$$p''_{Ds} = \frac{1}{2}\left[\frac{t_D}{\Delta t_D^2(1 + t/\Delta t)}\right]\left[\frac{t_D(2 + t/\Delta t)}{\Delta t_D^2(1 + t/\Delta t)}\right] \qquad (E.8)$$

which gives the following when $(t/\Delta t) \to 0$:

$$p''_{Ds} = t_D/(\Delta t_D^3) \qquad (E.9)$$

or

$$\log p''_{Ds} = -3 \log \Delta t_D + \log t_D \ . \qquad (E.10)$$

Equation E.10 shows that p''_{Ds} at long shut-in times is a function of producing time t_D.

E.2 Conversion to Real Parameters

In view of Eq. C.4, dimensionless p''_{Ds} is related to p''_{ws} by:

$$p''_{Ds} = \left(\frac{\phi\mu c r_w^2}{k}\right)^2 \left(\frac{2\pi kh}{q\mu}\right) \left|\frac{\partial^2 p_{ws}}{\partial \Delta t^2}\right| . \qquad (E.11)$$

Multiplying Eq. E.11 by Δt_D^2 we have

$$p''_{Ds} \cdot \Delta t_D^2 = \left(\frac{2\pi kh}{q\mu}\right) |p''_{ws}| \cdot (\Delta t^2) \qquad (E.12)$$

From Eq. C.7 of Appendix C, we get for Eq. E.6:

$$|p''_{ws}| = \frac{1}{\Delta t^2}\left(\frac{q\mu}{4\pi kh}\right) \qquad (E.13)$$

or

$$\log |p''_{ws}| = -2 \log \Delta t + \log[q\mu/(4\pi kh)] \qquad (E.14)$$

and for Eq. E.9:

$$|p''_{ws}| = \frac{t}{\Delta t^3}\left(\frac{q\mu}{2\pi kh}\right) \qquad (E.15)$$

or

$$\log |p''_{ws}| = -3 \log \Delta t + \log t + \log[q\mu/(2\pi kh)]. \qquad (E.16)$$

E.3 Conversion to Oil Field Units

In view of Eq. C.9, Eq. E.11 in oil field units is:

$$p''_{Ds} = (1.0184 \times 10^5)[\phi\mu c r_w^2/k]^2 \left(\frac{kh}{q\mu B}\right) |p''_{ws}| \qquad (E.17)$$

and Eq. E.12 yields:

$$p''_{Ds} \cdot \Delta t_D^2 = \frac{kh}{141.3\ q\mu B} |p''_{ws}| \cdot \Delta t^2 . \qquad (E.18)$$

Further, from Eq. E.17 and Eq. E.18 can be used to determine the ϕc and kh products.

APPENDIX F

TYPE-CURVE PLOTS

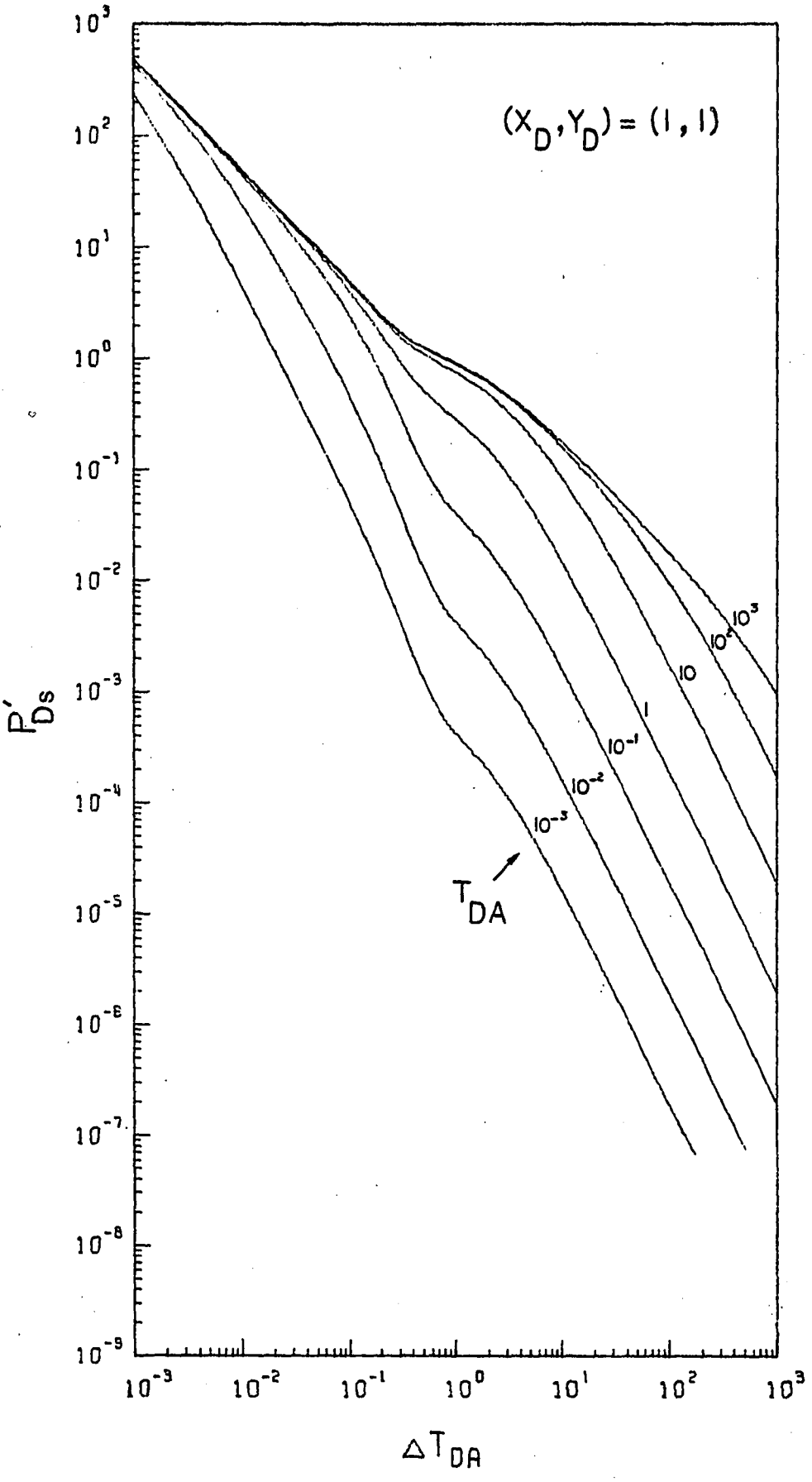

FIGURE F.1: Type curve plot of p'_{Ds} vs Δt_{DA} for a well located at $(x_D, y_D) = (1,1)$ between two perpendicular sealing faults.

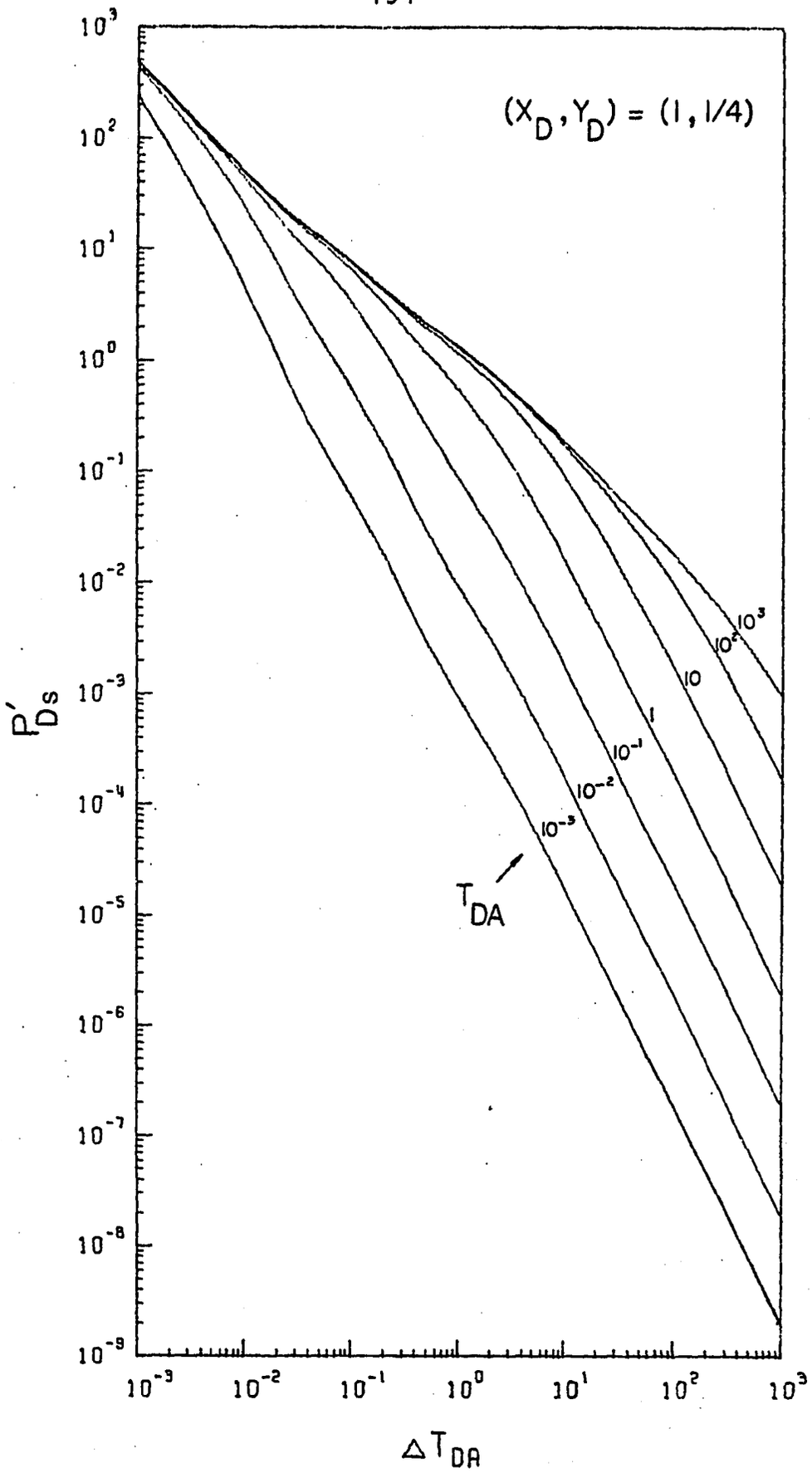

FIGURE F.2: Type-curve plot of p'_{Ds} vs Δt_{DA} for a well located at $(x_D, y_D) = (1, 1/4)$ between two perpendicular sealing faults.

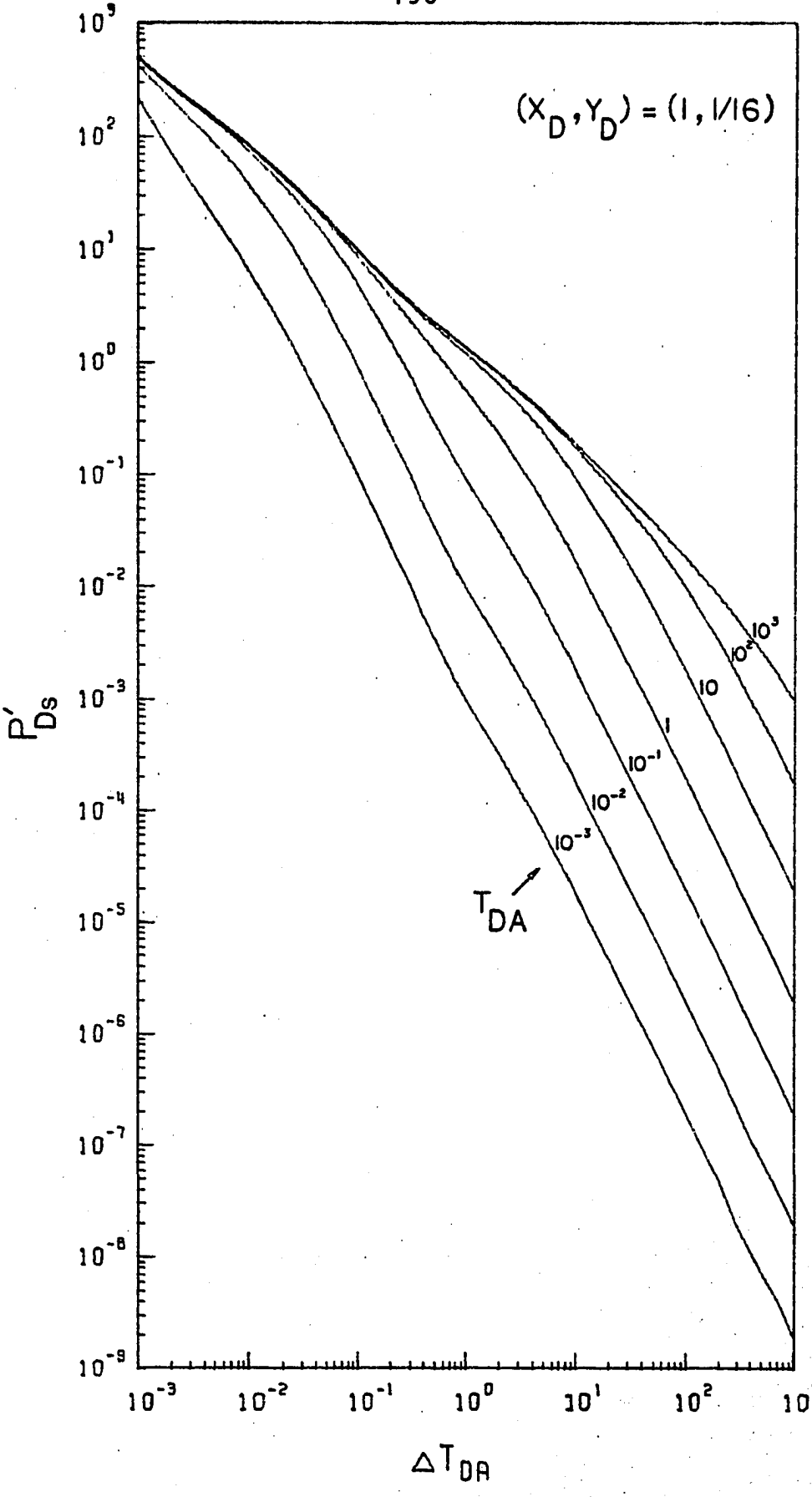

FIGURE F.3: Type-curve plot of p'_{Ds} vs Δt_{DA} for a well located at $(x_D, y_D) = (1, 1/16)$ between two perpendicular sealing faults.

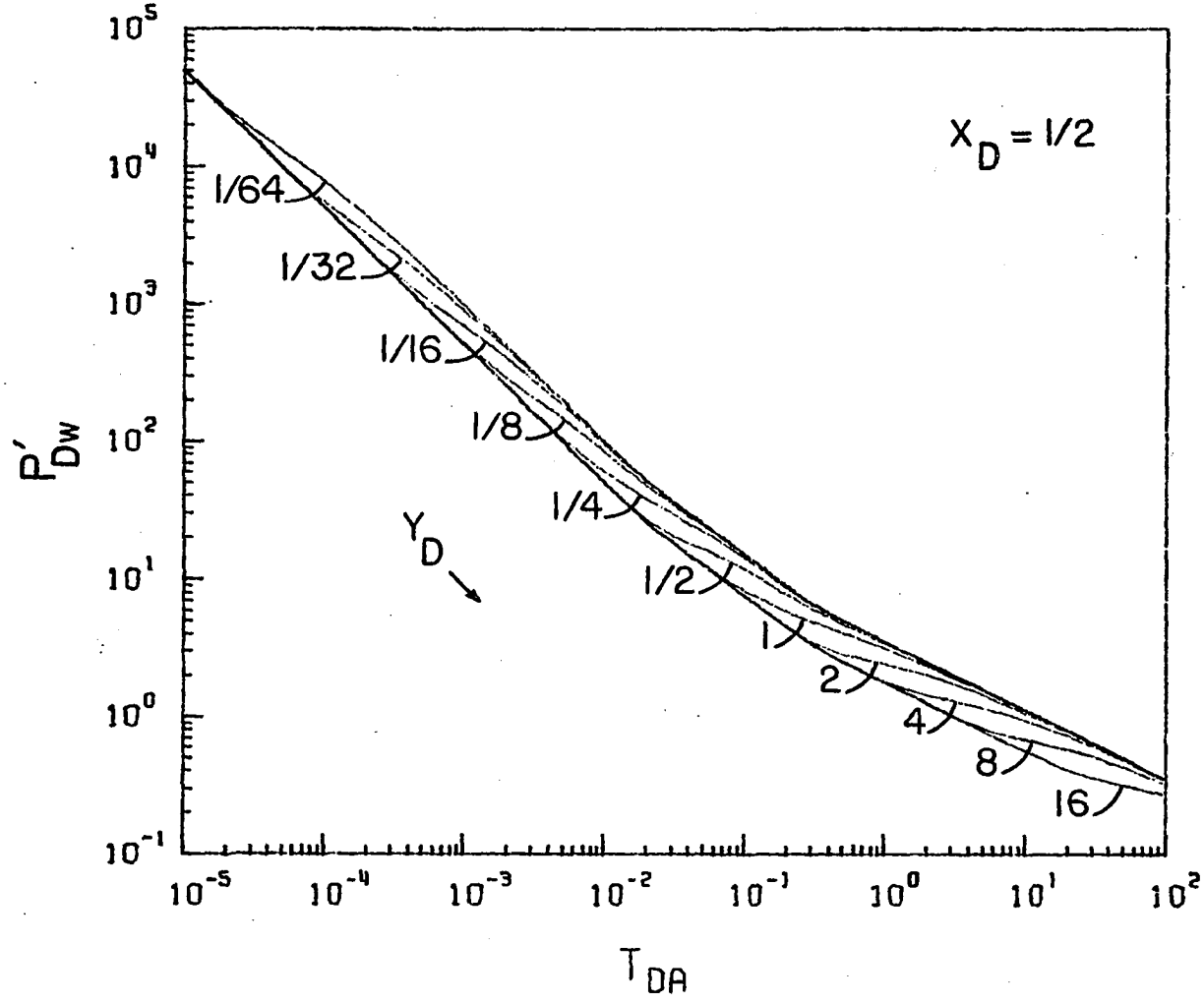

FIGURE F.4: Type-curve plot of p'_{Dw} vs t_{DA} for a well located between three perpendicular sealing faults, when $x_D = 1/2$ and $1/64 \leq y_D \leq 16$.

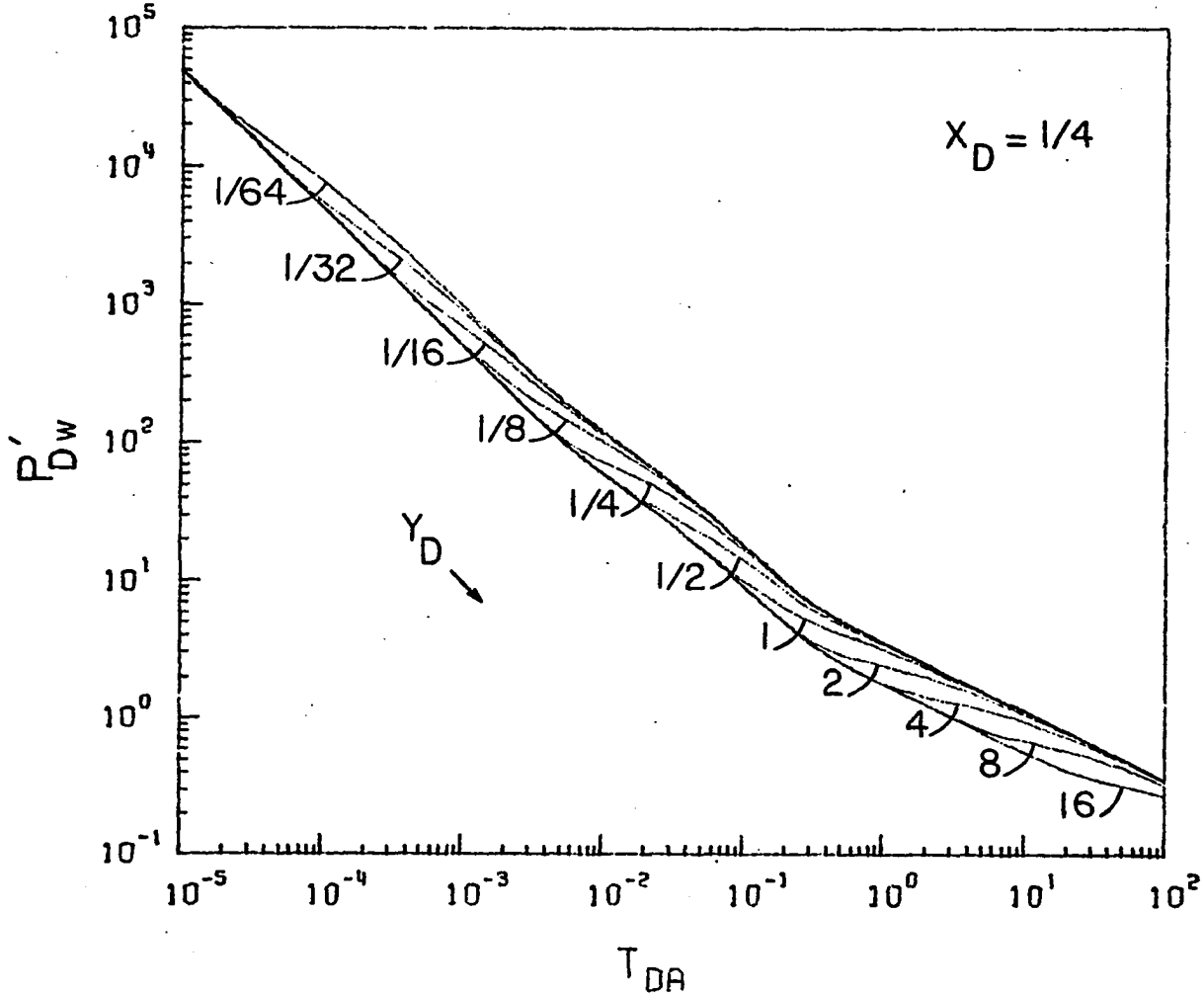

FIGURE F.5: Type-curve plot of p'_{Dw} vs t_{DA} for a well between three perpendicular sealing faults, when $x_D = 1/4$ and $1/64 \leq y_D \leq 1$.

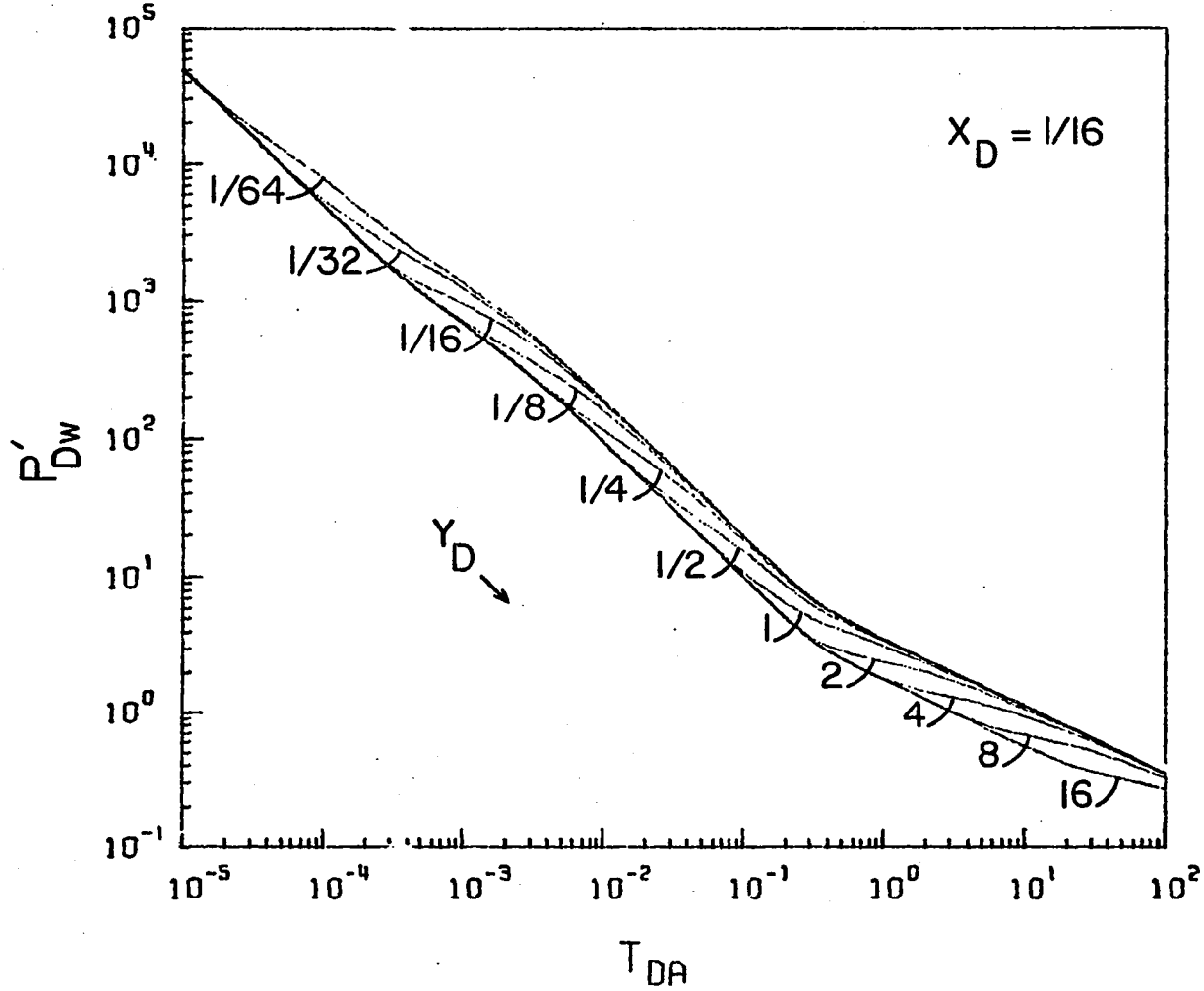

FIGURE F.6: Type-curve plot of p'_{Dw} vs t_{DA} for a well between three perpendicular sealing faults, when $x_D = 1/16$ and $1/64 \leq y_D \leq 16$.

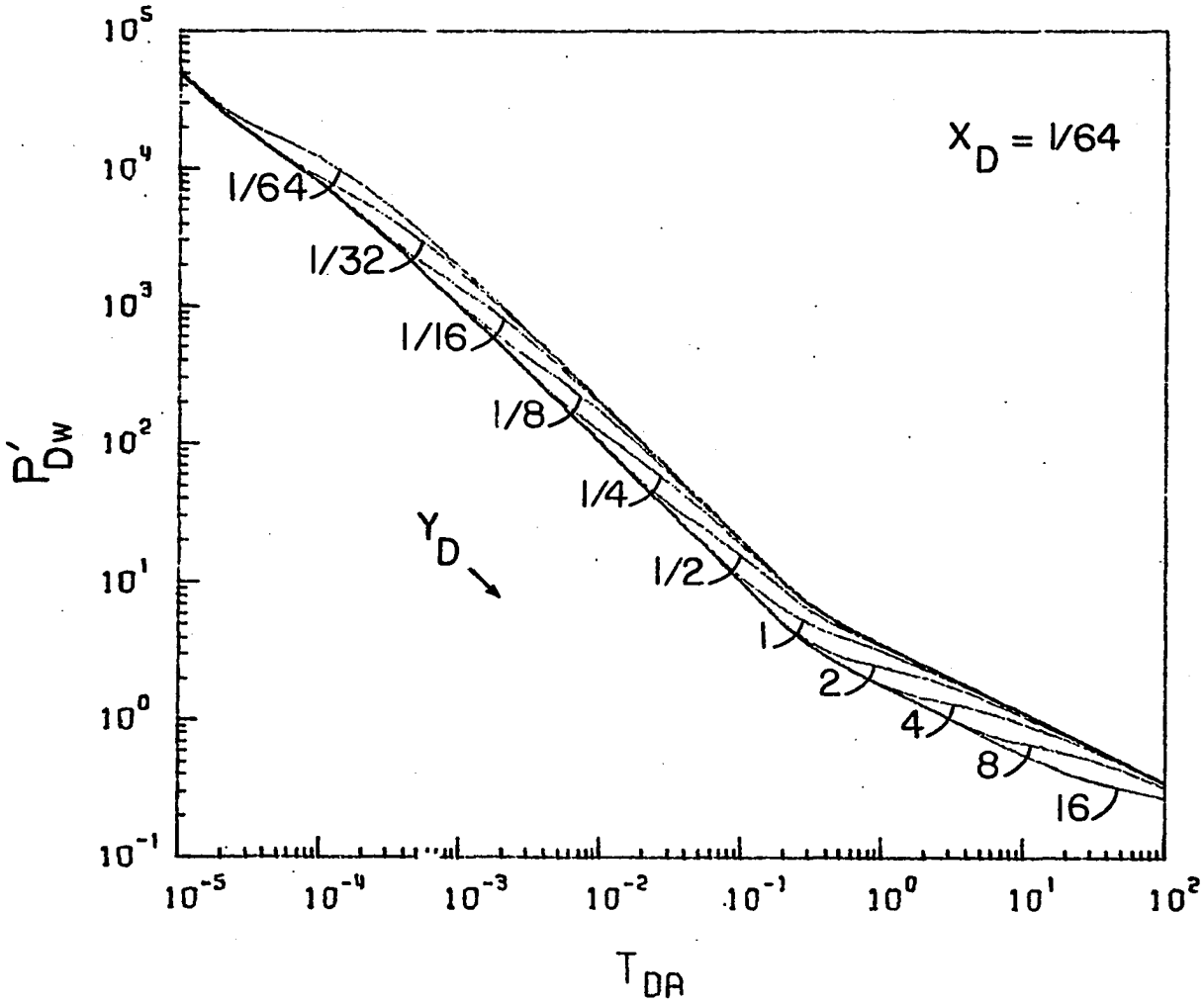

FIGURE F.7: Type-curve plot of p'_{DW} vs t_{DA} for a well between three perpendicular sealing faults, when $x_D = 1/64$ and $1/64 \leq y_D \leq 16$.

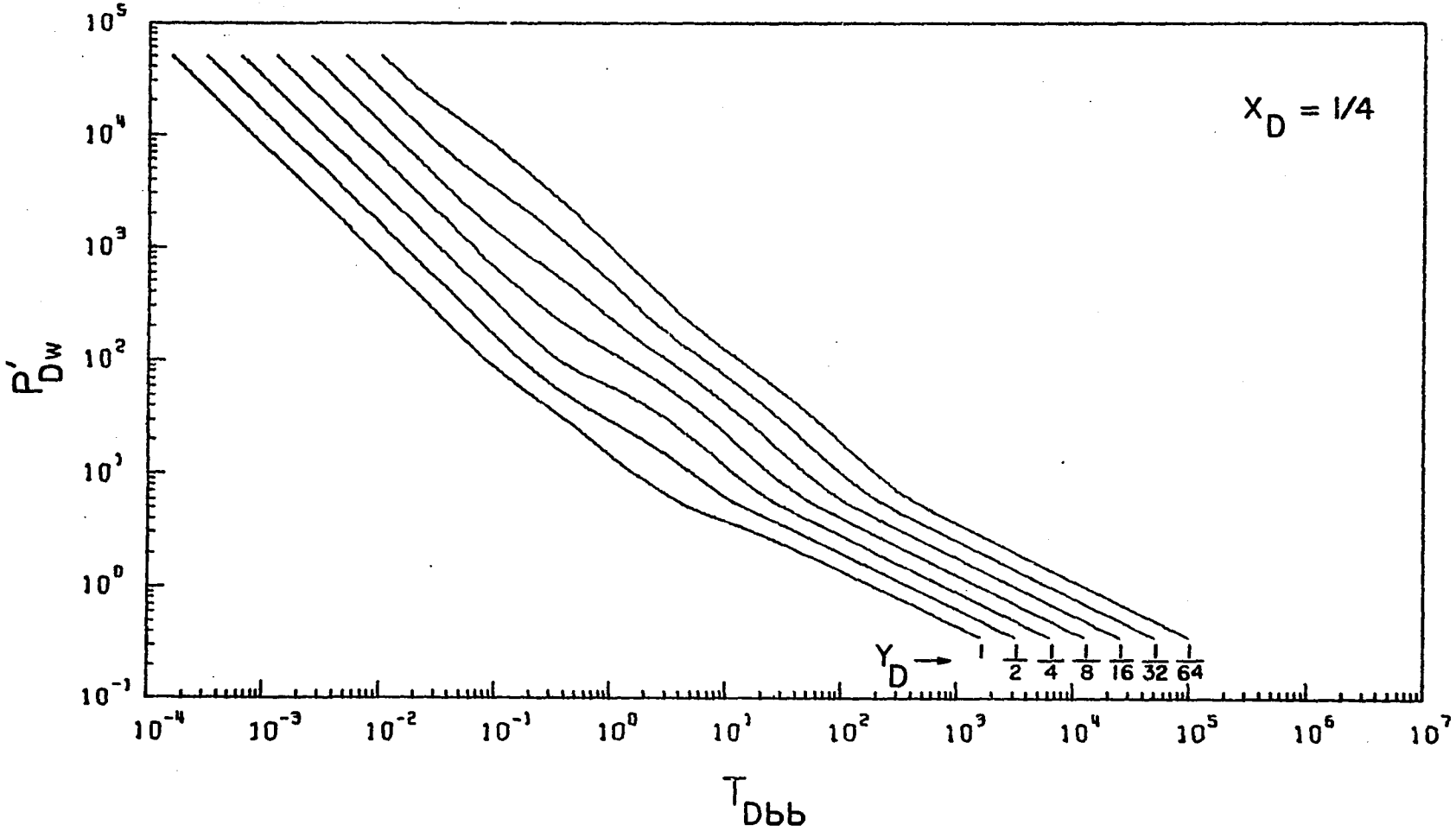

FIGURE F.8: Type-curve plot of p'_{Dw} vs t_{Dbb} for a well between three perpendicular sealing faults, when $x_D = 1/4$ and $1/64 \leq y_D \leq 1$.

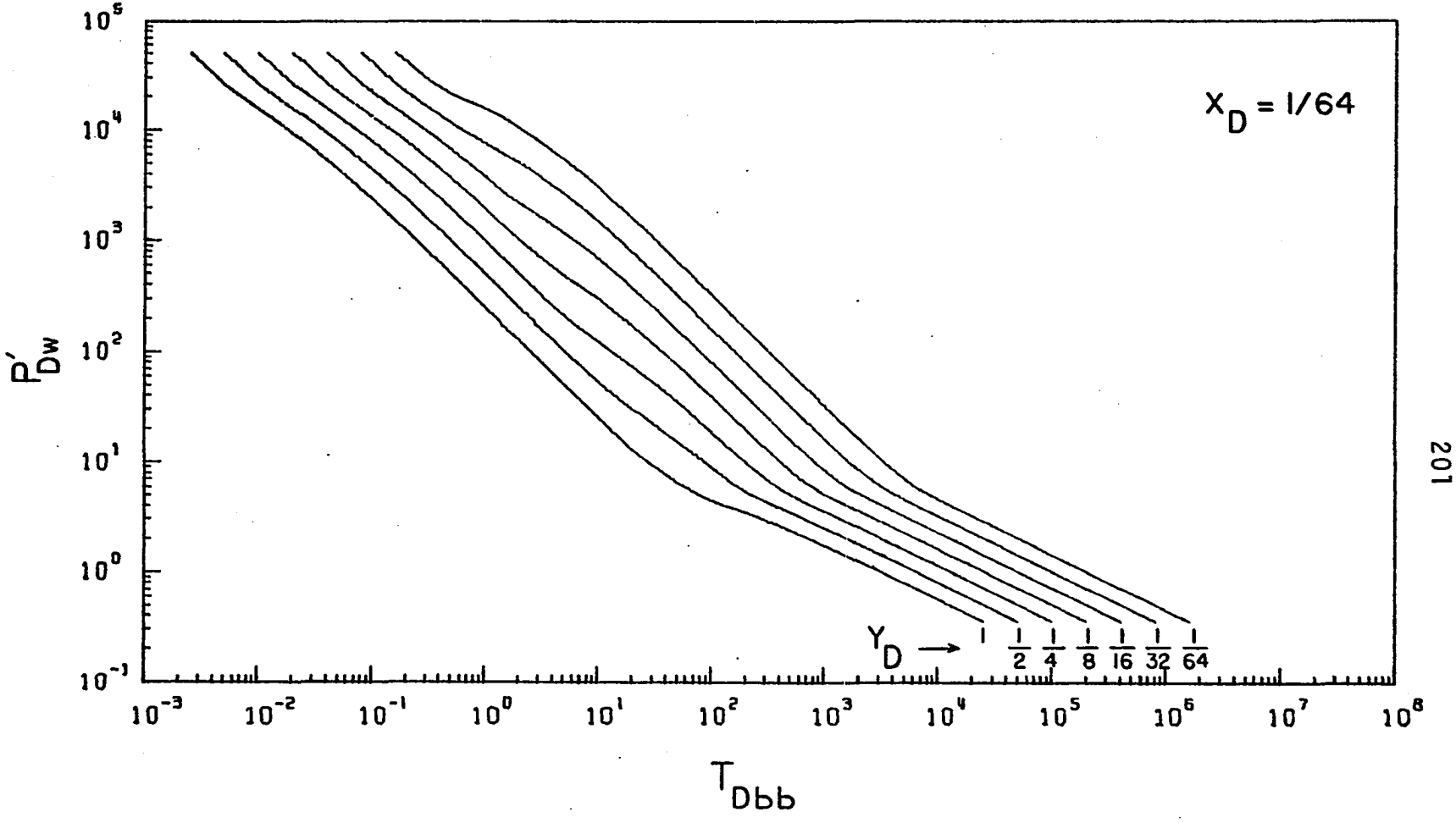

FIGURE F.9: Type plot of p'_{Dw} vs t_{Dbb} for a well between three perpendicular sealing faults, when $x_D = 1/64$ and $1/64 \leq y_D \leq 1$.

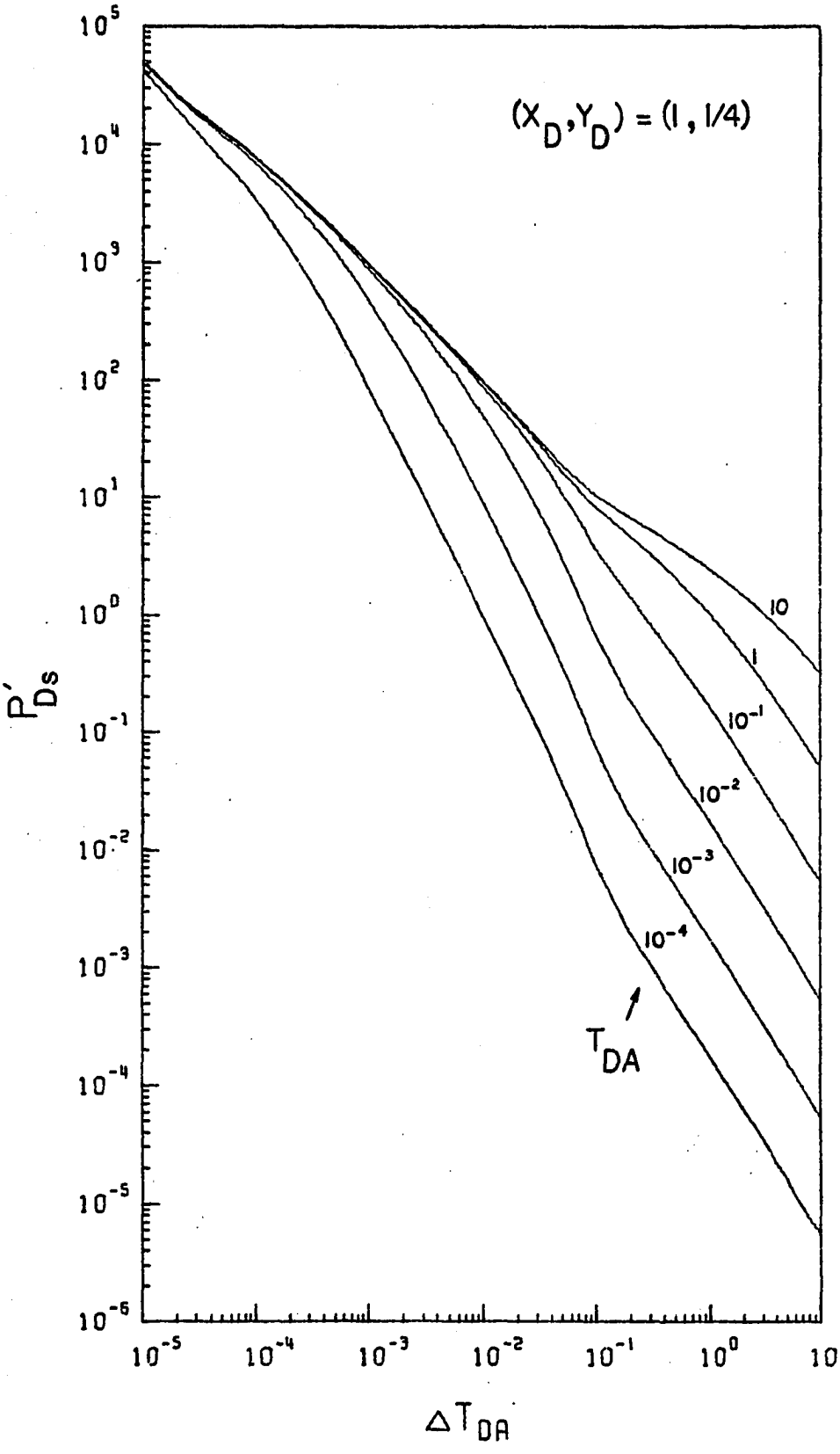

FIGURE F.10: Type-curve plot of p'_{Ds} vs Δt_{DA} for a well located at $(x_D, y_D) = (1, 1/4)$ between three perpendicular sealing faults.

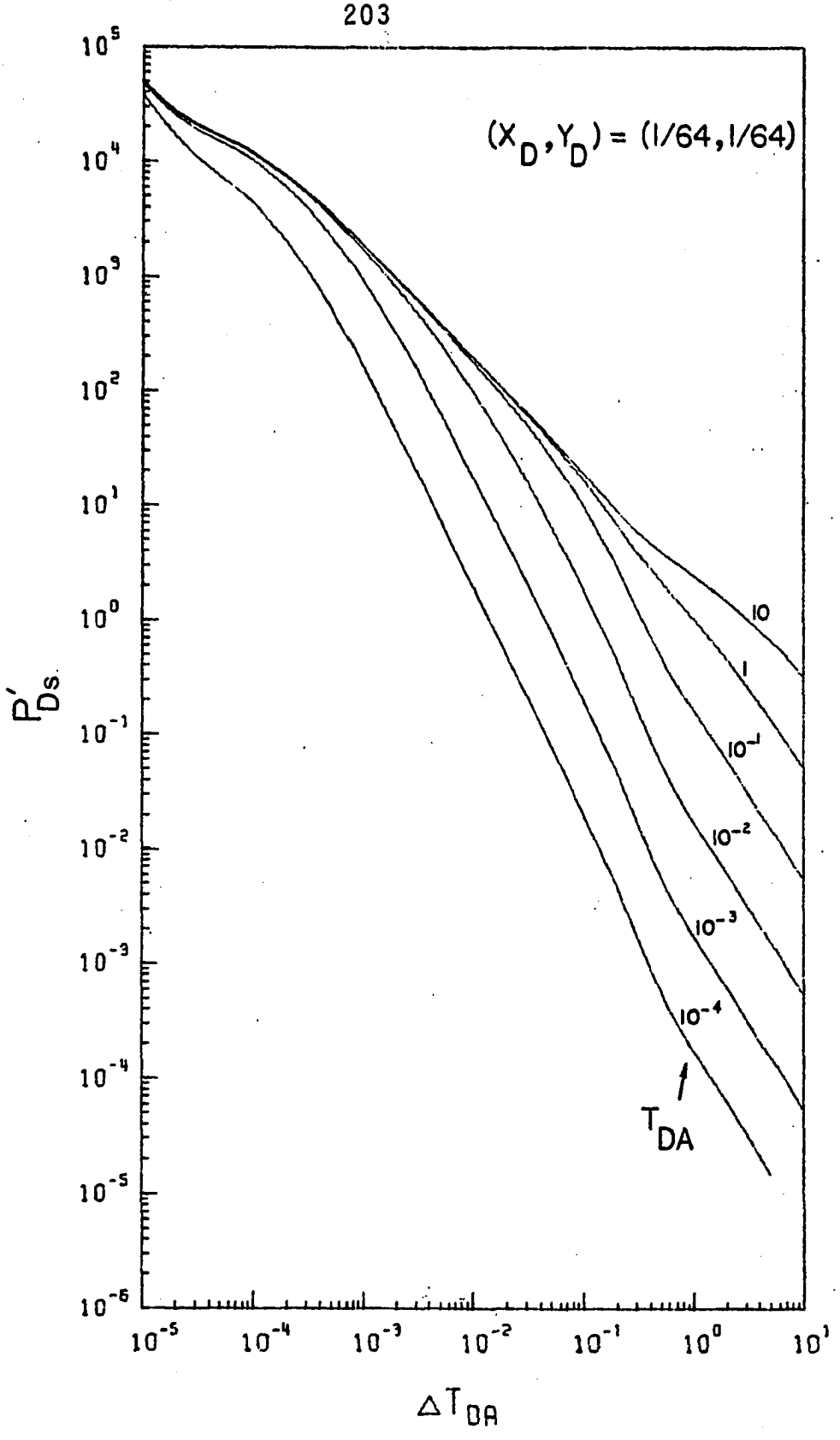

FIGURE F.11: Type-curve plot of p'_{Ds} vs Δt_{DA} for a well located at (x_D, y_D) = (1/64, 1/64) between three perpendicular sealing faults.

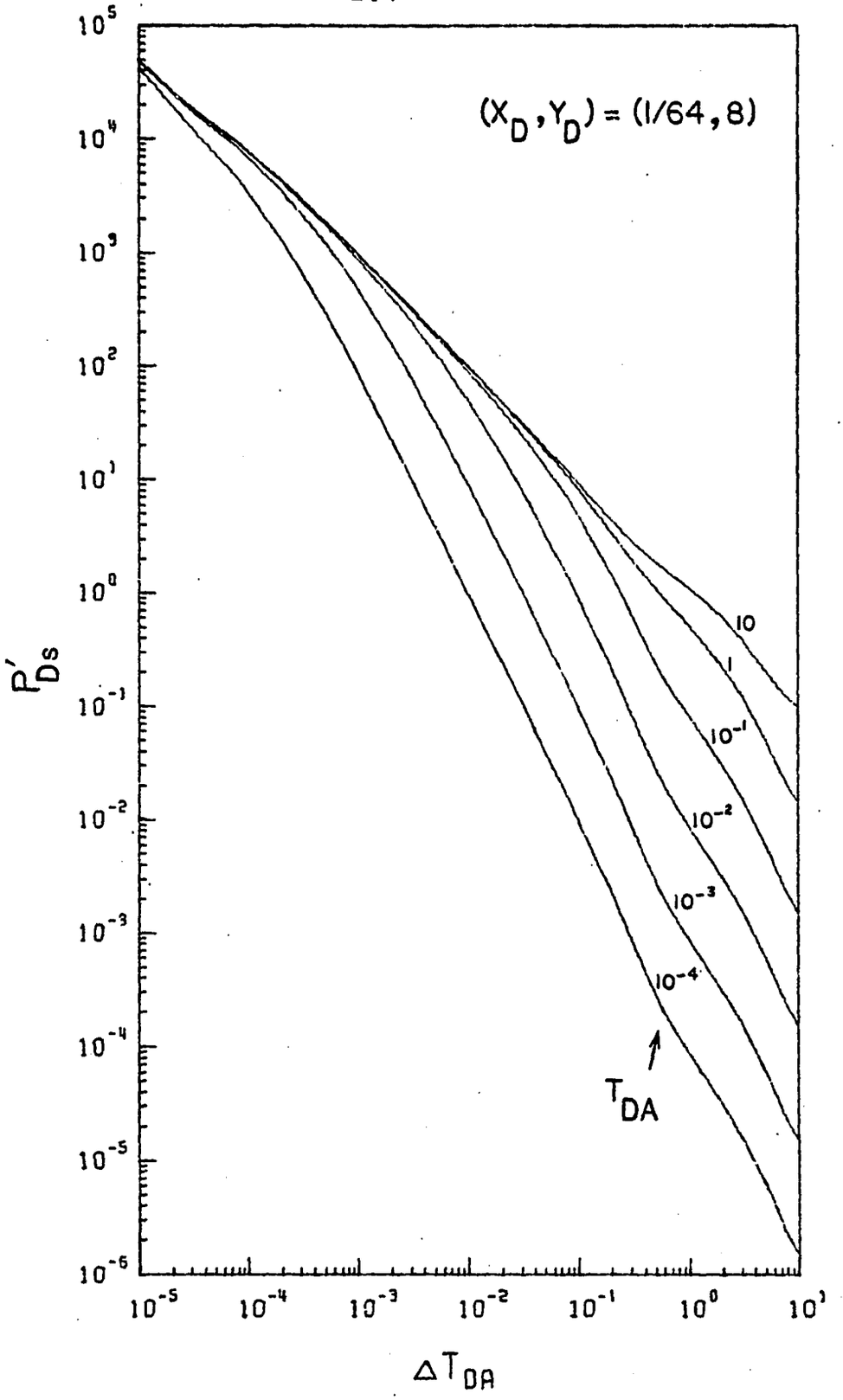

FIGURE F.12: Type-curve plot of p'_{Ds} vs Δt_{DA} for a well located at $(x_D, y_D) = (1/64, 8)$ between three perpendicular sealing faults.

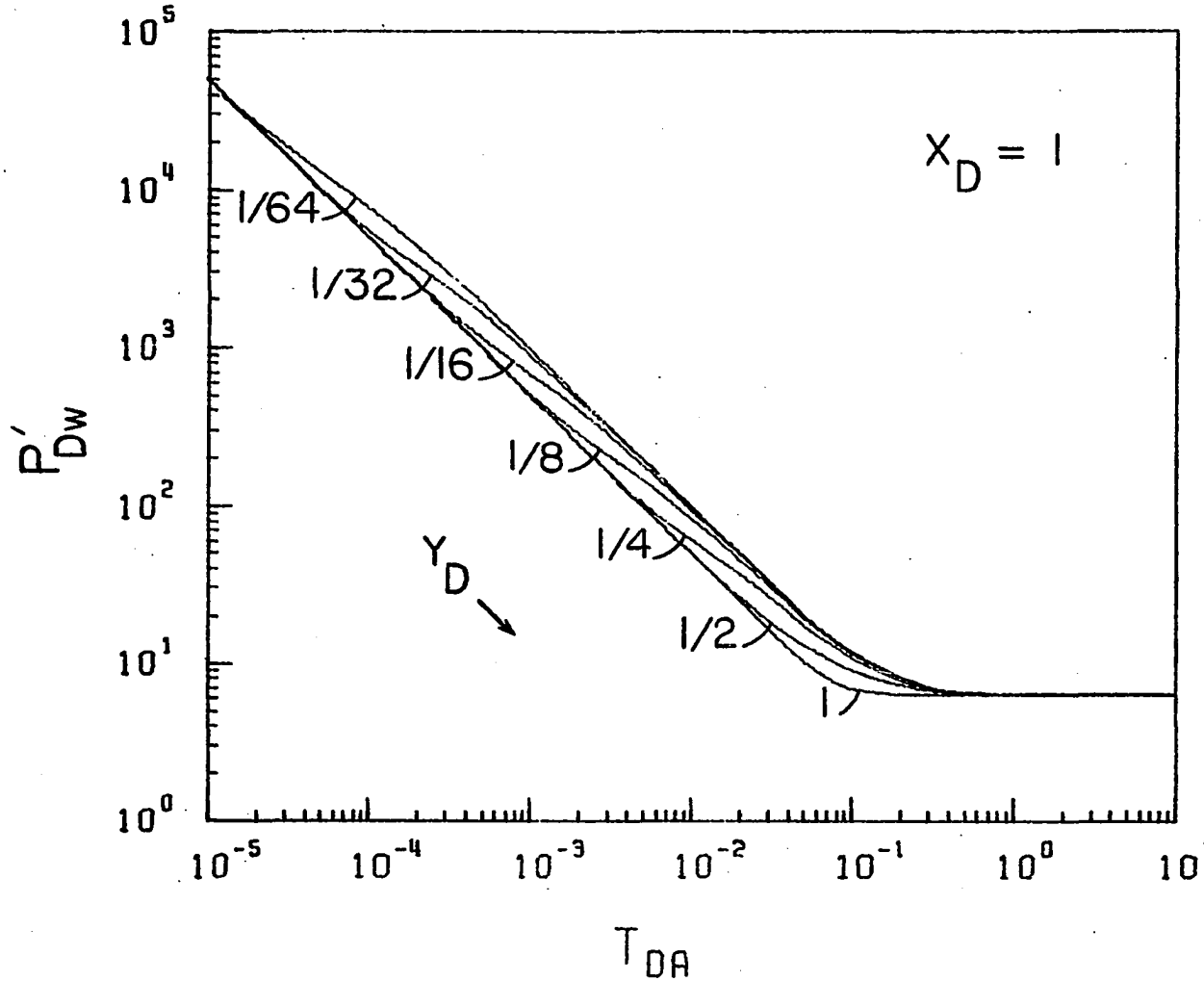

FIGURE F.13: Type-curve plot of p'_{Dw} vs t_{DA} for a well located inside a closed square, when $x_D = 1$ and $1/64 \leq y_D \leq 1$.

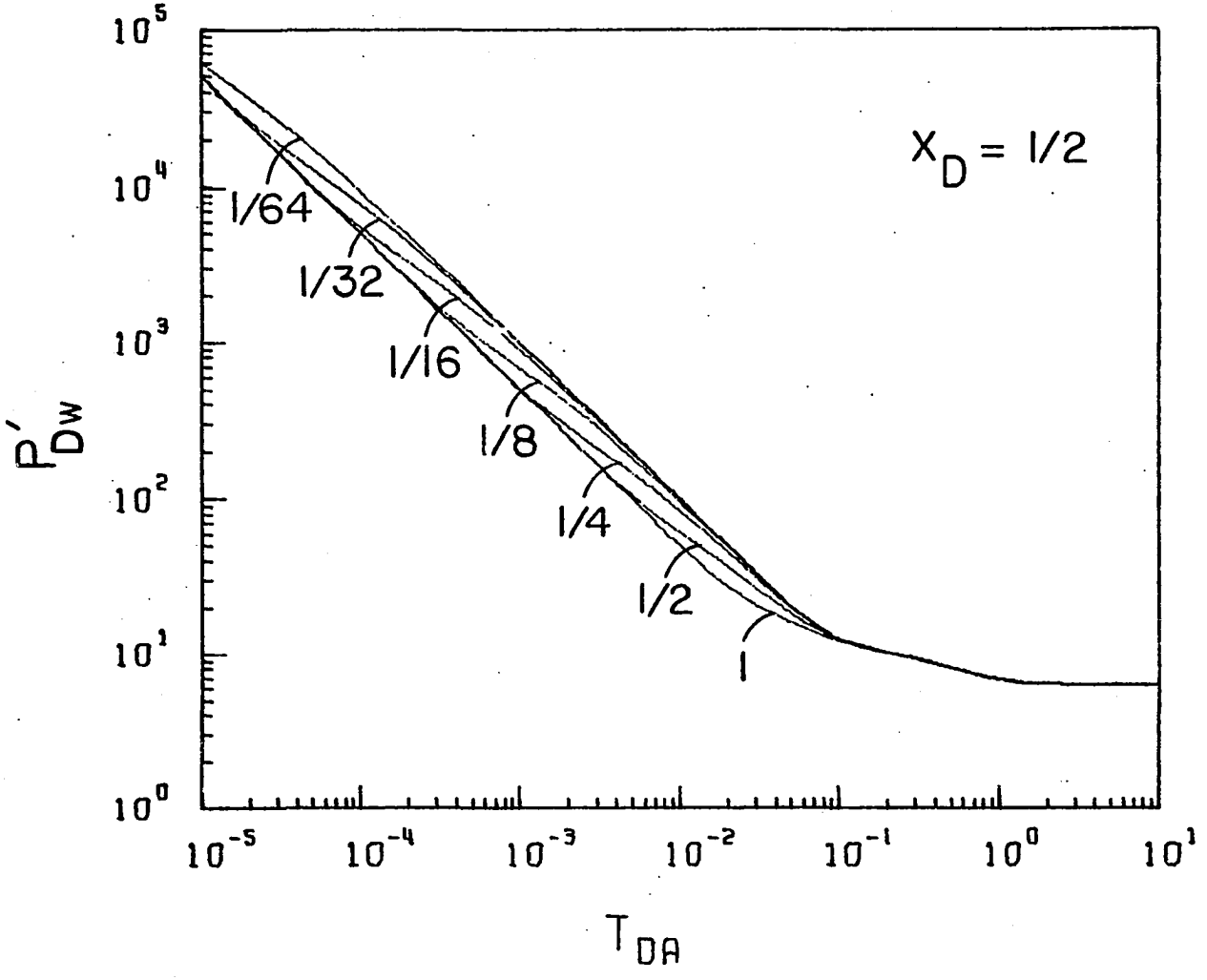

FIGURE F.14: Type-curve plot of p'_{Dw} vs t_{DA} for a well located inside a closed 4:1 rectangle, when $x_D = 1/2$ and $1/64 \leq y_D \leq 1$.

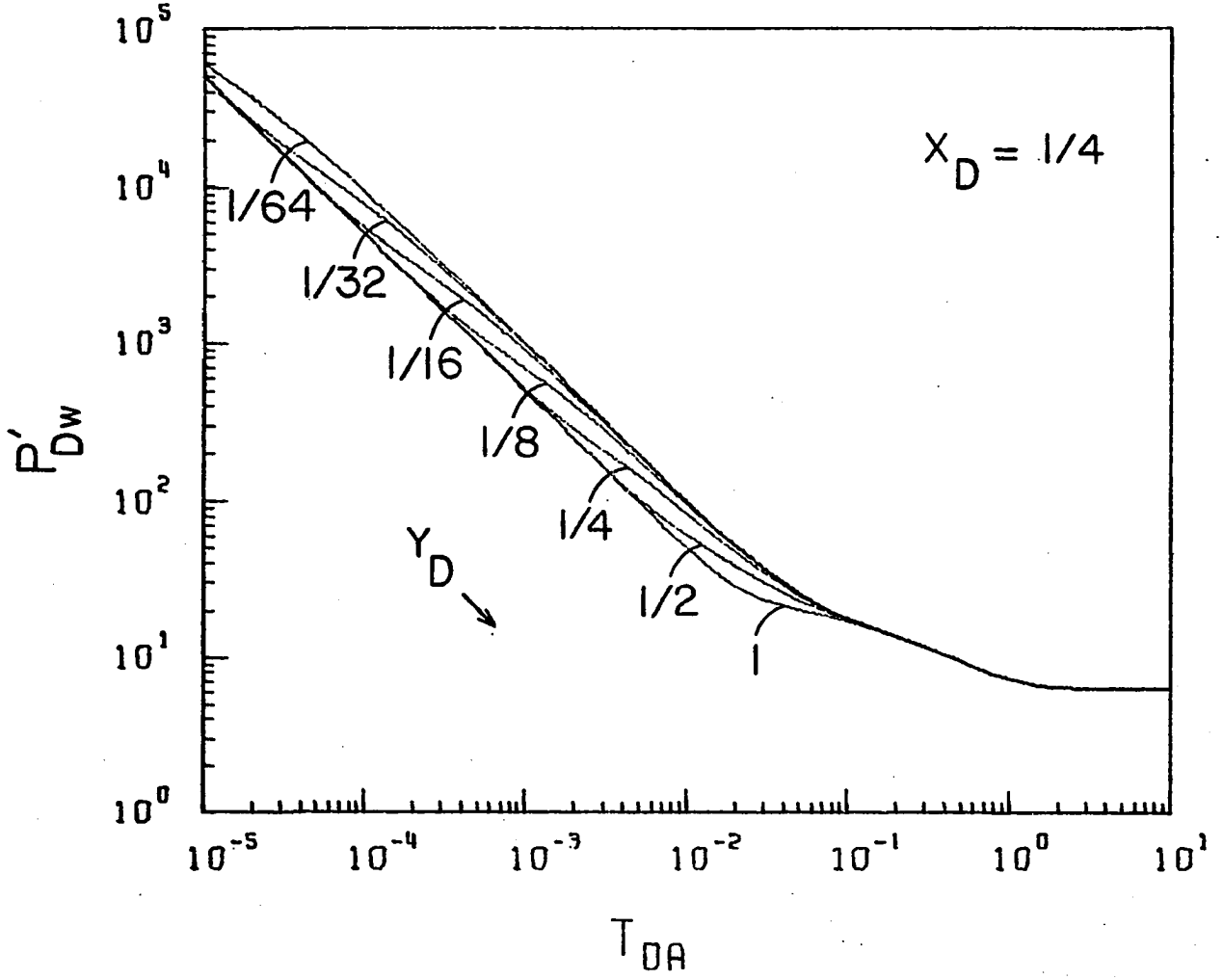

FIGURE F.15: Type-curve plot of p'_{Dw} vs t_{DA} for a well located inside a closed 4:1 rectangle, when $x_D = 1/4$ and $1/64 \leq y_D \leq 1$.

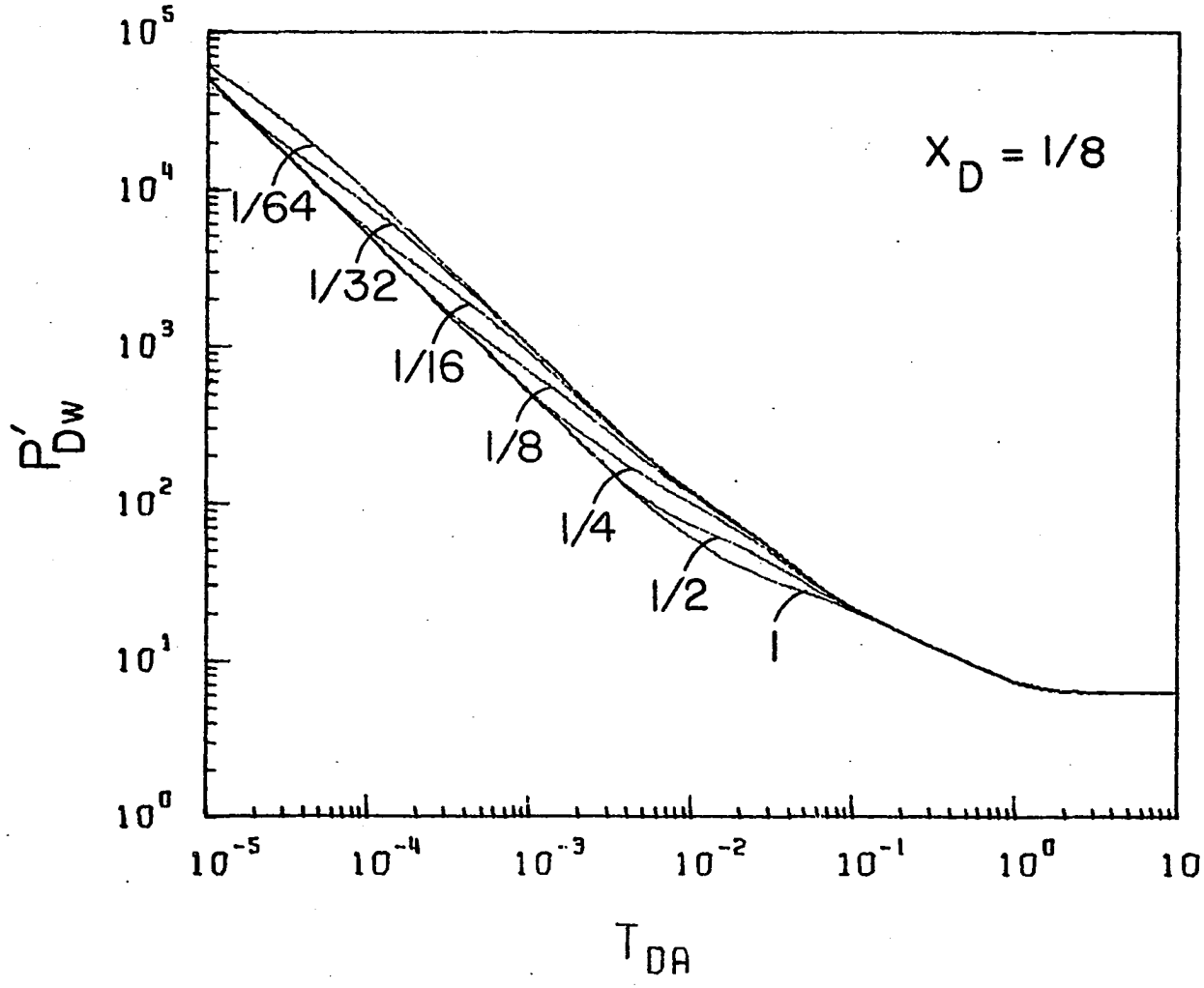

FIGURE F.16: Type-curve plot of p'_{Dw} vs t_{DA} for a well located inside a closed 4:1 rectangle, when $x_D = 1/8$ and $1/64 \leq y_D \leq 1$.

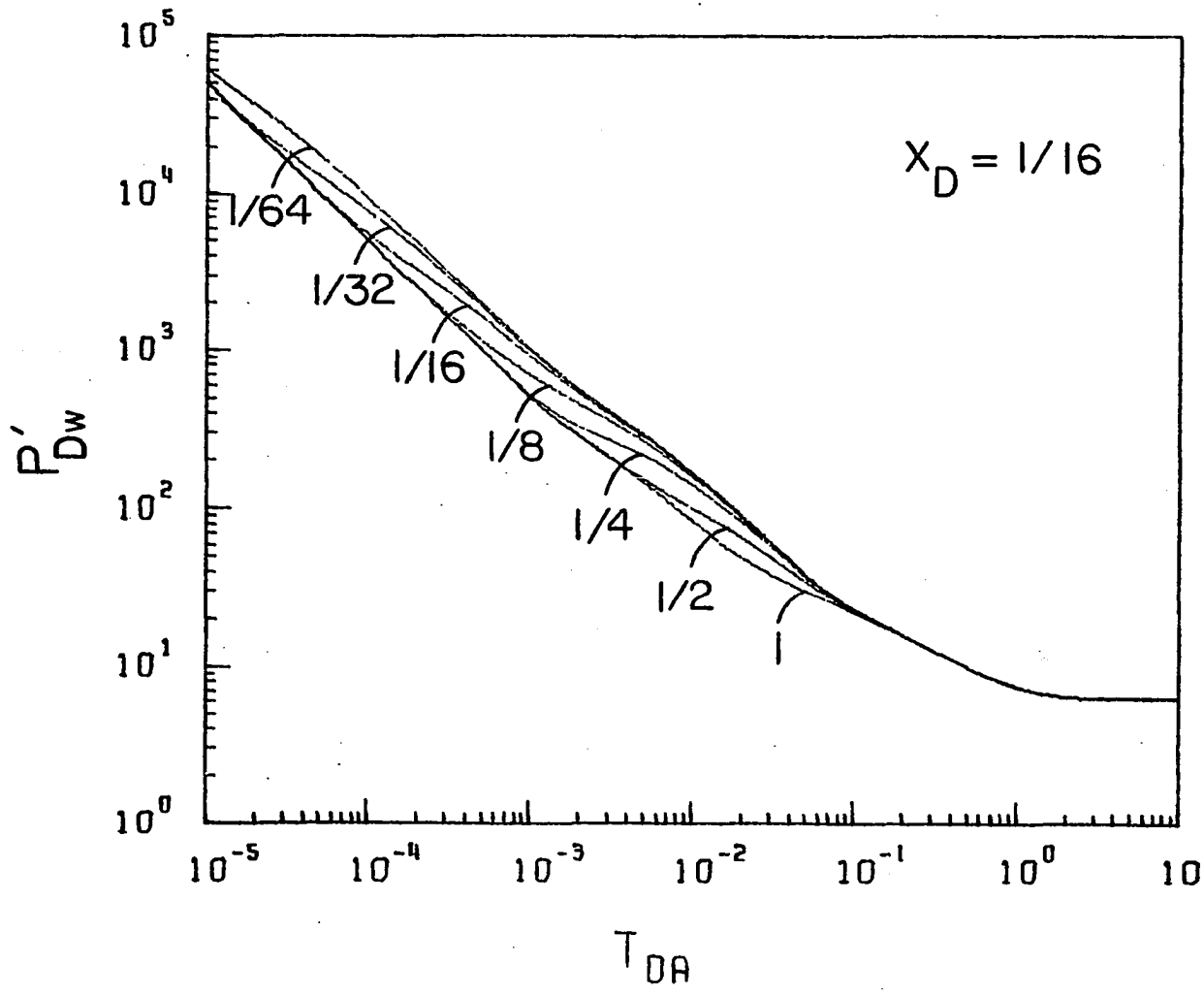

FIGURE F.17: Type-curve plot of p'_{Dw} vs t_{DA} for a well located inside a closed 4:1 rectangle, when $x_D = 1/16$ and $1/64 \leq y_D \leq 1$.

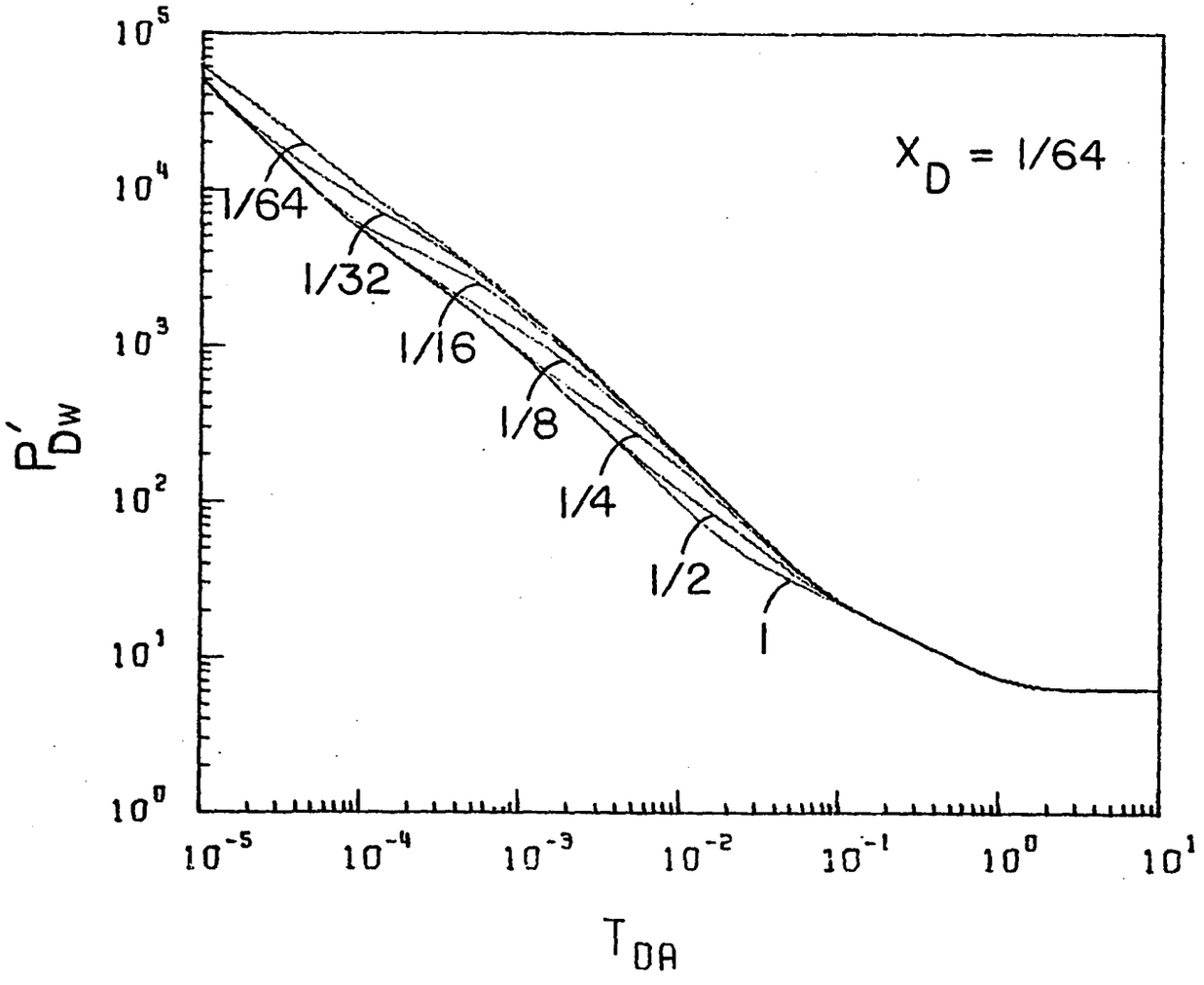

FIGURE F.18: Type-curve plot of p'_{Dw} vs t_{DA} for a well located inside a closed 4:1 rectangle, when x_D = 1/64 and $1/64 \leq y_D \leq 1$.

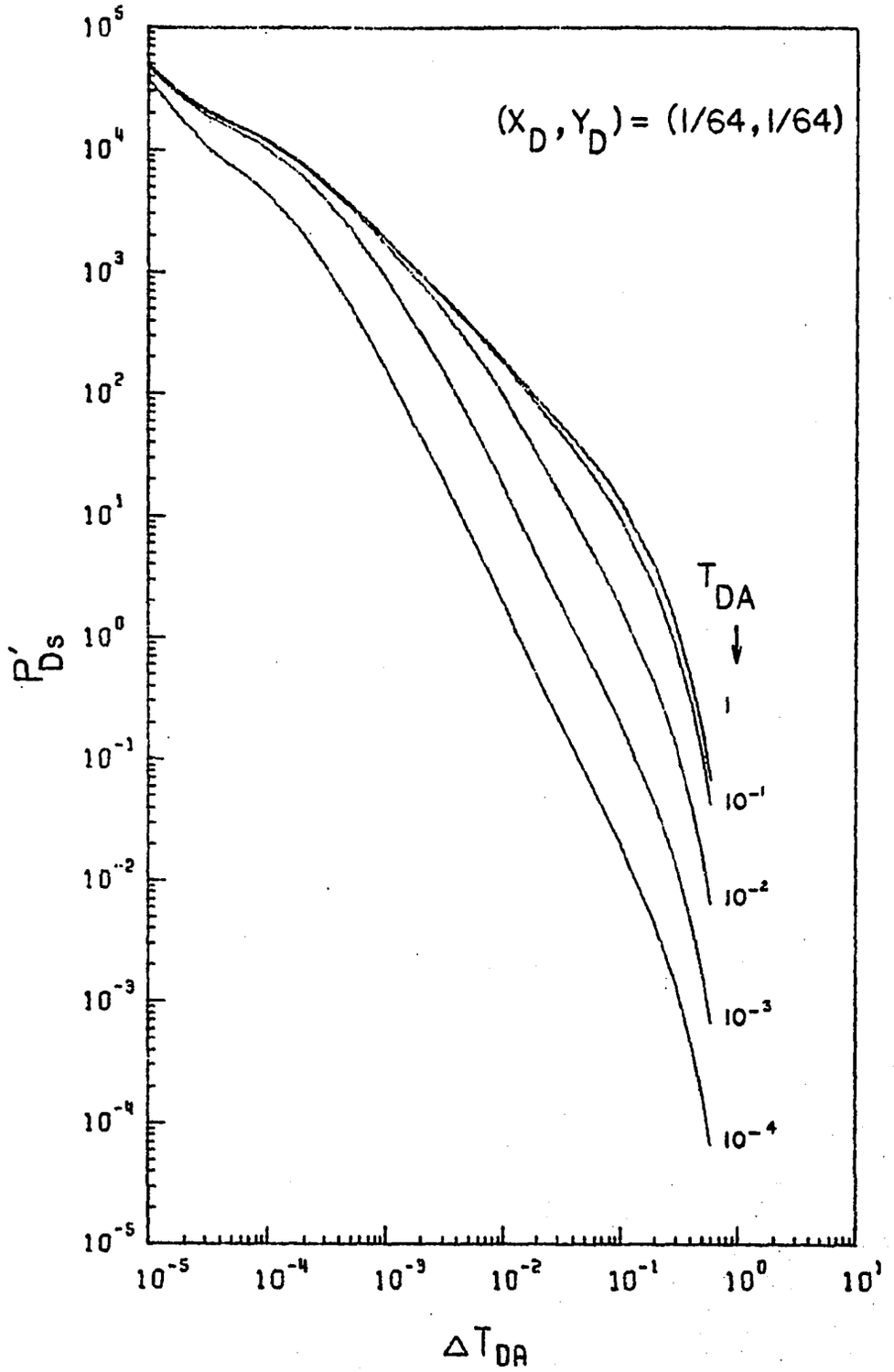

FIGURE F.19: Type-curve plot of p'_{Ds} vs Δt_{DA} for a well located at $(x_D, y_D) = (1/64, 1/64)$ inside a closed square.

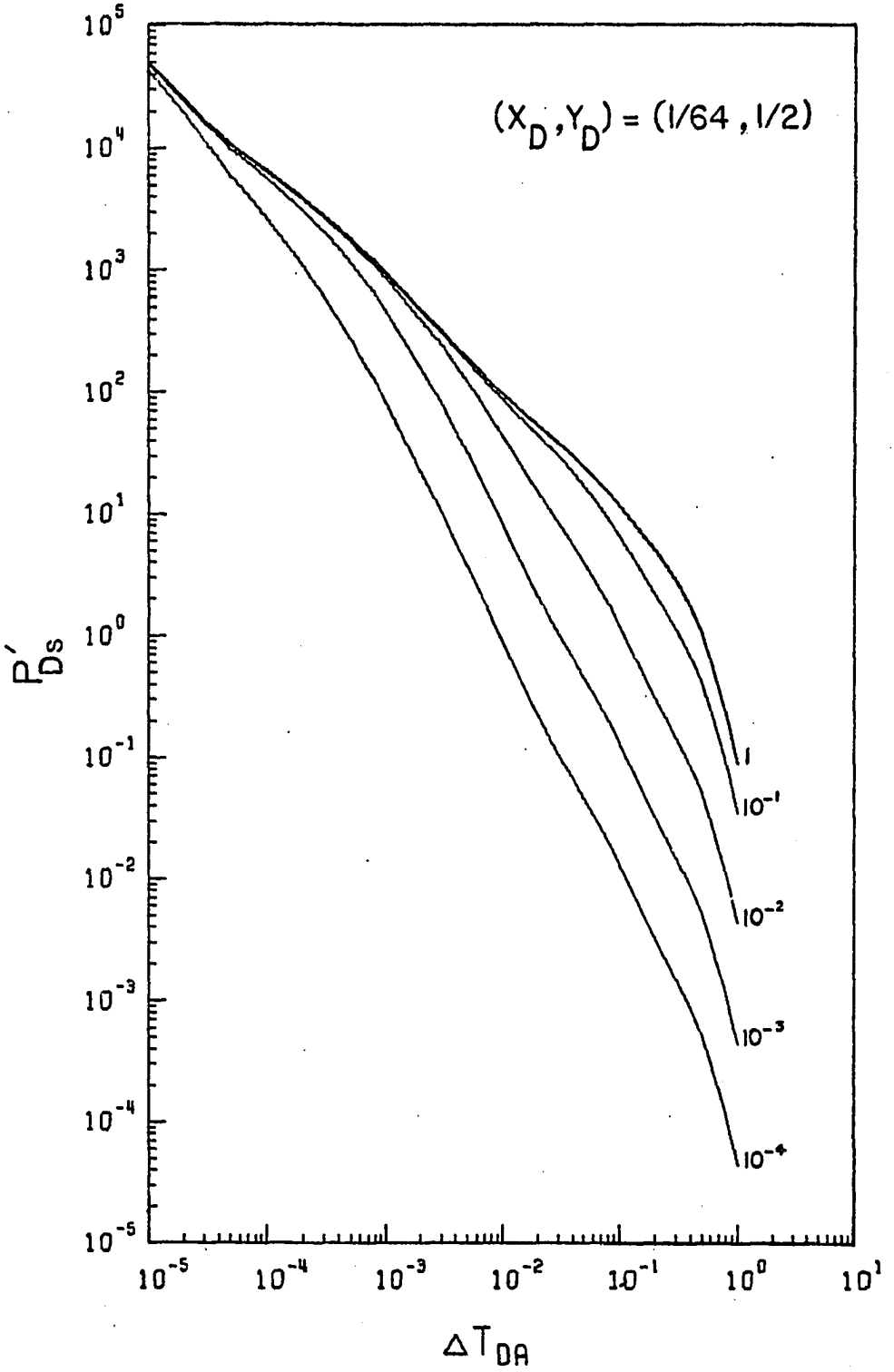

FIGURE F.20: Type-curve plot of p'_{Ds} vs Δt_{DA} for a well located at $(x_D, y_D) = (1/64, 1/2)$ inside a closed 2:1 rectangle.

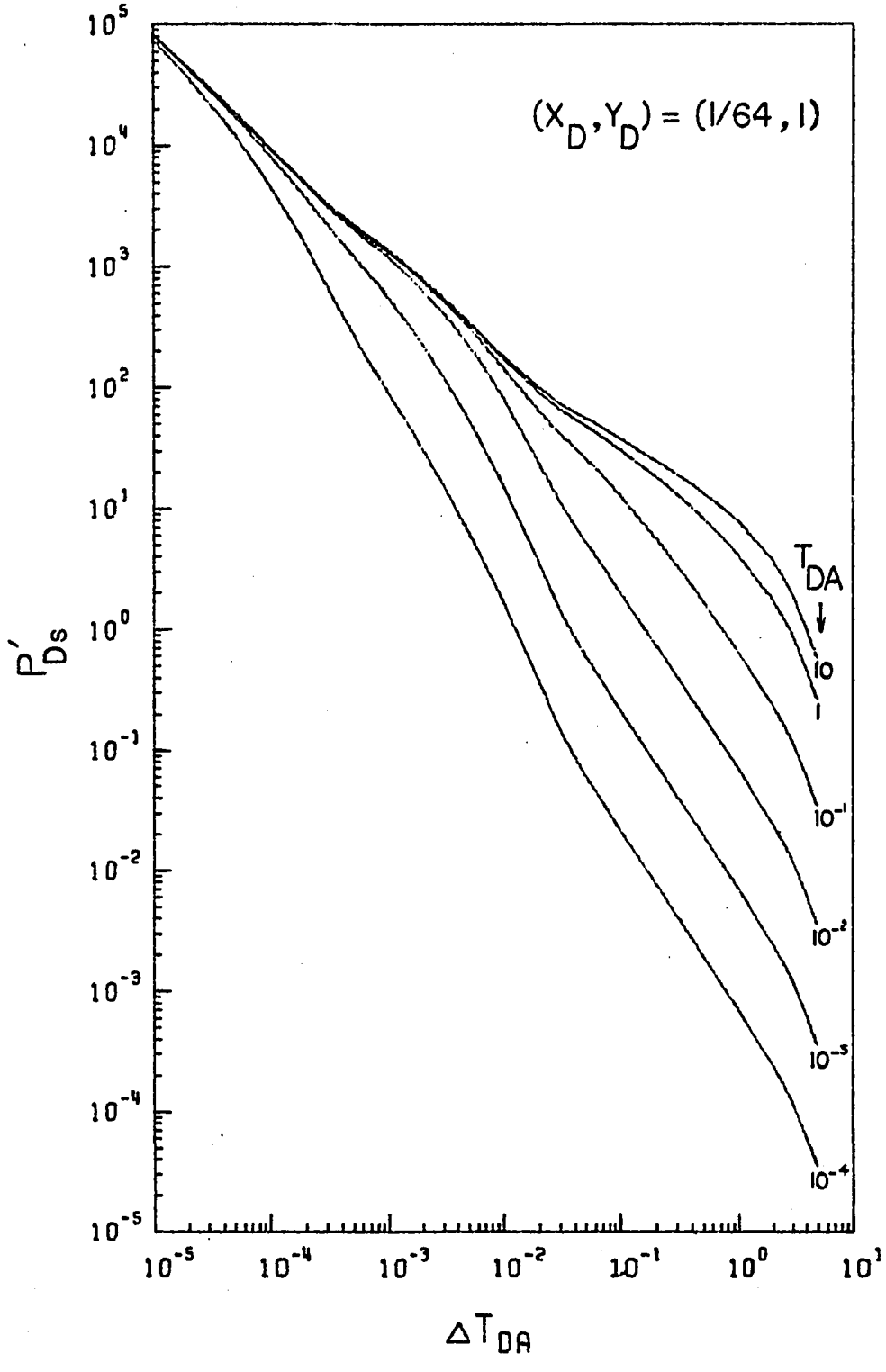

FIGURE F.21: Type-curve plot of p'_{Ds} vs Δt_{DA} for a well located at $(x_D, y_D) = (1/64, 1)$ inside a closed 4:1 rectangle.

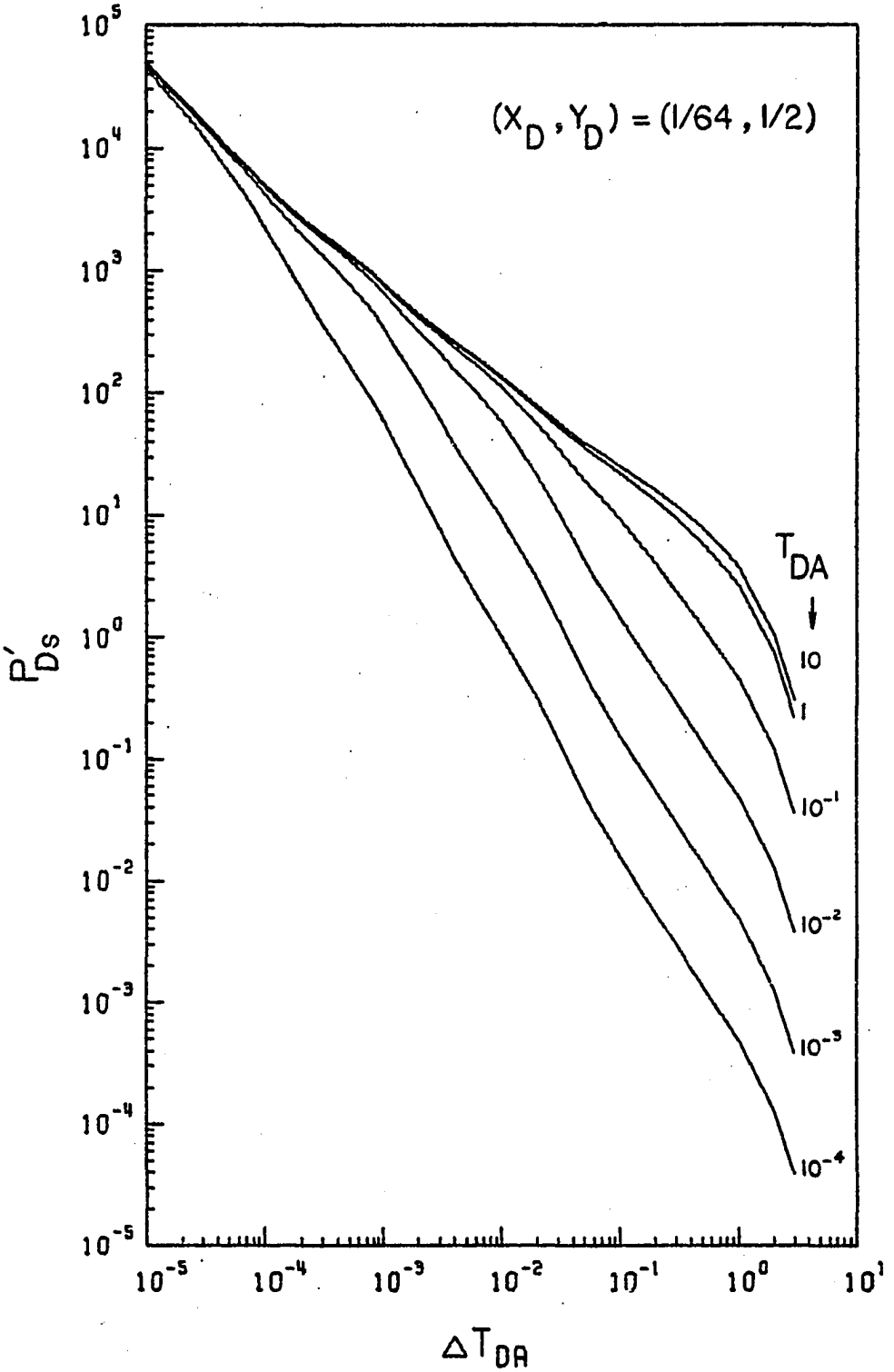

FIGURE F.22: Type-curve plot of p'_{Ds} vs Δt_{DA} for a well located at $(x_D, y_D) = (1/64, 1/2)$ inside a closed 8:1 rectangle.

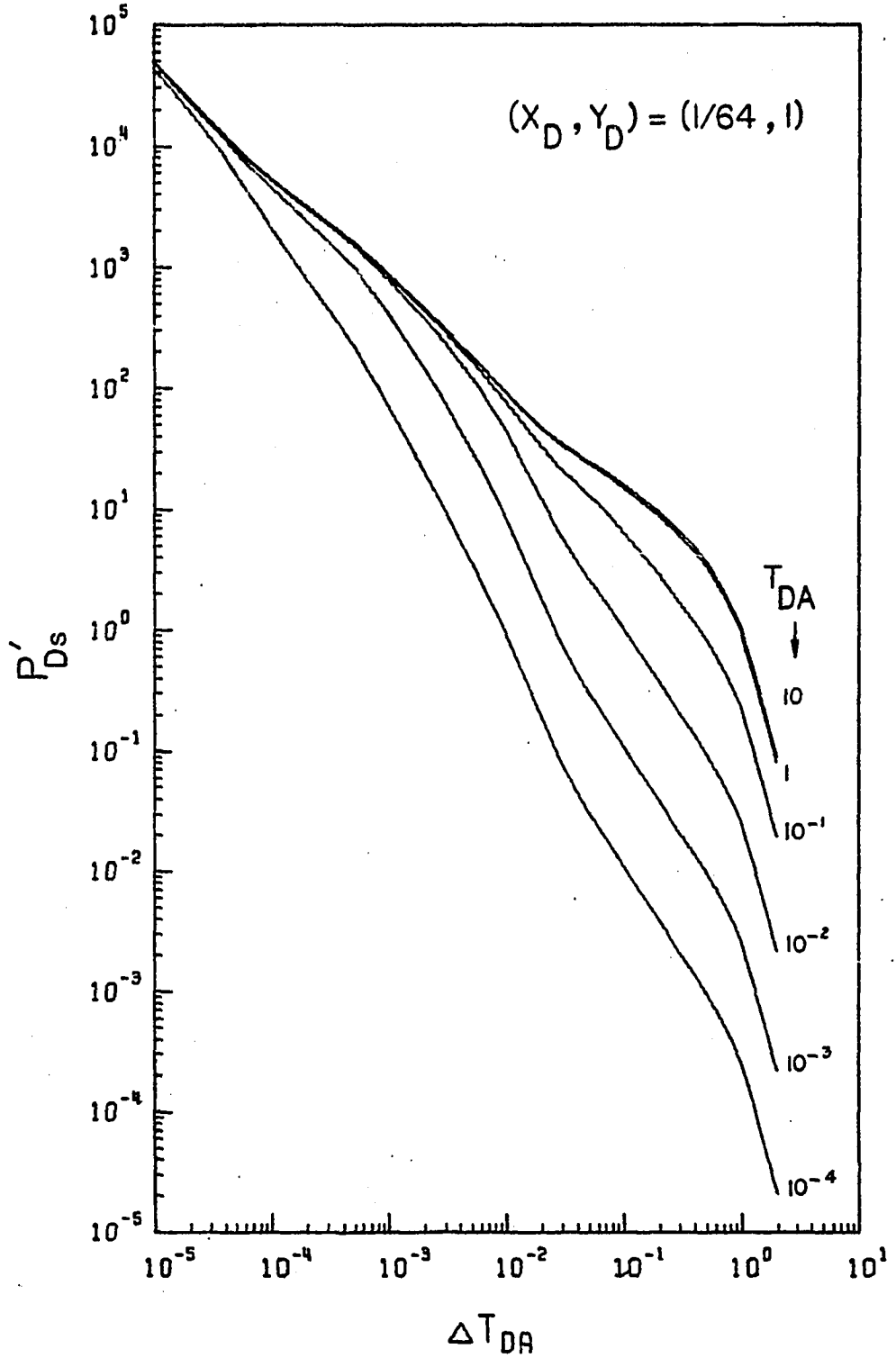

FIGURE F.23: Type-curve plot of p'_{Ds} vs Δt_{DA} for a well located at $(x_D, y_D) = (1/64, 1)$ inside a closed 16:1 rectangle.

TABLES

TABLE 1: p_{Dw}, p'_{Dw} and p''_{Dw} as Functions of Dimensionless Drawdown Times for a Well Between Two Perpendicular Sealing Faults

WELL LOCATION, (XD,YD) = (1.0000000, 1.0000000)

TDA	TDBY	TDBB	PD	PDP	PDPP
0.1000E-02	0.1000E-02	0.1000E-02	0.9115E 00	0.4524E 03	-0.4072E 06
0.2000E-02	0.2000E-02	0.2000E-02	0.1234E 01	0.2378E 03	-0.1130E 06
0.3000E-02	0.3000E-02	0.3000E-02	0.1429E 01	0.1612E 03	-0.5194E 05
0.4000E-02	0.4000E-02	0.4000E-02	0.1568E 01	0.1219E 03	-0.2972E 05
0.5000E-02	0.5000E-02	0.5000E-02	0.1677E 01	0.9802E 02	-0.1921E 05
0.6000E-02	0.6000E-02	0.6000E-02	0.1767E 01	0.8196E 02	-0.1343E 05
0.8000E-02	0.8000E-02	0.8000E-02	0.1909E 01	0.6172E 02	-0.7619E 04
0.1000E-01	0.1000E-01	0.1000E-01	0.2019E 01	0.4950E 02	-0.4901E 04
0.2000E-01	0.2000E-01	0.2000E-01	0.2363E 01	0.2488E 02	-0.1238E 04
0.3000E-01	0.3000E-01	0.3000E-01	0.2565E 01	0.1661E 02	-0.5519E 03
0.4000E-01	0.4000E-01	0.4000E-01	0.2708E 01	0.1247E 02	-0.3109E 03
0.5000E-01	0.5000E-01	0.5000E-01	0.2820E 01	0.9980E 01	-0.1992E 03
0.6000E-01	0.6000E-01	0.6000E-01	0.2911E 01	0.8319E 01	-0.1384E 03
0.8000E-01	0.8000E-01	0.8000E-01	0.3054E 01	0.6242E 01	-0.7792E 02
0.1000E 00	0.1000E 00	0.1000E 00	0.3166E 01	0.4995E 01	-0.4986E 02
0.2000E 00	0.2000E 00	0.2000E 00	0.3513E 01	0.2533E 01	-0.1181E 02
0.3000E 00	0.3000E 00	0.3000E 00	0.3723E 01	0.1787E 01	-0.4587E 01
0.4000E 00	0.4000E 00	0.4000E 00	0.3884E 01	0.1463E 01	-0.2270E 01
0.5000E 00	0.5000E 00	0.5000E 00	0.4021E 01	0.1289E 01	-0.1348E 01
0.6000E 00	0.6000E 00	0.6000E 00	0.4144E 01	0.1178E 01	-0.9230E 00
0.8000E 00	0.8000E 00	0.8000E 00	0.4364E 01	0.1034E 01	-0.5729E 00
0.1000E 01	0.1000E 01	0.1000E 01	0.4560E 01	0.9355E 00	-0.4322E 00
0.2000E 01	0.2000E 01	0.2000E 01	0.5333E 01	0.6452E 00	-0.2008E 00
0.3000E 01	0.3000E 01	0.3000E 01	0.5694E 01	0.4911E 00	-0.1181E 00
0.4000E 01	0.4000E 01	0.4000E 01	0.6334E 01	0.3955E 00	-0.7723E-01
0.5000E 01	0.5000E 01	0.5000E 01	0.6695E 01	0.3308E 00	-0.5424E-01
0.6000E 01	0.6000E 01	0.6000E 01	0.7001E 01	0.2841E 00	-0.4012E-01
0.8000E 01	0.8000E 01	0.8000E 01	0.7502E 01	0.2215E 00	-0.2444E-01
0.1000E 02	0.1000E 02	0.1000E 02	0.7902E 01	0.1814E 00	-0.1642E-01
0.2000E 02	0.2000E 02	0.2000E 02	0.9194E 01	0.9518E-01	-0.4527E-02
0.3000E 02	0.3000E 02	0.3000E 02	0.9972E 01	0.6450E-01	-0.2079E-02
0.4000E 02	0.4000E 02	0.4000E 02	0.1053E 02	0.4877E-01	-0.1189E-02
0.5000E 02	0.5000E 02	0.5000E 02	0.1097E 02	0.3921E-01	-0.7687E-03
0.6000E 02	0.6000E 02	0.6000E 02	0.1133E 02	0.3278E-01	-0.5374E-03
0.8000E 02	0.8000E 02	0.8000E 02	0.1189E 02	0.2469E-01	-0.3048E-03
0.1000E 03	0.1000E 03	0.1000E 03	0.1233E 02	0.1980E-01	-0.1960E-03
0.2000E 03	0.2000E 03	0.2000E 03	0.1371E 02	0.9950E-02	-0.4950E-04
0.3000E 03	0.3000E 03	0.3000E 03	0.1452E 02	0.6644E-02	-0.2207E-04
0.4000E 03	0.4000E 03	0.4000E 03	0.1509E 02	0.4988E-02	-0.1244E-04
0.5000E 03	0.5000E 03	0.5000E 03	0.1554E 02	0.3992E-02	-0.7968E-05
0.6000E 03	0.6000E 03	0.6000E 03	0.1590E 02	0.3328E-02	-0.5537E-05
0.8000E 03	0.8000E 03	0.8000E 03	0.1648E 02	0.2497E-02	-0.3117E-05
0.1000E 04	0.1000E 04	0.1000E 04	0.1692E 02	0.1998E-02	-0.1996E-05

TABLE 2: p_{Dw}, p'_{Dw} and p''_{Dw} as Functions of Dimensionless Drawdown Times for a Well Between Two Perpendicular Sealing Faults

WELL LOCATION, (XD,YD) = (1.0000000, 0.5000000)

TDA	TDRY	TDRB	PD	PDP	PDPP
0.1000E-02	0.4000E-02	0.2000E-02	0.9115E 00	0.4524E 03	-0.4072E 06
0.2000E-02	0.8000E-02	0.4000E-02	0.1234E 01	0.2378E 03	-0.1130E 06
0.3000E-02	0.1200E-01	0.6000E-02	0.1429E 01	0.1612E 03	-0.5194E 05
0.4000E-02	0.1600E-01	0.8000E-02	0.1568E 01	0.1219E 03	-0.2972E 05
0.5000E-02	0.2000E-01	0.1000E-01	0.1677E 01	0.9802E 02	-0.1921E 05
0.6000E-02	0.2400E-01	0.1200E-01	0.1767E 01	0.8196E 02	-0.1343E 05
0.8000E-02	0.3200E-01	0.1600E-01	0.1909E 01	0.6172E 02	-0.7619E 04
0.1000E-01	0.4000E-01	0.2000E-01	0.2019E 01	0.4950E 02	-0.4901E 04
0.2000E-01	0.8000E-01	0.4000E-01	0.2363E 01	0.2488E 02	-0.1237E 04
0.3000E-01	0.1200E 00	0.6000E-01	0.2565E 01	0.1662E 02	-0.5509E 03
0.4000E-01	0.1600E 00	0.8000E-01	0.2709E 01	0.1249E 02	-0.3078E 03
0.5000E-01	0.2000E 00	0.1000E 00	0.2820E 01	0.1005E 02	-0.1938E 03
0.6000E-01	0.2400E 00	0.1200E 00	0.2912E 01	0.8449E 01	-0.1316E 03
0.8000E-01	0.3200E 00	0.1600E 00	0.3060E 01	0.6517E 01	-0.7063E 02
0.1000E 00	0.4000E 00	0.2000E 00	0.3178E 01	0.5406E 01	-0.4372E 02
0.2000E 00	0.8000E 00	0.4000E 00	0.3586E 01	0.3237E 01	-0.1113E 02
0.3000E 00	0.1200E 01	0.6000E 00	0.3867E 01	0.2476E 01	-0.5219E 01
0.4000E 00	0.1600E 01	0.8000E 00	0.4093E 01	0.2076E 01	-0.3074E 01
0.5000E 00	0.2000E 01	0.1000E 01	0.4287E 01	0.1824E 01	-0.2089E 01
0.6000E 00	0.2400E 01	0.1200E 01	0.4460E 01	0.1644E 01	-0.1560E 01
0.8000E 00	0.3200E 01	0.1600E 01	0.4762E 01	0.1392E 01	-0.1026E 01
0.1000E 01	0.4000E 01	0.2000E 01	0.5022E 01	0.1217E 01	-0.7561E 00
0.2000E 01	0.8000E 01	0.4000E 01	0.5971E 01	0.7561E 00	-0.2845E 00
0.3000E 01	0.1200E 02	0.6000E 01	0.6613E 01	0.5493E 00	-0.1503E 00
0.4000E 01	0.1600E 02	0.8000E 01	0.7098E 01	0.4312E 00	-0.9274E-01
0.5000E 01	0.2000E 02	0.1000E 02	0.7489E 01	0.3549E 00	-0.6285E-01
0.6000E 01	0.2400E 02	0.1200E 02	0.7815E 01	0.3015E 00	-0.4538E-01
0.8000E 01	0.3200E 02	0.1600E 02	0.8342E 01	0.2317E 00	-0.2682E-01
0.1000E 02	0.4000E 02	0.2000E 02	0.8759E 01	0.1881E 00	-0.1769E-01
0.2000E 02	0.8000E 02	0.4000E 02	0.1009E 02	0.9696E-01	-0.4699E-02
0.3000E 02	0.1200E 03	0.6000E 02	0.1088E 02	0.6530E-01	-0.2132E-02
0.4000E 02	0.1600E 03	0.8000E 02	0.1144E 02	0.4923E-01	-0.1212E-02
0.5000E 02	0.2000E 03	0.1000E 03	0.1188E 02	0.3951E-01	-0.7803E-03
0.6000E 02	0.2400E 03	0.1200E 03	0.1224E 02	0.3299E-01	-0.5441E-03
0.8000E 02	0.3200E 03	0.1600E 03	0.1281E 02	0.2481E-01	-0.3077E-03
0.1000E 03	0.4000E 03	0.2000E 03	0.1326E 02	0.1988E-01	-0.1975E-03
0.2000E 03	0.8000E 03	0.4000E 03	0.1464E 02	0.9969E-02	-0.4969E-04
0.3000E 03	0.1200E 04	0.6000E 03	0.1544E 02	0.6653E-02	-0.2213E-04
0.4000E 03	0.1600E 04	0.8000E 03	0.1602E 02	0.4992E-02	-0.1246E-04
0.5000E 03	0.2000E 04	0.1000E 04	0.1646E 02	0.3995E-02	-0.7980E-05
0.6000E 03	0.2400E 04	0.1200E 04	0.1683E 02	0.3330E-02	-0.5544E-05
0.8000E 03	0.3200E 04	0.1600E 04	0.1740E 02	0.2498E-02	-0.3120E-05
0.1000E 04	0.4000E 04	0.2000E 04	0.1785E 02	0.1999E-02	-0.1997E-05

TABLE 3: p_{Dw}, p'_{Dw} and p''_{Dw} as Functions of Dimensionless Drawdown Times for a Well Between Two Perpendicular Sealing Faults

WELL LOCATION, (XD,YD) = (1.0000000, 0.2500000)

TDA	TDBY	TDBB	PD	PDP	PDPP
0.1000E-02	0.1600E-01	0.4000E-02	0.9115E 00	0.4524E 03	-0.4072E 06
0.2000E-02	0.3200E-01	0.8000E-02	0.1234E 01	0.2378E 03	-0.1130E 06
0.3000E-02	0.4800E-01	0.1200E-01	0.1429E 01	0.1612E 03	-0.5194E 05
0.4000E-02	0.6400E-01	0.1600E-01	0.1568E 01	0.1219E 03	-0.2972E 05
0.5000E-02	0.8000E-01	0.2000E-01	0.1677E 01	0.9802E 02	-0.1921E 05
0.6000E-02	0.9600E-01	0.2400E-01	0.1767E 01	0.8196E 02	-0.1343E 05
0.8000E-02	0.1280E 00	0.3200E-01	0.1909E 01	0.6175E 02	-0.7597E 04
0.1000E-01	0.1600E 00	0.4000E-01	0.2019E 01	0.4960E 02	-0.4850E 04
0.2000E-01	0.3200E 00	0.8000E-01	0.2369E 01	0.2597E 02	-0.1121E 04
0.3000E-01	0.4800E 00	0.1200E 00	0.2587E 01	0.1869E 02	-0.4769E 03
0.4000E-01	0.6400E 00	0.1600E 00	0.2754E 01	0.1509E 02	-0.2741E 03
0.5000E-01	0.8000E 00	0.2000E 00	0.2893E 01	0.1285E 02	-0.1849E 03
0.6000E-01	0.9600E 00	0.2400E 00	0.3013E 01	0.1126E 02	-0.1364E 03
0.8000E-01	0.1280E 01	0.3200E 00	0.3215E 01	0.9104E 01	-0.8575E 02
0.1000E 00	0.1600E 01	0.4000E 00	0.3382E 01	0.7672E 01	-0.5990E 02
0.2000E 00	0.3200E 01	0.8000E 00	0.3951E 01	0.4357E 01	-0.1817E 02
0.3000E 00	0.4800E 01	0.1200E 01	0.4317E 01	0.3127E 01	-0.8251E 01
0.4000E 00	0.6400E 01	0.1600E 01	0.4596E 01	0.2509E 01	-0.4631E 01
0.5000E 00	0.8000E 01	0.2000E 01	0.4827E 01	0.2137E 01	-0.3004E 01
0.6000E 00	0.9600E 01	0.2400E 01	0.5027E 01	0.1883E 01	-0.2152E 01
0.8000E 00	0.1280E 02	0.3200E 01	0.5368E 01	0.1548E 01	-0.1323E 01
0.1000E 01	0.1600E 02	0.4000E 01	0.5654E 01	0.1326E 01	-0.9295E 00
0.2000E 01	0.3200E 02	0.8000E 01	0.6665E 01	0.7909E 00	-0.3147E 00
0.3000E 01	0.4800E 02	0.1200E 02	0.7331E 01	0.5663E 00	-0.1605E 00
0.4000E 01	0.6400E 02	0.1600E 02	0.7829E 01	0.4412E 00	-0.9738E-01
0.5000E 01	0.8000E 02	0.2000E 02	0.8228E 01	0.3615E 00	-0.6534E-01
0.6000E 01	0.9600E 02	0.2400E 02	0.8560E 01	0.3062E 00	-0.4686E-01
0.8000E 01	0.1280E 03	0.3200E 02	0.9094E 01	0.2344E 00	-0.2747E-01
0.1000E 02	0.1600E 03	0.4000E 02	0.9516E 01	0.1899E 00	-0.1803E-01
0.2000E 02	0.3200E 03	0.8000E 02	0.1085E 02	0.9741E-01	-0.4744E-02
0.3000E 02	0.4800E 03	0.1200E 03	0.1164E 02	0.6551E-01	-0.2145E-02
0.4000E 02	0.6400E 03	0.1600E 03	0.1221E 02	0.4934E-01	-0.1217E-02
0.5000E 02	0.8000E 03	0.2000E 03	0.1265E 02	0.3958E-01	-0.7833E-03
0.6000E 02	0.9600E 03	0.2400E 03	0.1301E 02	0.3304E-01	-0.5458E-03
0.8000E 02	0.1280E 04	0.3200E 03	0.1358E 02	0.2484E-01	-0.3084E-03
0.1000E 03	0.1600E 04	0.4000E 03	0.1403E 02	0.1989E-01	-0.1979E-03
0.2000E 03	0.3200E 04	0.8000E 03	0.1541E 02	0.9973E-02	-0.4974E-04
0.3000E 03	0.4800E 04	0.1200E 04	0.1622E 02	0.6655E-02	-0.2214E-04
0.4000E 03	0.6400E 04	0.1600E 04	0.1679E 02	0.4993E-02	-0.1247E-04
0.5000E 03	0.8000E 04	0.2000E 04	0.1724E 02	0.3996E-02	-0.7983E-05
0.6000E 03	0.9600E 04	0.2400E 04	0.1760E 02	0.3330E-02	-0.5546E-05
0.8000E 03	0.1280E 05	0.3200E 04	0.1818E 02	0.2498E-02	-0.3121E-05
0.1000E 04	0.1600E 05	0.4000E 04	0.1862E 02	0.1999E-02	-0.1998E-05

TABLE 4: p_{Dw}, p'_{Dw} and p''_{Dw} as Functions of Dimensionless Drawdown Times for a Well Between Two Perpendicular Sealing Faults

WELL LOCATION, (XD,YD) = (1.0000000, 0.1250000)

TDA	TDBY	TDBB	PD	PDP	PDPP
0.1000E-02	0.6400E-01	0.8000E-02	0.9115E 00	0.4524E 03	-0.4072E 06
0.2000E-02	0.1280E 00	0.1600E-01	0.1234E 01	0.2379E 03	-0.1126E 06
0.3000E-02	0.1920E 00	0.2400E-01	0.1429E 01	0.1621E 03	-0.5066E 05
0.4000E-02	0.2560E 00	0.3200E-01	0.1570E 01	0.1244E 03	-0.2789E 05
0.5000E-02	0.3200E 00	0.4000E-01	0.1683E 01	0.1024E 03	-0.1734E 05
0.6000E-02	0.3840E 00	0.4800E-01	0.1778E 01	0.8812E 02	-0.1178E 05
0.8000E-02	0.5120E 00	0.6400E-01	0.1935E 01	0.7059E 02	-0.6563E 04
0.1000E-01	0.6400E 00	0.8000E-01	0.2065E 01	0.5998E 02	-0.4311E 04
0.2000E-01	0.1280E 01	0.1600E 00	0.2524E 01	0.3632E 02	-0.1363E 04
0.3000E-01	0.1920E 01	0.2400E 00	0.2833E 01	0.2651E 02	-0.7100E 03
0.4000E-01	0.2560E 01	0.3200E 00	0.3068E 01	0.2093E 02	-0.4398E 03
0.5000E-01	0.3200E 01	0.4000E 00	0.3258E 01	0.1730E 02	-0.2998E 03
0.6000E-01	0.3840E 01	0.4800E 00	0.3417E 01	0.1474E 02	-0.2176E 03
0.8000E-01	0.5120E 01	0.6400E 00	0.3675E 01	0.1138E 02	-0.1296E 03
0.1000E 00	0.6400E 01	0.8000E 00	0.3880E 01	0.9272E 01	-0.8595E 02
0.2000E 00	0.1280E 02	0.1600E 01	0.4538E 01	0.4843E 01	-0.2249E 02
0.3000E 00	0.1920E 02	0.2400E 01	0.4938E 01	0.3364E 01	-0.9640E 01
0.4000E 00	0.2560E 02	0.3200E 01	0.5235E 01	0.2653E 01	-0.5247E 01
0.5000E 00	0.3200E 02	0.4000E 01	0.5478E 01	0.2236E 01	-0.3336E 01
0.6000E 00	0.3840E 02	0.4800E 01	0.5686E 01	0.1956E 01	-0.2354E 01
0.8000E 00	0.5120E 02	0.6400E 01	0.6038E 01	0.1593E 01	-0.1417E 01
0.1000E 01	0.6400E 02	0.8000E 01	0.6332E 01	0.1357E 01	-0.9816E 00
0.2000E 01	0.1280E 03	0.1600E 02	0.7360E 01	0.8001E 00	-0.3230E 00
0.3000E 01	0.1920E 03	0.2400E 02	0.8032E 01	0.5707E 00	-0.1633E 00
0.4000E 01	0.2560E 03	0.3200E 02	0.8534E 01	0.4438E 00	-0.9860E-01
0.5000E 01	0.3200E 03	0.4000E 02	0.8935E 01	0.3632E 00	-0.6598E-01
0.6000E 01	0.3840E 03	0.4800E 02	0.9268E 01	0.3073E 00	-0.4724E-01
0.8000E 01	0.5120E 03	0.6400E 02	0.9804E 01	0.2351E 00	-0.2763E-01
0.1000E 02	0.6400E 03	0.8000E 02	0.1023E 02	0.1903E 00	-0.1811E-01
0.2000E 02	0.1280E 04	0.1600E 03	0.1156E 02	0.9752E-01	-0.4755E-02
0.3000E 02	0.1920E 04	0.2400E 03	0.1236E 02	0.6556E-01	-0.2149E-02
0.4000E 02	0.2560E 04	0.3200E 03	0.1293E 02	0.4937E-01	-0.1219E-02
0.5000E 02	0.3200E 04	0.4000E 03	0.1337E 02	0.3960E-01	-0.7840E-03
0.6000E 02	0.3840E 04	0.4800E 03	0.1373E 02	0.3305E-01	-0.5463E-03
0.8000E 02	0.5120E 04	0.6400E 03	0.1430E 02	0.2484E-01	-0.3086E-03
0.1000E 03	0.6400E 04	0.8000E 03	0.1474E 02	0.1990E-01	-0.1980E-03
0.2000E 03	0.1280E 05	0.1600E 04	0.1612E 02	0.9975E-02	-0.4975E-04
0.3000E 03	0.1920E 05	0.2400E 04	0.1693E 02	0.6655E-02	-0.2215E-04
0.4000E 03	0.2560E 05	0.3200E 04	0.1751E 02	0.4994E-02	-0.1247E-04
0.5000E 03	0.3200E 05	0.4000E 04	0.1795E 02	0.3996E-02	-0.7984E-05
0.6000E 03	0.3840E 05	0.4900E 04	0.1832E 02	0.3331E-02	-0.5546E-05
0.8000E 03	0.5120E 05	0.6400E 04	0.1889E 02	0.2498E-02	-0.3121E-05
0.1000E 04	0.6400E 05	0.8000E 04	0.1934E 02	0.1999E-02	-0.1998E-05

TABLE 5: p_{Ds}, p'_{Ds} and p''_{Ds} as Functions of Dimensionless Buildup Times for a Well Between Two Perpendicular Sealing Faults

WELL LOCATION, (XD,YD) = (1.0000000, 0.1250000)

PRODUCING TIME BEFORE SHUT-IN, TDA = 0.010

DEL(T)	TRAT	TDBY	PDS	PDSP	PDSS
0.1000E-02	0.1100E 02	0.6400E-01	0.1244E 01	-0.4313E 03	0.4718E 06
0.2000E-02	0.6000E 01	0.1280E 00	0.9582E 00	-0.1941E 03	0.1184E 06
0.3000E-02	0.4333E 01	0.1920E 00	0.8085E 00	-0.1162E 03	0.5059E 05
0.4000E-02	0.3500E 01	0.2560E 00	0.7126E 00	-0.7939E 02	0.2659E 05
0.5000E-02	0.3000E 01	0.3200E 00	0.6444E 00	-0.5885E 02	0.1575E 05
0.6000E-02	0.2667E 01	0.3840E 00	0.5924E 00	-0.4618E 02	0.1016E 05
0.8000E-02	0.2250E 01	0.5120E 00	0.5161E 00	-0.3177E 02	0.5083E 04
0.1000E-01	0.2000E 01	0.6400E 00	0.4610E 00	-0.2394E 02	0.3013E 04
0.2000E-01	0.1500E 01	0.1280E 01	0.3095E 00	-0.9861E 01	0.6593E 03
0.3000E-01	0.1333E 01	0.1920E 01	0.2353E 00	-0.5603E 01	0.2718E 03
0.4000E-01	0.1250E 01	0.2560E 01	0.1901E 00	-0.3639E 01	0.1406E 03
0.5000E-01	0.1200E 01	0.3200E 01	0.1596E 00	-0.2559E 01	0.8245E 02
0.6000E-01	0.1167E 01	0.3840E 01	0.1376E 00	-0.1898E 01	0.5257E 02
0.8000E-01	0.1125E 01	0.5120E 01	0.1079E 00	-0.1165E 01	0.2522E 02
0.1000E 00	0.1100E 01	0.6400E 01	0.8871E-01	-0.7870E 00	0.1403E 02
0.2000E 00	0.1050E 01	0.1280E 02	0.4735E-01	-0.2141E 00	0.2133E 01
0.3000E 00	0.1033E 01	0.1920E 02	0.3318E-01	-0.9312E-01	0.6498E 00
0.4000E 00	0.1025E 01	0.2560E 02	0.2628E-01	-0.5115E-01	0.2623E 00
0.5000E 00	0.1020E 01	0.3200E 02	0.2219E-01	-0.3272E-01	0.1272E 00
0.6000E 00	0.1017E 01	0.3840E 02	0.1944E-01	-0.2319E-01	0.7079E-01
0.8000E 00	0.1012E 01	0.5120E 02	0.1585E-01	-0.1403E-01	0.2935E-01
0.1000E 01	0.1010E 01	0.6400E 02	0.1352E-01	-0.9738E-02	0.1562E-01
0.2000E 01	0.1005E 01	0.1280E 03	0.7985E-02	-0.3216E-02	0.2634E-02
0.3000E 01	0.1003E 01	0.1920E 03	0.5699E-02	-0.1628E-02	0.9344E-03
0.4000E 01	0.1002E 01	0.2560E 03	0.4434E-02	-0.9837E-03	0.4374E-03
0.5000E 01	0.1002E 01	0.3200E 03	0.3627E-02	-0.6586E-03	0.2393E-03
0.6000E 01	0.1002E 01	0.3840E 03	0.3071E-02	-0.4717E-03	0.1450E-03
0.8000E 01	0.1001E 01	0.5120E 03	0.2349E-02	-0.2759E-03	0.6485E-04
0.1000E 02	0.1001E 01	0.6400E 03	0.1903E-02	-0.1809E-03	0.3442E-04
0.2000E 02	0.1000E 01	0.1280E 04	0.9747E-03	-0.4750E-04	0.4631E-05
0.3000E 02	0.1000E 01	0.1920E 04	0.6552E-03	-0.2146E-04	0.1407E-05
0.4000E 02	0.1000E 01	0.2560E 04	0.4940E-03	-0.1218E-04	0.6012E-06
0.5000E 02	0.1000E 01	0.3200E 04	0.3958E-03	-0.7834E-05	0.3101E-06
0.6000E 02	0.1000E 01	0.3840E 04	0.3309E-03	-0.5458E-05	0.1804E-06
0.8000E 02	0.1000E 01	0.5120E 04	0.2470E-03	-0.3085E-05	0.7660E-07
0.1000E 03	0.1000E 01	0.6400E 04	0.1965E-03	-0.1978E-05	0.3936E-07
0.2000E 03	0.1000E 01	0.1280E 05	0.9155E-04	-0.4917E-06	0.4933E-08
0.3000E 03	0.1000E 01	0.1920E 05	0.7629E-04	-0.2198E-06	0.1441E-08
0.4000E 03	0.1000E 01	0.2560E 05	0.4578E-04	-0.1229E-06	0.6075E-09
0.5000E 03	0.1000E 01	0.3200E 05	0.3052E-04	-0.7823E-07	0.3120E-09
0.6000E 03	0.1000E 01	0.3840E 05	0.4578E-04	-0.5425E-07	0.1810E-09
0.8000E 03	0.1000E 01	0.5120E 05	0.4578E-04	-0.3050E-07	0.7640E-10
0.1000E 04	0.1000E 01	0.6400E 05	0.1526E-04	-0.1956E-07	0.3820E-10

TABLE 6: p_{Ds}, p'_{Ds} and p''_{Ds} as Functions of Dimensionless Buildup Times for a Well Between Two Perpendicular Sealing Faults

WELL LOCATION, (XD,YD) = (1.0000000, 0.1250000)

PRODUCING TIME BEFORE SHUT-IN, TDA = 0.100

DEL(T)	TRAT	TDBY	PDS	PDSP	PDSS
0.1000E-02	0.1010E 03	0.6400E-01	0.3014E 01	-0.4785E 03	0.4754E 06
0.2000E-02	0.5100E 02	0.1280E 00	0.2683E 01	-0.2379E 03	0.1215E 06
0.3000E-02	0.3433E 02	0.1920E 00	0.2491E 01	-0.1572E 03	0.5327E 05
0.4000E-02	0.2600E 02	0.2560E 00	0.2355E 01	-0.1178E 03	0.2895E 05
0.5000E-02	0.2100E 02	0.3200E 00	0.2250E 01	-0.9503E 02	0.1785E 05
0.6000E-02	0.1767E 02	0.3840E 00	0.2163E 01	-0.8036E 02	0.1205E 05
0.8000E-02	0.1350E 02	0.5120E 00	0.2022E 01	-0.6253E 02	0.6633E 04
0.1000E-01	0.1100E 02	0.6400E 00	0.1908E 01	-0.5187E 02	0.4314E 04
0.2000E-01	0.6000E 01	0.1280E 01	0.1528E 01	-0.2859E 02	0.1311E 04
0.3000E-01	0.4333E 01	0.1920E 01	0.1294E 01	-0.1929E 02	0.6603E 03
0.4000E-01	0.3500E 01	0.2560E 01	0.1129E 01	-0.1418E 02	0.3954E 03
0.5000E-01	0.3000E 01	0.3200E 01	0.1005E 01	-0.1097E 02	0.2606E 03
0.6000E-01	0.2667E 01	0.3840E 01	0.9064E 00	-0.8782E 01	0.1828E 03
0.8000E-01	0.2250E 01	0.5120E 01	0.7608E 00	-0.6044E 01	0.1020E 03
0.1000E 00	0.2000E 01	0.6400E 01	0.6573E 00	-0.4432E 01	0.6352E 02
0.2000E 00	0.1500E 01	0.1280E 02	0.4000E 00	-0.1490E 01	0.1286E 02
0.3000E 00	0.1333E 01	0.1920E 02	0.2873E 00	-0.7112E 00	0.4394E 01
0.4000E 00	0.1250E 01	0.2560E 02	0.2429E 00	-0.4176E 00	0.1912E 01
0.5000E 00	0.1200E 01	0.3200E 02	0.2088E 00	-0.2797E 00	0.9817E 00
0.6000E 00	0.1167E 01	0.3840E 02	0.1849E 00	-0.2046E 00	0.5715E 00
0.8000E 00	0.1125E 01	0.5120E 02	0.1526E 00	-0.1284E 00	0.2521E 00
0.1000E 01	0.1100E 01	0.6400E 02	0.1311E 00	-0.9091E-01	0.1392E 00
0.2000E 01	0.1050E 01	0.1280E 03	0.7844E-01	-0.3103E-01	0.2493E-01
0.3000E 01	0.1033E 01	0.1920E 03	0.5627E-01	-0.1587E-01	0.8993E-02
0.4000E 01	0.1025E 01	0.2560E 03	0.4390E-01	-0.9645E-02	0.4246E-02
0.5000E 01	0.1020E 01	0.3200E 03	0.3599E-01	-0.6480E-02	0.2336E-02
0.6000E 01	0.1017E 01	0.3840E 03	0.3050E-01	-0.4653E-02	0.1420E-02
0.8000E 01	0.1012E 01	0.5120E 03	0.2337E-01	-0.2731E-02	0.6385E-03
0.1000E 02	0.1010E 01	0.6400E 03	0.1894E-01	-0.1794E-02	0.3400E-03
0.2000E 02	0.1005E 01	0.1280E 04	0.9729E-02	-0.4732E-03	0.4603E-04
0.3000E 02	0.1003E 01	0.1920E 04	0.6544E-02	-0.2142E-03	0.1402E-04
0.4000E 02	0.1002E 01	0.2560E 04	0.4930E-02	-0.1216E-03	0.5995E-05
0.5000E 02	0.1002E 01	0.3200E 04	0.3956E-02	-0.7823E-04	0.3095E-05
0.6000E 02	0.1002E 01	0.3840E 04	0.3303E-02	-0.5453E-04	0.1801E-05
0.8000E 02	0.1001E 01	0.5120E 04	0.2482E-02	-0.3082E-04	0.7651E-06
0.1000E 03	0.1001E 01	0.6400E 04	0.1987E-02	-0.1977E-04	0.3933E-06
0.2000E 03	0.1000E 01	0.1280E 05	0.9918E-03	-0.4977E-05	0.4956E-07
0.3000E 03	0.1000E 01	0.1920E 05	0.6714E-03	-0.2213E-05	0.1471E-07
0.4000E 03	0.1000E 01	0.2560E 05	0.5035E-03	-0.1244E-05	0.6216E-08
0.5000E 03	0.1000E 01	0.3200E 05	0.3967E-03	-0.7972E-06	0.3187E-08
0.6000E 03	0.1000E 01	0.3840E 05	0.3357E-03	-0.5541E-06	0.1845E-08
0.8000E 03	0.1000E 01	0.5120E 05	0.2594E-03	-0.3115E-06	0.7785E-09
0.1000E 04	0.1000E 01	0.6400E 05	0.1984E-03	-0.1995E-06	0.3984E-09

TABLE 7: p_{Ds}, p'_{Ds} and p''_{Ds} as Functions of Dimensionless Buildup Times for a Well Between Two Perpendicular Sealing Faults

WELL LOCATION, (XD,YD) = (1.0000000, 0.1250000)

PRODUCING TIME BEFORE SHUT-IN, TDA = 1.000

DEL(T)	TRAT	TDDY	PDS	PDSP	PDSS
0.1000E-02	0.1001E 04	0.6400E-01	0.5458E 01	-0.4863E 03	0.4755E 06
0.2000E-02	0.5010E 03	0.1280E 00	0.5119E 01	-0.2456E 03	0.1216E 06
0.3000E-02	0.3343E 03	0.1920E 00	0.4919E 01	-0.1648E 03	0.5336E 05
0.4000E-02	0.2510E 03	0.2560E 00	0.4776E 01	-0.1254E 03	0.2903E 05
0.5000E-02	0.2010E 03	0.3200E 00	0.4663E 01	-0.1025E 03	0.1793E 05
0.6000E-02	0.1677E 03	0.3840E 00	0.4568E 01	-0.8780E 02	0.1212E 05
0.8000E-02	0.1260E 03	0.5120E 00	0.4413E 01	-0.6982E 02	0.6707E 04
0.1000E-01	0.1010E 03	0.6400E 00	0.4284E 01	-0.5901E 02	0.4385E 04
0.2000E-01	0.5100E 02	0.1280E 01	0.3837E 01	-0.3508E 02	0.1371E 04
0.3000E-01	0.3433E 02	0.1920E 01	0.3541E 01	-0.2522E 02	0.7118E 03
0.4000E-01	0.2600E 02	0.2560E 01	0.3319E 01	-0.1963E 02	0.4400E 03
0.5000E-01	0.2100E 02	0.3200E 01	0.3142E 01	-0.1600E 02	0.2995E 03
0.6000E-01	0.1767E 02	0.3840E 01	0.2995E 01	-0.1345E 02	0.2170E 03
0.8000E-01	0.1350E 02	0.5120E 01	0.2762E 01	-0.1011E 02	0.1289E 03
0.1000E 00	0.1100E 02	0.6400E 01	0.2583E 01	-0.8010E 01	0.8518E 02
0.2000E 00	0.6000E 01	0.1280E 02	0.2048E 01	-0.3656E 01	0.2177E 02
0.3000E 00	0.4333E 01	0.1920E 02	0.1763E 01	-0.2246E 01	0.8996E 01
0.4000E 00	0.3500E 01	0.2560E 02	0.1575E 01	-0.1595E 01	0.4674E 01
0.5000E 00	0.3000E 01	0.3200E 02	0.1435E 01	-0.1232E 01	0.2822E 01
0.6000E 00	0.2667E 01	0.3840E 02	0.1324E 01	-0.1001E 01	0.1891E 01
0.8000E 00	0.2250E 01	0.5120E 02	0.1154E 01	-0.7220E 00	0.1034E 01
0.1000E 01	0.2000E 01	0.6400E 02	0.1028E 01	-0.5571E 00	0.6587E 00
0.2000E 01	0.1500E 01	0.1280E 03	0.6724E 00	-0.2294E 00	0.1597E 00
0.3000E 01	0.1333E 01	0.1920E 03	0.5019E 00	-0.1269E 00	0.6467E-01
0.4000E 01	0.1250E 01	0.2560E 03	0.4008E 00	-0.8065E-01	0.3261E-01
0.5000E 01	0.1200E 01	0.3200E 03	0.3337E 00	-0.5583E-01	0.1874E-01
0.6000E 01	0.1167E 01	0.3840E 03	0.2859E 00	-0.4095E-01	0.1175E-01
0.8000E 01	0.1125E 01	0.5120E 03	0.2223E 00	-0.2473E-01	0.5509E-02
0.1000E 02	0.1100E 01	0.6400E 03	0.1818E 00	-0.1654E-01	0.3012E-02
0.2000E 02	0.1050E 01	0.1280E 04	0.9522E-01	-0.4534E-02	0.4319E-03
0.3000E 02	0.1033E 01	0.1920E 04	0.6451E-01	-0.2081E-02	0.1342E-03
0.4000E 02	0.1025E 01	0.2560E 04	0.4877E-01	-0.1189E-02	0.5802E-04
0.5000E 02	0.1020E 01	0.3200E 04	0.3921E-01	-0.7688E-03	0.3015E-04
0.6000E 02	0.1017E 01	0.3840E 04	0.3278E-01	-0.5374E-03	0.1762E-04
0.8000E 02	0.1012E 01	0.5120E 04	0.2469E-01	-0.3048E-03	0.7525E-05
0.1000E 03	0.1010E 01	0.6400E 04	0.1980E-01	-0.1960E-03	0.3882E-05
0.2000E 03	0.1005E 01	0.1280E 05	0.9949E-02	-0.4951E-04	0.4925E-06
0.3000E 03	0.1003E 01	0.1920E 05	0.6653E-02	-0.2208E-04	0.1467E-06
0.4000E 03	0.1002E 01	0.2560E 05	0.4990E-02	-0.1244E-04	0.6203E-07
0.5000E 03	0.1002E 01	0.3200E 05	0.3993E-02	-0.7968E-05	0.3181E-07
0.6000E 03	0.1002E 01	0.3840E 05	0.3342E-02	-0.5537E-05	0.1843E-07
0.8000E 03	0.1001E 01	0.5120E 05	0.2502E-02	-0.3117E-05	0.7783E-08
0.1000E 04	0.1001E 01	0.6400E 05	0.1999E-02	-0.1996E-05	0.3987E-08

TABLE 8: p_{Ds}, p'_{Ds} and p''_{Ds} as Functions of Dimensionless Buildup Times for a Well Between Two Perpendicular Sealing Faults

WELL LOCATION, (XD,YD) = (1.0000000, 0.1250000)
PRODUCING TIME BEFORE SHUT-IN, TDA = 10.000

DELT	TRAT	TDBY	PDS	PDSP	PDSS
0.1000E-02	0.1000E 05	0.6400E-01	0.9352E 01	-0.4875E 03	0.4755E 06
0.2000E-02	0.5001E 04	0.1280E 00	0.9012E 01	-0.2468E 03	0.1216E 06
0.3000E-02	0.3334E 04	0.1920E 00	0.8811E 01	-0.1660E 03	0.5336E 05
0.4000E-02	0.2501E 04	0.2560E 00	0.8666E 01	-0.1265E 03	0.2903E 05
0.5000E-02	0.2001E 04	0.3200E 00	0.8552E 01	-0.1037E 03	0.1793E 05
0.6000E-02	0.1668E 04	0.3840E 00	0.8456E 01	-0.8896E 02	0.1213E 05
0.8000E-02	0.1251E 04	0.5120E 00	0.8298E 01	-0.7098E 02	0.6708E 04
0.1000E-01	0.1001E 04	0.6400E 00	0.8168E 01	-0.6017E 02	0.4385E 04
0.2000E-01	0.5010E 03	0.1280E 01	0.7709E 01	-0.3622E 02	0.1372E 04
0.3000E-01	0.3343E 03	0.1920E 01	0.7401E 01	-0.2636E 02	0.7127E 03
0.4000E-01	0.2510E 03	0.2560E 01	0.7168E 01	-0.2076E 02	0.4409E 03
0.5000E-01	0.2010E 03	0.3200E 01	0.6979E 01	-0.1712E 02	0.3004E 03
0.6000E-01	0.1677E 03	0.3840E 01	0.6822E 01	-0.1456E 02	0.2179E 03
0.8000E-01	0.1260E 03	0.5120E 01	0.6567E 01	-0.1120E 02	0.1298E 03
0.1000E 00	0.1010E 03	0.6400E 01	0.6366E 01	-0.9087E 01	0.8600E 02
0.2000E 00	0.5100E 02	0.1280E 02	0.5727E 01	-0.4657E 01	0.2248E 02
0.3000E 00	0.3433E 02	0.1920E 02	0.5346E 01	-0.3179E 01	0.9625E 01
0.4000E 00	0.2600E 02	0.2560E 02	0.5067E 01	-0.2470E 01	0.5231E 01
0.5000E 00	0.2100E 02	0.3200E 02	0.4842E 01	-0.2054E 01	0.3320E 01
0.6000E 00	0.1767E 02	0.3840E 02	0.4651E 01	-0.1776E 01	0.2339E 01
0.8000E 00	0.1350E 02	0.5120E 02	0.4335E 01	-0.1416E 01	0.1402E 01
0.1000E 01	0.1100E 02	0.6400E 02	0.4077E 01	-0.1183E 01	0.9666E 00
0.2000E 01	0.6000E 01	0.1280E 03	0.3216E 01	-0.6402E 00	0.3102E 00
0.3000E 01	0.4333E 01	0.1920E 03	0.2697E 01	-0.4226E 00	0.1523E 00
0.4000E 01	0.3500E 01	0.2560E 03	0.2338E 01	-0.3060E 00	0.8909E-01
0.5000E 01	0.3000E 01	0.3200E 03	0.2070E 01	-0.2342E 00	0.5767E-01
0.6000E 01	0.2667E 01	0.3840E 03	0.1862E 01	-0.1862E 00	0.3990E-01
0.8000E 01	0.2250E 01	0.5120E 03	0.1554E 01	-0.1270E 00	0.2180E-01
0.1000E 02	0.2000E 01	0.6400E 03	0.1337E 01	-0.9281E-01	0.1336E-01
0.2000E 02	0.1500E 01	0.1280E 04	0.7944E 00	-0.3197E-01	0.2607E-02
0.3000E 02	0.1333E 01	0.1920E 04	0.5670E 00	-0.1618E-01	0.9300E-03
0.4000E 02	0.1250E 01	0.2560E 04	0.4413E 00	-0.9775E-02	0.4349E-03
0.5000E 02	0.1200E 01	0.3200E 04	0.3613E 00	-0.6544E-02	0.2377E-03
0.6000E 02	0.1167E 01	0.3840E 04	0.3058E 00	-0.4688E-02	0.1440E-03
0.8000E 02	0.1125E 01	0.5120E 04	0.2342E 00	-0.2745E-02	0.6442E-04
0.1000E 03	0.1100E 01	0.6400E 04	0.1897E 00	-0.1801E-02	0.3421E-04
0.2000E 03	0.1050E 01	0.1280E 05	0.9734E-01	-0.4738E-03	0.4614E-05
0.3000E 03	0.1033E 01	0.1920E 05	0.6548E-01	-0.2143E-03	0.1404E-05
0.4000E 03	0.1025E 01	0.2560E 05	0.4932E-01	-0.1216E-03	0.6001E-06
0.5000E 03	0.1020E 01	0.3200E 05	0.3957E-01	-0.7828E-04	0.3097E-06
0.6000E 03	0.1017E 01	0.3840E 05	0.3304E-01	-0.5455E-04	0.1802E-06
0.8000E 03	0.1012E 01	0.5120E 05	0.2484E-01	-0.3083E-04	0.7654E-07
0.1000E 04	0.1010E 01	0.6400E 05	0.1990E-01	-0.1978E-04	0.3935E-07

TABLE 9: p_{Dw}, p'_{Dw} and p''_{Dw} as Functions of Dimensionless Drawdown Times for a Well Between Three Perpendicular Sealing Faults

WELL LOCATION, (XD,YD) = (0.0312500, 0.0156250)

TDA	TDBX	TDBY	TDBB	TDABX	PD	PDP	PDPP
0.1000E-04	0.4096E-01	0.1638E 00	0.8192E-01	0.6502E-03	0.2252E 01	0.4980E 05	-0.4881E 10
0.2000E-04	0.8192E-01	0.3277E 00	0.1638E 00	0.1300E-02	0.2603E 01	0.2610E 05	-0.1121E 10
0.3000E-04	0.1229E 00	0.4915E 00	0.2458E 00	0.1950E-02	0.2823E 01	0.1882E 05	-0.4767E 09
0.4000E-04	0.1638E 00	0.6554E 00	0.3277E 00	0.2601E-02	0.2991E 01	0.1523E 05	-0.2712E 09
0.6000E-04	0.2458E 00	0.9830E 00	0.4915E 00	0.3901E-02	0.3254E 01	0.1153E 05	-0.1269E 09
0.8000E-04	0.3277E 00	0.1311E 01	0.6554E 00	0.5201E-02	0.3464E 01	0.9593E 04	-0.7421E 08
0.1000E-03	0.4096E 00	0.1638E 01	0.8192E 00	0.6502E-02	0.3643E 01	0.8384E 04	-0.4940E 08
0.2000E-03	0.8192E 00	0.3277E 01	0.1638E 01	0.1300E-01	0.4318E 01	0.5623E 04	-0.1665E 08
0.3000E-03	0.1229E 01	0.4915E 01	0.2458E 01	0.1950E-01	0.4812E 01	0.4367E 04	-0.9588E 07
0.4000E-03	0.1638E 01	0.6554E 01	0.3277E 01	0.2601E-01	0.5207E 01	0.3585E 04	-0.6404E 07
0.5000E-03	0.2048E 01	0.8192E 01	0.4096E 01	0.3251E-01	0.5537E 01	0.3042E 04	-0.4605E 07
0.6000E-03	0.2458E 01	0.9830E 01	0.4915E 01	0.3901E-01	0.5820E 01	0.2642E 04	-0.3474E 07
0.8000E-03	0.3277E 01	0.1311E 02	0.6554E 01	0.5201E-01	0.6289E 01	0.2091E 04	-0.2180E 07
0.1000E-02	0.4096E 01	0.1638E 02	0.8192E 01	0.6502E-01	0.6669E 01	0.1731E 04	-0.1494E 07
0.2000E-02	0.8192E 01	0.3277E 02	0.1638E 02	0.1300E 00	0.7916E 01	0.9284E 03	-0.4306E 06
0.3000E-02	0.1229E 02	0.4915E 02	0.2458E 02	0.1950E 00	0.8679E 01	0.6342E 03	-0.2010E 06
0.4000E-02	0.1638E 02	0.6554E 02	0.3277E 02	0.2601E 00	0.9230E 01	0.4815E 03	-0.1159E 06
0.5000E-02	0.2048E 02	0.8192E 02	0.4096E 02	0.3251E 00	0.9661E 01	0.3881E 03	-0.7530E 05
0.6000E-02	0.2458E 02	0.9830E 02	0.4915E 02	0.3901E 00	0.1002E 02	0.3250E 03	-0.5282E 05
0.8000E-02	0.3277E 02	0.1311E 03	0.6554E 02	0.5201E 00	0.1058E 02	0.2453E 03	-0.3009E 05
0.1000E-01	0.4096E 02	0.1638E 03	0.8192E 02	0.6502E 00	0.1102E 02	0.1970E 03	-0.1940E 05
0.2000E-01	0.8192E 02	0.3277E 03	0.1638E 03	0.1300E 01	0.1239E 02	0.9924E 02	-0.4924E 04
0.3000E-01	0.1229E 03	0.4915E 03	0.2458E 03	0.1950E 01	0.1319E 02	0.6633E 02	-0.2200E 04
0.4000E-01	0.1638E 03	0.6554E 03	0.3277E 03	0.2601E 01	0.1377E 02	0.4981E 02	-0.1241E 04
0.5000E-01	0.2048E 03	0.8192E 03	0.4096E 03	0.3251E 01	0.1421E 02	0.3988E 02	-0.7951E 03
0.6000E-01	0.2458E 03	0.9830E 03	0.4915E 03	0.3901E 01	0.1458E 02	0.3325E 02	-0.5527E 03
0.8000E-01	0.3277E 03	0.1311E 04	0.6554E 03	0.5201E 01	0.1515E 02	0.2495E 02	-0.3113E 03
0.1000E 00	0.4096E 03	0.1638E 04	0.8192E 03	0.6502E 01	0.1560E 02	0.1997E 02	-0.1992E 03
0.2000E 00	0.8192E 03	0.3277E 04	0.1638E 04	0.1300E 02	0.1699E 02	0.1013E 02	-0.4722E 02
0.3000E 00	0.1229E 04	0.4915E 04	0.2458E 04	0.1950E 02	0.1783E 02	0.7140E 01	-0.1850E 02
0.4000E 00	0.1638E 04	0.6554E 04	0.3277E 04	0.2601E 02	0.1847E 02	0.5820E 01	-0.9404E 01
0.5000E 00	0.2048E 04	0.8192E 04	0.4096E 04	0.3251E 02	0.1901E 02	0.5085E 01	-0.5794E 01
0.6000E 00	0.2458E 04	0.9830E 04	0.4915E 04	0.3901E 02	0.1949E 02	0.4601E 01	-0.4075E 01
0.8000E 00	0.3277E 04	0.1311E 05	0.6554E 04	0.5201E 02	0.2034E 02	0.3966E 01	-0.2508E 01
0.1000E 01	0.4096E 04	0.1638E 05	0.8192E 04	0.6502E 02	0.2109E 02	0.3545E 01	-0.1776E 01
0.2000E 01	0.8192E 04	0.3277E 05	0.1638E 05	0.1300E 03	0.2403E 02	0.2507E 01	-0.6266E 00
0.3000E 01	0.1229E 05	0.4915E 05	0.2458E 05	0.1950E 03	0.2628E 02	0.2047E 01	-0.3411E 00
0.4000E 01	0.1638E 05	0.6554E 05	0.3277E 05	0.2601E 03	0.2818E 02	0.1772E 01	-0.2216E 00
0.5000E 01	0.2048E 05	0.8192E 05	0.4096E 05	0.3251E 03	0.2985E 02	0.1585E 01	-0.1585E 00
0.6000E 01	0.2458E 05	0.9830E 05	0.4915E 05	0.3901E 03	0.3137E 02	0.1447E 01	-0.1206E 00
0.8000E 01	0.3277E 05	0.1311E 06	0.6554E 05	0.5201E 03	0.3405E 02	0.1253E 01	-0.7833E-01
0.1000E 02	0.4096E 05	0.1638E 06	0.8192E 05	0.6502E 03	0.3642E 02	0.1121E 01	-0.5605E-01
0.2000E 02	0.8192E 05	0.3277E 06	0.1638E 06	0.1300E 04	0.4571E 02	0.7927E 00	-0.1982E-01
0.3000E 02	0.1229E 06	0.4915E 06	0.2458E 06	0.1950E 04	0.5283E 02	0.6472E 00	-0.1079E-01
0.4000E 02	0.1638E 06	0.6554E 06	0.3277E 06	0.2601E 04	0.5884E 02	0.5605E 00	-0.7006E-02
0.5000E 02	0.2048E 06	0.8192E 06	0.4096E 06	0.3251E 04	0.6413E 02	0.5013E 00	-0.5013E-02
0.6000E 02	0.2458E 06	0.9830E 06	0.4915E 06	0.3901E 04	0.6892E 02	0.4576E 00	-0.3814E-02
0.8000E 02	0.3277E 06	0.1311E 07	0.6554E 06	0.5201E 04	0.7741E 02	0.3963E 00	-0.2480E-02
0.1000E 03	0.4096E 06	0.1638E 07	0.8192E 06	0.6502E 04	0.8490E 02	0.3544E 00	-0.1780E-02

TABLE 10: p_{Dw}, p'_{Dw} and p''_{Dw} as Functions of Dimensionless Drawdown Times for a Well Between Three Perpendicular Sealing Faults

WELL LOCATION, (XD,YD) = (0.0312500,16.0000000)

TDA	TDBX	TDBY	TDBB	TDABX	PD	PDP	PDPP
0.1000E-04	0.4096E-01	0.1562E-06	0.8000E-04	0.6502E-03	0.2252E 01	0.4969E 05	-0.4938E 10
0.2000E-04	0.8192E-01	0.3125E-06	0.1600E-03	0.1300E-02	0.2597E 01	0.2492E 05	-0.1242E 10
0.3000E-04	0.1229E 00	0.4687E-06	0.2400E-03	0.1950E-02	0.2799E 01	0.1664E 05	-0.5521E 09
0.4000E-04	0.1638E 00	0.6250E-06	0.3200E-03	0.2601E-02	0.2943E 01	0.1251E 05	-0.3080E 09
0.6000E-04	0.2458E 00	0.9375E-06	0.4800E-03	0.3901E-02	0.3147E 01	0.8467E 04	-0.1313E 09
0.8000E-04	0.3277E 00	0.1250E-05	0.6400E-03	0.5201E-02	0.3295E 01	0.6541E 04	-0.7042E 08
0.1000E-03	0.4096E 00	0.1562E-05	0.8000E-03	0.6502E-02	0.3414E 01	0.5432E 04	-0.4366E 08
0.2000E-03	0.8192E 00	0.3125E-05	0.1600E-02	0.1300E-01	0.3824E 01	0.3237E 04	-0.1168E 08
0.3000E-03	0.1229E 01	0.4687E-05	0.2400E-02	0.1950E-01	0.4101E 01	0.2405E 04	-0.6012E 07
0.4000E-03	0.1638E 01	0.6250E-05	0.3200E-02	0.2601E-01	0.4316E 01	0.1929E 04	-0.3785E 07
0.5000E-03	0.2048E 01	0.7812E-05	0.4000E-02	0.3251E-01	0.4492E 01	0.1614E 04	-0.2628E 07
0.6000E-03	0.2458E 01	0.9375E-05	0.4800E-02	0.3901E-01	0.4642E 01	0.1388E 04	-0.1937E 07
0.8000E-03	0.3277E 01	0.1250E-04	0.6400E-02	0.5201E-01	0.4887E 01	0.1086E 04	-0.1181E 07
0.1000E-02	0.4096E 01	0.1562E-04	0.8000E-02	0.6502E-01	0.5083E 01	0.8917E 03	-0.7960E 06
0.2000E-02	0.8192E 01	0.3125E-04	0.1600E-01	0.1300E 00	0.5720E 01	0.4713E 03	-0.2221E 06
0.3000E-02	0.1229E 02	0.4687E-04	0.2400E-01	0.1950E 00	0.6106E 01	0.3203E 03	-0.1026E 06
0.4000E-02	0.1638E 02	0.6250E-04	0.3200E-01	0.2601E 00	0.6384E 01	0.2426E 03	-0.5885E 05
0.5000E-02	0.2048E 02	0.7812E-04	0.4000E-01	0.3251E 00	0.6602E 01	0.1952E 03	-0.3812E 05
0.6000E-02	0.2458E 02	0.9375E-04	0.4800E-01	0.3901E 00	0.6780E 01	0.1633E 03	-0.2668E 05
0.8000E-02	0.3277E 02	0.1250E-03	0.6400E-01	0.5201E 00	0.7063E 01	0.1231E 03	-0.1516E 05
0.1000E-01	0.4096E 02	0.1562E-03	0.8000E-01	0.6502E 00	0.7283E 01	0.9879E 02	-0.9760E 04
0.2000E-01	0.8192E 02	0.3125E-03	0.1600E 00	0.1300E 01	0.7970E 01	0.4970E 02	-0.2470E 04
0.3000E-01	0.1229E 03	0.4687E-03	0.2400E 00	0.1950E 01	0.8373E 01	0.3320E 02	-0.1102E 04
0.4000E-01	0.1638E 03	0.6250E-03	0.3200E 00	0.2601E 01	0.8660E 01	0.2492E 02	-0.6212E 03
0.5000E-01	0.2048E 03	0.7812E-03	0.4000E 00	0.3251E 01	0.8882E 01	0.1995E 02	-0.3981E 03
0.6000E-01	0.2458E 03	0.9375E-03	0.4800E 00	0.3901E 01	0.9064E 01	0.1663E 02	-0.2767E 03
0.8000E-01	0.3277E 03	0.1250E-02	0.6400E 00	0.5201E 01	0.9352E 01	0.1248E 02	-0.1558E 03
0.1000E 00	0.4096E 03	0.1562E-02	0.8000E 00	0.6502E 01	0.9574E 01	0.9989E 01	-0.9967E 02
0.2000E 00	0.8192E 03	0.3125E-02	0.1600E 01	0.1300E 02	0.1027E 02	0.5065E 01	-0.2362E 02
0.3000E 00	0.1229E 04	0.4687E-02	0.2400E 01	0.1950E 02	0.1069E 02	0.3570E 01	-0.9252E 01
0.4000E 00	0.1638E 04	0.6250E-02	0.3200E 01	0.2601E 02	0.1101E 02	0.2910E 01	-0.4703E 01
0.5000E 00	0.2048E 04	0.7813E-02	0.4000E 01	0.3251E 02	0.1128E 02	0.2543E 01	-0.2898E 01
0.6000E 00	0.2458E 04	0.9375E-02	0.4800E 01	0.3901E 02	0.1152E 02	0.2300E 01	-0.2038E 01
0.8000E 00	0.3277E 04	0.1250E-01	0.6400E 01	0.5201E 02	0.1195E 02	0.1983E 01	-0.1254E 01
0.1000E 01	0.4096E 04	0.1563E-01	0.8000E 01	0.6502E 02	0.1232E 02	0.1773E 01	-0.8881E 00
0.2000E 01	0.8192E 04	0.3125E-01	0.1600E 02	0.1300E 03	0.1379E 02	0.1253E 01	-0.3133E 00
0.3000E 01	0.1229E 05	0.4686E-01	0.2400E 02	0.1950E 03	0.1492E 02	0.1023E 01	-0.1706E 00
0.4000E 01	0.1638E 05	0.6250E-01	0.3200E 02	0.2601E 03	0.1587E 02	0.8862E 00	-0.1108E 00
0.5000E 01	0.2048E 05	0.7813E-01	0.4000E 02	0.3251E 03	0.1670E 02	0.7927E 00	-0.7926E-01
0.6000E 01	0.2458E 05	0.9375E-01	0.4800E 02	0.3901E 03	0.1746E 02	0.7236E 00	-0.6027E-01
0.8000E 01	0.3277E 05	0.1250E 00	0.6400E 02	0.5201E 03	0.1880E 02	0.6269E 00	-0.3897E-01
0.1000E 02	0.4096E 05	0.1563E 00	0.8000E 02	0.6502E 03	0.1999E 02	0.5614E 00	-0.2748E-01
0.2000E 02	0.8192E 05	0.3125E 00	0.1600E 03	0.1300E 04	0.2470E 02	0.4125E 00	-0.7727E-02
0.3000E 02	0.1229E 06	0.4688E 00	0.2400E 03	0.1950E 04	0.2854E 02	0.3619E 00	-0.3307E-02
0.4000E 02	0.1638E 06	0.6250E 00	0.3200E 03	0.2601E 04	0.3202E 02	0.3368E 00	-0.1947E-02
0.5000E 02	0.2048E 06	0.7813E 00	0.4000E 03	0.3251E 04	0.3530E 02	0.3204E 00	-0.1419E-02
0.6000E 02	0.2458E 06	0.9375E 00	0.4800E 03	0.3901E 04	0.3844E 02	0.3076E 00	-0.1163E-02
0.8000E 02	0.3277E 06	0.1250E 01	0.6400E 03	0.5201E 04	0.4438E 02	0.2872E 00	-0.9066E-03
0.1000E 03	0.4096E 06	0.1563E 01	0.8000E 03	0.6502E 04	0.4995E 02	0.2706E 00	-0.7617E-03

TABLE 11: p_{Dw}, p'_{Dw} and p''_{Dw} as Functions of Dimensionless Drawdown Times for a Well Between Three Perpendicular Sealing Faults

WELL LOCATION, (XD,YD) = (0.1250000, 0.0156250)

TDA	TDBX	TDBY	TDBB	TDABX	PD	PDP	PDPP
0.1000E-04	0.2560E-02	0.1638E 00	0.2048E-01	0.1707E-03	0.2252E 01	0.4980E 05	-0.4881E 10
0.2000E-04	0.5120E-02	0.3277E 00	0.4096E-01	0.3413E-03	0.2603E 01	0.2610E 05	-0.1121E 10
0.3000E-04	0.7680E-02	0.4915E 00	0.6144E-01	0.5120E-03	0.2823E 01	0.1881E 05	-0.4781E 09
0.4000E-04	0.1024E-01	0.6554E 00	0.8192E-01	0.6827E-03	0.2991E 01	0.1520E 05	-0.2758E 09
0.6000E-04	0.1536E-01	0.9830E 00	0.1229E 00	0.1024E-02	0.3252E 01	0.1134E 05	-0.1377E 09
0.8000E-04	0.2048E-01	0.1311E 01	0.1638E 00	0.1365E-02	0.3455E 01	0.9159E 04	-0.8664E 08
0.1000E-03	0.2560E-01	0.1638E 01	0.2048E 00	0.1707E-02	0.3623E 01	0.7713E 04	-0.6052E 08
0.2000E-03	0.5120E-01	0.3277E 01	0.4096E 00	0.3413E-02	0.4194E 01	0.4342E 04	-0.1889E 08
0.3000E-03	0.7680E-01	0.4915E 01	0.6144E 00	0.5120E-02	0.4554E 01	0.3026E 04	-0.9164E 07
0.4000E-03	0.1024E 00	0.6554E 01	0.8192E 00	0.6827E-02	0.4818E 01	0.2323E 04	-0.5394E 07
0.5000E-03	0.1280E 00	0.8192E 01	0.1024E 01	0.8533E-02	0.5027E 01	0.1886E 04	-0.3543E 07
0.6000E-03	0.1536E 00	0.9830E 01	0.1229E 01	0.1024E-01	0.5200E 01	0.1588E 04	-0.2494E 07
0.8000E-03	0.2048E 00	0.1311E 02	0.1638E 01	0.1365E-01	0.5477E 01	0.1213E 04	-0.1405E 07
0.1000E-02	0.2560E 00	0.1638E 02	0.2048E 01	0.1707E-01	0.5695E 01	0.9899E 03	-0.8843E 06
0.2000E-02	0.5120E 00	0.3277E 02	0.4096E 01	0.3413E-01	0.6421E 01	0.5623E 03	-0.2087E 06
0.3000E-02	0.7680E 00	0.4915E 02	0.6144E 01	0.5120E-01	0.6903E 01	0.4197E 03	-0.9954E 05
0.4000E-02	0.1024E 01	0.6554E 02	0.8192E 01	0.6827E-01	0.7280E 01	0.3415E 03	-0.6193E 05
0.5000E-02	0.1280E 01	0.8192E 02	0.1024E 02	0.8533E-01	0.7594E 01	0.2898E 03	-0.4339E 05
0.6000E-02	0.1536E 01	0.9830E 02	0.1229E 02	0.1024E 00	0.7865E 01	0.2523E 03	-0.3245E 05
0.8000E-02	0.2048E 01	0.1311E 03	0.1638E 02	0.1365E 00	0.8314E 01	0.2009E 03	-0.2036E 05
0.1000E-01	0.2560E 01	0.1638E 03	0.2048E 02	0.1707E 00	0.8680E 01	0.1672E 03	-0.1403E 05
0.2000E-01	0.5120E 01	0.3277E 03	0.4096E 02	0.3413E 00	0.9894E 01	0.9099E 02	-0.4142E 04
0.3000E-01	0.7680E 01	0.4915E 03	0.6144E 02	0.5120E 00	0.1064E 02	0.6253E 02	-0.1955E 04
0.4000E-01	0.1024E 02	0.6554E 03	0.8192E 02	0.6827E 00	0.1119E 02	0.4764E 02	-0.1135E 04
0.5000E-01	0.1280E 02	0.8192E 03	0.1024E 03	0.8533E 00	0.1162E 02	0.3847E 02	-0.7401E 03
0.6000E-01	0.1536E 02	0.9830E 03	0.1229E 03	0.1024E 01	0.1197E 02	0.3227E 02	-0.5206E 03
0.8000E-01	0.2048E 02	0.1311E 04	0.1638E 03	0.1365E 01	0.1253E 02	0.2440E 02	-0.2975E 03
0.1000E 00	0.2560E 02	0.1638E 04	0.2048E 03	0.1707E 01	0.1296E 02	0.1961E 02	-0.1921E 03
0.2000E 00	0.5120E 02	0.3277E 04	0.4096E 03	0.3413E 01	0.1434E 02	0.1005E 02	-0.4622E 02
0.3000E 00	0.7680E 02	0.4915E 04	0.6144E 03	0.5120E 01	0.1517E 02	0.7116E 01	-0.1822E 02
0.4000E 00	0.1024E 03	0.6554E 04	0.8192E 03	0.6827E 01	0.1581E 02	0.5813E 01	-0.9318E 01
0.5000E 00	0.1280E 03	0.8192E 04	0.1024E 04	0.8533E 01	0.1635E 02	0.5082E 01	-0.5766E 01
0.6000E 00	0.1536E 03	0.9830E 04	0.1229E 04	0.1024E 02	0.1683E 02	0.4600E 01	-0.4066E 01
0.8000E 00	0.2048E 03	0.1311E 05	0.1638E 04	0.1365E 02	0.1769E 02	0.3966E 01	-0.2507E 01
0.1000E 01	0.2560E 03	0.1638E 05	0.2048E 04	0.1707E 02	0.1843E 02	0.3545E 01	-0.1776E 01
0.2000E 01	0.5120E 03	0.3277E 05	0.4096E 04	0.3413E 02	0.2137E 02	0.2507E 01	-0.6266E 00
0.3000E 01	0.7680E 03	0.4915E 05	0.6144E 04	0.5120E 02	0.2362E 02	0.2047E 01	-0.3411E 00
0.4000E 01	0.1024E 04	0.6554E 05	0.8192E 04	0.6827E 02	0.2552E 02	0.1772E 01	-0.2216E 00
0.5000E 01	0.1280E 04	0.8192E 05	0.1024E 05	0.8533E 02	0.2720E 02	0.1585E 01	-0.1585E 00
0.6000E 01	0.1536E 04	0.9830E 05	0.1229E 05	0.1024E 03	0.2871E 02	0.1447E 01	-0.1206E 00
0.8000E 01	0.2048E 04	0.1311E 06	0.1638E 05	0.1365E 03	0.3140E 02	0.1253E 01	-0.7833E-01
0.1000E 02	0.2560E 04	0.1638E 06	0.2048E 05	0.1707E 03	0.3376E 02	0.1121E 01	-0.5605E-01
0.2000E 02	0.5120E 04	0.3277E 06	0.4096E 05	0.3413E 03	0.4305E 02	0.7927E 00	-0.1982E-01
0.3000E 02	0.7680E 04	0.4915E 06	0.6144E 05	0.5120E 03	0.5018E 02	0.6472E 00	-0.1079E-01
0.4000E 02	0.1024E 05	0.6554E 06	0.8192E 05	0.6827E 03	0.5618E 02	0.5605E 00	-0.7006E-02
0.5000E 02	0.1280E 05	0.8192E 06	0.1024E 06	0.8533E 03	0.6148E 02	0.5013E 00	-0.5013E-02
0.6000E 02	0.1536E 05	0.9830E 06	0.1229E 06	0.1024E 04	0.6626E 02	0.4576E 00	-0.3814E-02
0.8000E 02	0.2048E 05	0.1311E 07	0.1638E 06	0.1365E 04	0.7476E 02	0.3963E 00	-0.2480E-02
0.1000E 03	0.2560E 05	0.1638E 07	0.2048E 06	0.1707E 04	0.8224E 02	0.3544E 00	-0.1780E-02

TABLE 12: p_{Dw}, p'_{Dw} and p''_{Dw} as Functions of Dimensionless Drawdown Times for a Well Between Three Perpendicular Sealing Faults

WELL LOCATION, (XD,YD) = (0.1250000,16.0000000)

TDA	TDBX	TDBY	TDBB	TDABX	PD	PDP	PDPP
0.1000E-04	0.2560E-02	0.1562E-06	0.2000E-04	0.1707E-03	0.2252E 01	0.4969E 05	-0.4938E 10
0.2000E-04	0.5120E-02	0.3125E-06	0.4000E-04	0.3413E-03	0.2597E 01	0.2492E 05	-0.1242E 10
0.3000E-04	0.7680E-02	0.4687E-06	0.6000E-04	0.5120E-03	0.2799E 01	0.1663E 05	-0.5532E 09
0.4000E-04	0.1024E-01	0.6250E-06	0.8000E-04	0.6827E-03	0.2943E 01	0.1248E 05	-0.3115E 09
0.6000E-04	0.1536E-01	0.9375E-06	0.1200E-03	0.1024E-02	0.3145E 01	0.8325E 04	-0.1386E 09
0.8000E-04	0.2048E-01	0.1250E-05	0.1600E-03	0.1365E-02	0.3289E 01	0.6245E 04	-0.7800E 08
0.1000E-03	0.2560E-01	0.1562E-05	0.2000E-03	0.1707E-02	0.3401E 01	0.4997E 04	-0.4994E 08
0.2000E-03	0.5120E-01	0.3125E-05	0.4000E-03	0.3413E-02	0.3747E 01	0.2499E 04	-0.1249E 08
0.3000E-03	0.7680E-01	0.4687E-05	0.6000E-03	0.5120E-02	0.3950E 01	0.1666E 04	-0.5553E 07
0.4000E-03	0.1024E 00	0.6250E-05	0.8000E-03	0.6827E-02	0.4093E 01	0.1250E 04	-0.3122E 07
0.5000E-03	0.1280E 00	0.7812E-05	0.1000E-02	0.8533E-02	0.4205E 01	0.1000E 04	-0.1994E 07
0.6000E-03	0.1536E 00	0.9375E-05	0.1200E-02	0.1024E-01	0.4296E 01	0.8345E 03	-0.1377E 07
0.8000E-03	0.2048E 00	0.1250E-04	0.1600E-02	0.1365E-01	0.4441E 01	0.6297E 03	-0.7581E 06
0.1000E-02	0.2560E 00	0.1562E-04	0.2000E-02	0.1707E-01	0.4554E 01	0.5100E 03	-0.4707E 06
0.2000E-02	0.5120E 00	0.3125E-04	0.4000E-02	0.3413E-01	0.4924E 01	0.2854E 03	-0.1081E 06
0.3000E-02	0.7680E 00	0.4687E-04	0.6000E-02	0.5120E-01	0.5168E 01	0.2120E 03	-0.5099E 05
0.4000E-02	0.1024E 01	0.6250E-04	0.8000E-02	0.6827E-01	0.5359E 01	0.1721E 03	-0.3152E 05
0.5000E-02	0.1280E 01	0.7812E-04	0.1000E-01	0.8533E-01	0.5517E 01	0.1458E 03	-0.2200E 05
0.6000E-02	0.1536E 01	0.9375E-04	0.1200E-01	0.1024E 00	0.5653E 01	0.1268E 03	-0.1642E 05
0.8000E-02	0.2048E 01	0.1250E-03	0.1600E-01	0.1365E 00	0.5878E 01	0.1009E 03	-0.1027E 05
0.1000E-01	0.2560E 01	0.1562E-03	0.2000E-01	0.1707E 00	0.6062E 01	0.8383E 02	-0.7062E 04
0.2000E-01	0.5120E 01	0.3125E-03	0.4000E-01	0.3413E 00	0.6670E 01	0.4556E 02	-0.2077E 04
0.3000E-01	0.7680E 01	0.4687E-03	0.6000E-01	0.5120E 00	0.7046E 01	0.3130E 02	-0.9798E 03
0.4000E-01	0.1024E 02	0.6250E-03	0.8000E-01	0.6827E 00	0.7318E 01	0.2384E 02	-0.5682E 03
0.5000E-01	0.1280E 02	0.7812E-03	0.1000E 00	0.8533E 00	0.7532E 01	0.1925E 02	-0.3705E 03
0.6000E-01	0.1536E 02	0.9375E-03	0.1200E 00	0.1024E 01	0.7708E 01	0.1614E 02	-0.2605E 03
0.8000E-01	0.2048E 02	0.1250E-02	0.1600E 00	0.1365E 01	0.7988E 01	0.1220E 02	-0.1489E 03
0.1000E 00	0.2560E 02	0.1562E-02	0.2000E 00	0.1707E 01	0.8206E 01	0.9810E 01	-0.9610E 02
0.2000E 00	0.5120E 02	0.3125E-02	0.4000E 00	0.3413E 01	0.8892E 01	0.5025E 01	-0.2312E 02
0.3000E 00	0.7680E 02	0.4687E-02	0.6000E 00	0.5120E 01	0.9310E 01	0.3558E 01	-0.9113E 01
0.4000E 00	0.1024E 03	0.6250E-02	0.8000E 00	0.6827E 01	0.9630E 01	0.2907E 01	-0.4660E 01
0.5000E 00	0.1280E 03	0.7813E-02	0.1000E 01	0.8533E 01	0.9901E 01	0.2541E 01	-0.2884E 01
0.6000E 00	0.1536E 03	0.9375E-02	0.1200E 01	0.1024E 02	0.1014E 02	0.2300E 01	-0.2033E 01
0.8000E 00	0.2048E 03	0.1250E-01	0.1600E 01	0.1365E 02	0.1057E 02	0.1933E 01	-0.1253E 01
0.1000E 01	0.2560E 03	0.1563E-01	0.2000E 01	0.1707E 02	0.1094E 02	0.1773E 01	-0.8881E 00
0.2000E 01	0.5120E 03	0.3125E-01	0.4000E 01	0.3413E 02	0.1241E 02	0.1253E 01	-0.3133E 00
0.3000E 01	0.7680E 03	0.4688E-01	0.6000E 01	0.5120E 02	0.1354E 02	0.1023E 01	-0.1706E 00
0.4000E 01	0.1024E 04	0.6250E-01	0.8000E 01	0.6827E 02	0.1449E 02	0.8862E 00	-0.1109E 00
0.5000E 01	0.1280E 04	0.7813E-01	0.1000E 02	0.8533E 02	0.1532E 02	0.7927E 00	-0.7926E-01
0.6000E 01	0.1536E 04	0.9375E-01	0.1200E 02	0.1024E 03	0.1608E 02	0.7236E 00	-0.6027E-01
0.8000E 01	0.2048E 04	0.1250E 00	0.1600E 02	0.1365E 03	0.1742E 02	0.6269E 00	-0.3897E-01
0.1000E 02	0.2560E 04	0.1563E 00	0.2000E 02	0.1707E 03	0.1861E 02	0.5614E 00	-0.2748E-01
0.2000E 02	0.5120E 04	0.3125E 00	0.4000E 02	0.3413E 03	0.2332E 02	0.4125E 00	-0.7727E-02
0.3000E 02	0.7680E 04	0.4688E 00	0.6000E 02	0.5120E 03	0.2716E 02	0.3619E 00	-0.3307E-02
0.4000E 02	0.1024E 05	0.6250E 00	0.8000E 02	0.6827E 03	0.3064E 02	0.3368E 00	-0.1947E-02
0.5000E 02	0.1280E 05	0.7813E 00	0.1000E 03	0.8533E 03	0.3392E 02	0.3204E 00	-0.1419E-02
0.6000E 02	0.1536E 05	0.9375E 00	0.1200E 03	0.1024E 04	0.3706E 02	0.3076E 00	-0.1163E-02
0.8000E 02	0.2048E 05	0.1250E 01	0.1600E 03	0.1365E 04	0.4300E 02	0.2872E 00	-0.9066E-03
0.1000E 03	0.2560E 05	0.1563E 01	0.2000E 03	0.1707E 04	0.4857E 02	0.2706E 00	-0.7617E-03

TABLE 13: p_{Ds}, p'_{Ds} and p''_{Ds} as Functions of Dimensionless Buildup Times for a Well Between Three Perpendicular Sealing Faults

WELL LOCATION, (XD,YD) = (0.5000000, 0.0156250)

PRODUCING TIME BEFORE SHUT IN, TCA = 0.0100

DEL(T)	TRAT	TDBX	TDBY	TDBB	PDS	PDSP	PDSS
0.1000E-04	0.1001E 04	0.1600E-03	0.1638E 00	0.5120E-02	0.5716E 01	-0.4970E 05	0.4881E 10
0.2000E-04	0.5010E 03	0.3200E-03	0.3277E 00	0.1024E-01	0.5366E 01	-0.2600E 05	0.1121E 10
0.3000E-04	0.3343E 03	0.4800E-03	0.4915E 00	0.1536E-01	0.5147E 01	-0.1871E 05	0.4781E 09
0.4000E-04	0.2510E 03	0.6400E-03	0.6554E 00	0.2048E-01	0.4980E 01	-0.1510E 05	0.2758E 09
0.5000E-04	0.2010E 03	0.8000E-03	0.8192E 00	0.2560E-01	0.4841E 01	-0.1284E 05	0.1865E 09
0.6000E-04	0.1677E 03	0.9600E-03	0.9830E 00	0.3072E-01	0.4721E 01	-0.1124E 05	0.1377E 09
0.8000E-04	0.1260E 03	0.1280E-02	0.1311E 01	0.4096E-01	0.4520E 01	-0.9060E 04	0.8663E 08
0.1000E-03	0.1010E 03	0.1600E-02	0.1638E 01	0.5120E-01	0.4354E 01	-0.7614E 04	0.6051E 08
0.2000E-03	0.5100E 02	0.3200E-02	0.3277E 01	0.1024E 00	0.3793E 01	-0.4244E 04	0.1888E 08
0.3000E-03	0.3433E 02	0.4800E-02	0.4915E 01	0.1536E 00	0.3443E 01	-0.2929E 04	0.9155E 07
0.4000E-03	0.2600E 02	0.6400E-02	0.6554E 01	0.2048E 00	0.3188E 01	-0.2227E 04	0.5388E 07
0.5000E-03	0.2100E 02	0.8000E-02	0.8192E 01	0.2560E 00	0.2989E 01	-0.1790E 04	0.3545E 07
0.6000E-03	0.1767E 02	0.9600E-02	0.9830E 01	0.3072E 00	0.2825E 01	-0.1492E 04	0.2507E 07
0.8000E-03	0.1350E 02	0.1280E-01	0.1311E 02	0.4096E 00	0.2569E 01	-0.1111E 04	0.1441E 07
0.1000E-02	0.1100E 02	0.1600E-01	0.1638E 02	0.5120E 00	0.2371E 01	-0.8794E 03	0.9335E 06
0.2000E-02	0.6000E 01	0.3200E-01	0.3277E 02	0.1024E 01	0.1780E 01	-0.4089E 03	0.2358E 06
0.3000E-02	0.4333E 01	0.4800E-01	0.4915E 02	0.1536E 01	0.1460E 01	-0.2526E 03	0.1032E 06
0.4000E-02	0.3500E 01	0.6400E-01	0.6554E 02	0.2048E 01	0.1249E 01	-0.1760E 03	0.5668E 05
0.5000E-02	0.3000E 01	0.8000E-01	0.8192E 02	0.2560E 01	0.1098E 01	-0.1312E 03	0.3531E 05
0.6000E-02	0.2667E 01	0.9600E-01	0.9830E 02	0.3072E 01	0.9819E 00	-0.1022E 03	0.2383E 05
0.8000E-02	0.2250E 01	0.1280E 00	0.1311E 03	0.4096E 01	0.8160E 00	-0.6739E 02	0.1262E 05
0.1000E-01	0.2000E 01	0.1600E 00	0.1638E 03	0.5120E 01	0.7025E 00	-0.4777E 02	0.7579E 04
0.2000E-01	0.1500E 01	0.3200E 00	0.3277E 03	0.1024E 02	0.4374E 00	-0.1467E 02	0.1300E 04
0.3000E-01	0.1333E 01	0.4800E 00	0.4915E 03	0.1536E 02	0.3350E 00	-0.7228E 01	0.4087E 03
0.4000E-01	0.1250E 01	0.6400E 00	0.6554E 03	0.2048E 02	0.2782E 00	-0.4503E 01	0.1795E 03
0.5000E-01	0.1200E 01	0.8000E 00	0.8192E 03	0.2560E 02	0.2405E 00	-0.3177E 01	0.9759E 02
0.6000E-01	0.1167E 01	0.9600E 00	0.9830E 03	0.3072E 02	0.2128E 00	-0.2406E 01	0.6082E 02
0.8000E-01	0.1125E 01	0.1280E 01	0.1311E 04	0.4096E 02	0.1743E 00	-0.1552E 01	0.3001E 02
0.1000E 00	0.1100E 01	0.1600E 01	0.1638E 04	0.5120E 02	0.1482E 00	-0.1091E 01	0.1764E 02
0.2000E 00	0.1050E 01	0.3200E 01	0.3277E 04	0.1024E 03	0.8865E-01	-0.3184E 00	0.3090E 01
0.3000E 00	0.1033E 01	0.4800E 01	0.4915E 04	0.1536E 03	0.6735E-01	-0.1416E 00	0.9537E 00
0.4000E 00	0.1025E 01	0.6400E 01	0.6554E 04	0.2048E 03	0.5672E-01	-0.8013E-01	0.3846E 00
0.5000E 00	0.1020E 01	0.8000E 01	0.8192E 04	0.2560E 03	0.5022E-01	-0.5309E-01	0.1876E 00
0.6000E 00	0.1017E 01	0.9600E 01	0.9830E 04	0.3072E 03	0.4569E-01	-0.3890E-01	0.1068E 00
0.8000E 00	0.1012E 01	0.1280E 02	0.1311E 05	0.4096E 03	0.3953E-01	-0.2469E-01	0.4727E-01
0.1000E 01	0.1010E 01	0.1600E 02	0.1638E 05	0.5120E 03	0.3536E-01	-0.1761E-01	0.2644E-01
0.2000E 01	0.1005E 01	0.3200E 02	0.3277E 05	0.1024E 04	0.2504E-01	-0.6243E-02	0.4670E-02
0.3000E 01	0.1003E 01	0.4800E 02	0.4915E 05	0.1536E 04	0.2046E-01	-0.3401E-02	0.1698E-02
0.4000E 01	0.1002E 01	0.6400E 02	0.6554E 05	0.2048E 04	0.1770E-01	-0.2211E-02	0.8283E-03
0.5000E 01	0.1002E 01	0.8000E 02	0.8192E 05	0.2560E 04	0.1585E-01	-0.1581E-02	0.4744E-03
0.6000E 01	0.1002E 01	0.9600E 02	0.9830E 05	0.3072E 04	0.1447E-01	-0.1204E-02	0.3008E-03
0.8000E 01	0.1001E 01	0.1280E 03	0.1311E 06	0.4096E 04	0.1253E-01	-0.7811E-03	0.1466E-03
0.1000E 02	0.1001E 01	0.1600E 03	0.1638E 06	0.5120E 04	0.1120E-01	-0.5598E-03	0.8394E-04

TABLE 14: p_{Ds}, p'_{Ds} and p''_{Ds} as Functions of Dimensionless Buildup Times for a Well Between Three Perpendicular Sealing Faults

WELL LOCATION, (XD,YD) = (0.5000000, 0.0156250)

PRODUCING TIME BEFORE SHUT IN, TDA = 0.1000

DEL(T)	TRAT	TDBX	TDBY	TDBD	PDS	PDSP	PDSS
0.1000E-04	0.1000E 05	0.1600E-03	0.1638E 00	0.5120E-02	0.8447E 01	-0.4978E 05	0.4881E 10
0.2000E-04	0.5001E 04	0.3200E-03	0.3277E 00	0.1024E-01	0.8096E 01	-0.2609E 05	0.1121E 10
0.3000E-04	0.3334E 04	0.4800E-03	0.4915E 00	0.1536E-01	0.7877E 01	-0.1880E 05	0.4781E 09
0.4000E-04	0.2501E 04	0.6400E-03	0.6554E 00	0.2048E-01	0.7709E 01	-0.1518E 05	0.2758E 09
0.5000E-04	0.2001E 04	0.8000E-03	0.8192E 00	0.2560E-01	0.7569E 01	-0.1292E 05	0.1865E 09
0.6000E-04	0.1668E 04	0.9600E-03	0.9830E 00	0.3072E-01	0.7448E 01	-0.1132E 05	0.1377E 09
0.8000E-04	0.1251E 04	0.1280E-02	0.1311E 01	0.4096E-01	0.7245E 01	-0.9144E 04	0.8664E 08
0.1000E-03	0.1001E 04	0.1600E-02	0.1638E 01	0.5120E-01	0.7078E 01	-0.7697E 04	0.6052E 08
0.2000E-03	0.5010E 03	0.3200E-02	0.3277E 01	0.1024E 00	0.6509E 01	-0.4326E 04	0.1889E 08
0.3000E-03	0.3343E 03	0.4800E-02	0.4915E 01	0.1536E 00	0.6150E 01	-0.3011E 04	0.9164E 07
0.4000E-03	0.2510E 03	0.6400E-02	0.6554E 01	0.2048E 00	0.5887E 01	-0.2308E 04	0.5397E 07
0.5000E-03	0.2010E 03	0.8000E-02	0.8192E 01	0.2560E 00	0.5680E 01	-0.1870E 04	0.3553E 07
0.6000E-03	0.1677E 03	0.9600E-02	0.9830E 01	0.3072E 00	0.5508E 01	-0.1571E 04	0.2515E 07
0.8000E-03	0.1260E 03	0.1280E-01	0.1311E 02	0.4096E 00	0.5236E 01	-0.1189E 04	0.1456E 07
0.1000E-02	0.1010E 03	0.1600E-01	0.1638E 02	0.5120E 00	0.5023E 01	-0.9551E 03	0.9415E 06
0.2000E-02	0.5100E 02	0.3200E-01	0.3277E 02	0.1024E 01	0.4360E 01	-0.4773E 03	0.2424E 06
0.3000E-02	0.3433E 02	0.4800E-01	0.4915E 02	0.1536E 01	0.3975E 01	-0.3149E 03	0.1088E 06
0.4000E-02	0.2600E 02	0.6400E-01	0.6554E 02	0.2048E 01	0.3705E 01	-0.2332E 03	0.6145E 05
0.5000E-02	0.2100E 02	0.8000E-01	0.8192E 02	0.2560E 01	0.3498E 01	-0.1840E 03	0.3941E 05
0.6000E-02	0.1767E 02	0.9600E-01	0.9830E 02	0.3072E 01	0.3331E 01	-0.1511E 03	0.2738E 05
0.8000E-02	0.1350E 02	0.1280E 00	0.1311E 03	0.4096E 01	0.3074E 01	-0.1101E 03	0.1536E 05
0.1000E-01	0.1100E 02	0.1600E 00	0.1638E 03	0.5120E 01	0.2880E 01	-0.8559E 02	0.9737E 04
0.2000E-01	0.6000E 01	0.3200E 00	0.3277E 03	0.1024E 02	0.2316E 01	-0.3876E 02	0.2173E 04
0.3000E-01	0.4333E 01	0.4800E 00	0.4915E 03	0.1536E 02	0.2008E 01	-0.2489E 02	0.8838E 03
0.4000E-01	0.3500E 01	0.6400E 00	0.6554E 03	0.2048E 02	0.1795E 01	-0.1837E 02	0.4845E 03
0.5000E-01	0.3000E 01	0.8000E 00	0.8192E 03	0.2560E 02	0.1632E 01	-0.1448E 02	0.3128E 03
0.6000E-01	0.2667E 01	0.9600E 00	0.9830E 03	0.3072E 02	0.1501E 01	-0.1185E 02	0.2218E 03
0.8000E-01	0.2250E 01	0.1280E 01	0.1311E 04	0.4096E 02	0.1301E 01	-0.8459E 01	0.1298E 03
0.1000E 00	0.2000E 01	0.1600E 01	0.1638E 04	0.5120E 02	0.1155E 01	-0.6359E 01	0.8481E 02
0.2000E 00	0.1500E 01	0.3200E 01	0.3277E 04	0.1024E 03	0.7764E 00	-0.2220E 01	0.1878E 02
0.3000E 00	0.1333E 01	0.4800E 01	0.4915E 04	0.1536E 03	0.6207E 00	-0.1094E 01	0.6441E 01
0.4000E 00	0.1250E 01	0.6400E 01	0.6554E 04	0.2048E 03	0.5358E 00	-0.6637E 00	0.2803E 01
0.5000E 00	0.1200E 01	0.8000E 01	0.8192E 04	0.2560E 03	0.4807E 00	-0.4605E 00	0.1460E 01
0.6000E 00	0.1167E 01	0.9600E 01	0.9830E 04	0.3072E 03	0.4408E 00	-0.3475E 00	0.8736E 00
0.8000E 00	0.1125E 01	0.1280E 02	0.1311E 05	0.4096E 03	0.3847E 00	-0.2276E 00	0.4112E 00
0.1000E 01	0.1100E 01	0.1600E 02	0.1638E 05	0.5120E 03	0.3460E 00	-0.1651E 00	0.2373E 00
0.2000E 01	0.1050E 01	0.3200E 02	0.3277E 05	0.1024E 04	0.2476E 00	-0.6041E-01	0.4422E-01
0.3000E 01	0.1033E 01	0.4800E 02	0.4915E 05	0.1536E 04	0.2030E 00	-0.3328E-01	0.1637E-01
0.4000E 01	0.1025E 01	0.6400E 02	0.6554E 05	0.2048E 04	0.1761E 00	-0.2175E-01	0.8056E-02
0.5000E 01	0.1020E 01	0.8000E 02	0.8192E 05	0.2560E 04	0.1577E 00	-0.1562E-01	0.4640E-02
0.6000E 01	0.1017E 01	0.9600E 02	0.9830E 05	0.3072E 04	0.1441E 00	-0.1191E-01	0.2953E-02
0.8000E 01	0.1012E 01	0.1280E 03	0.1311E 06	0.4096E 04	0.1249E 00	-0.7762E-02	0.1446E-02
0.1000E 02	0.1010E 01	0.1600E 03	0.1638E 06	0.5120E 04	0.1118E 00	-0.5564E-02	0.8303E-03

TABLE 15: p_{Ds}, p'_{Ds} and p''_{Ds} as Functions of Dimensionless Buildup Times for a Well Between Three Perpendicular Sealing Faults

WELL LOCATION, (XD,YD) = (0.5000000, 0.0156250)
PRODUCING TIME BEFORE SHUT IN, TDA = 1.0000

DEL(T)	TRAT	TDBX	TDBY	TDBB	PDS	PDSP	PDSS
0.1000E-04	0.1000E 06	0.1600E-03	0.1638E 00	0.5120E-02	0.1361E 02	-0.4950E 05	0.4881E 10
0.2000E-04	0.5000E 05	0.3200E-03	0.3277E 00	0.1024E-01	0.1326E 02	-0.2610E 05	0.1121E 10
0.3000E-04	0.3333E 05	0.4800E-03	0.4915E 00	0.1536E-01	0.1304E 02	-0.1881E 05	0.4781E 09
0.4000E-04	0.2500E 05	0.6400E-03	0.6554E 00	0.2048E-01	0.1288E 02	-0.1519E 05	0.2758E 09
0.5000E-04	0.2000E 05	0.8000E-03	0.8192E 00	0.2560E-01	0.1274E 02	-0.1293E 05	0.1865E 09
0.6000E-04	0.1667E 05	0.9600E-03	0.9830E 00	0.3072E-01	0.1261E 02	-0.1133E 05	0.1377E 09
0.8000E-04	0.1250E 05	0.1280E-02	0.1311E 01	0.4096E-01	0.1241E 02	-0.9156E 04	0.8664E 08
0.1000E-03	0.1000E 05	0.1600E-02	0.1638E 01	0.5120E-01	0.1224E 02	-0.7709E 04	0.6052E 08
0.2000E-03	0.5001E 04	0.3200E-02	0.3277E 01	0.1024E 00	0.1167E 02	-0.4338E 04	0.1885E 08
0.3000E-03	0.3334E 04	0.4800E-02	0.4915E 01	0.1536E 00	0.1131E 02	-0.3023E 04	0.9164E 07
0.4000E-03	0.2501E 04	0.6400E-02	0.6554E 01	0.2048E 00	0.1105E 02	-0.2319E 04	0.5397E 07
0.5000E-03	0.2001E 04	0.8000E-02	0.8192E 01	0.2560E 00	0.1084E 02	-0.1881E 04	0.3554E 07
0.6000E-03	0.1668E 04	0.9600E-02	0.9830E 01	0.3072E 00	0.1067E 02	-0.1582E 04	0.2516E 07
0.8000E-03	0.1251E 04	0.1280E-01	0.1311E 02	0.4096E 00	0.1039E 02	-0.1200E 04	0.1450E 07
0.1000E-02	0.1001E 04	0.1600E-01	0.1638E 02	0.5120E 00	0.1018E 02	-0.9668E 03	0.9416E 06
0.2000E-02	0.5010E 03	0.3200E-01	0.3277E 02	0.1024E 01	0.9504E 01	-0.4889E 03	0.2429E 06
0.3000E-02	0.3343E 03	0.4800E-01	0.4915E 02	0.1536E 01	0.9107E 01	-0.3264E 03	0.1089E 06
0.4000E-02	0.2510E 03	0.6400E-01	0.6554E 02	0.2048E 01	0.8826E 01	-0.2446E 03	0.6155E 05
0.5000E-02	0.2010E 03	0.8000E-01	0.8192E 02	0.2560E 01	0.8608E 01	-0.1953E 03	0.3951E 05
0.6000E-02	0.1677E 03	0.9600E-01	0.9830E 02	0.3072E 01	0.8430E 01	-0.1623E 03	0.2749E 05
0.8000E-02	0.1260E 03	0.1280E 00	0.1311E 03	0.4096E 01	0.8150E 01	-0.1210E 03	0.1546E 05
0.1000E-01	0.1010E 03	0.1600E 00	0.1638E 03	0.5120E 01	0.7935E 01	-0.9636E 02	0.9836E 04
0.2000E-01	0.5100E 02	0.3200E 00	0.3277E 03	0.1024E 02	0.7268E 01	-0.4861E 02	0.2257E 04
0.3000E-01	0.3433E 02	0.4800E 00	0.4915E 03	0.1536E 02	0.6865E 01	-0.3395E 02	0.9573E 03
0.4000E-01	0.2600E 02	0.6400E 00	0.6554E 03	0.2048E 02	0.6565E 01	-0.2674E 02	0.5486E 03
0.5000E-01	0.2100E 02	0.8000E 00	0.8192E 03	0.2560E 02	0.6322E 01	-0.2226E 02	0.3691E 03
0.6000E-01	0.1767E 02	0.9600E 00	0.9830E 03	0.3072E 02	0.6116E 01	-0.1909E 02	0.2715E 03
0.8000E-01	0.1350E 02	0.1280E 01	0.1311E 04	0.4096E 02	0.5780E 01	-0.1482E 02	0.1693E 03
0.1000E 00	0.1100E 02	0.1600E 01	0.1638E 04	0.5120E 02	0.5513E 01	-0.1200E 02	0.1167E 03
0.2000E 00	0.6000E 01	0.3200E 01	0.3277E 04	0.1024E 03	0.4689E 01	-0.5790E 01	0.3208E 02
0.3000E 00	0.4333E 01	0.4800E 01	0.4915E 04	0.1536E 03	0.4230E 01	-0.3697E 01	0.1345E 02
0.4000E 00	0.3500E 01	0.6400E 01	0.6554E 04	0.2048E 03	0.3915E 01	-0.2717E 01	0.7137E 01
0.5000E 00	0.3000E 01	0.8000E 01	0.8192E 04	0.2560E 03	0.3673E 01	-0.2155E 01	0.4439E 01
0.6000E 00	0.2667E 01	0.9600E 01	0.9830E 04	0.3072E 03	0.3477E 01	-0.1786E 01	0.3069E 01
0.8000E 00	0.2250E 01	0.1280E 02	0.1311E 05	0.4096E 03	0.3171E 01	-0.1322E 01	0.1758E 01
0.1000E 01	0.2000E 01	0.1600E 02	0.1638E 05	0.5120E 03	0.2937E 01	-0.1038E 01	0.1148E 01
0.2000E 01	0.1500E 01	0.3200E 02	0.3277E 05	0.1024E 04	0.2253E 01	-0.4600E 00	0.2655E 00
0.3000E 01	0.1333E 01	0.4800E 02	0.4915E 05	0.1536E 04	0.1900E 01	-0.2742E 00	0.1195E 00
0.4000E 01	0.1250E 01	0.6400E 02	0.6554E 05	0.2048E 04	0.1674E 01	-0.1871E 00	0.6302E-01
0.5000E 01	0.1200E 01	0.8000E 02	0.8192E 05	0.2560E 04	0.1513E 01	-0.1381E 00	0.3793E-01
0.6000E 01	0.1167E 01	0.9600E 02	0.9830E 05	0.3072E 04	0.1391E 01	-0.1074E 00	0.2490E-01
0.8000E 01	0.1125E 01	0.1280E 03	0.1311E 06	0.4096E 04	0.1216E 01	-0.7168E-01	0.1265E-01
0.1000E 02	0.1100E 01	0.1600E 03	0.1638E 06	0.5120E 04	0.1094E 01	-0.5217E-01	0.7467E-02

TABLE 16: p_{Ds}, p'_{Ds} and p''_{Ds} as Functions of Dimensionless Buildup Times for a Well Between Three Perpendicular Sealing Faults

WELL LOCATION, (XD,YD) = (0.5000000, 0.0156250)
PRODUCING TIME BEFORE SHUT IN, TCA = 10.0000

DEL(T)	TRAT	TDBX	TDBY	TDBB	PDS	PDSP	PDSS
0.1000E-04	0.1000E 07	0.1600E-03	0.1638E 00	0.5120E-02	0.2894E 02	-0.4988E 05	0.4881E 10
0.2000E-04	0.5000E 06	0.3200E-03	0.3277E 00	0.1024E-01	0.2859E 02	-0.2610E 05	0.1121E 10
0.3000E-04	0.3333E 06	0.4800E-03	0.4915E 00	0.1536E-01	0.2837E 02	-0.1881E 05	0.4781E 09
0.4000E-04	0.2500E 06	0.6400E-03	0.6554E 00	0.2048E-01	0.2821E 02	-0.1520E 05	0.2758E 09
0.5000E-04	0.2000E 06	0.8000E-03	0.8192E 00	0.2560E-01	0.2807E 02	-0.1294E 05	0.1865E 09
0.6000E-04	0.1667E 06	0.9600E-03	0.9830E 00	0.3072E-01	0.2794E 02	-0.1134E 05	0.1377E 09
0.8000E-04	0.1250E 06	0.1280E-02	0.1311E 01	0.4096E-01	0.2774E 02	-0.9158E 04	0.8664E 08
0.1000E-03	0.1000E 06	0.1600E-02	0.1638E 01	0.5120E-01	0.2757E 02	-0.7712E 04	0.6052E 08
0.2000E-03	0.5000E 05	0.3200E-02	0.3277E 01	0.1024E 00	0.2700E 02	-0.4341E 04	0.1889E 08
0.3000E-03	0.3333E 05	0.4800E-02	0.4915E 01	0.1536E 00	0.2664E 02	-0.3025E 04	0.9164E 07
0.4000E-03	0.2500E 05	0.6400E-02	0.6554E 01	0.2048E 00	0.2638E 02	-0.2322E 04	0.5397E 07
0.5000E-03	0.2000E 05	0.8000E-02	0.8192E 01	0.2560E 00	0.2617E 02	-0.1884E 04	0.3554E 07
0.6000E-03	0.1667E 05	0.9600E-02	0.9830E 01	0.3072E 00	0.2600E 02	-0.1585E 04	0.2516E 07
0.8000E-03	0.1250E 05	0.1280E-01	0.1311E 02	0.4096E 00	0.2572E 02	-0.1203E 04	0.1450E 07
0.1000E-02	0.1000E 05	0.1600E-01	0.1638E 02	0.5120E 00	0.2551E 02	-0.9692E 03	0.9416E 06
0.2000E-02	0.5001E 04	0.3200E-01	0.3277E 02	0.1024E 01	0.2483E 02	-0.4914E 03	0.2425E 06
0.3000E-02	0.3334E 04	0.4800E-01	0.4915E 02	0.1536E 01	0.2443E 02	-0.3289E 03	0.1089E 06
0.4000E-02	0.2501E 04	0.6400E-01	0.6554E 02	0.2048E 01	0.2415E 02	-0.2470E 03	0.6156E 05
0.5000E-02	0.2001E 04	0.8000E-01	0.8192E 02	0.2560E 01	0.2393E 02	-0.1977E 03	0.3951E 05
0.6000E-02	0.1668E 04	0.9600E-01	0.9830E 02	0.3072E 01	0.2375E 02	-0.1647E 03	0.2749E 05
0.8000E-02	0.1251E 04	0.1280E 00	0.1311E 03	0.4096E 01	0.2346E 02	-0.1235E 03	0.1546E 05
0.1000E-01	0.1001E 04	0.1600E 00	0.1638E 03	0.5120E 01	0.2324E 02	-0.9877E 02	0.9838E 04
0.2000E-01	0.5010E 03	0.3200E 00	0.3277E 03	0.1024E 02	0.2255E 02	-0.5100E 02	0.2259E 04
0.3000E-01	0.3343E 03	0.4800E 00	0.4915E 03	0.1536E 02	0.2212E 02	-0.3633E 02	0.9589E 03
0.4000E-01	0.2510E 03	0.6400E 00	0.6554E 03	0.2048E 02	0.2180E 02	-0.2910E 02	0.5502E 03
0.5000E-01	0.2010E 03	0.8000E 00	0.8192E 03	0.2560E 02	0.2153E 02	-0.2460E 02	0.3707E 03
0.6000E-01	0.1677E 03	0.9600E 00	0.9830E 03	0.3072E 02	0.2130E 02	-0.2142E 02	0.2731E 03
0.8000E-01	0.1260E 03	0.1280E 01	0.1311E 04	0.4096E 02	0.2092E 02	-0.1711E 02	0.1708E 03
0.1000E 00	0.1010E 03	0.1600E 01	0.1638E 04	0.5120E 02	0.2061E 02	-0.1427E 02	0.1182E 03
0.2000E 00	0.5100E 02	0.3200E 01	0.3277E 04	0.1024E 03	0.1957E 02	-0.7916E 01	0.3337E 02
0.3000E 00	0.3433E 02	0.4800E 01	0.4915E 04	0.1536E 03	0.1890E 02	-0.5702E 01	0.1459E 02
0.4000E 00	0.2600E 02	0.6400E 01	0.6554E 04	0.2048E 03	0.1839E 02	-0.4613E 01	0.8154E 01
0.5000E 00	0.2100E 02	0.8000E 01	0.8192E 04	0.2560E 03	0.1796E 02	-0.3955E 01	0.5352E 01
0.6000E 00	0.1767E 02	0.9600E 01	0.9830E 04	0.3072E 03	0.1759E 02	-0.3500E 01	0.3893E 01
0.8000E 00	0.1350E 02	0.1280E 02	0.1311E 05	0.4096E 03	0.1696E 02	-0.2886E 01	0.2442E 01
0.1000E 01	0.1100E 02	0.1600E 02	0.1638E 05	0.5120E 03	0.1642E 02	-0.2476E 01	0.1726E 01
0.2000E 01	0.6000E 01	0.3200E 02	0.3277E 05	0.1024E 04	0.1453E 02	-0.1483E 01	0.5840E 00
0.3000E 01	0.4333E 01	0.4800E 02	0.4915E 05	0.1536E 04	0.1328E 02	-0.1063E 01	0.3033E 00
0.4000E 01	0.3500E 01	0.6400E 02	0.6554E 05	0.2048E 04	0.1235E 02	-0.8250E 00	0.1877E 00
0.5000E 01	0.3000E 01	0.8000E 02	0.8192E 05	0.2560E 04	0.1161E 02	-0.6700E 00	0.1280E 00
0.6000E 01	0.2667E 01	0.9600E 02	0.9830E 05	0.3072E 04	0.1099E 02	-0.5610E 00	0.9290E-01
0.8000E 01	0.2250E 01	0.1280E 03	0.1311E 06	0.4096E 04	0.1003E 02	-0.4178E 00	0.5512E-01
0.1000E 02	0.2000E 01	0.1600E 03	0.1638E 06	0.5120E 04	0.9287E 01	-0.3283E 00	0.3623E-01

TABLE 17: p_{Dw}, p'_{Dw} and p''_{Dw} as Functions of Dimensionless Drawdown Times for a Well Inside a Closed Square

WELL LOCATION, (XD,YD) = (1.0000000, 1.0000000)

TDA	TDDX	TDDY	TDDY	TDBY	TDBB	PD	PDP	PDPP
0.1000E-04	0.1000E-04	0.1000E-04	0.4000E-04	0.4000E-04	0.4000E-04	0.2252E 01	0.4969E 05	-0.4938E 10
0.1500E-04	0.1500E-04	0.1500E-04	0.6000E-04	0.6000E-04	0.6000E-04	0.2454E 01	0.3319E 05	-0.2204E 10
0.2000E-04	0.2000E-04	0.2000E-04	0.8000E-04	0.8000E-04	0.8000E-04	0.2597E 01	0.2492E 05	-0.1242E 10
0.3000E-04	0.3000E-04	0.3000E-04	0.1200E-03	0.1200E-03	0.1200E-03	0.2799E 01	0.1663E 05	-0.5532E 09
0.4000E-04	0.4000E-04	0.4000E-04	0.1600E-03	0.1600E-03	0.1600E-03	0.2943E 01	0.1248E 05	-0.3115E 09
0.5000E-04	0.5000E-04	0.5000E-04	0.2000E-03	0.2000E-03	0.2000E-03	0.3054E 01	0.9989E 04	-0.1995E 09
0.6000E-04	0.6000E-04	0.6000E-04	0.2400E-03	0.2400E-03	0.2400E-03	0.3145E 01	0.8325E 04	-0.1386E 09
0.8000E-04	0.8000E-04	0.8000E-04	0.3200E-03	0.3200E-03	0.3200E-03	0.3289E 01	0.6245E 04	-0.7800E 08
0.1000E-03	0.1000E-03	0.1000E-03	0.4000E-03	0.4000E-03	0.4000E-03	0.3401E 01	0.4997E 04	-0.4994E 08
0.1500E-03	0.1500E-03	0.1500E-03	0.6000E-03	0.6000E-03	0.6000E-03	0.3603E 01	0.3332E 04	-0.2220E 08
0.2000E-03	0.2000E-03	0.2000E-03	0.8000E-03	0.8000E-03	0.8000E-03	0.3747E 01	0.2499E 04	-0.1249E 08
0.3000E-03	0.3000E-03	0.3000E-03	0.1200E-02	0.1200E-02	0.1200E-02	0.3950E 01	0.1666E 04	-0.5553E 07
0.4000E-03	0.4000E-03	0.4000E-03	0.1600E-02	0.1600E-02	0.1600E-02	0.4093E 01	0.1250E 04	-0.3124E 07
0.5000E-03	0.5000E-03	0.5000E-03	0.2000E-02	0.2000E-02	0.2000E-02	0.4205E 01	0.9999E 03	-0.2000E 07
0.6000E-03	0.6000E-03	0.6000E-03	0.2400E-02	0.2400E-02	0.2400E-02	0.4296E 01	0.8332E 03	-0.1389E 07
0.8000E-03	0.8000E-03	0.8000E-03	0.3200E-02	0.3200E-02	0.3200E-02	0.4440E 01	0.6250E 03	-0.7811E 06
0.1000E-02	0.1000E-02	0.1000E-02	0.4000E-02	0.4000E-02	0.4000E-02	0.4552E 01	0.5000E 03	-0.4999E 06
0.1500E-02	0.1500E-02	0.1500E-02	0.6000E-02	0.6000E-02	0.6000E-02	0.4754E 01	0.3333E 03	-0.2222E 06
0.2000E-02	0.2000E-02	0.2000E-02	0.8000E-02	0.8000E-02	0.8000E-02	0.4899E 01	0.2500E 03	-0.1250E 06
0.3000E-02	0.3000E-02	0.3000E-02	0.1200E-01	0.1200E-01	0.1200E-01	0.5101E 01	0.1667E 03	-0.5555E 05
0.4000E-02	0.4000E-02	0.4000E-02	0.1600E-01	0.1600E-01	0.1600E-01	0.5245E 01	0.1250E 03	-0.3125E 05
0.5000E-02	0.5000E-02	0.5000E-02	0.2000E-01	0.2000E-01	0.2000E-01	0.5356E 01	0.1000E 03	-0.2000E 05
0.6000E-02	0.6000E-02	0.6000E-02	0.2400E-01	0.2400E-01	0.2400E-01	0.5447E 01	0.8333E 02	-0.1389E 05
0.8000E-02	0.8000E-02	0.8000E-02	0.3200E-01	0.3200E-01	0.3200E-01	0.5591E 01	0.6250E 02	-0.7812E 04
0.1000E-01	0.1000E-01	0.1000E-01	0.4000E-01	0.4000E-01	0.4000E-01	0.5703E 01	0.5000E 02	-0.5000E 04
0.1500E-01	0.1500E-01	0.1500E-01	0.6000E-01	0.6000E-01	0.6000E-01	0.5906E 01	0.3333E 02	-0.2222E 04
0.2000E-01	0.2000E-01	0.2000E-01	0.8000E-01	0.8000E-01	0.8000E-01	0.6049E 01	0.2500E 02	-0.1250E 04
0.3000E-01	0.3000E-01	0.3000E-01	0.1200E 00	0.1200E 00	0.1200E 00	0.6252E 01	0.1668E 02	-0.5516E 03
0.4000E-01	0.4000E-01	0.4000E-01	0.1600E 00	0.1600E 00	0.1600E 00	0.6397E 01	0.1260E 02	-0.2998E 03
0.5000E-01	0.5000E-01	0.5000E-01	0.2000E 00	0.2000E 00	0.2000E 00	0.6510E 01	0.1027E 02	-0.1781E 03
0.6000E-01	0.6000E-01	0.6000E-01	0.2400E 00	0.2400E 00	0.2400E 00	0.6605E 01	0.8858E 01	-0.1106E 03
0.8000E-01	0.8000E-01	0.8000E-01	0.3200E 00	0.3200E 00	0.3200E 00	0.6765E 01	0.7397E 01	-0.4577E 02
0.1000E 00	0.1000E 00	0.1000E 00	0.4000E 00	0.4000E 00	0.4000E 00	0.6906E 01	0.6778E 01	-0.1989E 02
0.1500E 00	0.1500E 00	0.1500E 00	0.6000E 00	0.6000E 00	0.6000E 00	0.7231E 01	0.6351E 01	-0.2674E 01
0.2000E 00	0.2000E 00	0.2000E 00	0.8000E 00	0.8000E 00	0.8000E 00	0.7547E 01	0.6293E 01	-0.3719E 00
0.3000E 00	0.3000E 00	0.3000E 00	0.1200E 01	0.1200E 01	0.1200E 01	0.8175E 01	0.6283E 01	-0.4919E-01
0.4000E 00	0.4000E 00	0.4000E 00	0.1600E 01	0.1600E 01	0.1600E 01	0.8804E 01	0.6283E 01	0.0
0.5000E 00	0.5000E 00	0.5000E 00	0.2000E 01	0.2000E 01	0.2000E 01	0.9432E 01	0.6283E 01	0.0
0.6000E 00	0.6000E 00	0.6000E 00	0.2400E 01	0.2400E 01	0.2400E 01	0.1006E 02	0.6283E 01	0.0
0.8000E 00	0.8000E 00	0.8000E 00	0.3200E 01	0.3200E 01	0.3200E 01	0.1132E 02	0.6283E 01	0.0
0.1000E 01	0.1000E 01	0.1000E 01	0.4000E 01	0.4000E 01	0.4000E 01	0.1257E 02	0.6283E 01	0.0
0.1500E 01	0.1500E 01	0.1500E 01	0.6000E 01	0.6000E 01	0.6000E 01	0.1572E 02	0.6283E 01	0.0
0.2000E 01	0.2000E 01	0.2000E 01	0.8000E 01	0.8000E 01	0.8000E 01	0.1886E 02	0.6283E 01	0.0
0.3000E 01	0.3000E 01	0.3000E 01	0.1200E 02	0.1200E 02	0.1200E 02	0.2514E 02	0.6283E 01	0.0
0.4000E 01	0.4000E 01	0.4000E 01	0.1600E 02	0.1600E 02	0.1600E 02	0.3142E 02	0.6283E 01	0.0
0.5000E 01	0.5000E 01	0.5000E 01	0.2000E 02	0.2000E 02	0.2000E 02	0.3771E 02	0.6283E 01	0.0
0.6000E 01	0.6000E 01	0.6000E 01	0.2400E 02	0.2400E 02	0.2400E 02	0.4399E 02	0.6283E 01	0.0
0.8000E 01	0.8000E 01	0.8000E 01	0.3200E 02	0.3200E 02	0.3200E 02	0.5656E 02	0.6283E 01	0.0
0.1000E 02	0.1000E 02	0.1000E 02	0.4000E 02	0.4000E 02	0.4000E 02	0.6912E 02	0.6283E 01	0.0

TABLE 18: p_{Dw}, p'_{Dw} and p''_{Dw} as Functions of Dimensionless Drawdown Times for a Well Located Inside a Closed 2:1 Rectangle

WELL LOCATION, (XD,YD) = (0.0625000, 0.0156250)

TDA	TDDX	TDDY	TDBX	TDBY	TDBB	PD	PDP	PDPP
0.1000E-04	0.5000E-05	0.2000E-04	0.5120E-02	0.3277E 00	0.4096E-01	0.2258E 01	0.5205E 05	-0.4453E 10
0.1500E-04	0.7500E-05	0.3000E-04	0.7680E-02	0.4915E 00	0.6144E-01	0.2477E 01	0.3755E 05	-0.1903E 10
0.2000E-04	0.1000E-04	0.4000E-04	0.1024E-01	0.6554E 00	0.8192E-01	0.2645E 01	0.3036E 05	-0.1099E 10
0.3000E-04	0.1500E-04	0.6000E-04	0.1536E-01	0.9830E 00	0.1229E 00	0.2906E 01	0.2266E 05	-0.5498E 09
0.4000E-04	0.2000E-04	0.8000E-04	0.2048E-01	0.1311E 01	0.1638E 00	0.3109E 01	0.1831E 05	-0.3461E 09
0.5000E-04	0.2500E-04	0.1000E-03	0.2560E-01	0.1638E 01	0.2048E 00	0.3277E 01	0.1542E 05	-0.2418E 09
0.6000E-04	0.3000E-04	0.1200E-03	0.3072E-01	0.1966E 01	0.2458E 00	0.3420E 01	0.1334E 05	-0.1796E 09
0.8000E-04	0.4000E-04	0.1600E-03	0.4096E-01	0.2621E 01	0.3277E 00	0.3656E 01	0.1051E 05	-0.1110E 09
0.1000E-03	0.5000E-04	0.2000E-03	0.5120E-01	0.3277E 01	0.4096E 00	0.3847E 01	0.8682E 04	-0.7554E 08
0.1500E-03	0.7500E-04	0.3000E-03	0.7680E-01	0.4915E 01	0.6144E 00	0.4208E 01	0.6052E 04	-0.3665E 08
0.2000E-03	0.1000E-03	0.4000E-03	0.1024E 00	0.6554E 01	0.8192E 00	0.4472E 01	0.4646E 04	-0.2157E 08
0.3000E-03	0.1500E-03	0.6000E-03	0.1536E 00	0.9830E 01	0.1229E 01	0.4854E 01	0.3177E 04	-0.9974E 07
0.4000E-03	0.2000E-03	0.8000E-03	0.2048E 00	0.1311E 02	0.1638E 01	0.5130E 01	0.2426E 04	-0.5620E 07
0.5000E-03	0.2500E-03	0.1000E-02	0.2560E 00	0.1638E 02	0.2048E 01	0.5349E 01	0.1980E 04	-0.3537E 07
0.6000E-03	0.3000E-03	0.1200E-02	0.3072E 00	0.1966E 02	0.2458E 01	0.5531E 01	0.1688E 04	-0.2403E 07
0.8000E-03	0.4000E-03	0.1600E-02	0.4096E 00	0.2621E 02	0.3277E 01	0.5830E 01	0.1333E 04	-0.1310E 07
0.1000E-02	0.5000E-03	0.2000E-02	0.5120E 00	0.3277E 02	0.4096E 01	0.6074E 01	0.1125E 04	-0.8349E 06
0.1500E-02	0.7500E-03	0.3000E-02	0.7680E 00	0.4915E 02	0.6144E 01	0.6556E 01	0.8394E 03	-0.3982E 06
0.2000E-02	0.1000E-02	0.4000E-02	0.1024E 01	0.6554E 02	0.8192E 01	0.6934E 01	0.6831E 03	-0.2477E 06
0.3000E-02	0.1500E-02	0.6000E-02	0.1536E 01	0.9830E 02	0.1229E 02	0.7518E 01	0.5046E 03	-0.1298E 06
0.4000E-02	0.2000E-02	0.8000E-02	0.2048E 01	0.1311E 03	0.1638E 02	0.7967E 01	0.4019E 03	-0.8143E 05
0.5000E-02	0.2500E-02	0.1000E-01	0.2560E 01	0.1638E 03	0.2048E 02	0.8333E 01	0.3343E 03	-0.5612E 05
0.6000E-02	0.3000E-02	0.1200E-01	0.3072E 01	0.1966E 03	0.2458E 02	0.8642E 01	0.2863E 03	-0.4108E 05
0.8000E-02	0.4000E-02	0.1600E-01	0.4096E 01	0.2621E 03	0.3277E 02	0.9146E 01	0.2225E 03	-0.2478E 05
0.1000E-01	0.5000E-02	0.2000E-01	0.5120E 01	0.3277E 03	0.4096E 02	0.9548E 01	0.1820E 03	-0.1657E 05
0.1500E-01	0.7500E-02	0.3000E-01	0.7680E 01	0.4915E 03	0.6144E 02	0.1030E 02	0.1251E 03	-0.7822E 04
0.2000E-01	0.1000E-01	0.4000E-01	0.1024E 02	0.6554E 03	0.8192E 02	0.1084E 02	0.9528E 02	-0.4539E 04
0.3000E-01	0.1500E-01	0.6000E-01	0.1536E 02	0.9830E 03	0.1229E 03	0.1162E 02	0.6453E 02	-0.2082E 04
0.4000E-01	0.2000E-01	0.8000E-01	0.2048E 02	0.1311E 04	0.1638E 03	0.1218E 02	0.4879E 02	-0.1190E 04
0.5000E-01	0.2500E-01	0.1000E 00	0.2560E 02	0.1638E 04	0.2048E 03	0.1262E 02	0.3923E 02	-0.7685E 03
0.6000E-01	0.3000E-01	0.1200E 00	0.3072E 02	0.1966E 04	0.2458E 03	0.1297E 02	0.3281E 02	-0.5357E 03
0.8000E-01	0.4000E-01	0.1600E 00	0.4096E 02	0.2621E 04	0.3277E 03	0.1354E 02	0.2479E 02	-0.2986E 03
0.1000E 00	0.5000E-01	0.2000E 00	0.5120E 02	0.3277E 04	0.4096E 03	0.1399E 02	0.2007E 02	-0.1854E 03
0.1500E 00	0.7500E-01	0.3000E 00	0.7680E 02	0.4915E 04	0.6144E 03	0.1482E 02	0.1419E 02	-0.7297E 02
0.2000E 00	0.1000E 00	0.4000E 00	0.1024E 03	0.6554E 04	0.8192E 03	0.1546E 02	0.1159E 02	-0.3713E 02
0.3000E 00	0.1500E 00	0.6000E 00	0.1536E 03	0.9830E 04	0.1229E 04	0.1648E 02	0.9196E 01	-0.1571E 02
0.4000E 00	0.2000E 00	0.8000E 00	0.2048E 03	0.1311E 05	0.1638E 04	0.1734E 02	0.8022E 01	-0.8899E 01
0.5000E 00	0.2500E 00	0.1000E 01	0.2560E 03	0.1638E 05	0.2048E 04	0.1810E 02	0.7340E 01	-0.5486E 01
0.6000E 00	0.3000E 00	0.1200E 01	0.3072E 03	0.1966E 05	0.2458E 04	0.1881E 02	0.6928E 01	-0.3486E 01
0.8000E 00	0.4000E 00	0.1600E 01	0.4096E 03	0.2621E 05	0.3277E 04	0.2015E 02	0.6523E 01	-0.1476E 01
0.1000E 01	0.5000E 00	0.2000E 01	0.5120E 03	0.3277E 05	0.4096E 04	0.2144E 02	0.6373E 01	-0.6395E 00
0.1500E 01	0.7500E 00	0.3000E 01	0.7680E 03	0.4915E 05	0.6144E 04	0.2460E 02	0.6291E 01	0.2051E-01
0.2000E 01	0.1000E 01	0.4000E 01	0.1024E 04	0.6554E 05	0.8192E 04	0.2774E 02	0.6284E 01	0.2622E 00
0.3000E 01	0.1500E 01	0.6000E 01	0.1536E 04	0.9830E 05	0.1229E 05	0.3402E 02	0.6283E 01	0.0
0.4000E 01	0.2000E 01	0.8000E 01	0.2048E 04	0.1311E 06	0.1638E 05	0.4031E 02	0.6283E 01	0.0
0.5000E 01	0.2500E 01	0.1000E 02	0.2560E 04	0.1638E 06	0.2048E 05	0.4659E 02	0.6283E 01	0.0
0.6000E 01	0.3000E 01	0.1200E 02	0.3072E 04	0.1966E 06	0.2458E 05	0.5287E 02	0.6283E 01	0.0
0.8000E 01	0.4000E 01	0.1600E 02	0.4096E 04	0.2621E 06	0.3277E 05	0.6544E 02	0.6283E 01	0.0
0.1000E 02	0.5000E 01	0.2000E 02	0.5120E 04	0.3277E 06	0.4096E 05	0.7801E 02	0.6283E 01	0.0

TABLE 19: p_{Dw}, p'_{Dw} and p''_{Dw} as Functions of Dimensionless Drawdown Times for a Well Located Inside a Closed 4:1 Rectangle

WELL LOCATION, (XD,YD) = (0.0312500, 0.1250000)

TDA	TDDX	TDDY	TDBX	TDBY	TDBB	PD	PDP	PDPP
0.1000E-04	0.2500E-05	0.4000E-04	0.1024E-01	0.1024E-01	0.1024E-01	0.2252E 01	0.4969E 05	-0.4938E 10
0.1500E-04	0.3750E-05	0.6000E-04	0.1536E-01	0.1536E-01	0.1536E-01	0.2454E 01	0.3319E 05	-0.2204E 10
0.2000E-04	0.5000E-05	0.8000E-04	0.2048E-01	0.2048E-01	0.2048E-01	0.2597E 01	0.2492E 05	-0.1242E 10
0.3000E-04	0.7500E-05	0.1200E-03	0.3072E-01	0.3072E-01	0.3072E-01	0.2799E 01	0.1663E 05	-0.5532E 09
0.4000E-04	0.1000E-04	0.1600E-03	0.4096E-01	0.4096E-01	0.4096E-01	0.2943E 01	0.1248E 05	-0.3115E 09
0.5000E-04	0.1250E-04	0.2000E-03	0.5120E-01	0.5120E-01	0.5120E-01	0.3054E 01	0.9988E 04	-0.1995E 09
0.6000E-04	0.1500E-04	0.2400E-03	0.6144E-01	0.6144E-01	0.6144E-01	0.3145E 01	0.8325E 04	-0.1386E 09
0.8000E-04	0.2000E-04	0.3200E-03	0.8192E-01	0.8192E-01	0.8192E-01	0.3289E 01	0.6245E 04	-0.7799E 08
0.1000E-03	0.2500E-04	0.4000E-03	0.1024E 00	0.1024E 00	0.1024E 00	0.3401E 01	0.4997E 04	-0.4989E 08
0.1500E-03	0.3750E-04	0.6000E-03	0.1536E 00	0.1536E 00	0.1536E 00	0.3603E 01	0.3342E 04	-0.2184E 08
0.2000E-03	0.5000E-04	0.8000E-03	0.2048E 00	0.2048E 00	0.2048E 00	0.3748E 01	0.2537E 04	-0.1175E 08
0.3000E-03	0.7500E-04	0.1200E-02	0.3072E 00	0.3072E 00	0.3072E 00	0.3959E 01	0.1797E 04	-0.4541E 07
0.4000E-03	0.1000E-03	0.1600E-02	0.4096E 00	0.4096E 00	0.4096E 00	0.4121E 01	0.1477E 04	-0.2248E 07
0.5000E-03	0.1250E-03	0.2000E-02	0.5120E 00	0.5120E 00	0.5120E 00	0.4259E 01	0.1304E 04	-0.1342E 07
0.6000E-03	0.1500E-03	0.2400E-02	0.6144E 00	0.6144E 00	0.6144E 00	0.4384E 01	0.1193E 04	-0.9254E 06
0.8000E-03	0.2000E-03	0.3200E-02	0.8192E 00	0.8192E 00	0.8192E 00	0.4607E 01	0.1048E 04	-0.5814E 06
0.1000E-02	0.2500E-03	0.4000E-02	0.1024E 01	0.1024E 01	0.1024E 01	0.4806E 01	0.9475E 03	-0.4412E 06
0.1500E-02	0.3750E-03	0.6000E-02	0.1536E 01	0.1536E 01	0.1536E 01	0.5233E 01	0.7716E 03	-0.2848E 06
0.2000E-02	0.5000E-03	0.8000E-02	0.2048E 01	0.2048E 01	0.2048E 01	0.5587E 01	0.6510E 03	-0.2046E 06
0.3000E-02	0.7500E-03	0.1200E-01	0.3072E 01	0.3072E 01	0.3072E 01	0.6152E 01	0.4943E 03	-0.1198E 06
0.4000E-02	0.1000E-02	0.1600E-01	0.4096E 01	0.4096E 01	0.4096E 01	0.6595E 01	0.3976E 03	-0.7807E 05
0.5000E-02	0.1250E-02	0.2000E-01	0.5120E 01	0.5120E 01	0.5120E 01	0.6958E 01	0.3322E 03	-0.5472E 05
0.6000E-02	0.1500E-02	0.2400E-01	0.6144E 01	0.6144E 01	0.6144E 01	0.7265E 01	0.2851E 03	-0.4042E 05
0.8000E-02	0.2000E-02	0.3200E-01	0.8192E 01	0.8192E 01	0.8192E 01	0.7767E 01	0.2221E 03	-0.2458E 05
0.1000E-01	0.2500E-02	0.4000E-01	0.1024E 02	0.1024E 02	0.1024E 02	0.8168E 01	0.1818E 03	-0.1649E 05
0.1500E-01	0.3750E-02	0.6000E-01	0.1536E 02	0.1536E 02	0.1536E 02	0.8918E 01	0.1251E 03	-0.7812E 04
0.2000E-01	0.5000E-02	0.8000E-01	0.2048E 02	0.2048E 02	0.2048E 02	0.9462E 01	0.9529E 02	-0.4537E 04
0.3000E-01	0.7500E-02	0.1200E 00	0.3072E 02	0.3072E 02	0.3072E 02	0.1024E 02	0.6459E 02	-0.2074E 04
0.4000E-01	0.1000E-01	0.1600E 00	0.4096E 02	0.4096E 02	0.4096E 02	0.1080E 02	0.4902E 02	-0.1163E 04
0.5000E-01	0.1250E-01	0.2000E 00	0.5120E 02	0.5120E 02	0.5120E 02	0.1124E 02	0.3981E 02	-0.7249E 03
0.6000E-01	0.1500E-01	0.2400E 00	0.6144E 02	0.6144E 02	0.6144E 02	0.1161E 02	0.3388E 02	-0.4825E 03
0.8000E-01	0.2000E-01	0.3200E 00	0.8192E 02	0.8192E 02	0.8192E 02	0.1221E 02	0.2695E 02	-0.2468E 03
0.1000E 00	0.2500E-01	0.4000E 00	0.1024E 03	0.1024E 03	0.1024E 03	0.1271E 02	0.2314E 02	-0.1473E 03
0.1500E 00	0.3750E-01	0.6000E 00	0.1536E 03	0.1536E 03	0.1536E 03	0.1373E 02	0.1834E 02	-0.6445E 02
0.2000E 00	0.5000E-01	0.8000E 00	0.2048E 03	0.2048E 03	0.2048E 03	0.1458E 02	0.1583E 02	-0.3982E 02
0.3000E 00	0.7500E-01	0.1200E 01	0.3072E 03	0.3072E 03	0.3072E 03	0.1600E 02	0.1292E 02	-0.2147E 02
0.4000E 00	0.1000E 00	0.1600E 01	0.4096E 03	0.4096E 03	0.4096E 03	0.1720E 02	0.1120E 02	-0.1394E 02
0.5000E 00	0.1250E 00	0.2000E 01	0.5120E 03	0.5120E 03	0.5120E 03	0.1826E 02	0.1002E 02	-0.9911E 01
0.6000E 00	0.1500E 00	0.2400E 01	0.6144E 03	0.6144E 03	0.6144E 03	0.1921E 02	0.9169E 01	-0.7406E 01
0.8000E 00	0.2000E 00	0.3200E 01	0.8192E 03	0.8192E 03	0.8192E 03	0.2092E 02	0.8029E 01	-0.4437E 01
0.1000E 01	0.2500E 00	0.4000E 01	0.1024E 04	0.1024E 04	0.1024E 04	0.2246E 02	0.7347E 01	-0.2763E 01
0.1500E 01	0.3750E 00	0.6000E 01	0.1536E 04	0.1536E 04	0.1536E 04	0.2590E 02	0.6593E 01	-0.8543E 00
0.2000E 01	0.5000E 00	0.8000E 01	0.2048E 04	0.2048E 04	0.2048E 04	0.2913E 02	0.6373E 01	-0.1762E 00
0.3000E 01	0.7500E 00	0.1200E 02	0.3072E 04	0.3072E 04	0.3072E 04	0.3545E 02	0.6291E 01	0.2878E 00
0.4000E 01	0.1000E 01	0.1600E 02	0.4096E 04	0.4096E 04	0.4096E 04	0.4174E 02	0.6284E 01	0.5152E 00
0.5000E 01	0.1250E 01	0.2000E 02	0.5120E 04	0.5120E 04	0.5120E 04	0.4802E 02	0.6283E 01	0.7123E 00
0.6000E 01	0.1500E 01	0.2400E 02	0.6144E 04	0.6144E 04	0.6144E 04	0.5430E 02	0.6283E 01	0.0
0.8000E 01	0.2000E 01	0.3200E 02	0.8192E 04	0.8192E 04	0.8192E 04	0.6687E 02	0.6283E 01	0.0
0.1000E 02	0.2500E 01	0.4000E 02	0.1024E 05	0.1024E 05	0.1024E 05	0.7944E 02	0.6283E 01	0.0

TABLE 20: p_{Dw}, p'_{Dw} and p''_{Dw} as Functions of Dimensionless Drawdown Times for a Well Located Inside a Closed 8:1 Rectangle

WELL LOCATION, (XD,YD) = (0.0156250, 1.0000000)

TDA	TDDX	TDDY	TDBX	TDBY	TDBB	PD	PDP	PDPP
0.1000E-04	0.1250E-05	0.8000E-04	0.2048E-01	0.3200E-03	0.2560E-02	0.2252E 01	0.4969E 05	-0.4938E 10
0.1500E-04	0.1875E-05	0.1200E-03	0.3072E-01	0.4800E-03	0.3840E-02	0.2454E 01	0.3319E 05	-0.2204E 10
0.2000E-04	0.2500E-05	0.1600E-03	0.4096E-01	0.6400E-03	0.5120E-02	0.2597E 01	0.2492E 05	-0.1242E 10
0.3000E-04	0.3750E-05	0.2400E-03	0.6144E-01	0.9600E-03	0.7680E-02	0.2799E 01	0.1663E 05	-0.5532E 09
0.4000E-04	0.5000E-05	0.3200E-03	0.8192E-01	0.1280E-02	0.1024E-01	0.2943E 01	0.1248E 05	-0.3115E 09
0.5000E-04	0.6250E-05	0.4000E-03	0.1024E 00	0.1600E-02	0.1280E-01	0.3054E 01	0.9988E 04	-0.1994E 09
0.6000E-04	0.7500E-05	0.4800E-03	0.1229E 00	0.1920E-02	0.1536E-01	0.3145E 01	0.8327E 04	-0.1383E 09
0.8000E-04	0.1000E-04	0.6400E-03	0.1638E 00	0.2560E-02	0.2048E-01	0.3289E 01	0.6259E 04	-0.7711E 08
0.1000E-03	0.1250E-04	0.8000E-03	0.2048E 00	0.3200E-02	0.2560E-01	0.3401E 01	0.5035E 04	-0.4847E 08
0.1500E-03	0.1875E-04	0.1200E-02	0.3072E 00	0.4800E-02	0.3840E-01	0.3608E 01	0.3461E 04	-0.2027E 08
0.2000E-03	0.2500E-04	0.1600E-02	0.4096E 00	0.6400E-02	0.5120E-01	0.3760E 01	0.2717E 04	-0.1092E 08
0.3000E-03	0.3750E-04	0.2400E-02	0.6144E 00	0.9600E-02	0.7680E-01	0.3991E 01	0.1994E 04	-0.4868E 07
0.4000E-03	0.5000E-04	0.3200E-02	0.8192E 00	0.1280E-01	0.1024E 00	0.4170E 01	0.1619E 04	-0.2921E 07
0.5000E-03	0.6250E-04	0.4000E-02	0.1024E 01	0.1600E-01	0.1280E 00	0.4319E 01	0.1376E 04	-0.2017E 07
0.6000E-03	0.7500E-04	0.4800E-02	0.1229E 01	0.1920E-01	0.1536E 00	0.4448E 01	0.1203E 04	-0.1503E 07
0.8000E-03	0.1000E-03	0.6400E-02	0.1638E 01	0.2560E-01	0.2048E 00	0.4663E 01	0.9644E 03	-0.9465E 06
0.1000E-02	0.1250E-03	0.8000E-02	0.2048E 01	0.3200E-01	0.2560E 00	0.4839E 01	0.8068E 03	-0.6570E 06
0.1500E-02	0.1875E-03	0.1200E-01	0.3072E 01	0.4800E-01	0.3840E 00	0.5177E 01	0.5740E 03	-0.3304E 06
0.2000E-02	0.2500E-03	0.1600E-01	0.4096E 01	0.6400E-01	0.5120E 00	0.5430E 01	0.4458E 03	-0.1990E 06
0.3000E-02	0.3750E-03	0.2400E-01	0.6144E 01	0.9600E-01	0.7680E 00	0.5798E 01	0.3083E 03	-0.9502E 05
0.4000E-02	0.5000E-03	0.3200E-01	0.8192E 01	0.1280E 00	0.1024E 01	0.6067E 01	0.2358E 03	-0.5520E 05
0.5000E-02	0.6250E-03	0.4000E-01	0.1024E 02	0.1600E 00	0.1280E 01	0.6279E 01	0.1914E 03	-0.3559E 05
0.6000E-02	0.7500E-03	0.4800E-01	0.1229E 02	0.1920E 00	0.1536E 01	0.6455E 01	0.1619E 03	-0.2441E 05
0.8000E-02	0.1000E-02	0.6400E-01	0.1638E 02	0.2560E 00	0.2048E 01	0.6739E 01	0.1262E 03	-0.1292E 05
0.1000E-01	0.1250E-02	0.8000E-01	0.2048E 02	0.3200E 00	0.2560E 01	0.6970E 01	0.1062E 03	-0.7685E 04
0.1500E-01	0.1875E-02	0.1200E 00	0.3072E 02	0.4800E 00	0.3840E 01	0.7431E 01	0.8197E 02	-0.3091E 04
0.2000E-01	0.2500E-02	0.1600E 00	0.4096E 02	0.6400E 00	0.5120E 01	0.7809E 01	0.7030E 02	-0.1795E 04
0.3000E-01	0.3750E-02	0.2400E 00	0.6144E 02	0.9600E 00	0.7680E 01	0.8441E 01	0.5743E 02	-0.9445E 03
0.4000E-01	0.5000E-02	0.3200E 00	0.8192E 02	0.1280E 01	0.1024E 02	0.8974E 01	0.4983E 02	-0.6154E 03
0.5000E-01	0.6250E-02	0.4000E 00	0.1024E 03	0.1600E 01	0.1280E 02	0.9445E 01	0.4462E 02	-0.4419E 03
0.6000E-01	0.7500E-02	0.4800E 00	0.1229E 03	0.1920E 01	0.1536E 02	0.9871E 01	0.4077E 02	-0.3370E 03
0.8000E-01	0.1000E-01	0.6400E 00	0.1638E 03	0.2560E 01	0.2048E 02	0.1063E 02	0.3534E 02	-0.2195E 03
0.1000E 00	0.1250E-01	0.8000E 00	0.2048E 03	0.3200E 01	0.2560E 02	0.1130E 02	0.3163E 02	-0.1574E 03
0.1500E 00	0.1875E-01	0.1200E 01	0.3072E 03	0.4800E 01	0.3840E 02	0.1272E 02	0.2585E 02	-0.8587E 02
0.2000E 00	0.2500E-01	0.1600E 01	0.4096E 03	0.6400E 01	0.5120E 02	0.1392E 02	0.2239E 02	-0.5585E 02
0.3000E 00	0.3750E-01	0.2400E 01	0.6144E 03	0.9600E 01	0.7680E 02	0.1593E 02	0.1829E 02	-0.3044E 02
0.4000E 00	0.5000E-01	0.3200E 01	0.8192E 03	0.1280E 02	0.1024E 03	0.1763E 02	0.1584E 02	-0.1978E 02
0.5000E 00	0.6250E-01	0.4000E 01	0.1024E 04	0.1600E 02	0.1280E 03	0.1913E 02	0.1417E 02	-0.1416E 02
0.6000E 00	0.7500E-01	0.4800E 01	0.1229E 04	0.1920E 02	0.1536E 03	0.2048E 02	0.1294E 02	-0.1077E 02
0.8000E 00	0.1000E 00	0.6400E 01	0.1638E 04	0.2560E 02	0.2048E 03	0.2288E 02	0.1121E 02	-0.6990E 01
0.1000E 01	0.1250E 00	0.8000E 01	0.2048E 04	0.3200E 02	0.2560E 03	0.2500E 02	0.1003E 02	-0.4968E 01
0.1500E 01	0.1875E 00	0.1200E 02	0.3072E 04	0.4800E 02	0.3840E 03	0.2952E 02	0.8264E 01	-0.2511E 01
0.2000E 01	0.2500E 00	0.1600E 02	0.4096E 04	0.6400E 02	0.5120E 03	0.3340E 02	0.7349E 01	-0.1363E 01
0.3000E 01	0.3750E 00	0.2400E 02	0.6144E 04	0.9600E 02	0.7680E 03	0.4030E 02	0.6593E 01	-0.3372E 00
0.4000E 01	0.5000E 00	0.3200E 02	0.8192E 04	0.1280E 03	0.1024E 04	0.4676E 02	0.6283E 01	0.0
0.5000E 01	0.6250E 00	0.4000E 02	0.1024E 05	0.1600E 03	0.1280E 04	0.5309E 02	0.6283E 01	0.0
0.6000E 01	0.7500E 00	0.4800E 02	0.1229E 05	0.1920E 03	0.1536E 04	0.5939E 02	0.6283E 01	0.0
0.8000E 01	0.1000E 01	0.6400E 02	0.1638E 05	0.2560E 03	0.2048E 04	0.7196E 02	0.6283E 01	0.0
0.1000E 02	0.1250E 01	0.8000E 02	0.2048E 05	0.3200E 03	0.2560E 04	0.8453E 02	0.6283E 01	0.0

TABLE 21: p_{Dw}, p'_{Dw} and p''_{Dw} as Functions of Dimensionless Drawdown Times for a Well Located Inside a Closed 16:1 Rectangle

WELL LOCATION, (XD,YC) = (0.0078125, 0.1250000)

TDA	TDDX	TDDY	TDBX	TDBY	TDBB	PD	PDP	PDPP
0.1000E-04	0.6250E-06	0.1600E-03	0.4096E-01	0.4096E-01	0.4096E-01	0.2252E 01	0.4969E 05	-0.4938E 10
0.1500E-04	0.9375E-06	0.2400E-03	0.6144E-01	0.6144E-01	0.6144E-01	0.2454E 01	0.3319E 05	-0.2204E 10
0.2000E-04	0.1250E-05	0.3200E-03	0.8192E-01	0.8192E-01	0.8192E-01	0.2597E 01	0.2492E 05	-0.1242E 10
0.3000E-04	0.1875E-05	0.4800E-03	0.1229E 00	0.1229E 00	0.1229E 00	0.2799E 01	0.1664E 05	-0.5509E 09
0.4000E-04	0.2500E-05	0.6400E-03	0.1638E 00	0.1638E 00	0.1638E 00	0.2943E 01	0.1254E 05	-0.3044E 09
0.5000E-04	0.3125E-05	0.8000E-03	0.2048E 00	0.2048E 00	0.2048E 00	0.3056E 01	0.1014E 05	-0.1876E 09
0.6000E-04	0.3750E-05	0.9600E-03	0.2458E 00	0.2458E 00	0.2458E 00	0.3149E 01	0.8612E 04	-0.1237E 09
0.8000E-04	0.5000E-05	0.1280E-02	0.3277E 00	0.3277E 00	0.3277E 00	0.3301E 01	0.6850E 04	-0.6196E 08
0.1000E-03	0.6250E-05	0.1600E-02	0.4096E 00	0.4096E 00	0.4096E 00	0.3428E 01	0.5905E 04	-0.3592E 08
0.1500E-03	0.9375E-05	0.2400E-02	0.6144E 00	0.6144E 00	0.6144E 00	0.3691E 01	0.4770E 04	-0.1479E 08
0.2000E-03	0.1250E-04	0.3200E-02	0.8192E 00	0.8192E 00	0.8192E 00	0.3914E 01	0.4192E 04	-0.9256E 07
0.3000E-03	0.1875E-04	0.4800E-02	0.1229E 01	0.1229E 01	0.1229E 01	0.4294E 01	0.3471E 04	-0.5785E 07
0.4000E-03	0.2500E-04	0.6400E-02	0.1638E 01	0.1638E 01	0.1638E 01	0.4615E 01	0.2976E 04	-0.4243E 07
0.5000E-03	0.3125E-04	0.8000E-02	0.2048E 01	0.2048E 01	0.2048E 01	0.4893E 01	0.2604E 04	-0.3273E 07
0.6000E-03	0.3750E-04	0.9600E-02	0.2458E 01	0.2458E 01	0.2458E 01	0.5139E 01	0.2312E 04	-0.2600E 07
0.8000E-03	0.5000E-04	0.1280E-01	0.3277E 01	0.3277E 01	0.3277E 01	0.5556E 01	0.1886E 04	-0.1747E 07
0.1000E-02	0.6250E-04	0.1600E-01	0.4096E 01	0.4096E 01	0.4096E 01	0.5902E 01	0.1590E 04	-0.1249E 07
0.1500E-02	0.9375E-04	0.2400E-01	0.6144E 01	0.6144E 01	0.6144E 01	0.6572E 01	0.1141E 04	-0.6467E 06
0.2000E-02	0.1250E-03	0.3200E-01	0.8192E 01	0.8192E 01	0.8192E 01	0.7074E 01	0.8884E 03	-0.3933E 06
0.3000E-02	0.1875E-03	0.4800E-01	0.1229E 02	0.1229E 02	0.1229E 02	0.7809E 01	0.6156E 03	-0.1892E 06
0.4000E-02	0.2500E-03	0.6400E-01	0.1638E 02	0.1638E 02	0.1638E 02	0.8346E 01	0.4708E 03	-0.1107E 06
0.5000E-02	0.3125E-03	0.8000E-01	0.2048E 02	0.2048E 02	0.2048E 02	0.8769E 01	0.3812E 03	-0.7259E 05
0.6000E-02	0.3750E-03	0.9600E-01	0.2458E 02	0.2458E 02	0.2458E 02	0.9118E 01	0.3202E 03	-0.5119E 05
0.8000E-02	0.5000E-03	0.1280E 00	0.3277E 02	0.3277E 02	0.3277E 02	0.9674E 01	0.2428E 03	-0.2921E 05
0.1000E-01	0.6250E-03	0.1600E 00	0.4096E 02	0.4096E 02	0.4096E 02	0.1011E 02	0.1961E 03	-0.1861E 05
0.1500E-01	0.9375E-03	0.2400E 00	0.6144E 02	0.6144E 02	0.6144E 02	0.1052E 02	0.1355E 03	-0.7720E 04
0.2000E-01	0.1250E-02	0.3200E 00	0.8192E 02	0.8192E 02	0.8192E 02	0.1152E 02	0.1078E 03	-0.3950E 04
0.3000E-01	0.1875E-02	0.4800E 00	0.1229E 03	0.1229E 03	0.1229E 03	0.1245E 02	0.8291E 02	-0.1588E 04
0.4000E-01	0.2500E-02	0.6400E 00	0.1638E 03	0.1638E 03	0.1638E 03	0.1322E 02	0.7093E 02	-0.9200E 03
0.5000E-01	0.3125E-02	0.8000E 00	0.2048E 03	0.2048E 03	0.2048E 03	0.1388E 02	0.6330E 02	-0.6371E 03
0.6000E-01	0.3750E-02	0.9600E 00	0.2458E 03	0.2458E 03	0.2458E 03	0.1449E 02	0.5778E 02	-0.4809E 03
0.8000E-01	0.5000E-02	0.1280E 01	0.3277E 03	0.3277E 03	0.3277E 03	0.1556E 02	0.5006E 02	-0.3119E 03
0.1000E 00	0.6250E-02	0.1600E 01	0.4096E 03	0.4096E 03	0.4096E 03	0.1651E 02	0.4479E 02	-0.2234E 03
0.1500E 00	0.9375E-02	0.2400E 01	0.6144E 03	0.6144E 03	0.6144E 03	0.1852E 02	0.3658E 02	-0.1217E 03
0.2000E 00	0.1250E-01	0.3200E 01	0.8192E 03	0.8192E 03	0.8192E 03	0.2022E 02	0.3169E 02	-0.7912E 02
0.3000E 00	0.1875E-01	0.4800E 01	0.1229E 04	0.1229E 04	0.1229E 04	0.2307E 02	0.2588E 02	-0.4309E 02
0.4000E 00	0.2500E-01	0.6400E 01	0.1638E 04	0.1638E 04	0.1638E 04	0.2547E 02	0.2241E 02	-0.2800E 02
0.5000E 00	0.3125E-01	0.8000E 01	0.2048E 04	0.2048E 04	0.2048E 04	0.2759E 02	0.2005E 02	-0.2004E 02
0.6000E 00	0.3750E-01	0.9600E 01	0.2458E 04	0.2458E 04	0.2458E 04	0.2950E 02	0.1830E 02	-0.1525E 02
0.8000E 00	0.5000E-01	0.1280E 02	0.3277E 04	0.3277E 04	0.3277E 04	0.3290E 02	0.1585E 02	-0.9904E 01
0.1000E 01	0.6250E-01	0.1600E 02	0.4096E 04	0.4096E 04	0.4096E 04	0.3589E 02	0.1418E 02	-0.7087E 01
0.1500E 01	0.9375E-01	0.2400E 02	0.6144E 04	0.6144E 04	0.6144E 04	0.4226E 02	0.1158E 02	-0.3855E 01
0.2000E 01	0.1250E 00	0.3200E 02	0.8192E 04	0.8192E 04	0.8192E 04	0.4764E 02	0.1003E 02	-0.2485E 01
0.3000E 01	0.1875E 00	0.4800E 02	0.1229E 05	0.1229E 05	0.1229E 05	0.5668E 02	0.8265E 01	-0.1248E 01
0.4000E 01	0.2500E 00	0.6400E 02	0.1638E 05	0.1638E 05	0.1638E 05	0.6444E 02	0.7349E 01	-0.6526E 00
0.5000E 01	0.3125E 00	0.8000E 02	0.2048E 05	0.2048E 05	0.2048E 05	0.7152E 02	0.6858E 01	-0.2997E 00
0.6000E 01	0.3750E 00	0.9600E 02	0.2458E 05	0.2458E 05	0.2458E 05	0.7824E 02	0.6593E 01	-0.7053E-01
0.8000E 01	0.5000E 00	0.1280E 03	0.3277E 05	0.3277E 05	0.3277E 05	0.9116E 02	0.6374E 01	0.2079E 00
0.1000E 02	0.6250E 00	0.1600E 03	0.4096E 05	0.4096E 05	0.4096E 05	0.1038E 03	0.6309E 01	0.3776E 00

TABLE 22: p_{Ds}, p'_{Ds} and p''_{Ds} as Functions of Dimensionless Build Up Times for a Well Located Inside a Closed 4:1 Rectangle

WELL LOCATION, (XD,YD) = (0.0156250, 0.5000000)
PRODUCING TIME BEFORE SHUT IN, TDA = 0.0010

DEL(T)	TRAT	TDRX	TDRY	TDRB	TDADX	PDS	PDSP	PDSS
0.1000E-04	0.1010E 03	0.4096E-01	0.6400E-03	0.5120E-02	0.3225E-03	0.2840E 01	-0.4880E 05	0.4937E 10
0.2000E-04	0.5100E 02	0.8192E-01	0.1280E-02	0.1024E-01	0.6450E-03	0.2504E 01	-0.2405E 05	0.1241E 10
0.3000E-04	0.3433E 02	0.1229E 00	0.1920E-02	0.1536E-01	0.9676E-03	0.2310E 01	-0.1577E 05	0.5513E 09
0.4000E-04	0.2600E 02	0.1638E 00	0.2560E-02	0.2048E-01	0.1290E-02	0.2175E 01	-0.1165E 05	0.3072E 09
0.5000E-04	0.2100E 02	0.2048E 00	0.3200E-02	0.2560E-01	0.1613E-02	0.2072E 01	-0.9210E 04	0.1929E 09
0.6000E-04	0.1767E 02	0.2458E 00	0.3840E-02	0.3072E-01	0.1935E-02	0.1988E 01	-0.7621E 04	0.1306E 09
0.8000E-04	0.1350E 02	0.3277E 00	0.5120E-02	0.4096E-01	0.2580E-02	0.1857E 01	-0.5708E 04	0.6973E 08
0.1000E-03	0.1100E 02	0.4096E 00	0.6400E-02	0.5120E-01	0.3225E-02	0.1754E 01	-0.4613E 04	0.4299E 08
0.2000E-03	0.6000E 01	0.8192E 00	0.1280E-01	0.1024E 00	0.6450E-02	0.1423E 01	-0.2480E 04	0.1111E 08
0.3000E-03	0.4333E 01	0.1229E 01	0.1920E-01	0.1536E 00	0.9676E-02	0.1219E 01	-0.1702E 04	0.5517E 07
0.4000E-03	0.3500E 01	0.1638E 01	0.2560E-01	0.2048E 00	0.1290E-01	0.1072E 01	-0.1272E 04	0.3353E 07
0.5000E-03	0.3000E 01	0.2048E 01	0.3200E-01	0.2560E 00	0.1613E-01	0.9595E 00	-0.9970E 03	0.2247E 07
0.6000E-03	0.2667E 01	0.2458E 01	0.3840E-01	0.3072E 00	0.1935E-01	0.8698E 00	-0.8072E 03	0.1600E 07
0.8000E-03	0.2250E 01	0.3277E 01	0.5120E-01	0.4096E 00	0.2580E-01	0.7348E 00	-0.5652E 03	0.9108E 06
0.1000E-02	0.2000E 01	0.4096E 01	0.6400E-01	0.5120E 00	0.3225E-01	0.6374E 00	-0.4202E 03	0.5745E 06
0.2000E-02	0.1500E 01	0.8192E 01	0.1280E 00	0.1024E 01	0.6450E-01	0.3869E 00	-0.1494E 03	0.1213E 06
0.3000E-02	0.1333E 01	0.1229E 02	0.1920E 00	0.1536E 01	0.9676E-01	0.2811E 00	-0.7458E 02	0.4485E 05
0.4000E-02	0.1250E 01	0.1638E 02	0.2560E 00	0.2048E 01	0.1290E 00	0.2239E 00	-0.4367E 02	0.2084E 05
0.5000E-02	0.1200E 01	0.2048E 02	0.3200E 00	0.2560E 01	0.1613E 00	0.1887E 00	-0.2839E 02	0.1102E 05
0.6000E-02	0.1167E 01	0.2458E 02	0.3840E 00	0.3072E 01	0.1935E 00	0.1649E 00	-0.1995E 02	0.6385E 04
0.8000E-02	0.1125E 01	0.3277E 02	0.5120E 00	0.4096E 01	0.2580E 00	0.1345E 00	-0.1164E 02	0.2637E 04
0.1000E-01	0.1100E 01	0.4096E 02	0.6400E 00	0.5120E 01	0.3225E 00	0.1155E 00	-0.7868E 01	0.1339E 04
0.2000E-01	0.1050E 01	0.8192E 02	0.1280E 01	0.1024E 02	0.6450E 00	0.7118E-01	-0.2594E 01	0.2050E 03
0.3000E-01	0.1033E 01	0.1229E 03	0.1920E 01	0.1536E 02	0.9676E 00	0.5257E-01	-0.1334E 01	0.7632E 02
0.4000E-01	0.1025E 01	0.1638E 03	0.2560E 01	0.2048E 02	0.1290E 01	0.4223E-01	-0.7985E 00	0.3703E 02
0.5000E-01	0.1020E 01	0.2048E 03	0.3200E 01	0.2560E 02	0.1613E 01	0.3576E-01	-0.5216E 00	0.2043E 02
0.6000E-01	0.1017E 01	0.2458E 03	0.3840E 01	0.3072E 02	0.1935E 01	0.3141E-01	-0.3628E 00	0.1222E 02
0.8000E-01	0.1012E 01	0.3277E 03	0.5120E 01	0.4096E 02	0.2580E 01	0.2599E-01	-0.2020E 00	0.5119E 01
0.1000E 00	0.1010E 01	0.4096E 03	0.6400E 01	0.5120E 02	0.3225E 01	0.2276E-01	-0.1297E 00	0.2506E 01
0.2000E 00	0.1005E 01	0.8192E 03	0.1280E 02	0.1024E 03	0.6450E 01	0.1583E-01	-0.3965E-01	0.3047E 00
0.3000E 00	0.1003E 01	0.1229E 04	0.1920E 02	0.1536E 03	0.9676E 01	0.1293E-01	-0.2150E-01	0.1074E 00
0.4000E 00	0.1002E 01	0.1638E 04	0.2560E 02	0.2048E 03	0.1290E 02	0.1120E-01	-0.1395E-01	0.5269E-01
0.5000E 00	0.1002E 01	0.2048E 04	0.3200E 02	0.2560E 03	0.1613E 02	0.1003E-01	-0.9809E-02	0.3088E-01
0.6000E 00	0.1002E 01	0.2458E 04	0.3840E 02	0.3072E 03	0.1935E 02	0.9171E-02	-0.7370E-02	0.2036E-01
0.8000E 00	0.1001E 01	0.3277E 04	0.5120E 02	0.4096E 03	0.2580E 02	0.8026E-02	-0.4344E-02	0.1079E-01
0.1000E 01	0.1001E 01	0.4096E 04	0.6400E 02	0.5120E 03	0.3225E 02	0.7339E-02	-0.2629E-02	0.6436E-02
0.2000E 01	0.1000E 01	0.8192E 04	0.1280E 03	0.1024E 04	0.6450E 02	0.6393E-02	-0.2222E-03	0.8479E-03
0.3000E 01	0.1000E 01	0.1229E 05	0.1920E 03	0.1536E 04	0.9676E 02	0.6283E-02	0.0	0.0
0.4000E 01	0.1000E 01	0.1638E 05	0.2560E 03	0.2048E 04	0.1290E 03	0.6283E-02	0.0	0.0
0.5000E 01	0.1000E 01	0.2048E 05	0.3200E 03	0.2560E 04	0.1613E 03	0.6283E-02	0.0	0.0
0.6000E 01	0.1000E 01	0.2458E 05	0.3840E 03	0.3072E 04	0.1935E 03	0.6283E-02	0.0	0.0
0.8000E 01	0.1000E 01	0.3277E 05	0.5120E 03	0.4096E 04	0.2580E 03	0.6283E-02	0.0	0.0
0.1000E 02	0.1000E 01	0.4096E 05	0.6400E 03	0.5120E 04	0.3225E 03	0.6283E-02	0.0	0.0

TABLE 23: p_{Ds}, p'_{Ds} and p''_{Ds} as Functions of Dimensionless Build Up Times for a Well Located Inside a Closed 4:1 Rectangle

WELL LOCATION, (XD,YD) = (0.0156250, 0.5000000)
PRODUCING TIME BEFORE SHUT IN, TDA = 0.0100

DEL(T)	TRAT	TDBX	TDBY	TDBR	TDABX	PDS	PDSP	PDSS
0.1000E-04	0.1001E 04	0.4096E-01	0.6400E-03	0.5120E-02	0.3225E-03	0.5121E 01	-0.4957E 05	0.4938E 10
0.2000E-04	0.5010E 03	0.8192E-01	0.1280E-02	0.1024E-01	0.6450E-03	0.4778E 01	-0.2480E 05	0.1242E 10
0.3000E-04	0.3343E 03	0.1229E 00	0.1920E-02	0.1536E-01	0.9676E-03	0.4577E 01	-0.1652E 05	0.5521E 09
0.4000E-04	0.2510E 03	0.1638E 00	0.2560E-02	0.2048E-01	0.1290E-02	0.4434E 01	-0.1239E 05	0.3080E 09
0.5000E-04	0.2010E 03	0.2048E 00	0.3200E-02	0.2560E-01	0.1613E-02	0.4323E 01	-0.9944E 04	0.1936E 09
0.6000E-04	0.1677E 03	0.2458E 00	0.3840E-02	0.3072E-01	0.1935E-02	0.4232E 01	-0.8348E 04	0.1313E 09
0.8000E-04	0.1260E 03	0.3277E 00	0.5120E-02	0.4096E-01	0.2580E-02	0.4087E 01	-0.6422E 04	0.7042E 08
0.1000E-03	0.1010E 03	0.4096E 00	0.6400E-02	0.5120E-01	0.3225E-02	0.3970E 01	-0.5313E 04	0.4366E 08
0.2000E-03	0.5100E 02	0.8192E 00	0.1280E-01	0.1024E 00	0.6450E-02	0.3572E 01	-0.3119E 04	0.1167E 08
0.3000E-03	0.3433E 02	0.1229E 01	0.1920E-01	0.1536E 00	0.9675E-02	0.3307E 01	-0.2288E 04	0.6004E 07
0.4000E-03	0.2600E 02	0.1638E 01	0.2560E-01	0.2048E 00	0.1290E-01	0.3103E 01	-0.1813E 04	0.3777E 07
0.5000E-03	0.2100E 02	0.2048E 01	0.3200E-01	0.2560E 00	0.1613E-01	0.2939E 01	-0.1498E 04	0.2620E 07
0.6000E-03	0.1767E 02	0.2458E 01	0.3840E-01	0.3072E 00	0.1935E-01	0.2801E 01	-0.1273E 04	0.1929E 07
0.8000E-03	0.1350E 02	0.3277E 01	0.5120E-01	0.4096E 00	0.2580E-01	0.2579E 01	-0.9725E 03	0.1174E 07
0.1000E-02	0.1100E 02	0.4096E 01	0.6400E-01	0.5120E 00	0.3225E-01	0.2405E 01	-0.7800E 03	0.7888E 06
0.2000E-02	0.6000E 01	0.8192E 01	0.1280E 00	0.1024E 01	0.6450E-01	0.1876E 01	-0.3665E 03	0.2152E 06
0.3000E-02	0.4333E 01	0.1229E 02	0.1920E 00	0.1536E 01	0.9676E-01	0.1591E 01	-0.2229E 03	0.9468E 05
0.4000E-02	0.3500E 01	0.1638E 02	0.2560E 00	0.2048E 01	0.1290E 00	0.1406E 01	-0.1535E 03	0.5047E 05
0.5000E-02	0.3000E 01	0.2048E 02	0.3200E 00	0.2560E 01	0.1613E 00	0.1274E 01	-0.1143E 03	0.3014E 05
0.6000E-02	0.2667E 01	0.2458E 02	0.3840E 00	0.3072E 01	0.1935E 00	0.1172E 01	-0.9003E 02	0.1954E 05
0.8000E-02	0.2250E 01	0.3277E 02	0.5120E 00	0.4096E 01	0.2580E 00	0.1023E 01	-0.6222E 02	0.9848E 04
0.1000E-01	0.2000E 01	0.4096E 02	0.6400E 00	0.5120E 01	0.3225E 00	0.9155E 00	-0.4701E 02	0.5872E 04
0.2000E-01	0.1500E 01	0.8192E 02	0.1280E 01	0.1024E 02	0.6450E 00	0.6179E 00	-0.1925E 02	0.1325E 04
0.3000E-01	0.1333E 01	0.1229E 03	0.1920E 01	0.1536E 02	0.9676E 00	0.4748E 00	-0.1061E 02	0.5557E 03
0.4000E-01	0.1250E 01	0.1638E 03	0.2560E 01	0.2048E 02	0.1290E 01	0.3909E 00	-0.6604E 01	0.2853E 03
0.5000E-01	0.1200E 01	0.2048E 03	0.3200E 01	0.2560E 02	0.1613E 01	0.3367E 00	-0.4434E 01	0.1630E 03
0.6000E-01	0.1167E 01	0.2458E 03	0.3840E 01	0.3072E 02	0.1935E 01	0.2993E 00	-0.3152E 01	0.9989E 02
0.8000E-01	0.1125E 01	0.3277E 03	0.5120E 01	0.4096E 02	0.2580E 01	0.2515E 00	-0.1815E 01	0.4338E 02
0.1000E 00	0.1100E 01	0.4096E 03	0.6400E 01	0.5120E 02	0.3225E 01	0.2221E 00	-0.1194E 01	0.2184E 02
0.2000E 00	0.1050E 01	0.8192E 03	0.1280E 02	0.1024E 03	0.6450E 01	0.1566E 00	-0.3834E 00	0.2874E 01
0.3000E 00	0.1033E 01	0.1229E 04	0.1920E 02	0.1536E 03	0.9676E 01	0.1283E 00	-0.2102E 00	0.1035E 01
0.4000E 00	0.1025E 01	0.1638E 04	0.2560E 02	0.2048E 03	0.1290E 02	0.1114E 00	-0.1372E 00	0.5128E 00
0.5000E 00	0.1020E 01	0.2048E 04	0.3200E 02	0.2560E 03	0.1613E 02	0.9981E-01	-0.9764E-01	0.3024E 00
0.6000E 00	0.1017E 01	0.2458E 04	0.3840E 02	0.3072E 03	0.1935E 02	0.9137E-01	-0.7280E-01	0.2002E 00
0.8000E 00	0.1012E 01	0.3277E 04	0.5120E 02	0.4096E 03	0.2580E 02	0.8011E-01	-0.4296E-01	0.1066E 00
0.1000E 01	0.1010E 01	0.4096E 04	0.6400E 02	0.5120E 03	0.3225E 02	0.7335E-01	-0.2602E-01	0.6370E-01
0.2000E 01	0.1005E 01	0.8192E 04	0.1280E 03	0.1024E 04	0.6450E 02	0.6374E-01	-0.2198E-02	0.8415E-02
0.3000E 01	0.1003E 01	0.1229E 05	0.1920E 03	0.1536E 04	0.9676E 02	0.6283E-01	0.0	0.0
0.4000E 01	0.1002E 01	0.1638E 05	0.2560E 03	0.2048E 04	0.1290E 03	0.6283E-01	0.0	0.0
0.5000E 01	0.1002E 01	0.2048E 05	0.3200E 03	0.2560E 04	0.1613E 03	0.6283E-01	0.0	0.0
0.6000E 01	0.1002E 01	0.2458E 05	0.3840E 03	0.3072E 04	0.1935E 03	0.6283E-01	0.0	0.0
0.8000E 01	0.1001E 01	0.3277E 05	0.5120E 03	0.4096E 04	0.2580E 03	0.6283E-01	0.0	0.0
0.1000E 02	0.1001E 01	0.4096E 05	0.6400E 03	0.5120E 04	0.3225E 03	0.6283E-01	0.0	0.0

TABLE 24: p_{Ds}, p'_{Ds} and p''_{Ds} as Functions of Dimensionless Build Up Times for a Well Located Inside a Closed 4:1 Rectangle

WELL LOCATION, (XD,YD) = (0.0156250, 0.5000000)
PRODUCING TIME BEFORE SHUT IN, TDA = 0.1000

DEL(T)	TRAT	TDBX	TDBY	TDBR	TDABX	PDS	PDSP	PDSS
0.1000E-04	0.1000E 05	0.4096E-01	0.6400E-03	0.5120E-02	0.3225E-03	0.8914E 01	-0.4967E 05	0.4938E 10
0.2000E-04	0.5001E 04	0.8192E-01	0.1280E-02	0.1024E-01	0.6450E-03	0.8569E 01	-0.2490E 05	0.1242E 10
0.3000E-04	0.3334E 04	0.1229E 00	0.1920E-02	0.1536E-01	0.9676E-03	0.8367E 01	-0.1661E 05	0.5521E 09
0.4000E-04	0.2501E 04	0.1638E 00	0.2560E-02	0.2048E-01	0.1290E-02	0.8224E 01	-0.1249E 05	0.3080E 09
0.5000E-04	0.2001E 04	0.2048E 00	0.3200E-02	0.2560E-01	0.1613E-02	0.8112E 01	-0.1004E 05	0.1936E 09
0.6000E-04	0.1668E 04	0.2458E 00	0.3840E-02	0.3072E-01	0.1935E-02	0.8020E 01	-0.8444E 04	0.1313E 09
0.8000E-04	0.1251E 04	0.3277E 00	0.5120E-02	0.4096E-01	0.2580E-02	0.7873E 01	-0.6518E 04	0.7042E 08
0.1000E-03	0.1001E 04	0.4096E 00	0.6400E-02	0.5120E-01	0.3225E-02	0.7754E 01	-0.5409E 04	0.4366E 08
0.2000E-03	0.5010E 03	0.8192E 00	0.1280E-01	0.1024E 00	0.6450E-02	0.7347E 01	-0.3214E 04	0.1168E 08
0.3000E-03	0.3343E 03	0.1229E 01	0.1920E-01	0.1536E 00	0.9676E-02	0.7072E 01	-0.2382E 04	0.6012E 07
0.4000E-03	0.2510E 03	0.1638E 01	0.2560E-01	0.2048E 00	0.1290E-01	0.6859E 01	-0.1906E 04	0.3785E 07
0.5000E-03	0.2010E 03	0.2048E 01	0.3200E-01	0.2560E 00	0.1613E-01	0.6685E 01	-0.1591E 04	0.2627E 07
0.6000E-03	0.1677E 03	0.2458E 01	0.3840E-01	0.3072E 00	0.1935E-01	0.6538E 01	-0.1365E 04	0.1937E 07
0.8000E-03	0.1260E 03	0.3277E 01	0.5120E-01	0.4096E 00	0.2580E-01	0.6298E 01	-0.1063E 04	0.1181E 07
0.1000E-02	0.1010E 03	0.4096E 01	0.6400E-01	0.5120E 00	0.3225E-01	0.6106E 01	-0.9690E 03	0.7959E 06
0.2000E-02	0.5100E 02	0.8192E 01	0.1280E 00	0.1024E 01	0.6450E-01	0.5491E 01	-0.4489E 03	0.2213E 06
0.3000E-02	0.3433E 02	0.1229E 02	0.1920E 00	0.1536E 01	0.9676E-01	0.5127E 01	-0.2996E 03	0.9999E 05
0.4000E-02	0.2600E 02	0.1638E 02	0.2560E 00	0.2048E 01	0.1290E 00	0.4866E 01	-0.2252E 03	0.5515E 05
0.5000E-02	0.2100E 02	0.2048E 02	0.3200E 00	0.2560E 01	0.1613E 00	0.4666E 01	-0.1816E 03	0.3431E 05
0.6000E-02	0.1767E 02	0.2458E 02	0.3840E 00	0.3072E 01	0.1935E 00	0.4500E 01	-0.1533E 03	0.2329E 05
0.8000E-02	0.1350E 02	0.3277E 02	0.5120E 00	0.4096E 01	0.2580E 00	0.4231E 01	-0.1187E 03	0.1293E 05
0.1000E-01	0.1100E 02	0.4096E 02	0.6400E 00	0.5120E 01	0.3225E 00	0.4016E 01	-0.9787E 02	0.8461E 04
0.2000E-01	0.6000E 01	0.8192E 02	0.1280E 01	0.1024E 02	0.6450E 00	0.3312E 01	-0.5187E 02	0.2605E 04
0.3000E-01	0.4333E 01	0.1229E 03	0.1920E 01	0.1536E 02	0.9676E 00	0.2896E 01	-0.3348E 02	0.1292E 04
0.4000E-01	0.3500E 01	0.1638E 03	0.2560E 01	0.2048E 02	0.1290E 01	0.2615E 01	-0.2362E 02	0.7465E 03
0.5000E-01	0.3000E 01	0.2048E 03	0.3200E 01	0.2560E 02	0.1613E 01	0.2410E 01	-0.1768E 02	0.4690E 03
0.6000E-01	0.2667E 01	0.2458E 03	0.3840E 01	0.3072E 02	0.1935E 01	0.2254E 01	-0.1385E 02	0.3123E 03
0.8000E-01	0.2250E 01	0.3277E 03	0.5120E 01	0.4096E 02	0.2580E 01	0.2027E 01	-0.9379E 01	0.1577E 03
0.1000E 00	0.2000E 01	0.4096E 03	0.6400E 01	0.5120E 02	0.3225E 01	0.1865E 01	-0.6975E 01	0.9110E 02
0.2000E 00	0.1500E 01	0.8192E 03	0.1280E 02	0.1024E 03	0.6450E 01	0.1425E 01	-0.2910E 01	0.1826E 02
0.3000E 00	0.1333E 01	0.1229E 04	0.1920E 02	0.1536E 03	0.9676E 01	0.1201E 01	-0.1731E 01	0.7570E 01
0.4000E 00	0.1250E 01	0.1638E 04	0.2560E 02	0.2048E 03	0.1290E 02	0.1059E 01	-0.1177E 01	0.4044E 01
0.5000E 00	0.1200E 01	0.2048E 04	0.3200E 02	0.2560E 03	0.1613E 02	0.9582E 00	-0.8564E 00	0.2511E 01
0.6000E 00	0.1167E 01	0.2458E 04	0.3840E 02	0.3072E 03	0.1935E 02	0.8937E 00	-0.6459E 00	0.1720E 01
0.8000E 00	0.1125E 01	0.3277E 04	0.5120E 02	0.4096E 03	0.2580E 02	0.7832E 00	-0.3844E 00	0.9468E 00
0.1000E 01	0.1100E 01	0.4096E 04	0.6400E 02	0.5120E 03	0.3225E 02	0.7227E 00	-0.2333E 00	0.5734E 00
0.2000E 01	0.1050E 01	0.8192E 04	0.1280E 03	0.1024E 04	0.6450E 02	0.6363E 00	-0.1975E-01	0.7840E-01
0.3000E 01	0.1033E 01	0.1229E 05	0.1920E 03	0.1536E 04	0.9676E 02	0.6283E 00	0.0	0.0
0.4000E 01	0.1025E 01	0.1638E 05	0.2560E 03	0.2048E 04	0.1290E 03	0.6283E 00	0.0	0.0
0.5000E 01	0.1020E 01	0.2048E 05	0.3200E 03	0.2560E 04	0.1613E 03	0.6283E 00	0.0	0.0
0.6000E 01	0.1017E 01	0.2458E 05	0.3840E 03	0.3072E 04	0.1935E 03	0.6283E 00	0.0	0.0
0.8000E 01	0.1012E 01	0.3277E 05	0.5120E 03	0.4096E 04	0.2580E 03	0.6283E 00	0.0	0.0
0.1000E 02	0.1010E 01	0.4096E 05	0.6400E 03	0.5120E 04	0.3225E 03	0.6283E 00	0.0	0.0

TABLE 25: p_{Ds}, p'_{Ds} and p''_{Ds} as Functions of Dimensionless Build Up Times for a Well Located Inside a Closed 4:1 Rectangle

WELL LOCATION, (XD,YD) = (0.0156250, 0.5000000)

PRODUCING TIME BEFORE SHUT IN, TDA = 1.0000

DEL(T)	TRAT	TDBX	TDBY	TDBB	TDABX	PDS	PDSP	PDSS
0.1000E-04	0.1000E 06	0.4096E-01	0.6400E-03	0.5120E-02	0.3225E-03	0.1867E 02	-0.4968E 05	0.4938E 10
0.2000E-04	0.5000E 05	0.8192E-01	0.1280E-02	0.1024E-01	0.6450E-03	0.1832E 02	-0.2491E 05	0.1242E 10
0.3000E-04	0.3333E 05	0.1229E 00	0.1920E-02	0.1536E-01	0.9676E-03	0.1812E 02	-0.1663E 05	0.5521E 09
0.4000E-04	0.2500E 05	0.1638E 00	0.2560E-02	0.2048E-01	0.1290E-02	0.1797E 02	-0.1250E 05	0.3080E 09
0.5000E-04	0.2000E 05	0.2048E 00	0.3200E-02	0.2560E-01	0.1613E-02	0.1786E 02	-0.1006E 05	0.1936E 09
0.6000E-04	0.1667E 05	0.2458E 00	0.3840E-02	0.3072E-01	0.1935E-02	0.1777E 02	-0.8460E 04	0.1313E 09
0.8000E-04	0.1250E 05	0.3277E 00	0.5120E-02	0.4096E-01	0.2580E-02	0.1762E 02	-0.6533E 04	0.7042E 08
0.1000E-03	0.1000E 05	0.4096E 00	0.6400E-02	0.5120E-01	0.3225E-02	0.1750E 02	-0.5425E 04	0.4366E 08
0.2000E-03	0.5001E 04	0.8192E 00	0.1280E-01	0.1024E 00	0.6450E-02	0.1709E 02	-0.3229E 04	0.1168E 08
0.3000E-03	0.3334E 04	0.1229E 01	0.1920E-01	0.1536E 00	0.9676E-02	0.1682E 02	-0.2398E 04	0.6012E 07
0.4000E-03	0.2501E 04	0.1638E 01	0.2560E-01	0.2048E 00	0.1290E-01	0.1660E 02	-0.1921E 04	0.3785E 07
0.5000E-03	0.2001E 04	0.2048E 01	0.3200E-01	0.2560E 00	0.1613E-01	0.1643E 02	-0.1606E 04	0.2628E 07
0.6000E-03	0.1668E 04	0.2458E 01	0.3840E-01	0.3072E 00	0.1935E-01	0.1628E 02	-0.1381E 04	0.1937E 07
0.8000E-03	0.1251E 04	0.3277E 01	0.5120E-01	0.4096E 00	0.2580E-01	0.1604E 02	-0.1078E 04	0.1181E 07
0.1000E-02	0.1001E 04	0.4096E 01	0.6400E-01	0.5120E 00	0.3225E-01	0.1584E 02	-0.8843E 03	0.7960E 06
0.2000E-02	0.5010E 03	0.8192E 01	0.1280E 00	0.1024E 01	0.6450E-01	0.1521E 02	-0.4641E 03	0.2215E 06
0.3000E-02	0.3343E 03	0.1229E 02	0.1920E 00	0.1536E 01	0.9676E-01	0.1483E 02	-0.3147E 03	0.1001E 06
0.4000E-02	0.2510E 03	0.1638E 02	0.2560E 00	0.2048E 01	0.1290E 00	0.1456E 02	-0.2401E 03	0.5527E 05
0.5000E-02	0.2010E 03	0.2048E 02	0.3200E 00	0.2560E 01	0.1613E 00	0.1434E 02	-0.1965E 03	0.3443E 05
0.6000E-02	0.1677E 03	0.2458E 02	0.3840E 00	0.3072E 01	0.1935E 00	0.1416E 02	-0.1681E 03	0.2341E 05
0.8000E-02	0.1260E 03	0.3277E 02	0.5120E 00	0.4096E 01	0.2580E 00	0.1386E 02	-0.1333E 03	0.1304E 05
0.1000E-01	0.1010E 03	0.4096E 02	0.6400E 00	0.5120E 01	0.3225E 00	0.1362E 02	-0.1122E 03	0.8568E 04
0.2000E-01	0.5100E 02	0.8192E 02	0.1280E 01	0.1024E 02	0.6450E 00	0.1278E 02	-0.6520E 02	0.2696E 04
0.3000E-01	0.3433E 02	0.1229E 03	0.1920E 01	0.1536E 02	0.9676E 00	0.1223E 02	-0.4597E 02	0.1370E 04
0.4000E-01	0.2600E 02	0.1638E 03	0.2560E 01	0.2048E 02	0.1290E 01	0.1183E 02	-0.3538E 02	0.8147E 03
0.5000E-01	0.2100E 02	0.2048E 03	0.3200E 01	0.2560E 02	0.1613E 01	0.1151E 02	-0.2880E 02	0.5295E 03
0.6000E-01	0.1767E 02	0.2458E 03	0.3840E 01	0.3072E 02	0.1935E 01	0.1125E 02	-0.2439E 02	0.3665E 03
0.8000E-01	0.1350E 02	0.3277E 03	0.5120E 01	0.4096E 02	0.2580E 01	0.1082E 02	-0.1893E 02	0.2023E 03
0.1000E 00	0.1100E 02	0.4096E 03	0.6400E 01	0.5120E 02	0.3225E 01	0.1047E 02	-0.1571E 02	0.1287E 03
0.2000E 00	0.6000E 01	0.8192E 03	0.1280E 02	0.1024E 03	0.6450E 01	0.9310E 01	-0.8916E 01	0.3806E 02
0.3000E 00	0.4333E 01	0.1229E 04	0.1920E 02	0.1536E 03	0.9676E 01	0.8572E 01	-0.6148E 01	0.2017E 02
0.4000E 00	0.3500E 01	0.1638E 04	0.2560E 02	0.2048E 03	0.1290E 02	0.8044E 01	-0.4527E 01	0.1289E 02
0.5000E 00	0.3000E 01	0.2048E 04	0.3200E 02	0.2560E 03	0.1613E 02	0.7649E 01	-0.3437E 01	0.9080E 01
0.6000E 00	0.2667E 01	0.2458E 04	0.3840E 02	0.3072E 03	0.1935E 02	0.7346E 01	-0.2649E 01	0.6762E 01
0.8000E 00	0.2250E 01	0.3277E 04	0.5120E 02	0.4096E 03	0.2580E 02	0.6931E 01	-0.1601E 01	0.4079E 01
0.1000E 01	0.2000E 01	0.4096E 04	0.6400E 02	0.5120E 03	0.3225E 02	0.6678E 01	-0.9754E 00	0.2603E 01
0.2000E 01	0.1500E 01	0.8192E 04	0.1280E 03	0.1024E 04	0.6450E 02	0.6317E 01	-0.8266E-01	0.4693E 00
0.3000E 01	0.1333E 01	0.1229E 05	0.1920E 03	0.1536E 04	0.9676E 02	0.6283E 01	0.0	0.0
0.4000E 01	0.1250E 01	0.1638E 05	0.2560E 03	0.2048E 04	0.1290E 03	0.6283E 01	0.0	0.0
0.5000E 01	0.1200E 01	0.2048E 05	0.3200E 03	0.2560E 04	0.1613E 03	0.6283E 01	0.0	0.0
0.6000E 01	0.1167E 01	0.2458E 05	0.3840E 03	0.3072E 04	0.1935E 03	0.6283E 01	0.0	0.0
0.8000E 01	0.1125E 01	0.3277E 05	0.5120E 03	0.4096E 04	0.2580E 03	0.6283E 01	0.0	0.0
0.1000E 02	0.1100E 01	0.4096E 05	0.6400E 03	0.5120E 04	0.3225E 03	0.6283E 01	0.0	0.0

TABLE 26: p_{Ds}, p'_{Ds} and p''_{Ds} as Functions of Dimensionless Build Up Times for a Well Located Inside a Closed 4:1 Rectangle

WELL LOCATION, (XD,YD) = (0.0156250, 0.5000000)
PRODUCING TIME BEFORE SHUT IN, TDA = 10.0000

DEL(T)	TRAT	TDBX	TDBY	TDBB	TDABX	PDS	PDSP	PDSS
0.1000E-04	0.1000E 07	0.4096E-01	0.6400E-03	0.5120E-02	0.3225E-03	0.7565E 02	-0.4968E 05	0.4938E 10
0.2000E-04	0.5000E 06	0.8192E-01	0.1280E-02	0.1024E-01	0.6450E-03	0.7530E 02	-0.2492E 05	0.1242E 10
0.3000E-04	0.3333E 06	0.1229E 00	0.1920E-02	0.1536E-01	0.9676E-03	0.7510E 02	-0.1663E 05	0.5521E 09
0.4000E-04	0.2500E 06	0.1638E 00	0.2560E-02	0.2048E-01	0.1290E-02	0.7495E 02	-0.1250E 05	0.3080E 09
0.5000E-04	0.2000E 06	0.2048E 00	0.3200E-02	0.2560E-01	0.1613E-02	0.7484E 02	-0.1006E 05	0.1936E 09
0.6000E-04	0.1667E 06	0.2458E 00	0.3840E-02	0.3072E-01	0.1935E-02	0.7475E 02	-0.8461E 04	0.1313E 09
0.8000E-04	0.1250E 06	0.3277E 00	0.5120E-02	0.4096E-01	0.2580E-02	0.7460E 02	-0.6534E 04	0.7042E 08
0.1000E-03	0.1000E 06	0.4096E 00	0.6400E-02	0.5120E-01	0.3225E-02	0.7448E 02	-0.5426E 04	0.4366E 08
0.2000E-03	0.5000E 05	0.8192E 00	0.1280E-01	0.1024E 00	0.6450E-02	0.7407E 02	-0.3230E 04	0.1168E 08
0.3000E-03	0.3333E 05	0.1229E 01	0.1920E-01	0.1536E 00	0.9676E-02	0.7380E 02	-0.2399E 04	0.6012E 07
0.4000E-03	0.2500E 05	0.1638E 01	0.2560E-01	0.2048E 00	0.1290E-01	0.7358E 02	-0.1922E 04	0.3785E 07
0.5000E-03	0.2000E 05	0.2048E 01	0.3200E-01	0.2560E 00	0.1613E-01	0.7341E 02	-0.1607E 04	0.2628E 07
0.6000E-03	0.1667E 05	0.2458E 01	0.3840E-01	0.3072E 00	0.1935E-01	0.7326E 02	-0.1382E 04	0.1937E 07
0.8000E-03	0.1250E 05	0.3277E 01	0.5120E-01	0.4096E 00	0.2580E-01	0.7302E 02	-0.1079E 04	0.1181E 07
0.1000E-02	0.1000E 05	0.4096E 01	0.6400E-01	0.5120E 00	0.3225E-01	0.7282E 02	-0.8854E 03	0.7960E 06
0.2000E-02	0.5001E 04	0.8192E 01	0.1280E 00	0.1024E 01	0.6450E-01	0.7219E 02	-0.4652E 03	0.2215E 06
0.3000E-02	0.3334E 04	0.1229E 02	0.1920E 00	0.1536E 01	0.9676E-01	0.7181E 02	-0.3158E 03	0.1001E 06
0.4000E-02	0.2501E 04	0.1638E 02	0.2560E 00	0.2048E 01	0.1290E 00	0.7153E 02	-0.2412E 03	0.5527E 05
0.5000E-02	0.2001E 04	0.2048E 02	0.3200E 00	0.2560E 01	0.1613E 00	0.7132E 02	-0.1975E 03	0.3443E 05
0.6000E-02	0.1668E 04	0.2458E 02	0.3840E 00	0.3072E 01	0.1935E 00	0.7113E 02	-0.1691E 03	0.2341E 05
0.8000E-02	0.1251E 04	0.3277E 02	0.5120E 00	0.4096E 01	0.2580E 00	0.7083E 02	-0.1343E 03	0.1305E 05
0.1000E-01	0.1001E 04	0.4096E 02	0.6400E 00	0.5120E 01	0.3225E 00	0.7059E 02	-0.1132E 03	0.8572E 04
0.2000E-01	0.5010E 03	0.8192E 02	0.1280E 01	0.1024E 02	0.6450E 00	0.6974E 02	-0.6621E 02	0.2700E 04
0.3000E-01	0.3343E 03	0.1229E 03	0.1920E 01	0.1536E 02	0.9676E 00	0.6918E 02	-0.4696E 02	0.1374E 04
0.4000E-01	0.2510E 03	0.1638E 03	0.2560E 01	0.2048E 02	0.1290E 01	0.6877E 02	-0.3634E 02	0.8188E 03
0.5000E-01	0.2010E 03	0.2048E 03	0.3200E 01	0.2560E 02	0.1613E 01	0.6844E 02	-0.2974E 02	0.5335E 03
0.6000E-01	0.1677E 03	0.2458E 03	0.3840E 01	0.3072E 02	0.1935E 01	0.6817E 02	-0.2531E 02	0.3705E 03
0.8000E-01	0.1260E 03	0.3277E 03	0.5120E 01	0.4096E 02	0.2580E 01	0.6772E 02	-0.1981E 02	0.2061E 03
0.1000E 00	0.1010E 03	0.4096E 03	0.6400E 01	0.5120E 02	0.3225E 01	0.6736E 02	-0.1654E 02	0.1325E 03
0.2000E 00	0.5100E 02	0.8192E 03	0.1280E 02	0.1024E 03	0.6450E 01	0.6612E 02	-0.9566E 01	0.4141E 02
0.3000E 00	0.3433E 02	0.1229E 04	0.1920E 02	0.1536E 03	0.9676E 01	0.6533E 02	-0.6656E 01	0.2316E 02
0.4000E 00	0.2600E 02	0.1638E 04	0.2560E 02	0.2048E 03	0.1290E 02	0.6475E 02	-0.4924E 01	0.1561E 02
0.5000E 00	0.2100E 02	0.2048E 04	0.3200E 02	0.2560E 03	0.1613E 02	0.6432E 02	-0.3748E 01	0.1158E 02
0.6000E 00	0.1767E 02	0.2458E 04	0.3840E 02	0.3072E 03	0.1935E 02	0.6399E 02	-0.2891E 01	0.9078E 01
0.8000E 00	0.1350E 02	0.3277E 04	0.5120E 02	0.4096E 03	0.2580E 02	0.6354E 02	-0.1749E 01	0.6132E 01
0.1000E 01	0.1100E 02	0.4096E 04	0.6400E 02	0.5120E 03	0.3225E 02	0.6326E 02	-0.1066E 01	0.4480E 01
0.2000E 01	0.6000E 01	0.8192E 04	0.1280E 03	0.1024E 04	0.6450E 02	0.6287E 02	-0.9033E-01	0.2005E 01
0.3000E 01	0.4333E 01	0.1229E 05	0.1920E 03	0.1536E 04	0.9676E 02	0.6283E 02	0.0	0.0
0.4000E 01	0.3500E 01	0.1638E 05	0.2560E 03	0.2048E 04	0.1290E 03	0.6283E 02	0.0	0.0
0.5000E 01	0.3000E 01	0.2048E 05	0.3200E 03	0.2560E 04	0.1613E 03	0.6283E 02	0.0	0.0
0.6000E 01	0.2667E 01	0.2458E 05	0.3840E 03	0.3072E 04	0.1935E 03	0.6283E 02	0.0	0.0
0.8000E 01	0.2250E 01	0.3277E 05	0.5120E 03	0.4096E 04	0.2580E 03	0.6283E 02	0.0	0.0
0.1000E 02	0.2000E 01	0.4096E 05	0.6400E 03	0.5120E 04	0.3225E 03	0.6283E 02	0.0	0.0

NOMENCLATURE

A = well drainage area, or area of the rectangular reservoir, ft^2

a_x = distance to farthest fault in the x-axis, ft

a_y = distance to farthest fault in the y-axis, ft

b_x = distance to closest fault in the x-axis, ft

b_y = distance to closest fault in the y-axis, ft

B = formation volume factor, res vol/std vol

c = compressibility, psi^{-1}

C_A = shape factor of drainage area

h = formation thickness, ft

k = formation permeability

m = absolute value of slope of straight line portion of semilog pressure buildup or drawdown curves, psi/log cycle

p = pressure, psi

p_D = dimensionless pressure at a point

p_{DI} = dimensionless pressure contribution due to image wells

p_{DR} = dimensionless pressure contribution due to real well

p_{Dw} = dimensionless well pressure

p_{Ds} = dimensionless shut-in pressure

p_i = initial reservoir pressure, psi

p_{wf} = flowing wellbore pressure, psi

p_{ws} = shut-in wellbore pressure, psi

p'_D = first derivative of dimensionless pressure with respect to dimensionless time

p''_D = second derivative of dimensionless pressure with respect to dimensionless time

p'_{Dw} = time rate of change of dimensionless well pressure

p'_{wf} = time rate of change of flowing well pressure, psi/hr

Δp_{skin} = pressure drop across the skin, psi

q = production rate of well, STB/D

r = radial distance, ft

r_D = dimensionless radial distance

r_{DI} = dimensionless radial distance between the real well and the image well

r_{DR} = dimensionless radial distance between the real well and any point in the reservoir

r_{xe} = radial distance between the real well and image wells along the x-axis when n is even

r_{xo} = radial distance between the real well and image wells along the positive direction of the x-axis when n is odd

r_{xop} = radial distance between the real well and image wells along the negative direction of the y-axis when n is odd

r_E = distance between the real well and image wells of infinite lines parallel to the x-axis when m is even

r_O = distance between the real well and image wells of infinite lines parallel to the x-axis on the positive direction of the y-axis when m is odd

r_P = distance between the real well and image wells of infinite lines parallel to the x-axis on the negative direction of the y-axis when m is odd

r_{Dw} = dimensionless ratio $r_w/\sqrt{A}$

r_w = wellbore radius, ft

s = skin factor

t = producing time, hours

t_D = dimensionless producing time based on wellbore radius r_w

t_{DA} = dimensionless producing time based on drainage area A

t_{Db_x} = dimensionless producing time based on distance to fault b_x

t_{Dbb} = dimensionless producing time based on product $b_x b_y$

Δt = shut-in time, hours

Δt_{DA} = dimensionless shut-in time based on drainage area A

W_x = width of rectangle (or infinite strip) in the x-axis

W_y = width of rectangle in the y-axis

x_D = dimensionless x-coordinate of the real well

y_D = dimensionless y-coordinate of the real well

Greek Symbols

γ = Euler's constant

μ = fluid viscosity, cp

ϕ = porosity, fraction

ψ_w = correction factor at the well

Δ = difference operator

$\partial/\partial t$ = partial differential with time

ρ = fluid density, gm/cc

Mathematical Constants and Expressions

e = 2.71828··· (Napierian base)

$\gamma = \lim_{m\to\infty}\left[1 + \frac{1}{2} + \frac{1}{3} + \frac{1}{4} + \cdots + \frac{1}{m} - \ln(m)\right] = 0.57721\cdots$

e^{γ} = 1.78107···

ln = natural logarithm (to the base e)

log = logarithm to the base 10

π = 3.1459···

$$Ei(-x) = -\int_x^{\infty} \frac{e^{-u}}{u}\,du$$

$$Ei(y) = \int_{\infty}^{y} \frac{e^{u}}{u}\,du = \gamma + \ln y + \frac{y}{1\times 1!} + \frac{y^2}{2\times 2!} + \frac{y^3}{3\times 3!} + \cdots + \frac{y^n}{n\times n!}$$

$$\simeq \frac{e^y}{y}\left(1 + \frac{1!}{y} + \frac{2!}{y^2} + \frac{3!}{y^3} + \cdots + \frac{n!}{y^n}\right) \quad (y \to \infty)$$

Special Symbols Used in Tables

PD = p_{Dw}

PDP = p'_{Dw}

PDPP = p''_{Dw}

PDS = P_{Ds}

PDSP = P'_{Ds}

PDSS = P''_{Ds}

TRAT = $(t_{DA} + \Delta t_{DA})/\Delta t_{DA}$

DEL(T) = Δt_{DA}

REFERENCES

1. Moore, T. V., Schilthuis, R. J., and Hurst, W.: "The Determination of Permeability from Field Data," Proc., API Bull. 211 (1933) 4.
2. Theis, C. V.: "The Relationship Between the Lowering of Piezometric Surface and Rate and Duration of Discharge of Wells Using Ground-Water Storage," Trans., AGU (1935) II, 519.
3. Muskat, M.: The Flow of Homogeneous Fluids Through Porous Media, McGraw-Hill Book Co., Inc., New York (1937).
4. Elkins, L. F.: "Reservoir Performance and Well Spacing Silica Arbuckle Pool, Kansas," Drill. and Prod. Prac., API (1946) 109.
5. Arps, J. J. and Smith, A. E.: "Practical Use of Bottom-hole Pressure Buildup Curves," Drill. and Prod. Prac., API (1949) 155.
6. Horner, D. R.: "Pressure Buildup in Wells," Proc., Third World Pet. Cong., E. J. Brill, Leiden (1951) II, 503.
7. Miller, C. C., Dyes, A. B., and Hutchinson, C. A., Jr.: "The Estimation of Permeability and Reservoir Pressure from Bottom-hole Pressure Buildup Characteristics," Trans., AIME (1950) 189, 91-106.

8. Dolan, J. R., Einarsen, C. A., and Hill, G. A.: "Special Applications of Drill-Stem Test Pressure Data," Trans., AIME (1957) 210, 318-324.

9. Davis, E. Grady, Jr., and Hawkins, M. F., Jr.: "Linear Fluid-Barrier Detection by Well Pressure Measurements," J. Pet. Tech. (October, 1963) 1077-1079.

10. Gray, K. E.: "Approximating Well-to-Fault Distance From Pressure Buildup Tests," J. Pet. Tech. (July, 1965) 761-767.

11. Bixel, H. C., Larkin, B. K., and Van Poollen, H. K.: "Effect of Linear Discontinuities on Pressure Buildup and Drawdown Behavior," J. Pet. Tech. (August, 1963) 885-895.

12. Evrenos, A. I. and Rejda, E. A.: "A Digital Computer Application to the Investigation of Aquifer Properties," J. Pet. Tech. (July, 1965) 827-838.

13. Overpeck, A. C. and Holden, W. R.: "Well Imaging and Fault Detection in Anisotropic Reservoirs," J. Pet. Tech. (October, 1970) 1317-1325.

14. Rodgers, J. S. and McArthur, B. W.: "Implicit Solutions and Precision Pressure Measurements Provide Reliable Transient Analyses," Paper SPE 4056 presented at 47th Annual SPE Fall Meeting, San Antonio, Texas (October 8-11, 1972).

15. Prasad, Raj K.: "Pressure Transient Analysis in the Presence of Two Intersecting Boundaries," Paper SPE 4560 presented at 48th Annual SPE Fall Meeting, Las Vegas, Nevada (September 30-October 3, 1973).

16. Jones, P.: "Reservoir Limit Test on Gas Wells." Paper presented at SPE Gas Tech. Symp., Tyler, Texas (April 20-21, 1961).

17. van Poollen, H. K.: "Drawdown Curves Give Angle Between Intersecting Faults," The Oil and Gas Journal (December 20, 1965) 71-75.

18. Witherspoon, P. A., Javandel, I., Neuman, S. P., and Freeze, R. A.: Interpretation of Aquifer Gas Storage Conditions from Water Pumping Tests, Monograph on Project NS-38, American Gas Association, Inc., New York, 1967.

19. Ramey, H. J., Jr., Kumar, A., and Gulati, M. S.: Gas Well Test Analysis Under Water-Drive Conditions, Monograph on Project 61-51, American Gas Association, Inc., Virginia (1973).

20. Matthews, C. S., Brons, F., and Hazebroek, P.: "A Method for Determination of Average Pressure in a Bounded Reservoir," Trans., AIME (1954), 201, 182-191.

21. Brons, F. and Miller, W. C.: "A Simple Method for Correcting Spot Pressure Readings," J. Pet. Tech. (August, 1961), 803-805.

22. Dietz, D. N.: "Determination of Average Pressure from Build-up Surveys," J. Pet. Tech. (August, 1965), 955.

23. Matthews, C. S. and Russel, D. G.: Pressure Buildup and Flow Tests in Wells, SPE Monograph, Vol. 1, Society of Petr. Eng. of AIME, Dallas, Texas (1967).

24. Earlougher, R. C., Jr., Ramey, H. J., Jr., Miller, F. G. and Mueller, T. D.: "Pressure Distribution in Rectangular Reservoirs," J. Pet. Tech. (February, 1968), 199.

25. Earlougher, R. C., Jr., and Ramey, H. J., Jr.: "Interference Analysis in Bounded Systems," The J. Canad. Pet. (October-December, 1973), 33.

26. Tiab, D.: A New Approach to Detect and Locate Multiple Reservoir Boundaries by Transient Well Pressure Data, M.S. Thesis, New Mexico Institute of Mining and Technology, Socorro, New Mexico (1975).

27. Tiab, D., and Kumar, A.: "Application of p_D' Function to Interference Analysis," Paper SPE 6053 presented at the 51st Annual Fall Meeting of the Society of Petroleum Engineers of AIME, New Orleans, LA (October 3-6, 1976).

28. Tiab, D. and Kumar, A.: "Detection and Location of Two Parallel Sealing Faults Around a Well," Paper SPE 6056 presented at the 51st Annual Fall Meeting of the Society of Petroleum Engineers of AIME, New Orleans, LA (October 3-6, 1976).

29. van Everdingen, A. F. and Hurst, W.: "The Application of the Laplace Transformation to Flow Problems in Reservoirs," Trans., AIME (1949) 186, 305-324.

30. Clegg, M. W.: "Some Approximate Solutions of Radial Flow Problems Associated with Production at Constant Well Pressure," Paper SPE 1536 presented at 41st Annual Fall Meeting, Dallas, Texas (October 2-5, 1966).

31. Ramey, H. J., Jr.: "Application of the Line Source Solution to Flow in Porous Media--A Review," Prod. Monthly (May, 1967) 4.

32. Mueller, T. D. and Witherspoon, P. A.: "Pressure Interference Effects Within Reservoirs and Aquifers," J. Pet. Tech. (April, 1965) 471-474.

33. Abramowitz, M. and Stegun, I. A.: Handbook of Mathematical Functions, Dover Publications, Inc., New York (November, 1970), 255.

34. Chatas, A. T.: "A Practical Treatment of Nonsteady-State Flow Problems in Reservoir Systems," Petr. Eng. (1953) 25.

35. Mortada, M.: "A Practical Method for Treating Oilfield Interference in Water-Drive Reservoirs," Trans., AIME (1955) 204, 217.

36. Katz, D. L., Tek, M. R., Coats, K. H., Katx, M. L., Jones, S. C., and Miller, N. C.: Movement of Underground Water in Contact with Natural Gas, AGA, New York (February, 1963) 251-271.

37. Edwardson, M. J., Girner, H. M., Parkison, H. R., Williams, C. D., and Matthews, C. S.: "Calculation of Formation Temperature Disturbances Caused by Mud Circulation," J. Pet. Tech. (April, 1962) 416-426.

38. Ramey, H. J., Jr. and Cobb, W. M.: "A General Pressure Buildup Theory for a Well in a Closed Drainage Area," J. Pet. Tech. (December, 1971) 1493-1505

39. Claret, J. and Tempère, C.: "Une Nouvelle Region Productrice au Sahara Algerien: L'Anticlinorium d'Hassi Touareg," Proc., Seventh World Pet. Cong., Mexico (1967) II, 81-100.

40. Kumar, A. and Ramey, H. J., Jr.: "Well-Test Analysis for a Well in a Constant Pressure Square," Soc. Petr. Eng. J. (April, 1974) 107-116.

41. Earlougher, R. C., Jr.: "The Use of Interpolation to Obtain Shape Factors for Pressure Buildup Calculations," J. Pet. Tech. (May, 1968) 449-450.

42. Russel, D. G.: "Extensions of Pressure Buildup Analysis Methods," J. Pet. Tech. (December, 1966) 1624-1636.